Durham University

Joint Quantum Centre
WWW.JQC.ORG.UK

EGAS

49th Conference of the European Group on Atomic Systems

EPS

EGAS 2017, July 17–21, Durham University, UK

EGAS49

Book of Abstracts

PLENARY TALKS

Tuesday 8:45	**Magneto-optical trapping and sub-Doppler cooling of molecules** Ed Hinds (EPS Invited Speaker)
Tuesday 9:30	**Near-optimal atom-photon interfaces in the solid-state** Pascale Senellart
Tuesday 14:00	**Attosecond physics and the dream of an electron movie** Eva Lindroth
Wednesday 8:45	**Contactless photon-photon interactions** Charles Adams
Wednesday 9:30	**Structure and dynamics of nanoparticles in short wavelength light pulses** Thomas Möller
Thursday 8:45	**Quantum gas in a box** Zoran Hadzibabic
Thursday 14:00	**Atomic clock and quantum many-body physics** Jun Ye
Friday 8:45	**Dipolar quantum gases and liquids** Tilman Pfau
Friday 9:30	**Ultracold Dipolar Fermi Gas of NaK Molecules** Martin Zwierlein

INVITED TALKS

Tuesday 11:00	**Fast ion beams stored in cryogenic low-density environment: Collision experiments and low-energy internal excitations** Andreas Wolf
Tuesday 11:00	**Superconducting circuits for detecting and manipulating spins in solids** Denis Vion
Tuesday 15:90	**Imaging ultrafast molecular wave-packets with a single chirped UV pulse** Alicia Palacios
Tuesday 15:00	**Cold chemistry with cold molecules** Edvardas Narevicius
Wednesday 11:00	**Spectroscopy of highly charged ions in magnetic fusion plasmas: Research opportunities and diagnostic necessities** Peter Beiersdorfer
Wednesday 11:00	**Detection of entanglement and of features of quantum evolution with few local measurement and complementary properties** Chiara Macchiavello
Thursday 11:00	**Exploring quantum antiferromagnets with single-site resolution** Daniel Greif
Thursday 11:00	**Real-time dynamics of lattice gauge theories with a few-qubit quantum computer** Christine Muschik
Thursday 15:00	**Observation of the 1S-2S transition in trapped antihydrogen** Niels Madsen
Thursday 15:00	**Vector correlations in molecular photodissociation: Production of spin-polarized H-atoms and femtosecond stereodynamics** Oleg Vasyutinskii
Friday 11:00	**Two-dimensional arrays of single Rydberg atoms for the quantum simulation of spin systems** Thierry Lahaye

CONTRIBUTED TALKS

Tuesday 11:30 **Testing the Universality of Free Fall with Bragg atom interferometer**
M. K. Zhou, K. Zhang, Y. Cheng, L. L. Chen, L. S. Cao and Z. K. Hu

Tuesday 11:50 **Coherence of an interacting ultra-cold atomic ensemble in a trapped matter-wave sensor**
Alexis Bonnin, X. Alauze, C. Solaro, F. Combes, J. N. Fuchs, F. Piéchon and F. Pereira dos Santos

Tuesday 12:10 **Experimental constraints on non-Newtonian gravity via state of the art photoassociation spectroscopy**
Mateusz Borkowski, Alexei A. Buchachenko, Roman Ciuryło, Paul S. Julienne, Hirotaka Yamada, Kikuchi Yuu, Kekaru Takahashi, Yosuke Takasu and Yoshiro Takahashi

Tuesday 11:30 **Experimental signatures of an absorbing-state phase transition in a cold Rydberg gas**
C. Simonelli, M. Archimi, F. Castellucci, E. Arimondo, D. Ciampini, R. Gutierrez, M. Marcuzzi, I. Lesanovsky and O. Morsch

Tuesday 11:50 **A Rydberg-dressed magneto-optical trap**
A. D. Bounds, N. C. Keegan, R. K. Hanley, R. F. Faoro, E. M. Bridge, P. Huillery and M. P. A. Jones

Tuesday 12:10 **Quantum gas microscopy of spatial correlations in attractive and repulsive Fermi-Hubbard systems**
P. Schauss, D. Mitra, P. T. Brown, E. Guardado-Sanchez, S. S. Kondov, E. Khatami, T. Paiva, N. Trivedi, T. Devakul, D. A. Huse and W. S. Bakr

Tuesday 15:30 **Positron cooling and annihilation in noble gases**
D. G. Green, P. Mullan, M. Lee and G. F. Gribakin

Tuesday 15:50 **Self-organisation of light in optical media with competing nonlocal nonlinearities**
F. Maucher, T. Pohl, S. Skupin and W. Krolikowski

Tuesday 15:30 **Directional quantum controlled Chemistry: Generating alignment of ultracold photoassociation molecules**
S. Kallush, J. L. Carini, P. L. Gould and R. Kosloff

Tuesday 15:50 **Precision spectroscopy of cold formaldehyde in an electric trap**
Martin Ibrügger, A. Prehn, M. Zeppenfeld and G. Rempe

Wednesday 11:30 **Laboratory measurements compellingly support a charge-exchange mechanism for the "dark matter" ~ 3.5 keV X-ray line**
Chintan Shah, Sven Bernitt, Stepan Dobrodey, René Steinbrügge, Liyi Gu, Jelle Kaastra and José R. Crespo López-Urrutia

Wednesday 11:50 **Sideband heating of a single calcium ion trapped in a Penning trap: Preparation and coherence studies of a non-thermal state**
M. K. Joshi, P. Hrmo, V. Jarlaud, J. F. Goodwin, G. Stutter and R. C. Thompson

Wednesday 12:10 **Direct detection of giant molecules with a cloud of cold ions**
N. Bremare, C. Champenois, C. Dedonder-Lardeux, D. Guyomarc'h, A. Janulyte, J. Pedregosa-Gutierrez, C. Jouvet and M. Knoop

Wednesday 11:30 **Spectroscopy methods with quantum sensors**
Tuvia Gefen, Simon Schmitt, Liam P. McGuinness, Fedor Jelezko, Alex Retzker

Wednesday 11:50 **Towards coherent splitting and recombination of bright solitary matter waves**
A. Rakonjac, O. J. Wales, T. P. Billam, J. L. Helm, S. A. Gardiner and S. L. Cornish

Wednesday 12:10 **Improved sensitivity to the electron's electric dipole moment using YbF molecules**
Isabel M. Rabey, J. A. Devlin, C. Ho, B. E. Sauer, M. R. Tarbutt and E. A. Hinds

Thursday 11:30 **Single atom- and momentum-resolved investigation of thermal and quantum depletion in metastable Helium Bose condensates**
H. Cayla, C. Carcy, Q. Bouton, R. Chang, C. I. Westbrook, A. Aspect, M. Mancini and D. Clément

Thursday 11:50 **Supersolidity with Bose-Einstein condensates**
A. Morales, J. Leonard, P. Zupancic, T. Esslinger and T. Donner

Thursday 12:10 **Crossing over from attractive to repulsive interactions in a tunneling bosonic Josephson junction**
Giovanni Ferioli, G. Spagnolli, G. Semeghini, L. Masi, A. Trenkwalder, S. Coop, M. Landini, L. Pezzé, G. Modugno, M. Inguscio, A. Smerzi and M. Fattori

Thursday 11:30 **Single organic molecule coupling to a hybrid plasmonic waveguide**
S. Grandi, M. A. Nielsen, J. Cambiasso, S. Boissier, K. D. Major, C. Reardon, T. F. Krauss, R. F. Oulton, E. A. Hinds and A. S. Clark

Thursday 11:50 **Identifying optical transitions in highly charged ions with applications for metrology and searches of variation of the fine-structure constant**
H. Bekker, A. Windberger, N. Potters, J. Rauch, J. Berengut, A. Borschevsky and J. R. Crespo López-Urrutia

Thursday 12:10 **Monochromatic electron beam from Rydberg atoms**
E. Moufarej, Z. Mazzotta, M. Vielle-Grosjean, F. Robicheaux, Y. J. Picard and D. Comparat

Thursday 15:30 **An improved value of the atomic mass of the proton**
Florian Köhler-Langes, Fabian Heiße, Sascha Rau, Sven Junck, Andreas Mooser, Wolfgang Quint, Stefan Ulmer, Günter Werth, Klaus Blaum and Sven Sturm

Thursday 15:50 **Precision spectroscopy on the $2\,^3\mathrm{S} \rightarrow 2\,^1\mathrm{S}$ transition in ultracold helium inside a magic wavelength trap**
R. J. Rengelink, R. P. M. J. W. Notermans and W. Vassen

Thursday 15:30 **Electron-nuclear coupling through autoionizing states after strong-field excitation of H_2 molecules**
Yonghao Mi, Nicolas Camus, Lutz Fechner, Martin Laux, Robert Moshammer and Thomas Pfeifer

Thursday 15:50 **Control of 3D photoelectron wavepackets using single beam bichromatic and polarization shaped ultrashort laser pulses**
D. Pengel, S. Kerbstadt, D. Johannmeyer, L. Englert, T. Bayer and M. Wollenhaupt

Friday 11:30 **Nondestructive detection of polar molecules via Rydberg atoms**
M. Zeppenfeld and F. Jarisch

Friday 11:50 **Three-Body Förster resonances in a few interacting Rb Rydberg atoms**
I. I. Ryabtsev, D. B. Tretyakov, I. I. Beterov, E. A. Yakshina, V. M. Entin, P. Cheinet and P. Pillet

Friday 12:10 **Coherent control and trapping of ultracold $^{87}\mathrm{Rb}^{133}\mathrm{Cs}$ molecules**
Philip D. Gregory, Jacob A. Blackmore, Elizabeth M. Bridge, Jesus Aldegunde, Jeremy M. Hutson and Simon L. Cornish

POSTERS

Session A (Tuesday 16:30)

Poster A1 **Towards conductivity imaging of biological tissues with atomic magnetometers**
Cameron Deans, Luca Marmugi and Ferruccio Renzoni

Poster A2 **Modelling LMT atom interferometry in optical cavities**
M. Dovale, Aaron Jones, D. Brown, H. Miao and A. Freise

Poster A3 **Application of cavity ring-down spectroscopy for diagnostics of low temperature N_2H^+ dominated afterglow plasmas**
Ábel Kálosi, P. Dohnal, D. Shapko, R. Plasil and J. Glosík

Poster A4 **Multichannel optical atomic magnetometer operating in unshielded environment**
V. Biancalana, Antonio Vigilante, G. Bevilacqua, Y. Dancheva, E. Mariotti and C. Rossi

Poster A5 **Real-time monitoring of breath acetone in diabetic patients**
Arin Mizouri, Nada Al Taisan, Eckart Wrede, N. Hendrik Nahler and David Carty

Poster A6 **Dynamical studies in electron impact ionization of atoms and molecules**
S. Houamer, M. Chinoune and C. Dal Cappello

Poster A7 **The filleted atom revisited - a new dynamical description**
H. Agueny, M. Chovancova, M. Førre and J. P. Hansen

Poster A8 **Phase properties of the cutoff high-order harmonics**
M. Khokhlova and V. Strelkov

Poster A9 **Study of atomic delays in negative ions**
E. Lindroth and Marcus Dahlström

Poster A10 **Relativistic ionization dynamics for a hydrogen atom exposed to superintense XUV laser pulses**
E. Lindroth, Tor Kjellsson, Sølve Selstø and Morten Førre

Poster A11 **XUV-initiated high-harmonic generation in Ar^+**
Daniel D. A. Clarke, H. W. van der Hart and A. C. Brown

Poster A12 **Rydberg excitations of cold atoms inside a hollow-core fiber**
Maria Langbecker, Mohammad Noaman, Chantal Voss and Patrick Windpassinger

Poster A13 **Species-selective confinement of atoms dressed with multiple radiofrequencies**
E. Bentine, T. L. Harte, K. Luksch, A. Barker, J. Mur-Petit, B. Yuen and C. J. Foot

Poster A14 **An ε-pseudoclassical model for quantum resonances in a cold dilute atomic gas periodically driven by finite-duration standing-wave laser pulses**
B. T. Beswick, S. A. Gardiner, I. G. Hughes, H. P. A. G. Astier, M. F. Andersen and B. Daszuta

Poster A15 **Fibonacci anyon excitations of one-dimensional dipolar lattice bosons**
Tanja Đurić, Krzysztof Biedroń and Jakub Zakrzewski

Poster A16 **Laser cooling of molecules to below the Doppler limit**
L. Caldwell, S. Truppe, M. Hambach, H. J. Williams, N. J. Fitch, E. A. Hinds, B. E. Sauer and M. R. Tarbutt

Poster A17 **The long-range behavior of ab initio transition dipole moments and spin-orbit coupling matrix elements between the low-lying electronic states of LiRb and KRb molecules**
E. A. Bormotova and A.V. Stolyarov

Poster A18 **Prospects of the usage of the $A^1\Sigma^+ \sim b^3\Pi$ and $S^1\Pi \sim d^3\Pi$ complexes in ultracold LiRb molecule production**
E. A. Bormotova, S. V. Kozlov, E. A. Pazyuk and A. V. Stolyarov

Poster A19 **Towards non-destructive, real-time transport measurements of interacting Fermi gas**
Barbara Cilenti, K. Roux, O. Bettermann, V. Helson and J. Brantut

Poster A20 **Towards the implementation of quantum probes in spin-dependent optical lattice potentials**
Andrea Di Carli, C. Colquhoun and E.Haller

Poster A21 **Discovering new physics strategies with citizen science driven, human-computer hybrid optimization**
Ottó Elíasson, Jacob Sherson and the scienceathome.org team

Poster A22 **Observing metastability in a strongly-correlated many-body system**
L. Hruby, N. Dogra, M. Landini, K. Kroeger, T. Donner and T. Esslinger

Poster A23 **Blue-detuned magneto optical trap**
Kyle N. Jarvis, T. E. Wall, E. A. Hinds, B. E. Sauer and M. R. Tarbutt

Poster A24 **Spin mixing and protection of ferromagnetism in a spinor dipolar condensate**
Kaci Kechadi, Bruno Laburthe-Tolra and Paolo Pedri

Poster A25 **Nonlinear scattering of atomic bright solitons in disorder**
A. Boissé, G. Berthet and T. Bourdel

Poster A26 **Towards coherent splitting and recombination of bright solitary matter waves**
A. Rakonjac, O. J. Wales, T. P. Billam, J. L. Helm, S. A. Gardiner and S. L. Cornish

Poster A27 **A multipurpose experiment for ultracold lanthanides**
P. Ilzhöfer, G. Durastante, A. Patscheider, M. Sohmen, A. Trautmann, M. J. Mark and F. Ferlaino

Poster A28 **Reflection of noble gas endohedral structure in electron and positron scattering cross-sections**
Miron Amusia and L. V. Chernysheva

Poster A29 **Quantitative modeling of coherent atom-light interactions in 2, 3 and 4-level systems in the hyperfine Paschen-Back (HPB) regime**
J. Keaveney, D. J. Whiting, R. Mathew, C. S. Adams and I. G. Hughes

Poster A30 **Atom probing of thermally populated surface polaritons**
J. C de Aquino Carvalho, A. Laliotis, P. Chaves de Souza Segundo, I. Maurin, M. Ducloy and D. Bloch

Poster A31 **Sub-Doppler features in the backward-emitted fluorescence of a dense vapor and analogies with thin-cell spectroscopy**
J. C. de Aquino Carvalho, A. Laliotis, M. Chevrollier, M. Oriá and D. Bloch

Poster A32 **Slow molecular beams of heavy diatomic polar molecules**
Kevin Esajas, Artem Zapara and Steven Hoekstra

Poster A33 **Dielectric response of a particle embedded in media**
Johannes Fiedler and Stefan Y. Buhmann

Poster A34 **A new general cooling technique for ions by autoresonance in an electrostatic ion beam trap**
R. K. Gangwar, K. Saha, O. Heber, M. L. Rappaport and D. Zajfman

Poster A35 **Optical diagnostic of gas mixture plasmas with fine-structure resolved population-kinetic models**
R. K. Gangwar, Priti, S. Gupta, Dipti and R. Srivastava

Poster A36 **Single- and double-electron capture in the collisions of C^{4+} + He**
J. W. Gao, Y. Wu, N. Sisourat, J. G. Wang and A. Dubois

Poster A37 **Effect of gravity on magnetobound states of protonium**
Elijah Goodrich and Carlos A. Ordonez

Poster A38 **Experimental upgrades to measure the electron's electric dipole moment using YbF molecules**
Chris J. Ho, I. M. Rabey, J. A. Devlin, B. E. Sauer, M. R. Tarbutt and E. A. Hinds

Poster A39 **Molecular frame (e, 2e + ion) studies of CH_4 and CF_4**
Khokon Hossen, Xueguang Ren and Alexander Dorn

Poster A40 **Simultaneous magnetic trapping of O_2 molecules together with Li atoms**
N. Akerman, Michael Karpov, Y. Segev, S. Reitich, N. Bibelnik, J. Narevicius and E. Narevicius

Poster A41 **The hyperfine structure investigation of V I lines with Doppler reduced laser spectroscopic method**
Gö. Başar, I. K. Öztürk, F. Güzelçimen, Doğukan Bingöl, S. Kröger and Gü. Başar

Poster A42 **Identifying optical transitions in highly charged ions with applications for metrology and searches of variation of the fine-structure constant**
H. Bekker, A. Windberger, N. Potters, J. Rauch, J. Berengut, A. Borschevsky and J. R. Crespo López-Urrutia

Poster A43 **Isotope shift of the $2p^4\ ^3P_2 \rightarrow 2p^3 3p\ ^3P_2$ two-photon transition of O I and the triplet energy levels of atomic oxygen**
Christophe Blondel, Daniil Marinov, Jean-Paul Booth and Cyril Drag

Poster A44 **Probing the size of helium droplets with interatomic Coulombic decay: A theoretical insight**
S. Kazandjian, T. Miteva and N. Sisourat

Poster A45 **E2 transitions between hyperfine structure components of the H_2^+ molecular ion**
P. Danev, D. Bakalov, V. I. Korobov and S. Shiller

Poster A46 **Photodetachment of O^- from the $O(^3P)$ to the $O(^1S)$ threshold**
M. Génévriez, A. Dochain and X. Urbain

Poster A47 **Resonant Faraday rotation effect in Rb atoms with the use of a nano-cell: Impact of cell thicknesses on observed spectra**
Emmanuel Klinger, A. Sargsyan, A. Tonoyan, G. Hakhumyan, A. Amiryan, A. Papoyan, C. Leroy and D. Sarkisyan

Poster A48 **Selective reflection monitoring of forbidden at zero B-field atomic transitions of a Rb vapor nanocell**
A. Amiryan, A. Sargsyan, E. Klinger, S. Cartaleva, C. Leroy and D. Sarkisyan

Poster A49 **Algebraic order and quench dynamics in exciton-polariton condensates**
P. Comaron, G. Dagvadorj, A. Zamora, I. Carusotto, N. Proukakis and M. H. Szymańska

Poster A50 **Charge-state-resolved spectroscopy of highly charged tin ions for laser-plasma-based nanolithography EUV-light sources**
F. Torretti, J. Scheers, A. Windberger, W. Ubachs, R. Hoekstra, A. Ryabtsev, A. Borschevsky, J. Berengut, J. R. Crespo López-Urrutia and O. O. Versolato

Poster A51 **High-helicity vortex conversion in a rubidium vapor**
Aurélien Chopinaud, Marion Jacquey, Bruno Viaris de Lesegno and Laurence Pruvost

Session B (Wednesday 19:00)

Poster B1 **Colliding laser produced plasmas analysis: Fast imaging and spectroscopic study**
Domagoj Kos, O. Maguire, F. O'Reilly, P. Dunne and E. Sokell

Poster B2 **A novel off-axis electron gun for electron beam ion traps**
S. Kühn, Sven Bernitt, Peter Micke, Thomas Stöhlker and José R. Crespo López-Urrutia

Poster B3 **Observing the effect of wavefront aberrations in an atom interferometer by modulating the diameter of Raman beams**
Qin Luo, Le-le Chen, Xiao-Chun Duan, Min-kang Zhou and Zhong-kun Hu

Poster B4 **Transmission diffraction gratings for ultrasensitive biosensors and atomic physics**
A. Sierant, B. Jany, D. Bartoszek-Bober, J. Fiutowski, J. Adam and T. Kawalec

Poster B5 **Effect of the Raman beams' alignment in four-pulse atom gyroscope**
W. J. Xu, M. K. Zhou, X. C. Duan, M. M. Zhao, K. Zhang and Z. K. Hu

Poster B6 **Dielectronic-recombination processes in highly-charged heavy ions observed in ion traps**
A. Borovik, Jr., J. Dreiling, R. Silwal, Dipti, E. Takács, J. Gillaspy, R. Lomsadze, V. Ovsyannikov, K. Huber, A. Müller and Yu. Ralchenko

Poster B7 **Developments towards a transverse free-electron target for the storage ring CRYRING@ESR**
C. Brandau, A. Borovik, Jr., B. M. Döhring, B. Ebinger, C. Kozhuharov, T. Molkentin, A. Müller, Th. Stöhlker and S. Schippers, for the SPARC working group "Electron Targets"

Poster B8 **Simulating strong control fields in nuclear quantum optics**
K. P. Heeg, A. Kaldun, C. Strohm, P. Reiser, C. Ott, S. Rajagopalan, D. Lentrodt, J. Haber, H.-C. Wille, S. Goerttler, R. Rüffer, C. H. Keitel, R. Röhlsberger, T. Pfeifer and J. Evers

Poster B9 **X-ray laser spectroscopy with highly charged ions using radiation from synchrotrons and free-electron lasers**
S. Bernitt, R. Steinbrügge, S. Dobrodey, S. Kühn, P. Micke, J. K. Rudolph, S. W. Epp, T. Stöhlker and J. R. Crespo Löpez-Urrutia

Poster B10 **Theoretical studies of dipole blockade parameters using Förster resonances in Rb atoms**
Teodora Kirova, Arturs Cinins, Marcis Auzinsh and Ite A. Yu

Poster B11 **Single- and multi-layer platform of individually addressable atomic qubits for quantum simulation and quantum computation**
M. Schlosser, D. Ohl de Mello, D. Schäffner, T. Preuschoff, L. Kohfahl and G. Birkl

Poster B12 **Ionization spectra of highly Stark shifted rubidium Rydberg states**
J. Grimmel, M. Stecker, M. Kaiser, F. Karlewski, L. Torralbo-Campo, A. Günther and J. Fortágh

Poster B13 **Efficient preparation of circular states in He with n $\geq$ 70 using a modified version of the crossed-fields method**
A. Morgan, V. Zhelyazkova and S. D. Hogan

Poster B14 **A Rydberg-atom beam splitter**
J. Palmer and S. D. Hogan

Poster B15 **Rydberg-mediated long-range interactions between stored optical photons**
Hannes Busche, Paul Huillery, Simon W. Ball, Teodora Ilieva, Nicholas L. R. Spong, Matthew P. A. Jones and Charles S. Adams

Poster B16 **The coupled-channel deperturbation analysis of the mixed** $(1 \sim 2)^1\Pi$**,** $1^3\Pi$**,** $2^1\Sigma^+$ **and** $2^3\Sigma^+$ **states of KRb molecule**
Sergei V. Kozlov, E. A. Pazyuk and A. V. Stolyarov

Poster B17 **A cold atoms platform for testing the computational power of discord**
K. Krzyzanowska, R. Romain, M. Copley-May, A. Odufowora, C. MacCormick and S. Bergamini

Poster B18 **Towards measuring the absolute frequency of Rydberg levels in** ^{39}**K**
Prosenjit Majumder and Simon Cornish

Poster B19 **Creating Feshbach resonances for ultracold molecule formation with radiofrequency fields**
Daniel J. Owens, Ting Xie and Jeremy M. Hutson

Poster B20 **Inelastic losses in radiofrequency-dressed traps for ultracold atoms**
Daniel J. Owens and Jeremy M. Hutson

Poster B21 **Superstatistical energy distributions of an ion interacting with a neutral buffer gas**
I. Rouse and S. Willitsch

Poster B22 **An optical quasicrystal for ultracold atoms**
Matteo Sbroscia, Konrad Viebahn, Edward Carter and Ulrich Schneider

Poster B23 **Molecular beam brightening by shock-wave suppression**
Yair Segev, N. Bibelnik, N. Akerman, Y. Shagam, A. Luski, M. Karpov, J. Narevicius and E. Narevicius

Poster B24 **Many-body localization due to random interactions**
A. Sierant, B. Jany, D. Bartoszek-Bober, J. Fiutowski, J. Adam and T. Kawalec

Poster B25 **Observation of Fano-Feshbach resonances in ultracold gas of thulium**
Vladislav Tsyganok, E. T. Davletov, I. S. Cojocaru and A. V. Akimov

Poster B26 **A new design of a high-flux source of cold strontium atoms**
Dongyang Xu, Rowan Moore and Christopher Foot

Poster B27 **Collisions in ultracold polar bosonic RbCs molecules**
Elizabeth M. Bridge, Jacob A. Blackmore, Philip D. Gregory, Jesus Aldegunde, Jeremy M. Hutson and Simon L. Cornish

Poster B28 **Towards ultracold KCs molecules**
Zhengkun Fu, Apichayaporn Ratkata, Danielle Boddy, Jesus Aldegunde, Jeremy M. Hutson and Simon L. Cornish

Poster B29 **Laser cooling of YbF molecules for measuring the electron's electric dipole moment**
M. A. Trigatzis, J. Lim, J. R. Almond, N. J. Fitch, B. E. Sauer, E. A. Hinds and M. R. Tarbutt

Poster B30 **Retrieval of group refractive index in a dense atomic vapor helped by buffer gas-assisted radiation channeling**
A. Papoyan, S. Shmavonyan, Davit Khachatryan and G. Grigoryan

Poster B31 **Two-dimensional exciton spectrum in GaAs quantum well in tilted magnetic field**
E. A. Koval and O. A. Koval

Poster B32 **Cavity-enhanced frequency up-conversion in rubidium vapour**
R. F. Offer, J. W. C. Conway, E. Riis, S. Franke-Arnold and A. S. Arnold

Poster B33 **CPT Tests with protons and antiprotons**
G. Schneider, Hiroki Nagahama, Mustafa Besirli, Matthew Bohman, Matthias Borchert, James Harrington, Takashi Higuchi, Andreas Mooser, Natalie Schön, Stefan Sellner, Christian Smorra, Toya Tanaka, Klaus Blaum, Yasuyuki Matsuda, Christian Ospelkaus, Wolfgang Quint, Jochen Walz, Yasunori Yamazaki and Stefan Ulmer

Poster B34 **Notes on non-relativistic QED and Bethe logarithm**
D. Šimsa, J. Zamastil and V. Patkóš

Poster B35 **Electron collisions with selected hydrocarbons: relation between total cross section and physical properties of molecule**
Cz. Szmytkowski, S. Stefanowska, E. Ptasińska-Denga and P. Możejko

Poster B36 **Spectroscopy of trapped $^{138}Ba^{+}$ ions for atomic parity violation**
E. A. Dijck, N. Valappol, A. Hofsteenge, T. Meijknecht, L. Willmann and K. Jungmann

Poster B37 **Effect of confinement on the self-annihilation rate of positronium**
A. R. Swann, D. G. Green and G. F. Gribakin

Poster B38 **Many-body theory of positronium-atom scattering and pickoff annihilation**
D. G. Green, A. R. Swann and G. F. Gribakin

Poster B39 **Solution of Hartree-Fock equations in the B-spline basis**
David T. Waide, D. G. Green and G. F. Gribakin

Poster B40 **Radiative lifetimes of $HeLi^{+}(b^{3}\Sigma^{+})$**
Martina Zámečníková and P. Soldán

Poster B41 **Spectroscopy of ultracold dipolar $^{6}Li^{40}K$ molecules**
Sambit B. Pal, Mark Lam, Anbang Yang, Andrew Laugharn and Kai Dieckmann

Poster B42 **Stability of a frequency-comb-based transfer-lock using a passive Fabry-Perot resonator**
Sambit B. Pal, Mark Lam and Kai Dieckmann

Poster B43 **Experimental characterisation of the double minimum $3^{1}\Sigma_{u}^{+}$ state in Rb_2 up to the dissociation limit**
W. Jastrzebski, P. Kowalczyky and J. Szczepkowski

Poster B44 **X-Ray spectroscopy of the KLL-dielectronic recombination transitions with a Heidelberg compact EBIT**
P. Micke, S. Bernitt, S. Kühn, A. Surzhykov, T. Leopold, S. A. King, T. Pfeifer, P. O. Schmidt and J. R. Crespo López-Urrutia

Poster B45 **Single photon transient hot electron ionization of C_{60}**
K. Hansen and V. Zhaunerchyk

Poster B46 **EUV/SXR spectroscopy of Ge laser-produced plasma**
O. Maguire, D. Kos and E. Sokell

Poster B47 **Intra-cavity high-order harmonic generation for XUV spectroscopy of highly charged ions**
Janko Nauta, Andrii Borodin, Julian Stark, Peter Micke, Lisa Schmöger, Maria Schwarz, José R. Crespo López-Urrutia and Thomas Pfeifer

Poster B48 **Ultracold lithium for sympathetic cooling of dipolar molecules**
S. Wright, Thomas Wall and Michael Tarbutt

Poster B49 **Rydberg spectroscopy of ytterbium**
H. Lehec, A. Zuliani, W. Maineult, E. Luc-Koenig, P. Pillet and P. Cheinet

Poster B50 **Inverse crossover resonances applied to ^{171}Yb laser cooling**
J. J. McFerran, L. A. Salter and Emeric de Clercq

Poster B51 **Laser-induced fluorescence and optogalvanic spectroscopy used to find Landé g_J factors of La I**
Ł. M. Sobolewski, Laurentius Windholz and Jerzy Kwela

Session C (Thursday 16:30)

Poster C1 **Lifetimes and transition probabilities for high-lying levels in astrophysically interesting atoms using multi-photon excitation**
L. Engström, H. Lundberg, H. Nilsson and H. Hartman

Poster C2 **Probing variations of the fundamental constants with Cs clock referenced acetylene lines**
Florin Lucian Constantin

Poster C3 **Multifrequency generation with an ac-biased photomixer**
Florin Lucian Constantin

Poster C4 **Long term comparison between Raman atom interferometry based gravimeter and FG5 absolute gravimeter**
LingXiao Zhu, Anthony Rodgers, Victoria Smith, Graham Appleby, Yu-Hung Lien, Michael Holynski and Kai Bongs

Poster C5 **Ultrafast diffraction with cold electrons from laser-cooled atoms**
A. J. McCulloch, R. W. Speirs, D. Murphy, D. J. Thompson, J. Torrance, B. M. Sparkes and R. E.Scholten

Poster C6 **Towards an optical thermometer based on molecular spectroscopy to implement the new kelvin**
E. Moufarej, O. Kozlova, B. Darquie, S. K. Tokunaga, S. Briaudeau and C. Daussy

Poster C7 **Coherent and efficient microwave-to-optical conversion via six-wave mixing in Rydberg atoms**
Thibault Vogt, J. Han, C. Gross, D. Jaksch, M. Kiffner and W. Li

Poster C8 **Probing superfluidity in a quasi two-dimensional Bose gas through its local dynamics**
C. De Rossi, R. Dubessy, K. Merloti, M. de Goër de Herve, T. Badr, A. Perrin, L. Longchambon and H. Perrin

Poster C9 **Quantum chaos in ultracold collisions between Yb(^{1}S$_0$) and Yb(^{3}P$_2$)**
Dermot G. Green, Christophe L. Vaillant, Matthew D. Frye, Masato Morita and Jeremy M. Hutson

Poster C10 **Avoided crossings in near-threshold bound states of space-fixed dipoles**
John D. Reddel, Matthew D. Frye and Jeremy M. Hutson

Poster C11 **Imprinting knotted optical vortices onto atomic Bose-Einstein condensates**
S. A. Gardiner, I. G. Hughes and F. Maucher

Poster C12 **Strong coupling of a cold Potassium gas and a ring cavity**
R. Culver, A. Lampis, B. Megyeri, G. Harvie and Jon Goldwin

Poster C13 **Spin-orbit coupled interferometry with ring-trapped Bose-Einstein condensates**
J. L. Helm, T. P. Billam, A. Rakonjac, S. L. Cornish and S. A. Gardiner

Poster C14 **BOUND: a program for bound states of atomic and molecular pairs**
C. Ruth Le Sueur and Jeremy M. Hutson

Poster C15 **KCs: refinement of interaction potential and prediction of Feshbach resonances**
C. Ruth Le Sueur and Jeremy M. Hutson

Poster C16 **Theoretical study on the stability of a vortex ring in an axisymmetrically and harmonically trapped dipolar condensate**
I-Kang Liu (Gary) and Shih-Chuan Gou

Poster C17 **Control of quantum dynamics on an atom chip**
Cosimo Lovecchio, H.-V. Do and F. S. Cataliotti

Poster C18 **Probing correlations of cold-atom systems using multiple atomic impurities**
M. Streif, A. Buchleitner, D. Jaksch and J. Mur-Petit

Poster C19 **Phase profiles of atomic Bose-Einstein condensate mixtures**
K. L. Lee, I.-K. Liu, N. Jorgensen, L. Wacker, M. G. Skou, K. T. Skalmstang, J. J. Arlt and Nick Proukakis

Poster C20 **Decay of Josephson superflow via vortex-ring emission**
K. Xhani, K. L. Lee, L. Galantucci, C. F. Barenghi, A. Trombettoni, G. Valtolina, F. Scazza, A. Amico, C. Fort, M. Zaccanti, A. Burchianti, G. Roati, and Nick Proukakis

Poster C21 **Manipulating cold atoms with low frequency electromagnetic radiation**
G. A. Sinuco-Leon and B. M. Garraway

Poster C22 **Observation of attractive and repulsive polarons in a Bose-Einstein condensate**
N. B. Jørgensen, L. Wacker, K. T. Skalmstang, M. M. Parish, J. Levinsen, R. S. Christensen, G. M. Bruun and J. J. Arlt

Poster C23 **Spatially distributed multipartite entanglement and Einstein-Podolsky-Rosen steering of atomic clouds**
Philipp Kunkel, Maximilian Prüfer, Daniel Linnemann, Anika Frölian, Helmut Strobel, Thomas Gasenzer, Martin Gärttner and Markus K. Oberthaler

Poster C24 **Non-adiabatic quantum phase transition in a trapped spinor condensate**
Tomasz Świsłocki, E. Witkowska and M. Matuszewski

Poster C25 **Synthetic clock transitions and Rashba spin-orbit coupling**
Dimitris Trypogeorgos, Ana Valdés-Curiel, Nathan Lundblad and I. B. Spielman

Poster C26 **Spatial entanglement patterns and Einstein-Podolsky-Rosen steering in a Bose-Einstein condensate**
T. Zibold, M. Fadel, B. Décamps and P. Treutlein

Poster C27 **Study of ICD time evolution with THz - field - driven XUV streak camera**
F. Karimi, M. Pfau, M. Ranke, S. Walther, A. Dimitriou and U. Frühling

Poster C28 **4d - 4f photoabsorption in laser-produced thulium plasmas**
R. Stefanuik, E. Sokell, E. Long, P. Hayden and P. Dunne

Poster C29 **Photo-ionization in presence of circularly polarized fundamental and odd order harmonic fields**
I. A. Ivanov, Chang Hee Nam and Kyung Taec Kim

Poster C30 **Fano-CI method for decay widths of metastable excited states of atomic and molecular systems**
Pěemysl Kolorenč

Poster C31 **The ALPHA Experiment: Laser and microwave spectroscopy of antihydrogen atoms**
Daniel Maxwell and the ALPHA Collaboration

Poster C32 **Configuration interaction effects in unresolved** $n\mathrm{p}^6 n\mathrm{d}^{N+1}$ - $n\mathrm{p}^5 n\mathrm{d}^{N+2}$ + $n\mathrm{p}^6 n\mathrm{d}^N n\mathrm{f}^1$ **transition arrays: Contrasting behaviour for** $n = 4$ **and** $n = 5$
Luning Liu, Deirdre Kilbane, Padraig Dunne, John Sheil, Xinbing Wang and Gerry O'Sullivan

Poster C33 **Variation of the fine-structure constant and the electron-proton mass ratio in simple ions**
Natalia S. Oreshkina, Stefano M. Cavaletto, Niklas Michel, Christoph H. Keitel and Zoltán Harman

Poster C34 **High-density effects on the atomic structure and inner-shell transitions of astrophysical interest in oxygen ions**
J. Deprince, P. Palmeri, P. Quinet, S. Fritzsche, M. A. Bautista, C. Mendoza, T. R. Kallman and J. Garcia

Poster C35 **Theoretical insight into the atomic structure of neutral astatine, the rarest element on Earth**
P. Quinet and G. Sicorello

Poster C36 **High-precision relativistic calculations of isotope shifts in neutral antimony**
S. Gamrath, P. Palmeri, P. Quinet, S. Bouazza and M. R. Godefroid

Poster C37 **Electron-impact-induced long-chain modified arylpiperazine molecule fragmentation**
L. G. Romanova, V. S. Vukstich, A. V. Snegursky, A. V. Papp and T. A. Snegurskaya

Poster C38 **Structure and relative stabilities of chlorobenzene dications and trications produced by electron, proton and photon impact**
Wania Wolff, Benedikt Rudek, Woon Yong Baek, Felipe Fantuzzi and Marco A. C. Nascimento

Poster C39 **Ionization and fragmentation of building blocks of the DNA by electron, proton and nitrogen-ion impact**
Benedikt Rudek and WaniaWolff

Poster C40 **Ion desorption from nitrile-bearing astrophysical ice analogues studied by electron and heavy ion bombardment**
F. de A. Ribeiro, G. C. Almeida, W. Wolff, E. F. da Silveira, H. M. Boechat-Roberty and M. L. Rocco

Poster C41 **Population transfer in five level atoms**
E. Gazazyan

Poster C42 g **factor of lithium-like ions: Higher-order interelectronic-interaction effects**
D. A. Glazov, A. V. Volotka, V. M. Shabaev, I. I. Tupitsyn and G. Plunien

Poster C43 **Cross-relaxation studies with optically detected magnetic resonances in nitrogen - vacancy centres in diamond in external magnetic field**
Marcis Auzinsh, Andris Berzins, Laima Busaite, Ruvins Ferbers, Forian Gahbauer and Reinis Lazda

Poster C44 **Optically detected magnetic resonance studies of level anticrossing in nitrogen - vacancy centres in diamond crystals**
Marcis Auzinsh, Andris Berzins, Laima Busaite, Ruvins Ferbers, Forian Gahbauer and Reinis Lazda

Poster C45 **Shell model calculation of the atomic scattering factor in electric field**
S. Y. Yousif Al-Mulla

Poster C46 **STIRAP-like quantum search**
Nicholas Chancellor and Viv Kendon

Poster C47 **Adiabatic passage of Förster resonances for two-qubit gates and generation of Bell states of Rb and Cs atoms**
I. I. Beterov, G. N. Hamzina, M. Saffman, D. B. Tretyakov, V. M. Entin, E. A. Yakshina, S. Bergamini, E. A. Kuznetsova and I. I. Ryabtsev

Poster C48 **Hong-Ou-Mandel interference in an integrated quantum optical waveguide device**
V. Syvokon and Iryna Sharapova

Poster C49 **Theoretical study of Rydberg - EIT in thermal Rb atoms**
Arturs Cinins, T. Kirova, M. Auzinsh, Y. H. Chen and Ite. A. Yu

Poster C50 **Analytical evaluation of non-adiabaticity and efficiency of STIRAP using the saddle-point method**
Arturs Cinins, M. Bruvelis, D. K. Efimov, K. Miculis, N. N. Bezuglov and A. Ekers

Poster C51 **Toward optical detection of zero- and ultra-low field nuclear magnetic resonance**
S. Pustelny and P. Put

Magneto-optical trapping and sub-Doppler cooling of molecules.

S. Truppe, H. J. Williams, M. Hambach, L. Caldwell, N. J. Fitch, M. A. Trigatzis, J. Lim, J. R. Almond, E. A. Hinds*, B. E. Sauer and M. R. Tarbutt

Centre for Cold Matter, Imperial College London, SW7 2AZ, UK

Atomic physics has been revolutionised by the introduction of laser techniques to cool atoms far below the Doppler limit. Now, it has become possible to laser cool molecules, to collect them in a magneto-optical trap, to cool them below the Doppler limit [1] and to trap them with modest magnetic fields. These ultracold molecules open up a wide vista of future applications. To give a few examples, they can be optically or magnetically trapped to form arrays for quantum simulation, they can make a molecular fountain for testing fundamental physics at unprecedented levels of sensitivity, and they open a new energy range for the study of ultracold collisions and ultracold chemistry. I will review the current status of this field.

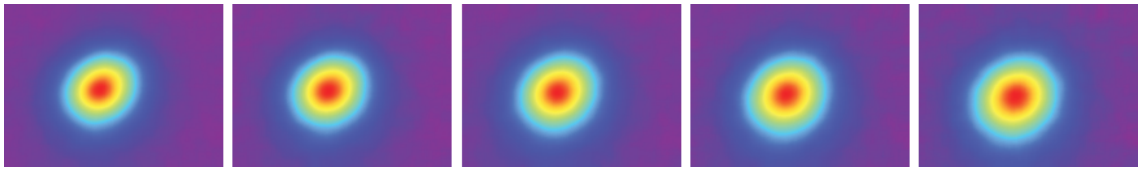

Fig. 1: Images of a CaF cloud expanding freely after cooling to 52(2) μK [1].

References

[1] S. Truppe *et al.*, arXiv:1703.00580v1

*Corresponding author: ed.hinds@imperial.ac.uk

To the list of contents

Near-optimal atom-photon interfaces in the solid-state

Pascale Senellart[*1]
1. Centre for Nanoscience and Nanotechnology – C2N – CNRS - UMR9001
Route de Nozay, 91460 Marcoussis, France

Today, optical quantum technologies are limited both by the low efficiency of heralded single-photon sources and by the probabilistic operation of two-photon gates. Deterministic sources and gates can in principle be obtained making use of the single-photon sensitivity of an atomic transition. In this context, artificial atoms in the form of semiconductor quantum dots have emerged as a promising system to scale up optical quantum technologies, offering the potential of integration and scalability.

In this talk, we will review our recent progresses along this research line. We will discuss how a single quantum dot can be positioned in an optical cavity in a fully controlled way, so as to control its spontaneous emission on demand [1-2]. Close to ideal atom-photon interfaces are obtained, where a single quantum dot interacts with a single mode of the optical field and is largely isolated from all sources of decoherence [3].
These systems are shown to be bright single-photon sources with single photon purity and indistinguishability exceeding 99%. The brightness of the sources exceeds by a factor 20 the one of currently used sources based on parametric down conversion [4-5]. We have also made progresses toward the development of deterministic two-photon gates [6], with devices performing as nonlinear switches at the single-photon level, converting a coherent pulse into a highly non-classical light wave-packet [7].

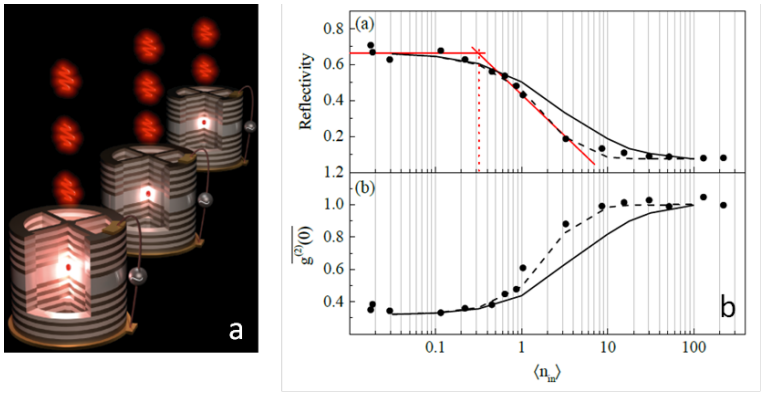

Fig. 1: (a) Artist view of the quantum-dot cavity devices performing as near optimal atom-photon interfaces. (b) Reflectivity (top) and second order intensity correlation function (bottom) of the directly reflected light as a function of the incident photon number (pulsed excitation).

References

[1] A. Dousse et al. , Phys. Rev. Lett. 101, 267404 (2008)
[2] A. Nowak et al., Nature Communications 5, 3240 (2014)
[3] V. Giesz et al., Nature Communications 7, 11986 (2016)
[4] N. Somaschi, et al., Nature Photonics 10, 340 (2016)
[5] J. Loredo et al., Optica 3, 433 (2016)
[6] A. Arnold, et al., Nature Communications 6, 6236 (2015)
[7] L. De Santis et al., arXiv:1607.05977, To appear in Nature Nanotechnology

*Corresponding author: pascale.senellart-mardon@u-psud.fr

To the list of contents

Fast Ion Beams Stored in Cryogenic Low-Density Environment: Collision Experiments and Low-Energy Internal Excitations

Andreas Wolf*
for the CSR team
Max-Planck-Institut für Kernphysik, Saupfercheckweg 1, 69117 Heidelberg, Germany

Internal structures and excitations of atomic, molecular and cluster ions are sensitively probed by their collisions and reactions. An important class of these reactions – such as ion–neutral reactions, dissociative recombination with electrons, or electron emission from molecular and cluster anions – leads to neutral products. These products are difficult to access with stationary targets. However, fast ion beams offer powerful single-particle detection methods by which neutral daughter products can be observed. The use of these efficient detection methods on the binary interactions of stored and possibly state-controlled particles is a main motivation behind the development of storage rings for atomic, molecular and cluster ions. In particular, electrostatic storage rings [1, 2] were developed for complex, heavy ionic species with energies in the multi-keV range.

Both the ion storage conditions and the control over the internal ionic excitations can be much improved by setting up cryogenic electrostatic storage rings. Devices of this type recently started operation at three laboratories world-wide [3, 4, 5]. In this talk, we present the Cryogenic Storage Ring (CSR) realized at the Max Planck Institute for Nuclear Physics in Heidelberg, Germany [5]. It is built to accept ion beams (cations and anions) of kinetic energy up to 300 keV per ionic charge and stores these ions on a 35 m long closed orbit. The ion orbit encompasses four 2 m long, field-free straight sections for collision experiments. The ion energy is high enough to enable experiments with a merged electron beam at matched electron and ion velocities, even for polyatomic molecules. Correspondingly, it is envisaged that phase-space cooling of such molecular ion beams will be possible (envisaged mass limit $\sim$160 u per ionic charge). Multi-particle coincidence detectors operated downstream of the merged-beam zones offer the detection of neutral products and to include them in the analysis of the collision kinematics.

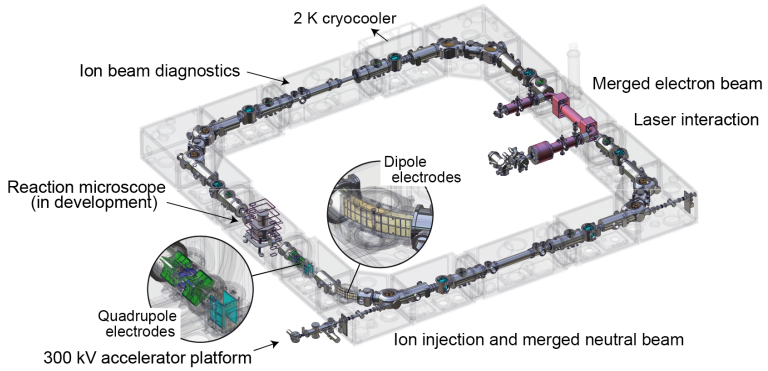

Fig. 1: Overview of the Cryogenic Storage Ring CSR (closed orbit circumference: 35 m).

The CSR was operated successfully at vacuum chamber temperatures of 6 K and ion beam storage time constants up to 45 min [5]. Moreover, it was used for experiments on resonant photodissociation of cations (CH^+ [6]) and near-threshold photodetachment of anions (OH^- [7]). In both cases, the rotational levels radiatively cooled towards a population dominated by $J = 0$. Photodissociation and photodetachment cross-sections as well as radiative lifetimes were investigated on the rotationally cold ions, stored in empty space without buffer gas over times of up to 20 min. Presently, merged-beams reaction zones with electrons and neutral atoms are taken into operation. The talk will present the performance of the CSR, results of first experiments at the facility and the progress of recent experiments using laser and merged particle beam interactions.

References

[1] S. Pape Møller and U.V. Pedersen, Phys. Scr. **T92**, 105 (2001).
[2] H. T. Schmidt, Phys. Scr. **T166**, 914063 (2015).
[3] H. T. Schmidt *et al.*, Rev. Sci. Instrum. **84**, 055115 (2013).
[4] Y. Enomoto *et al.*, J. Phys. Conf. Proc. **635**, 022028 (2015).
[5] R. von Hahn *et al.*, Rev. Sci. Instrum. **87**, 063115 (2016).
[6] A. O'Connor *et al.*, Phys. Rev. Lett. **116**, 113002 (2016).
[7] C. Meyer *et al.*, in preparation.

*Corresponding author: a.wolf@mpi-hd.mpg.de

To the list of contents

Testing the Universality of Free Fall with Bragg atom interferometer

M. K. Zhou[*1], **K. Zhang**[1], **Y. Cheng**[1], **L. L. Chen**[1], **L. S. Cao**[1], **Z. K. Hu**[†1]
1. MOE Key Laboratory of Fundamental Physical Quantities Measurements, School of Physics, Huazhong University of Science and Technology, Wuhan 430074, People's Republic of China

The validity of universality of free fall (UFF), as one of the fundamental postulations of General Relativity (GR), has excited a huge amount of experiments under various circumstances to search for the sign of the extended GR theory. We have performed a precision atomic interferometry experiment on testing the UFF considering atoms' spin degree of freedom. Our experiment employs the Bragg atom interferometer with ^{87}Rb atoms in different spin states of $|F=1,m_F=0\rangle$ and $|F=2,m_F=0\rangle$, and both the wave packets in these two states are diffracted in one pair of Bragg beams, which can help suppress the common-mode systematic errors. We have obtained an Eötvös ratio $\eta=(-2.8\pm4.2)\times10^{-9}$, and set a new record on the precision with a nearly 30 times improvement. Our experiment gives stronger restrictions on the possible UFF breaking mechanism. The new scheme also possesses a potential to improve various quantum tests of the UFF, e.g. with different species and search for possible spin-gravity couplings.

References

[1] Z. K. Hu, B. L. Sun, X. C. Duan, M. K. Zhou, L. L. Chen, S. Zhan, Q. Z. Zhang, and J. Luo, Phys. Rev. A **88**, 043610 (2013).
[2] X. C. Duan, X. B. Deng, M. K. Zhou, K. Zhang, W. J. Xu, F. Xiong, Y. Y. Xu, C. G. Shao, J. Luo, and Z. K. Hu, Phys. Rev. Lett. **117**, 023001 (2016).

[*]Corresponding author: zmk@hust.edu.cn
[†]Corresponding author: zkhu@mail.hust.edu.cn

To the list of contents

Coherence of an Interacting Ultra-Cold Atomic Ensemble in a Trapped Matter-Wave Sensor

Alexis Bonnin[*1], **X. Alauze**[1], **C. Solaro**[1], **F. Combes**[2], **J. N. Fuchs**[2,3], **F. Piéchon**[2], **F. Pereira dos Santos**[†1]

1. SYRTE, Observatoire de Paris, PSL Research University
CNRS, Sorbonne Université, UMPC Univ. Paris 06, LNE
61 avenue de L'observatoire, 75014 Paris, France
2. Laboratoire de Physique des Solides, CNRS UMR 8502
Univ. Paris-Sud, Univ. Paris-Saclay
F-91405 Orsay CEDEX, France
3. Laboratoire de Physique Théorique de la Matière Condensée
CNRS UMR 7600, Univ. Pierre et Marie Curie,
4 place Jussieu, 75252 Paris CEDEX 05, France

The FORCA-G project aims to develop a quantum-sensor for probing short range forces, *i.e* forces at a length scale of typically few micrometers. The sensor relies on a trapped atom interferometer using an ultra-cold ensemble of ^{87}Rb trapped in a vertical optical lattice ($\lambda = 532$nm). For shallow depths of the lattice, stimulated Raman transitions are used to induce a coherent coupling between different lattice sites, allowing us to realize atom interferometers capable of probing with very high sensitivity and accuracy the local potential experienced by the atoms. By using a symmetrized Ramsey-Raman interferometer, our force quantum-sensor reaches a state-of-the-art relative sensitivity of 1.8×10^{-6} at 1 s on the Bloch frequency, and thus on the local gravitational field [1][2].

In a recent work [3], we studied the impact of atomic interactions arising from the use of a dense and small ultra-cold atomic ensemble as a source for our trapped interferometer. The purpose of using such an atomic source is to reduce inhomogeneous dephasing and to obtain better addressability of the lattice sites and ultimately to populate only one of them. At densities of typically 10^{12} atoms/cm^3, we observe an unexpected behavior of the contrast of Ramsey interferometers, when applying a π-pulse to symmetrize the interferometer. These results are interpreted as a competition between the spin-echo technique and a spin self-rephasing (SSR) mechanism based on the identical spin rotation effect (ISRE [4]), see Fig.1. Originating from particle indistinguishability, SSR has been observed in trapped atomic clocks, where it can enhance the clock's coherence up to several seconds [5][6]. The study of these mechanisms due to atomic interactions seems thus to be of great interest for metrology and for developing more compact quantum-sensors based on trapped atomic ensembles, and capable of probing the external fields experienced by the atoms with a spatial resolution better that 1μm.

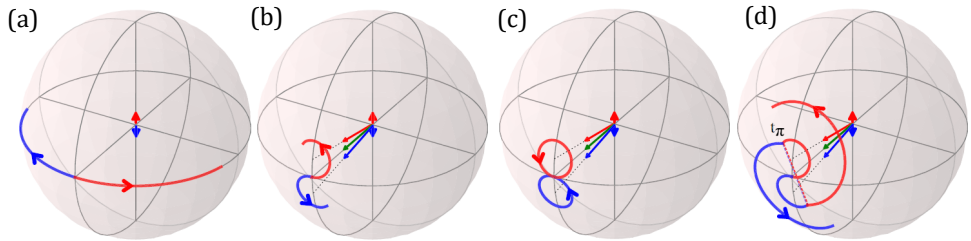

Fig. 1: *Competition between Spin Echo and Spin Self-Rephasing*. The atomic population is divided into two equal classes of hot (red) and cold (blue) atoms that are represented by their macrospins trajectories on the Bloch sphere. After the first $\pi/2$-pulse of the Ramsey sequence, the two macrospins are in the equatorial plane. (a) Inhomogeneous dephasing acts as a torque pointing in the vertical direction that is of opposite sign for the two classes of atoms (red and blue short arrows). (b) With the ISRE, the effective magnetic field seen by the atoms is the sum of the inhomogeneity and the exchange mean field proportional to the total spin (green arrow). As a consequence, the hot (cold) macrospin precesses around the red (blue) long arrow, so that if no π-pulse is applied they rephase at certain time T_{ex}: this is the SSR (c). If one applies a π-pulse when the two macrospins are out of the equatorial plane the rephasing is degraded (d).

References

[1] B . Pelle et al. "State-labeling Wannier-Stark atomic interferometers", Phys. Rev. A **87**, 023601 (2013).
[2] A . Hilico et al., "Contrast decay in a trapped-atom interferometer", Phys. Rev. A **91**, 053616 (2015).
[3] C . Solaro et al., "Competition between Spin-Echo and Spin Self-Repahsing in a Trapped Atom Interferometer", Phys. Rev. Lett. **117**, 163003 (2016).
[4] C . Lhuillier and F. Laloë, "Transport properties in a spin polarized gas, I", J. Phys. (Paris) **43**, 197 (1982).
[5] C . Deutsch et al., "Spin self-rephasing and very long coherence times in a trapped atomic ensemble", Phys. Rev. Lett. **105**, 020401 (2010).
[6] G . Kleine Büning et al., "Extended Coherence Time on the Clock Transition of Optically Trapped Rubidium", Phys. Rev. Lett. **106**, 240801 (2011).

[*]Corresponding author: alexis.bonnin@obspm.fr
[†]Corresponding author: franck.pereira@obspm.fr

To the list of contents

Experimental constraints on non-Newtonian gravity via state of the art photoassociation spectroscopy

Mateusz Borkowski[1], **Alexei A. Buchachenko**[2], **Roman Ciuryło**[1], **Paul S. Julienne**[3], **Hirotaka Yamada**[4], **Kikuchi Yuu**[4], **Kekaru Takahashi**[4], **Yosuke Takasu**[4], **Yoshiro Takahashi**[4,5]

1. Institute of Physics, Faculty of Physics, Astronomy and Informatics, Nicolaus Copernicus University, Grudziadzka 5, 87-100 Torun, Poland
2. Skolkovo Institute of Science and Technology, 100 Novaya Street, Skolkovo, Moscow Region, 143025, Russia
3. Joint Quantum Institute, National Institute of Standards and Technology and the University of Maryland, 100 Bureau Drive, Stop 8423, Gaithersburg, Maryland 20899-8423, USA
4. Department of Physics, Graduate School of Science, Kyoto University, Kyoto 606-8502, Japan
5. CREST, Japan Science and Technology Agency, Chiyoda-ku, Tokyo 102-0075, Japan

Deviations from the universal inverse-square law of gravitation have in recent decades been the subject of considerable experimental effort [1]. Corrections to the Newtonian law have been predicted by several extensions to the Standard Model of particle physics [2], where additional forces would appear due to the exchange of light bosons. Also, attempts at solving the hierarchy problem using extra dimensions (see e.g. [3]) also predict deviations from the $-1/R^2$ behavior at submillimeter scale. Experiments aim to constrain the magnitude of these deviations by providing limits on the magnitude α of the Yukawa-type form of the gravitational potential $V(R) = -G\frac{m_1 m_2}{R}(1+\alpha\exp(-R/\lambda))$ as a function of its range λ.

While the inverse-square gravitational interaction is well confirmed at macroscopic scales, for nanometers the current best constraints on α, are over *twenty* orders of magnitude larger than gravity itself. Such constraints are mostly provided by measurements of neutron scattering and of Casimir-Polder forces and only recently a new scheme using precise transition measurements in the H_2 molecule has been proposed. We propose a scheme based on the mass scaling behavior of photoassociation (PA) line positions. We have measured a total of 13 PA lines for three isotopes of the Yb_2 molecule. To achieve high precision, the measurements were performed using the Raman scheme in a Bose-Einstein condensate of Yb atoms (see Fig. 1, left). Systematic shifts have been eliminated by extrapolation (Fig. 1, right) leading to an unprecedented experimental accuracy of ≈ 500 Hz.

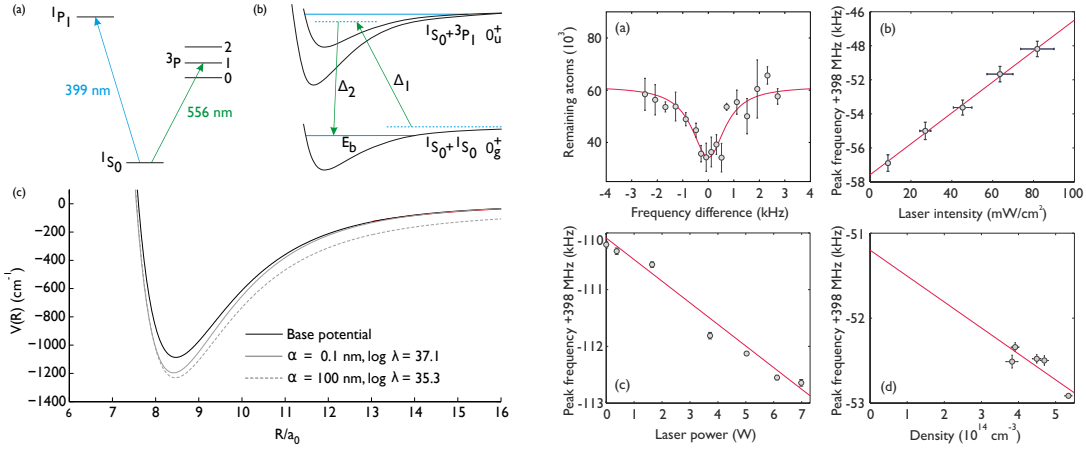

Fig. 1: Left: (a) transitions used in the experiment, (b) two-color photoassociation spectroscopy in Raman configuration, (c) impact of the Yukawa-modified gravitational potential on the atomic interaction. **Right:** High precision photoassociation spectroscopy. (a) An example Raman PA lineshape with FWHM $\approx$ 1 kHz, (b-d) extrapolation of systematic shifts caused by PA light shift, trapping laser light shift, and atomic density, respectively.

We calculate the theoretical line positions using an *ab initio*-based potential. The long range parameters and a short range 'quantum defect' of the potential are fitted to the PA data using least-squares to obtain a mass scaled model [4]. Incorporating the beyond-Born-Oppenheimer effects [5] into the model enabled us to achieve mass scaling to an accuracy of about 20 kHz. Finally, the non-Newtonian gravitational interaction is added. The value of α where the model loses its accuracy despite continued fitting is our experimental constraint on non-Newtonian gravity. Even though this is a proof of concept determination, our limits are already nearly on par with the best constraints provided by competing mature methods.

References

[1] E. G. Adelberger, B.R. Heckel, and A. E. Nelson, Annu. Rev. Nucl. Part. Sci. **53**, 77 (2003).
[2] J. E. Kim, Phys. Rep. 150, **1** (1987).
[3] N. Arkani-Hamed, S. Dimopoulos, and G. Dvali Phys. Rev. D **59**, 086004 (1999)
[4] M. Borkowski, *et al.* Phys. Rev. A **88**, 052708 (2013)
[5] J. J. Lutz, J. M. Hutson, J. Mol. Spectr. **330**, 43-56 (2016)

To the list of contents

Superconducting circuits for detecting and manipulating spins in solids

C. Grèzes[1] A. Bienfait[1], J. Pla[2], Y. Kubo[1], D. Vion[1], D. Esteve[1], B. Julsgaard [3], K. Moelmer [3], J. Isoya [4], J. J. L. Morton[2], and P. Bertet*[1]

1. Quantronics group, SPEC, CEA, CNRS, Université Paris-Saclay, CEA Saclay, 91191 Gif-sur-Yvette, France
2. London Centre for Nanotechnology, University College London, London WC1H 0AH, UK
3. Department of Physics and Astronomy, Aarhus University, Ny Munkegade 120, Aarhus C DK-8000, Denmark.
4. Research Center for Knowledge Communities, University of Tsukuba, Tsukuba 305-8550, Japan

The detection of spins in solids or biological materials by electron-spin resonance (ESR) spectroscopy has numerous applications in material science and biology. Besides, dilute spins in solids have long quantum coherence time, which makes them promising candidates for storing quantum information. In our laboratory, we use superconducting circuits to try to store and retrieve quantum information in spin ensembles, as well as to increase the ESR sensitivity and detect as few spins as possible. In this presentation, we will first show how a superconducting resonator can be strongly coupled to a spin ensemble [1], and how quantum information can be stored in and retrieve from the ensemble [2] [3] using circuits combining superconducting resonators and a Josephson quantum bit (see Fig. 1). In a second part, we will show how using the tools offered by circuit Quantum Electrodynamics (QED), namely high quality factor superconducting resonators and Josephson parametric amplifiers that operate at the quantum limit, we increase the sensitivity of ESR by four orders of magnitude over the state-of-the-art [4]. Finally, we will show how the energy relaxation time of the spins can be limited by spontaneous emission of microwave photons through the resonator, which opens the way to on-demand spin initialization via Purcell effect [5].

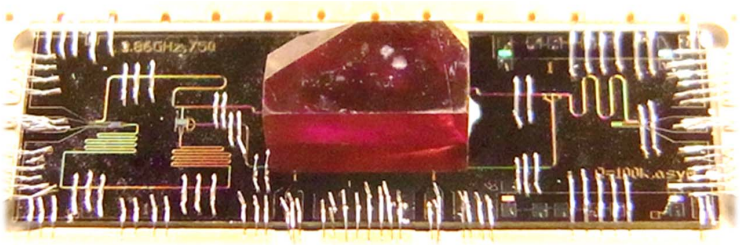

Fig. 1: Hybrid circuit with superconducting resonators and qubits coupled to an ensemble of NV centers in diamond.

References

[1] Y. Kubo et al., Phys. Rev. Lett. 105, 140502 (2010).
[2] Y. Kubo et al., Phys. Rev. Lett. 107, 220501 (2011).
[3] C. Grezes et al., Phys. Rev. A 92, 020301 (2015).
[4] A. Bienfait et al., Nature Nanotechnology 11, 253 (2016).
[5] A. Bienfait et al., Nature 531, 74 (2016).

*Corresponding author: patrice.bertet@cea.fr

To the list of contents

Experimental signatures of an absorbing-state phase transition in a cold Rydberg gas

C. Simonelli[1,2], M. Archimi[2], F. Castellucci[2], E. Arimondo[1,2], D. Ciampini[1,2], R. Gutierrez[3,4], M. Marcuzzi[3,4], I. Lesanovsky[3,4], O. Morsch*[1,2]

1. INO-CNR, Via G. Moruzzi 1, 56124 Pisa, Italy
2. Dipartimento di Fisica "E. Fermi", Università di Pisa, Largo Bruno Pontecorvo 3, 56127 Pisa, Italy
3. School of Physics and Astronomy, University of Nottingham, Nottingham, NG7 2RD, UK
4. Centre for the Mathematics and Theoretical Physics of Quantum Non-Equilibrium Systems, University of Nottingham, Nottingham, NG7 2RD, UK

Phase transitions in non-equilibrium systems have been extensively studied in recent years but continue to pose challenges. One example of such a phase transition is that between a non-fluctuating absorbing phase [1], e.g., an extinct population, and one in which the relevant order parameter, such as the population density, assumes a finite value. Here we report the observation of signatures of such a non-equilibrium phase transition in an open driven quantum system. In our experiment rubidium atoms in a quasi one-dimensional cold disordered gas are excited to Rydberg states under so-called facilitation conditions [2]. This conditional excitation process (which in the present work occurs in the incoherent regime and can thus be described by a rate equation) competes with spontaneous decay (see Fig. 1a) and leads to a crossover between a stationary state with no excitations and one with a finite number of Rydberg excitations. This crossover can be seen in the phase diagram of Fig. 1b, where the number of Rydberg excitations is plotted as a function of the driving strength and detuning from resonance for a system initially prepared in a state with a fixed number of seed excitations [3]. We relate the underlying physics to that of an absorbing state phase transition in the presence of a field which slightly offsets the system from criticality. We observe a characteristic power-law scaling of the Rydberg excitation density as well as increased fluctuations close to the transition point. Furthermore, we argue that the observed transition relies on the presence of atomic motion (due to the finite temperature of the atomic cloud) which introduces annealed disorder into the system and thus enables the formation of long-ranged correlations. Our study paves the road towards future investigations into the largely unexplored physics of non-equilibrium phase transitions in open many-body quantum systems. The experimental realization of such systems presented here promises to be a versatile platform for investigations both in the semi-classical (incoherent) and in the quantum (coherent) regime.

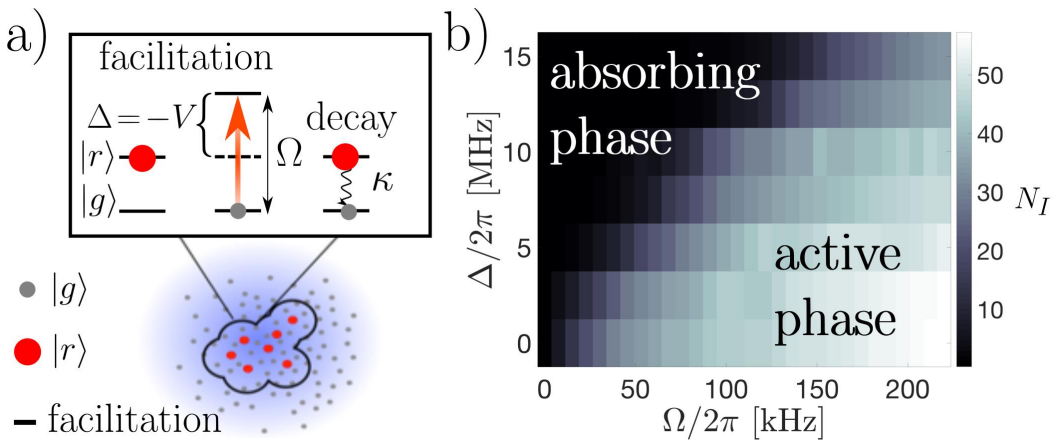

Fig. 1: (a) Microscopic processes leading to an absorbing state phase transition in a gas of cold Rydberg atoms with ground state $|g\rangle$ and excited state $|r\rangle$: facilitation (characterized by the van der Waals interaction $-V$ matching the detuning Δ for off-resonant excitation) and decay at rate κ. (b) Phase diagram of the experimental system: stationary number of Rydberg excitations N_I versus driving frequency Ω and detuning Δ.

References

[1] H. Hinrichsen, Adv. Phys. **49**, 815 (2000)
[2] N. Malossi, M. M. Valado, S. Scotto, P. Huillery, P. Pillet, D. Ciampini, E. Arimondo, and O. Morsch, Phys. Rev. Lett. **113**, 023006 (2014)
[3] M. Marcuzzi, E. Levi, W. Li, J. P. Garrahan, B. Olmos, and I. Lesanovsky, New J. Phys. **17**, 072003 (2015).

*Corresponding author: morsch@df.unipi.it

To the list of contents

A Rydberg-dressed magneto-optical trap

A.D. Bounds, N.C Keegan* **R.K. Hanley, R.F. Faoro, E.M. Bridge, P. Huillery, M.P.A. Jones.**[1]
1. Joint Quantum Centre (JQC) Durham–Newcastle, Department of Physics, Durham University
South Road, Durham DH1 3LE, UK

The strong dipolar interactions between Rydberg atoms have been exploited to perform numerous experimental studies of interacting many-body systems. A promising approach to create an interacting many-body quantum gas with tunable interactions is to off-resonantly couple a low-lying atomic state to a Rydberg state [1,2]. It has been shown that this so-called Rydberg dressing approach could facilitate the formation of interesting states of matter, such as supersolids [3,4]. Recently, experimental work has demonstrated the tunability of the Rydberg-dressed interaction in optical lattices [5,6], however the effect of these interactions in a randomly distributed ensemble are yet to be observed. Here we present a novel Rydberg-dressing experiment where the excited state of a narrow-line strontium MOT is coupled off-resonantly to a high-lying Rydberg state, producing an operational MOT with measurable Rydberg character. This is supported by a quantitative Monte-Carlo model of the MOT. We are able to measure the Rydberg character of the MOT through its sensitivity to an applied electric field, which without the Rydberg admixture would be nonexistent. Here we present recent experiments which strive to observe a mechanical effect of the long-range dressed interactions in a laser-cooled gas.

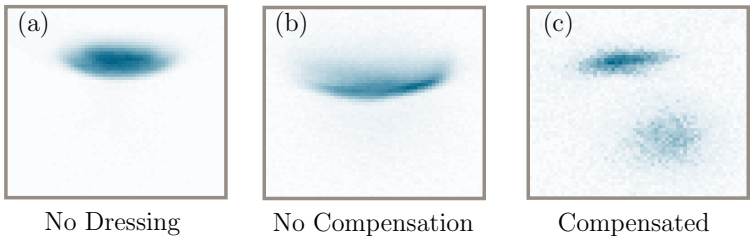

Fig. 1: MOT images after 10ms of dressing at different values of coupling beam Rabi frequency and MOT beam detunings. The coupling beam is detuned +12MHz from resonance. (a) MOT image in the absence of the coupling laser with a MOT beam detuning of −110kHz. (b-c) MOT image in the presence of the coupling beam with 4MHz Rabi frequency and MOT beam detuning of −110kHz and +190kHz respectively. The presence of the coupling beam causes an AC Stark shift of the MOT transition. If the MOT beam detuning remains unchanged (b), the MOT moves to a lower position. By compensating the AC Stark shift (c), the atoms remain in the coupling beam resulting in a functioning dressed MOT.

References

[1] L. Santos *et al.*, Phys. Rev. Lett. **85**, 1791 (2000).
[2] I. Bouchoule and K. Mölmer, Phys. Rev. A **65**, 041803 (2002)
[3] N. Henkel, R. Nath, and T. Pohl, Phys. Rev. Lett. **104**, 195302 (2010).
[4] G. Pupillo *et al.*, Phys. Rev. Lett. **104**, 223002 (2010).
[5] Y. Y. Jau *et al.*, Nat. Phys **12**, 71 (2015)
[6] J. Zeiher *et al.*, Nat. Phys **12**, 1095 (2016)

*Corresponding author: n.c.keegan@dur.ac.uk

To the list of contents

Quantum gas microscopy of spatial correlations in attractive and repulsive Fermi-Hubbard systems

P. Schauss[1], D. Mitra[1], P. T. Brown[1], E. Guardado-Sanchez[1], S. S. Kondov[1], E. Khatami[2], T. Paiva[3], N. Trivedi[4], T. Devakul[1], D. A. Huse[1], and W. S. Bakr*[1]

1. Department of Physics, Princeton University
Jadwin Hall, Princeton, NJ 08544, USA
2. Department of Physics and Astronomy, San Jose State University
San José, CA 95192, USA
3. Instituto de Fisica, Universidade Federal do Rio de Janeiro
Caixa Postal 68.528, 21941-972 Rio de Janeiro RJ, Brazil
4. Department of Physics, The Ohio State University
Columbus, OH 43210, USA

Quantum gas microscopes have taken the study of Hubbard physics in optical lattices to a new level, enabling site-resolved detection of strongly correlated states like Mott insulators and antiferromagnets. We present two experiments using a lithium-6 quantum gas microscope to study the Hubbard model in new regimes. In a first experiment, we investigate the spin correlations of the repulsive Hubbard model in the presence of spin-imbalance [1]. We observe short-range canted antiferromagnetism by measuring the anisotropy of spin correlations in two bases. In addition we find non-monotonic behavior of the spin polarization with doping resembling the behavior of the magnetic susceptibility in the cuprates.

In another experiment, we observe charge density wave correlations in the attractive Hubbard model at half filling [2]. These correlations provide a low-temperature thermometer for the attractive Hubbard model and constitute a lower bound on superfluid correlations in this system.

Our measurements on Fermi-Hubbard physics in the presence of spin-imbalance and doping challenge state-of-the-art numerical methods and contribute to the understanding of the low-temperature physics in these systems. The combination of spin-imbalance with attractive interactions will enable the search for signatures of non-zero momentum superfluids using quantum gas microscopy.

References

[1] P. T. Brown, D. Mitra, E. Guardado-Sanchez, P. Schauss, S. S. Kondov, E. Khatami, T. Paiva, N. Trivedi, D. A. Huse, and W. S. Bakr, arXiv:1612.07746 (2016)
[2] D. Mitra, P. T. Brown, E. Guardado-Sanchez, S. S. Kondov, T. Devakul, D. A. Huse, P. Schauss, and W. S. Bakr, in preparation.

*Corresponding author: wbakr@princeton.edu

To the list of contents

Attosecond physics and the dream of an electron movie

E. Lindroth[*1]
1. Department of Physics, Stockholm University, AlbaNova University Center, SE-106 91 Stockholm, Sweden

Advances in laser technology have made it possible to produce light-pulses with a duration as short as around hundred attoseconds. Since this is the time scale of electron dynamics it opens the exciting possibility to follow electron motion in the time domain. Interesting scenarios could be to follow it during a chemical reaction, or for a molecular break-up processes, during the charge-migration that is taking place before nuclear motion sets in. The methods to make this dream come true are still in a rapid development phase.

The dynamics, during for example a photoionization process, is encoded in the amplitude and *phase* of the released electron wave packet. A key quantity is the spectral derivative of this phase, the *group delay*. It reflects the delay or advance of the electron when it travels through the atomic potential to eventually emerge in the continuum: attosecond interferometric techniques have made such phase information obtainable.

During the last decade a number of photo-emission delay studies have been done showing for example distinct delay differences for different atomic orbitals [1-2], or for different bands in solids [3]. In the latter case these differences are giving information on the electron-transport dynamics towards the surface. More recently structures in the continuum such as Cooper minima and resonances [4-6], with rapid spectral phase variations, have been under investigation. In the talk I will discuss some of the experimental methods that have been developed, the role of theory[7], and how we can understand the time-domain measurement that has been performed for a basic processes such as photoionization.

References

[1] M. Schultze*et al.*, Science **328**, 16581 (2010).
[2] K. Klünder *et al.*, Phys. Rev. Lett. **106**, 143002 (2011).
[3] A. L. Cavalieri *et al.*, Nature **449**, 1029 (2007).
[4] M. Kotur *et al.*, Nat. Commun. **7**, 10566 (2016).
[5] V. Gruson *et al.*, Science **354**, 734 (2016).
[6] M. Sabbar *et al.*, Phys. Rev. Lett. **115**, 133001 (2015)
[7] J. M. Dahlström and E. Lindroth, J. Phys. B: At. Mol. Opt. Phys. **47**, 124012 (2014)

[*]Corresponding author: Eva.Lindroth@fysik.su.se

To the list of contents

Imaging ultrafast molecular wave-packets with a single chirped UV pulse

D. Jelovina[1], **J. Feist**[2,3], **F. Martín**[1,3,4], **A. Palacios**[*1]

1. Departamento de Química, Universidad Autónoma de Madrid, 28049 Madrid, Spain
2. Departamento de Física Teórica de la Materia Condensada, Universidad Autónoma de Madrid, 28049 Madrid, Spain
3. Condensed Matter Physics Center (IFIMAC), Universidad Autónoma de Madrid, 28049 Madrid, Spain
4. Instituto Madrileño de Estudios Avanzados (IMDEA) en Nanociencia, 28049 Madrid, Spain

Free-electron-laser facitilites and high-harmonic generation techniques implemented in tabletop setups can nowadays provide intense ultrashort UV pulses with durations in the femtosecond and attosecond range [1][2]. These pulses allow for monitoring and manipulating electron dynamics in matter at its intrinsic time scale. One of the primary goals of attosecond science is to use UV-pump / UV-probe schemes [3][4][5], where one pumps an atom (molecule), creating a superposition of electronic (vibronic) states whose field free evolution is captured by a second UV pulse. Because of technical challenges, these schemes have proven elusive due to the still low intensities that can be reached nowadays in the laboratory and due to difficulties in producing two independent ultrashort pulses with well-controlled time delays. Therefore, most of the existing experiments have been performed combining a UV ultrashort pulse with an IR field. The latter distorts the potential created by the electrons and nuclei of the isolated system itself, and therefore leads to the observation of IR-induced dynamics more than probing the UV-pumped ultrafast dynamics. In the present work, we propose an alternative approach: the use of a single chirped UV pulse, which can be realized in a lab, to emulate a conventional UV-UV pump-probe scheme [6].

We demonstrate that by tuning a single parameter, the spectral chirp of an ultrashort UV pulse, we can achieve a significant amount of control over molecular multiphoton ionization, changing the total ionization yield by more than a factor of ten. In addition, we show how it is possible to emulate a standard pump-probe setup to obtain direct time-resolved imaging of ultrafast molecular dynamics. The vibronic (vibrational+electronic) wave packet pumped in the singly excited molecule can be simultaneously probed through the ionization fragments generated by the same pulse. The chirp is the parameter that encodes the time delay between the pump and probe frequencies. We choose a quadratic frequency chirp, which is experimentally achievable even in broadband pulses with Fourier-limited durations as short as a few hundreds of attoseconds [2][7][8], and perform ab initio simulations on the H_2^+ molecule.

The full-dimensional time-dependent Schrödinger equation is solved numerically, using a finite element discrete variable representation [9] for the molecular wave function, including both electronic and nuclear degrees of freedom. We also introduce a sequential model to demonstrate the direct mapping of the pumped wave packet into the energy distribution of the charged fragments after the Coulomb explossion of the molecule [6]. Although we employ the H_2^+ molecule as benchmark target, the method should also be suitable to probe wave packet dynamics in more complex molecules.

References

[1] F. Krausz and M. Ivanov *Rev. Mod. Phys.* **81** 163 (2009).
[2] C. Bostedt *et al. Rev. Mod. Phys.* **88** 015007 (2016).
[3] P. Tzallas, E. Skantzakis, L. A. A. Nikolopoulos, G. D. Tsakiris and D. Charalambidis *Nat. Phys.* **7** 781 (2011).
[4] M. Wöstmann, R. Mitzner, T. Noll, S. Roling, B. Siemer, F. Siewert, S. Eppenhoff, F. Wahlert and H. Zacharias *JPB* **46** 164005 (2013).
[5] F. Campia *et al. Rev. Sci. Inst.* **87** 023106 (2016).
[6] D. Jelovina, J. Feist, F. Martín and A. Palacios **arXiv:1702.05269** (2017)
[7] Z. Chang *Phys. Rev. A* **71** 023813 (2005).
[8] M. Hofstetter *et al. Opt. Expr.* **19** 1767 (2011).
[9] A. Palacios, C. W. McCurdy and T. N. Rescigno *Phys. Rev. A* **76** 043420 (2007).

[*]Corresponding author: alicia.palacios@uam.es

To the list of contents

Positron cooling and annihilation in noble gases

D. G. Green*, **P. Mullan, M. Lee**†, **G. F. Gribakin**

School of Mathematics and Physics, Queen's University Belfast, University Road, Belfast BT7 1NN, UK

Observation of lifetime spectra for positrons annihilating in a gas was one of the first sources of information on positron interaction with atoms and molecules [1]. In particular, measurements of the normalised annihilation rate $Z_{\rm eff}(t)$ during positron thermalization provided information on the energy dependence of the scattering cross sections and $Z_{\rm eff}$. Understanding the dynamics of positron cooling, including the fraction of positrons surviving to thermalization, is critical for accurate interpretation of such experiments. Incomplete thermalization was suspected to be responsible for the lack of consensus among the $Z_{\rm eff}$ data in Xe [2], while modelling of $Z_{\rm eff}(t)$ [3] revealed deficiencies in the theoretical data for the heavier noble-gas atoms. Understanding of positron kinetics is also crucial for the development of efficient positron cooling in traps and accumulators [4], and for a cryogenically cooled, ultra-high-energy-resolution, trap-based positron beam [5].

Many-body theory (MBT) calculations provide an accurate description of the whole body of data on low-energy positron scattering and annihilation rates on noble-gas atoms [6]. In this work we use our MBT calculated elastic scattering cross sections, $Z_{\rm eff}$ and γ-spectra to study positron cooling and annihilation in noble gases via Monte-Carlo simulation and numerical solution of the Fokker-Planck equation. Both methods yield the positron probability density in momentum space $f(p,t)$ (see Fig. 1), from which we calculate the time-varying annihilation rate $Z_{\rm eff}(t) = \int Z_{\rm eff}(p) f(p,t) dp / \int f(p,t) dp$ and γ-spectra, and compare these with experiment, where available.

We find that a strikingly large fraction of positrons annihilate before thermalising: $\sim$90% in He (see right panel of Fig. 1), $\sim$100% in Ne (due to cooling effectively stalling in the relatively deep momentum-transfer cross section minimum), $\sim$85% in Ar, $\sim$95% in Kr and $\sim$99.97% in Xe, owing to the larger mass. For Ar, Kr and Xe, we find that $Z_{\rm eff}(t)$ is sensitive to the depletion of the distribution due to loss of annihilated particles. This is most notable in Xe, for which the vigorous increase in $Z_{\rm eff}$ at low positron momenta leads to a quasi-steady-state distribution whose low-momentum tail is suppressed relative to the Maxwell-Boltzmann distribution, and a steady-state 'thermal' annihilation rate $\bar{Z}_{\rm eff}$ $\sim$370 that is smaller than the true thermal $Z_{\rm eff} \sim 450$, thus explaining the discrepancy between gas-cell and trap-based measurements. Overall, the use of the accurate atomic data gives $Z_{\rm eff}(t)$ in better agreement with experiment for all noble gases except Ne, the experiment for which is proffered to have suffered from incomplete knowledge of the fraction of positrons surviving to thermalisation and/or the presence of impurities. We also show that the γ spectrum shape parameters are sensitive probes of the positron energy and cooling times, and thus provide an alternative and complementary probe to positron lifetime spectroscopy.

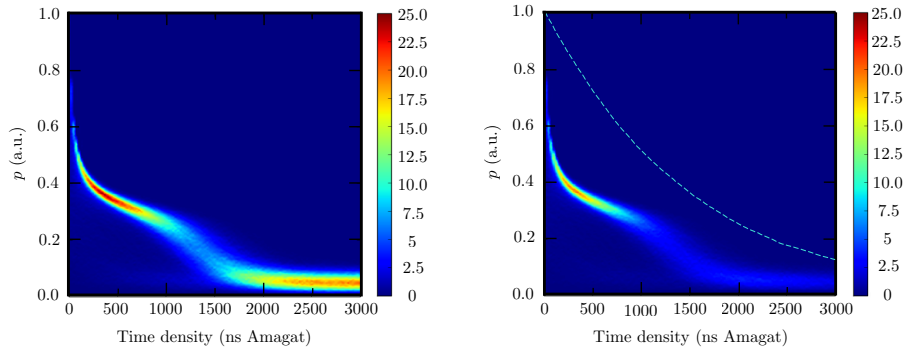

Fig. 1: $f(p,t)$ for positrons in He at 293K, initially distributed uniformly in energy up to the Ps-formation threshold: excluding (left) and including (right) annihilation. The latter distribution is normalized as $\int f(p,t)dp = F(t)$, where $F(t)$ is the fraction of positrons surviving at time t (shown by the dashed line on the right panel).

References

[1] P. G. Coleman *et al.*, J. Phys. B **8**, 1734 (1975); P. G. Coleman, T. C. Griffith and G. R. Heyland, *ibid.* **14**, 2509 (1981).
[2] G. L. Wright, M. Charlton, T. C. Griffith and G. R. Heyland, J. Phys. B **18**, 4327 (1985).
[3] R. I. Campeanu, Can. J. Phys. **60**, 615 (1982).
[4] I. Al-Qaradawi, M. Charlton, I. Borozan, R. Whitehead and I. Borozan, J. Phys. B **33**, 2725 (2000).
[5] M. R. Natisin, J. R. Danielson and C. M. Surko, J. Phys. B **47**, 225209 (2014); M. R. Natisin, J. R. Danielson and C. M. Surko, Appl. Phys. Lett. **108**, 024102 (2016).
[6] D. G. Green, J. A. Ludlow and G. F. Gribakin, Phys. Rev. A **90**, 032712 (2014); D. G. Green and G. F. Gribakin, Phys. Rev. Lett. **114**, 093201 (2015).

*Corresponding author: d.green@qub.ac.uk
†Present address: Bath University, Bath, United Kingdom

To the list of contents

Self-Organisation of Light in Optical Media with Competing Nonlocal Nonlinearities

F. Maucher[*1,2], **T. Pohl**[3,4], **S. Skupin**[5,6], **W. Krolikowski**[7,8]

1. Joint Quantum Centre (JQC) Durham-Newcastle, Department of Physics, Durham University, Durham DH1 3LE, United Kingdom
2. Department of Mathematical Sciences, Durham University, Durham DH1 3LE, United Kingdom
3. Max Planck Institute for the Physics of Complex Systems, 01187 Dresden, Germany
4. Department of Physics and Astronomy, 8000 Aarhus C, Denmark
5. Univ. Bordeaux—CNRS—CEA, Centre Lasers Intenses et Applications, UMR 5107, 33405 Talence, France
6. Univ. Lyon, Université Claude Bernard Lyon 1, CNRS, Institut Lumière Matière, F-69622, VILLEURBANNE, France
7. Laser Physics Centre, Research School of Physics and Engineering, Australian National University, Canberra, ACT 0200, Australia
8. Science Program, Texas A&M University at Qatar, Doha, Qatar

This talk will present recent work on nonlinear light propagation in the presence of competing local and nonlocal nonlinearities [1]. Such system can be realized in a gas of thermal alkali atoms [Fig. 1(a)]. Here, the nonlocality of the nonlinearity arises from the diffusive atomic motion and the simultaneous coupling of two incoherently coupled hyperfine levels to an excited state manifold gives rise to the competition between focusing and defocusing nonlinearities. For an appropriate choice of parameters, modulational instability occurs only for a finite band of wavelengths. Then, apart from spatial soliton formation, the different length scales of the nonlocality can give rise to filamentation and subsequent self-organised hexagonal lattice formation in the beam profile upon unidirectional propagation [Fig. 1(b)], akin to the superfluid-supersolid phase transition in Bose-Einstein condensates. The particular role of the topologically complex optical vorticity in the process of the pattern formation will be emphasized and the order of the phase-transition discussed [2].

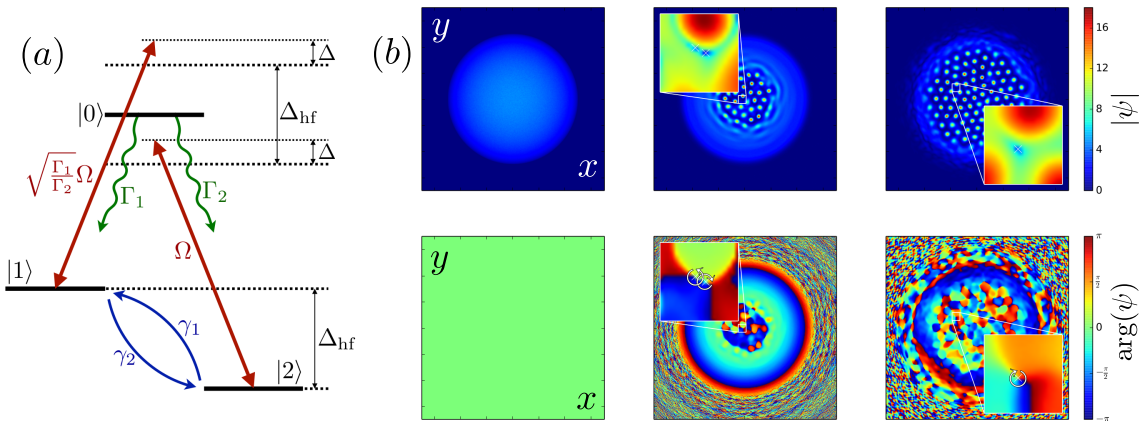

Fig. 1: (a) A thermal gas of alkali atoms with two hyperfine groundstates are coupled to an excited state manifold by the laser beam shown in (b), where the upper panel shows the amplitude and the lower panel the phase of the beam. The initial beam has a flat phase. Propagation of the beam gives rise to filamentation clearly visible in the amplitude profile accompanied by a complex phase structure including phase singularities highlighted in the insets. Further propagation then gives rise to a global ordering into crystals of light filaments with hexagonal symmetry.

References

[1] F. Maucher, T. Pohl, S. Skupin, and W. Krolikowski *Phys. Rev. Lett.*, **116**, 163902 (2016)
[2] F. Maucher, T. Pohl, S. Skupin, and W. Krolikowski, accepted for *Optical Data Processing and Storage*, (2017)

*Corresponding author: fabian.maucher@durham.ac.uk

To the list of contents

Cold chemistry with cold molecules

Edvardas Narevicius[*1]
1. Department of Chemical Physics, Weizmann Institute of Science, Rehovot 76100, Israel

We will discuss our efforts towards reaching ultra-cold temperatures with trapped molecules where molecular beams carrying both cold molecules and atoms have been decelerated and trapped in a permanent magnetic trap. I will present our plans and prospects of further cooling via evaporation or sympathetic collisions. In the second part of my talk we will focus on cold collisions with cold molecular partners that have been magnetically merged in order to reach collisions temperatures of $\sim$ 10 mK. I will show that quantum phenomena dominates collisions in this cold regime and discuss the importance of molecular degrees of freedom on cold reactions.

[*]Corresponding author: edvardas.narevicius@weizmann.ac.il

To the list of contents

Directional Quantum Controlled Chemistry: Generating Alignment of Ultracold Photoassociation Molecules

S. Kallush[*1,2], **J.L. Carini**[3], **P.L. Gould** [3], **R. Kosloff**[2]

1. Department of Physics and Optical Engineering, ORT-Braude College, P.O. Box 78, 21982 Karmiel, Israel

2. The Fritz Haber Research Center, The Hebrew University of Jerusalem, Jerusalem 91904, Israel

3. Department of Physics, University of Connecticut, Storrs, Connecticut 06269, USA

Quantum coherent control was conceived as a method to direct chemical reactions to a desirable outcome [1],[2],[3]. Despite the remarkable success of the application of control methods to induce uni-molecular manipulations like photo-isomerization[4], photo dissociation[5], the raison d'etre for coherent control in the context of chemistry, namely, the assembling of multiple atoms or molecules into a new molecule, was not realized until recently [6],[7]. The main obstacle has been the pre-entangelment of the reactants [8]. The approach to overcome this issue differs in hot and cold collisions. For reactions in the high ($T \gg 1K$) temperature regime, one has to first distill entangled pairs out of thermal incoherent mixture [9]. In the cold ($T \ll 1K$) regime, quantum phenomena close to threshold effects the low angular momentum states are pre-entangled. For the ultracold reactions, technological developments that gave access to the instant frequency in the time domain [10] were used to demonstrate coherent control effects for ultracold photoassociation[7].

We present a new aspect of quantum control of chemical reactions unique to photochemical reactions. Such control is able to align the products of the reaction along a well-defined spatial direction relative to the lab frame. We show that under conventional shaped photo-associated pulses in the *ns* regime a significant alignment is developed. The alignment We explore the dependency of and give several detecting approach

A theoretical investigating in pulsed photoassociation of ultracold ^{87}Rb atoms shows significant alignment of a specific vibarational state $v" = 39$ on the ground $^3\Sigma_u^+$ electronic state. The simulation is based on solving the time dependent Schrödinger equation with the pulse contained explicitly and performing thermal averaging. Significant alignment is obtained by transform limited pulses. Enhancement of the population transfer by chirped pulses decreases slightly decreases the alignment. Employing multipulses in synchornization with the vibrational and rotational periods leads to coherent enhancement of both population and alignment of the target state.

A linearly polarized REMPI probe that will be tuned to an electronic Π state induce electronic excitations perpendicular to the molecule axis. For molecules which are aligned to the lab fixed axis a difference in the molecular signal for REMPI pulse polarizations parallel and perpendicular to the pump should give a clear indication for the alignment. For the values that presented in this paper one can estimate the ratio of the signal to be at most at the order of $S_\perp/S_{||} \sim 3$. Once the photoassociation generats a $v" = 39$ molecule, additional alignment can be obtained by excitation de-excitation cycles leading to lower vibrational states.

The introduction of lab-frame spectroscopy into the coherently controlled ultracold reaction could raise several interesting applications. For hetronuclear ultracold molecules that posses permanent dipole moment, a controlled photoassociation can generate macroscopic *orientation* of whole ensemble. Furthermore, under BEC conditions, the induced macroscopic dipole could exhibit phenomena that origin in the quantum characters of the molecules but give signatures on the macroscopic scales. A concerted rotation of the quantum condensed phase can lead to effects which will have analogs in other classical-like condensed phase dynamics.

References

[1] D.J. Tannor and S.A. Rice, J. Chem. Phys.,**83**, 5013 (1985)
[2] D.J. Tannor, R. Kosloff and S.A. Rice, J. Chem. Phys., **85**, 5805 (1986).
[3] P. Brumer and M. Shapiro, Chem. Phys. Lett., **126**, 541 (1986).
[4] V. Prokhorenko, A.M. Nagy, S.A. Waschuk, L.S. Brown, R.R. Birge, and R.J.D. Miller, science, **313**, 1257 (2006).
[5] M. Shapiro and P. Brumer, *Principles of the Quantum Control of Molecular Processes* ISBN 0-471-24184-9. (Wiley-VCH, February 2003).

[6] L. Levin, W. Skomorowski, L. Rybak, R. Kosloff, C.P. Koch, and Z. Amitay, Phys. Rev. Lett., **114**, 233003 (2015).
[7] J.L. Carini, S. Kallush, R. Kosloff, and P.L. Gould, Phys. Rev. Lett., **115**, 173003 (2015).
[8] A. Abrashkevich, M. Shapiro, and P. Brumer, Phys. Rev. Lett., **81**, 3789 (1998).
[9] S. Amaran, R. Kosloff, M. Tomza, W. Skomorowski, F. Pawlowski, R. Moszynski, L. Rybak, L. Levin, Z. Amitay, M. Berglund, D. Reich, and C. Koch, J. Chem. Phys., **139**, 164124 (2013).
[10] rogers2007, C.E. Rogers, M.J. Wright, J.L. Carini, J.A. and Pechkis, and P.L. Gould, J. Opt. Soc. Am. B, **24**, 1249 (2007)

*Corresponding author: shimshonkallush@braude.ac.il

To the list of contents

Precision spectroscopy of cold formaldehyde in an electric trap

Martin Ibrügger[*1], **A. Prehn**[1], **M. Zeppenfeld**[1], **G. Rempe**[1]
1. Max Planck Institute of Quantum Optics, Hans-Kopfermann-Str. 1, 85748 Garching, Germany

Ultracold molecules are ideal systems for the investigation of fundamental physics. The rich internal structure renders them perfect candidates for measuring a variation of physical constants such as the proton-electron mass ratio and the fine structure constant. Due to high internal electric fields they are also well suited for measuring the electron's electric dipole moment. All these experiments require the highest attainable precision calling for trapping to increase interrogation times as is being done for atomic optical clocks. For neutral molecules however, in particular polyatomic molecules, there are few to none experiments combining spectroscopy with cooling and trapping. In our group we use optoelectrical Sisyphus cooling [1] to prepare large ensembles of up to $3 \cdot 10^5$ formaldehyde molecules (H_2CO) at sub-millikelvin temperatures [2]. Molecules are cooled and stored in an electric trap [3] which provides a box-like potential with a tunable and homogeneous offset field. Furthermore, we have good control over the internal state of the molecules and are able to prepare them with a purity of over 80 % in a single rotational state by optical pumping [4]. This setup provides us with an ideal environment to perform precision spectroscopy.

Here, we present microwave spectroscopy of trapped formaldehyde on a magic transition between rotational levels $J = 4$ and $J = 5$ with a splitting of 364 GHz. Tuning the trap's homogeneous electric field appropriately allows us to essentially eliminate Stark broadening which up to now has been the limiting factor, broadening transition lines on the order of MHz. We now achieve linewidths down to 3.8 kHz corresponding to an accuracy of 10^{-8} limited by the Doppler effect. By applying this technique to even colder molecules, which are readily available in our experiment, measurements with unprecedented precision for polyatomic molecules seem feasible.

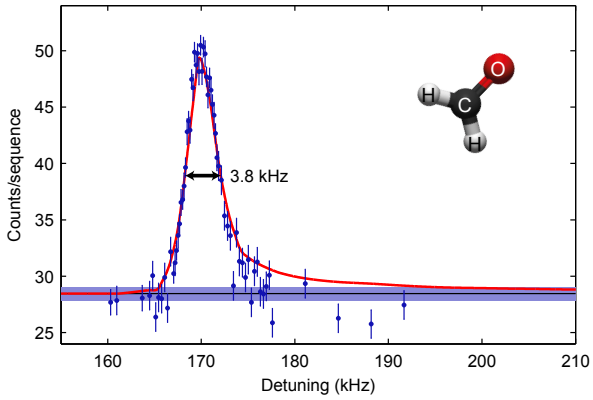

Fig. 1: Doppler-limited rotational transition line between $J = 4$ and $J = 5$ of trapped formaldehyde at 364 GHz. Measured data shown in blue and theoretical lineshape in red. Theory takes into account the energy distribution of the molecules and the electric field distribution in the trap.

References

[1] M. Zeppenfeld *et al.*, Nature **491**, 570 (2012).
[2] A. Prehn *et al.*, Phys. Rev. Lett. **116**, 063005 (2016).
[3] B.G.U. Englert *et al.*, Phys. Rev. Lett. **107**, 263003 (2011).
[4] R. Glöckner *et al.*, Phys. Rev. Lett. **115**, 233001 (2015).

*Corresponding author: martin.ibruegger@mpq.mpg.de

To the list of contents

Contactless photon-photon interactions

C. S. Adams[*1],
1. Joint Quantum Centre (JQC) Durham–Newcastle, Department of Physics, Durham University
South Road, Durham DH1 3LE, UK

The experimental demonstration of electromagnetically induced transparency (EIT) involving highly-excited Rydberg atoms [1] opened gate to a new field of non-linear quantum optics based on dipolar interactions [2]. A unique feature of Rydberg quantum optics is the ability for photons to interact without ever being in the same medium. Recently, we demonstrated the van der Waals repulsion between two photons stored in two media separated by 15 times the optical wavelength [2]. Effectively each photon sees a position dependent refractive index gradient created by a photon in the nearby medium, as illustrated in the Fig. 1.

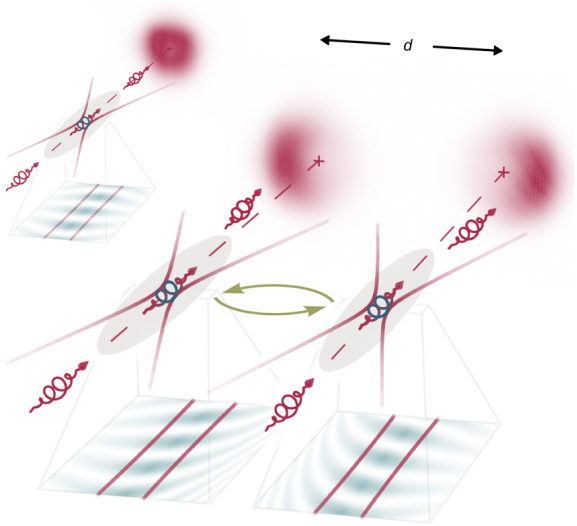

Fig. 1: Propagation of light (red) through two independent media (grey). The light couples to highly-excited Rydberg states which interact via long-range van der Waals interactions imprinting a phase gradient (shown below) leading to a deflection of the outgoing light. The inset shows the case of a single channel.

Such long-range interactions between photons provide an interesting platform for scalable multichannel photonic devices, or quantum simulation of strongly correlated many-body dynamics using light.

References

[1] A. Mohapatra, T. R. Jackson, and C. S. Adams, *Coherent optical detection of highly excited Rydberg states using electromagnetically induced transparency*, Phys. Rev. Lett. **98**, 113003 (2007).

[2] O. Firstenberg, C. S. Adams, and S. Hofferberth, *Nonlinear quantum optics mediated by Rydberg interactions*, J. Phys. B **49**, 152003 (2016).

[3] H. Busche, P. Huillery, S. W. Ball, T. Ilieva, M. P. A. Jones and C. S. Adams, *Contactless nonlinear optics mediated by long-range Rydberg interactions*, Nature Phys. doi:10.1038/nphys4058 (2017).

*Corresponding author: c.s.adams@durham.ac.uk

To the list of contents

Structure and dynamics of nanoparticles in short wavelength light pulses

Thomas Möller

Institut für Optik und Atomare Physik, Technische Universität Berlin
Hardenbergstrasse 36, 10627 Berlin. Germany

The interaction of high intensity, short-wavelength, short-pulse radiation with matter is a fundamental problem of current research[1]. Its understanding is essential for virtually all experiments with new super intense X-ray sources, in particular for flash imaging of nm sized particles. Clusters as finite systems with the density of bulk solids are ideal samples to study fundamental light–matter interaction processes in all wavelength regimes[2-5]. Recently, initial experiments with short wave length pulses have shown that single nm-sized gas phase particles and clusters can be imaged by single shot scattering[6-10]. Especially with free electron lasers new avenues are opened to investigate transition states[11] and ultrafast processes[12, 13] with unprecedented spatial and temporal resolution.

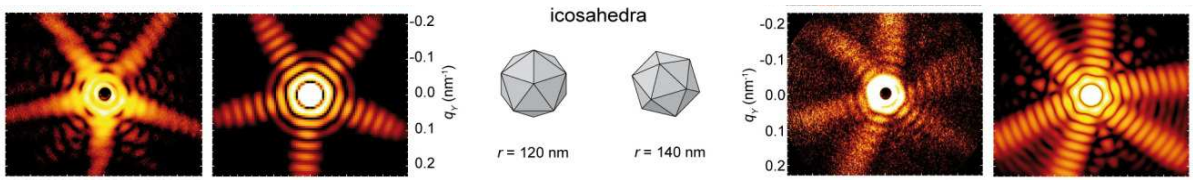

Fig. 1: Experimental and simulated scattering patterns of large silver nanoparticles [10].

While short wavelength radiation from hard x-ray sources is essential for the high spatial resolution, soft x-rays can provide 3D-information since the light also efficiently scattered to rather large angles[10]. This offers new routes for structure determination in cluster and nanometer-scale science.

References

1 A. A. Sorokin, S. V. Bobashev, T. Feigl, K. Tiedtke, H. Wabnitz, and M. Richter, Physical Review Letters **99** (2007).
2 T. Ditmire, T. Donnelly, A. M. Rubenchik, R. W. Falcone, and M. D. Perry, Phys. Rev. A **53**, 3379 (1996).
3 C. Bostedt, et al., Physical Review Letters **100**, 133401 (2008).
4 U. Saalmann, C. Siedschlag, and J. M. Rost, J. Phys. B **39**, R39 (2006).
5 T. Fennel, K. H. Meiwes-Broer, J. Tiggesbaumker, P. G. Reinhard, P. M. Dinh, and E. Suraud, Reviews of Modern Physics **82**, 1793 (2010).
6 C. Bostedt, M. Adolph, E. Eremina, M. Hoener, D. Rupp, S. Schorb, H. Thomas, A. R. B. de Castro, and T. Moller, Journal of Physics B-Atomic Molecular and Optical Physics **43**, 194011 (2010).
7 C. Bostedt, et al., Physical Review Letters **108**, 093401 (2012).
8 D. Rupp, et al., New Journal of Physics **14** (2012).
9 L. F. Gomez, et al., Science **345**, 906 (2014).
10 I. Barke, et al., Nature communications **6**, 4648 (2015).
11 D. Rupp, et al., Physical review letters **117** (2016).
12 T. Gorkhover, et al., Physical Review Letters **108** (2012).
13 T. Gorkhover, et al., Nature Photonics **10**, 93 (2016).

thomas.moeller@physik.tu-berlin.de

To the list of contents

Spectroscopy of Highly Charged Ions in Magnetic Fusion Plasmas: Research Opportunities and Diagnostic Necessities

P. Beiersdorfer[*1]
1. Physics Department, Lawrence Livermore National Laboratory, Livermore, CA 94550, USA

Highly charged ions play a crucial role in magnetic fusion research as diagnostics of, for example, electron and ion temperatures, transport, and bulk motion, and as contributors to the radiative plasma cooling [1],[2]. In order to develop specific spectral diagnostics a large amount of atomic data are needed. For example, there is a need for highly accurate wavelengths as references for measurements of bulk plasma motion, for accurate line excitation rates that encompass both electron-impact excitation and indirect line formation processes, for accurate position and resonance strength information of dielectronic recombination satellite lines that may broaden or shift diagnostic lines or that may provide electron temperature information, and for accurate ionization balance calculations.

Conversely, magnetic fusion plasmas are excellent sources for studying highly charged ions and their atomic properties as well as the collisional processes involved in their excitation. These studies include x-ray production by charge exchange, line identifications and accurate wavelength measurements, benchmark data for ionization balance calculations, and the calibration of astrophysical density diagnostics. An overview of opportunities for highly charged ion research with magnetic fusion plasmas was given recently [3].

We point out that the ions of several elements are of special current interest, notably the highly charged ions of argon, iron, krypton, xenon, and, foremost, of tungsten [3]. The electron temperatures thought to be achievable in the near future may produce W^{70+} ions and possibly ions with even higher charge states. This means that all but a few of the most highly charged ions are of potential interest as plasma diagnostics or are available for basic research.

This talk will give an overview of various research opportunities and diagnostic needs involving highly charged ions in magnetic fusion plasmas.

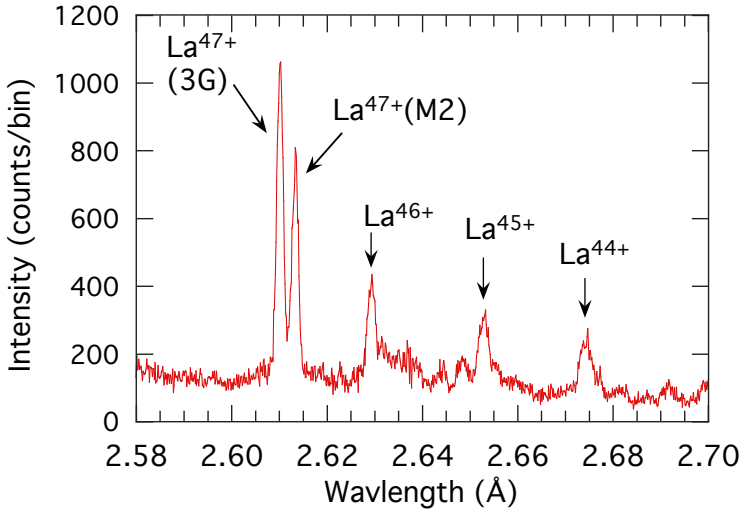

Fig. 1: Emission from highly charged lanthanum observed from a tokamak plasma. Lines $3G$ and $M2$ are $3s \rightarrow 2p$ transitions in neonlike La^{47+}.

This work was performed under the auspices of the U. S. Department of Energy by Lawrence Livermore National Laboratory under Contract DE-AC52-07NA27344 and supported by the Office of Fusion Energy Sciences.

References

[1] P . Beiersdorfer, J. Clementson, J. Dunn, M. F. Gu, K. Morris, Y. Podpaly, E. Wang, M. Bitter, R. Feder, K. W. Hill, D. Johnson, and R. Barnsley, J. Phys. B **43**, 144008 (2010).
[2] P . Beiersdorfer, M. J. May, J. H. Scofield, and S. B. Hansen, High Energy Dens. Phys. **8**, 271 (2012).
[3] P . Beiersdorfer, J. Phys. B **48**, 144017 (2015).

*Corresponding author: beiersdorfer1@llnl.gov

To the list of contents

Laboratory measurements compellingly support a charge-exchange mechanism for the "Dark matter" ∼3.5 keV X-ray line

Chintan Shah*[1], Sven Bernitt†[1,2,3], Stepan Dobrodey[1], René Steinbrügge[1], Liyi Gu[4], Jelle Kaastra[4,5], and José R. Crespo López-Urrutia[1]

1. Max–Planck–Institut für Kernphysik, Saupfercheckweg 1, 69117 Heidelberg, Germany
2. Friedrich-Schiller-Universität Jena, Fürstengraben 1, 07743 Jena, Germany
3. Helmholtz-Institut Jena, Fröbelstieg 3, 07743 Jena, Germany
4. SRON Netherlands Institute for Space Research, Utrecht, The Netherlands
5. Leiden Observatory, Leiden University, 2300 RA Leiden, The Netherlands

A mysterious X-ray signal at 3.5 keV from nearby galaxies and galaxy clusters [1] recently sparked tremendous interest in the scientific community and has given rise to a tide of publications attempting to explain the origin of this line. It has been hypothesized that the signal is the result of decaying sterile neutrinos – a potential dark matter particle candidate – presumably based on the fact that this X-ray line is not available in the standard spectral databases and models for thermal plasmas. Cautiously, Gu *et al.* [2] have pointed out an alternative explanation for this phenomenon: charge exchange between bare ions of sulfur and atomic hydrogen. Their model shows that X-rays should be emitted at 3.5 keV by a set of S^{15+} transitions from $n \geq 9$ to the ground states, where n is the principle quantum number.

We tested this hypothesis in the laboratory by measuring K-shell X-ray spectra of highly ionized sulfur ions following charge exchange with gaseous molecules in an electron beam ion trap. We produced bare S^{16+} and H-like S^{15+} ions and let them capture electrons in collisions with molecules, while recording X-ray spectra. The 3.5 keV transition clearly shows up in the charge-exchange induced spectrum under a broad range of conditions. The inferred X-ray energy of 3.47 ± 0.06 keV is in full accord with both the astrophysical observations and theoretical calculations, and confirms the novel scenario proposed by Gu [2][3]. Taking the experimental uncertainties and inaccuracies of the astrophysical measurements into account, we conclude that the charge exchange between bare sulfur and hydrogen atoms can outstandingly explain the mysterious signal at around 3.5 keV [3].

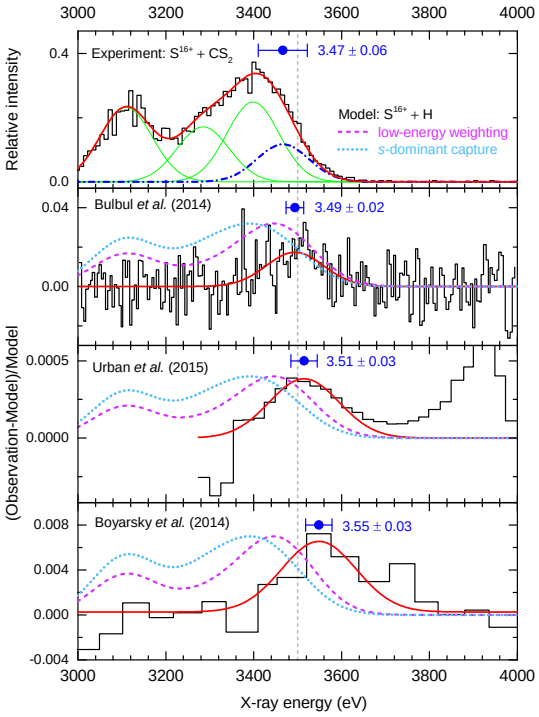

Fig. 1: Charge-exchange-induced X-ray spectrum in comparison with recently reported astrophysical observations. The experimental data and observations are compared with the charge exchange model of Gu.

References

[1] E. Bulbul *et al.*, *Astrophys. J* **13**, 789 (2014)
[2] L. Gu *et al.*, A & A **L11**, 584 (2015)
[3] C. Shah *et al.*, *Astrophys. J* **833**, 52, (2016)

*Corresponding author: chintan@mpi-hd.mpg.de
†Corresponding author: bernitt@mpi-hd.mpg.de

To the list of contents

Sideband heating of a single calcium ion trapped in a Penning trap: Preparation and coherence studies of a non-thermal state

M. K. Joshi[*1], **P. Hrmo** [1], **V. Jarlaud** [1], **J. F. Goodwin** [2], **G. Stutter** [3] **and R. C. Thompson**[1]

1. Imperial College London, SW7 2AZ, United Kingdom

2. Department of Physics, University of Oxford, Oxford OX1 3PU, United Kingdom

3. Department of Physics and Astronomy, Aarhus University, DK-8000 Aarhus C, Denmark.

Previously, we have demonstrated the ground state cooling of a single trapped calcium ion in a Penning trap[1]. A trapped calcium ion is initially cooled to its Doppler limit by a red detuned 397 nm laser light (resonant with the $S_{1/2} \leftrightarrow P_{1/2}$ transition) [2]. The next stage of cooling is carried out through a resolved sideband cooling scheme. A resolved sideband cooling requires a narrow linewidth transition and also a narrow linewidth laser tuned to the first red sideband of the transition (i.e. $S_{1/2} \leftrightarrow D_{5/2}$ for a calcium ion). In an extension to that work, we report here the coherent manipulation, both within and outside the Lamb-Dicke (L-D) regime, of a single ion qubit. Coherence studies of a ground state cooled ion are carried out by observing the Rabi oscillations and Ramsey interference fringes, and the coherence time is measured to be 1.5 ms.

In contrast to sideband cooling we also show the results of the sideband heating on a ground state cooled trapped ion. Sideband heating is demonstrated by tuning the 729 nm laser to a blue sideband of the transition. This eventually drives the population to high phonon states. Due to the presence of minima of the sideband strength, the population gets confined to a few phonon states [3]. Such a spectrum is shown in Fig. 1, where the sideband heating is carried out on the first blue sideband. In the right part of the figure, a simulated histogram of the population spread as a function of sideband heating time is shown. It can be seen that initially the population spreads out and then gets confined around a phonon state n = 160. This is the phonon state at which the blue sideband strength ceases, thus leads to a population build up. Realisation of these quantum states are vital and can be very useful to demonstrate the quantum studies outside the L-D regime.

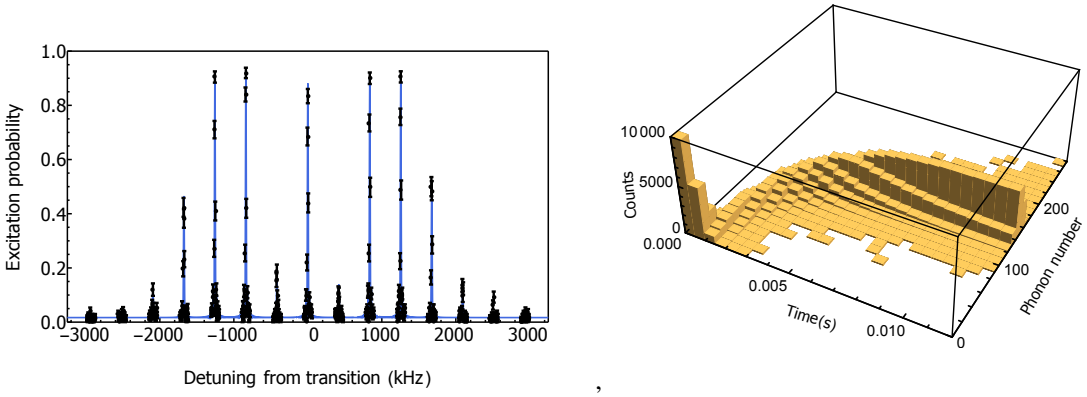

Fig. 1: Sideband heating of a calcium ion at 419 kHz axial frequency (Left). A simulated histogram plot of population in each phonon state as a function of time, where the sideband heating is carried out at the first blue sideband (Right).

Recently, we also have carried out the ground state cooling on ion Coulomb crystals (ICCs) [4]. The ground state cooling of an ICC is performed through a resolved sideband cooling scheme, similar to the single ion case. Due to the presence of multiple sidebands a complex cooling sequence was necessary and multiple laser frequencies are used repeatedly to efficiently cool the ions to their ground state. In future work we will carry out the coherence studies on such crystals.

References

[1] J. G. Goodwin, *et al.*, Phys. Rev. Lett. **116**, 143002 (2016).
[2] S. Mavadia, Nature Comm. **4**, 2571 (2013)..
[3] M. Joshi, *et al.*, in preparation.
[4] G. Stutter *et al.*, in preparation.

*Corresponding author: m.joshi@ic.ac.uk

To the list of contents

Direct Detection of Giant Molecules with a Cloud of Cold Ions

N. Bremare[1], C. Champenois[1], C. Dedonder-Lardeux[1], D. Guyomarc'h[1], A. Janulyte[1], J. Pedregosa-Gutierrez[1], C. Jouvet[1], and M. Knoop[*1]

1. Aix-Marseille University, CNRS, PIIM, UMR 7345, 13397 Marseille Cedex 20, France

Molecules with a mass above some 10^6 a.m.u. cannot be detected directly today, and there is a strong demand in mass spectrometry to directly detect viruses or antibodies, rather than to rely on fragmentation. We use the passage of a single, charged molecule through a cloud of laser-cooled, radio-frequency trapped ions as a direct detector for any molecule without mass limitation. The crossing of the ion cloud by a charged particle induces a perturbation of the ion cloud's equilibrium state. The temperature variation of the ion cloud is amplified by the radiofrequency heating induced by the confining potential, resulting in the modification of the fluorescence signal of the ion cloud. This fluorescence signal is macroscopic, and can be measured with standard means of non-intrusive photon collection and counting. Every single, charged particle that crosses the ion cloud induces a measurable perturbation of the ion cloud and may thus be detected, independently of its mass. The technology has so far been demonstrated theoretically and numerically [1], and the experimental prototype is delivering first signals.

The experimental set-up combines a versatile molecule source in high vacuum with a linear radiofrequency trap confining a laser-cooled cloud of Ca^+-ions in ultra-high vacuum. The molecular source produces a beam of lowly charged particles with a controlled energy dispersion in order to limit the divergence of the beam throughout the apparatus. Various electrostatic lenses channel these molecules through the trapped ion cloud which is created with a radial extension larger than 100 μm in order to facilitate the interaction with the molecule. Trapping and laser-cooling conditions are tuned so that the perturbation of the cloud and its fluorescence signal are persistent and can be easily detected.

This innovative detector is non-destructive and allows to re-use the molecule for other experiments, it can be coupled to a mass-separation stage (i.e. TOF). This sensor opens a new domain of applications: rapid detection of macromolecules (proteins and viruses for example) in a single step, simply, reliably and unambiguously.

References

[1] C. Champenois, C. Dedonder-Lardeux, C. Jouvet, L. Hilico, M. Knoop, J. Pedregosa, *Non-destructive detection method of charged particles without mass limitation*, European Patent EP14306498 (2014)

[*]Corresponding author: martina.knoop@univ-amu.fr

To the list of contents

Detection of entanglement and of features of quantum evolution with few local measurement and complementary properties

Chiara Macchiavello* [1]
1. Department of Physics, University of Pavia, via Bassi 6, 27100 Pavia, Italy

We will give an overview of several recent results concerning the detection of properties of composite states and of quantum evolutions by employing measurements of complementary properties. Two properties of a quantum systems are called complementary if they are such that, if one knows the value of one property, all possible values of the other property are equiprobable. We will first provide an interpretation of entanglement in composite systems based on classical correlations between measurement outcomes of complementary properties [1]. We will then present a general scheme to detect properties of quantum evolution in open quantum systems and of quantum communication channels. We will show in particular a practically feasible scheme to detect features of quantum channels such as being entanglement breaking or separable [2], and lower bounds to information-theoretic properties [3] that are important to quantify the ability of a quantum channel to transmit information, such as the quantum capacity. Such a scheme is based on the measurement of few local observables that coincide with complementary properties in the case of two-dimensional systems and offers the advantage of avoiding full quantum process tomography, that is a demanding procedure in terms of the number of measurements required. Its efficiency has been successfully tested with polarised photons [4]. We will finally show that a similar scheme can be employed to detect non-Markovianity of quantum evolution, by applying tools from spectral analysis to study the evolution of an open quantum system [5].

References

[1] L . Maccone, D. Bruss and C. Macchiavello, Phys. Rev. Lett. **114**, 130401 (2015).
[2] C . Macchiavello and M. Rossi, Phys. Rev. A **88**, 042335 (2013).
[3] C . Macchiavello and M.F. Sacchi, Phys. Rev. Lett. **116**, 140501 (2016).
[4] A . Orieux, L. Sansoni, M. Persechino, P. Mataloni, M. Rossi and C. Macchiavello, Phys. Rev. Lett. **111**, 220501 (2013); A. Cuevas, M. Proietti, M.A. Ciampini, S. Duranti, P. Mataloni, M.F. Sacchi and C. Macchiavello, arXiv:1612.07754.
[5] D . Chruscinski, C. Macchiavello and S. Maniscalco, Phys. Rev. Lett. **118**, 080404 (2017).

*Corresponding author: chiara.macchiavello@unipv.it

To the list of contents

Spectroscopy methods with quantum sensors

Tuvia Gefen[*1], **Simon Schmitt** [2], **Liam P. McGuinness** [2], **Fedor Jelezko** [2], **Alex Retzker**[†1]
1. Racah Institute of Physics, Hebrew University of Jerusalem, 91904 Jerusalem, Israel
2. Institute of Quantum Optics, Ulm University, 89081 Ulm, Germany

We consider the problem of quantum spectroscopy, namely reconstruction of the frequency components of a time dependent Hamiltonian. This task is of great interest to chemical analysis, nano-scale NMR and frequency standards. We examine theoretically and experimentally the following questions: Given an oscillating Hamiltonian, what is the best achievable precision in detecting the frequency and how well can we resolve between two close frequencies. It turns out that some misconceptions have led to suboptimal techniques and a considerable improvement can be introduced. This observation is demonstrated experimentally with a new technique [1]. We find, quite surprisingly, that the precision of the frequency tracking scales as $\frac{1}{T^{1.5}}$, while for long enough probe coherence time a scaling of $\frac{1}{T^2}$ is achievable (with a suitable control). We show that these control methods basically give rise to an accelerated phase accumulation which results in an enhanced sensitivity [2]. Relevance to nano-scale NMR and future challenges are also discussed.

References

[1] Simon Schmitt et al. *Sub-millihertz magnetic spectroscopy performed with a nanoscale quantum sensor*, accepted to Science (2017)
[2] Tuvia Gefen, Fedor Jelezko, and Alex Retzker, arXiv preprint arXiv:1702.07408 (2017).

[*]Corresponding author: tuvia.gefen@mail.huji.ac.il
[†]Corresponding author: retzker@phys.huji.ac.il

To the list of contents

Towards Coherent splitting and recombination of bright solitary matter waves

A. Rakonjac*[1], O. J. Wales[1], T. P. Billam[2], J. L. Helm[3], S. A. Gardiner[1], and S. L. Cornish†[1]

1. Joint Quantum Centre (JQC) Durham–Newcastle, Department of Physics, Durham University
South Road, Durham DH1 3LE, UK
2. Joint Quantum Centre (JQC) Durham–Newcastle, School of Mathematics and Statistics, Newcastle University
Newcastle upon Tyne NE1 7RU, UK
3. Dodd-Walls Centre for Photonic and Quantum Technologies, Department of Physics, University of Otago
730 Cumberland Street, Dunedin 9016, New Zealand

We report on the controlled creation, splitting, and recombination of bright solitary matter waves formed from Bose-Einstein condensates of ^{85}Rb atoms. These solitary wavepackets, or solitons, are long-lived, with lifetimes of over 20 seconds, and can propagate without observable dispersion over macroscopic distances. Following our previous work on classical reflection of solitons from a broad repulsive barrier [1] and quantum reflection from a narrow attractive well [2], we extend our investigations to solitons incident on a narrow repulsive gaussian barrier [3]. When the kinetic energy of the soliton wavepacket is comparable to the barrier height, we observe controllable splitting of the soliton into two daughter solitons. The splitting proportion varies according to incident velocity and barrier height with good agreement with 1-D and 3-D Gross-Pitaevskii simulations. After allowing the daughter solitons to oscillate in a weak harmonic potential, they recombine on the barrier and continue propagating as an apparent single soliton, though the recombination is in this case the result of velocity filtering rather than a coherent process. Future experiments with a narrower barrier should allow us to reach the coherent recombination regime.

The coherent splitting and recombination of solitons as well as their long lifetime leads the way to using such a scheme for soliton-based interferometry in a variety of configurations [4]. In particular, the scheme can be utilised in a ring geometry for Sagnac interferometry [5]. Future work includes implementing a soliton Sagnac interferometer using a 2-D painted ring potential and further experimental studies of bright matter-wave soliton dynamics that can be used to elucidate the wealth of theoretical work in the field, as well as to explore, for example, the realisation of Schrödinger cat states [6, 7] and the study of short-range atom-surface potentials [8].

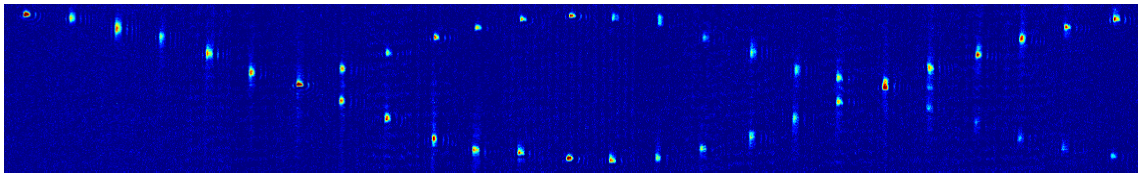

Fig. 1: A series of destructive absorption images at 30 ms time intervals showing splitting and apparent recombination of two equally populated daughter solitons on a narrow repulsive Gaussian barrier.

References

[1] A. L. Marchant, T. P. Billam, T. P. Wiles, M. M. H. Yu, S. A Gardiner, and S. L. Cornish, Nat. Commun. **4**, 1865 (2013)
[2] A. L. Marchant, T. P. Billam, M. M. H. Yu, A. Rakonjac, J. L. Helm, J. Polo, C. Weiss, S. A. Gardiner, and S. L. Cornish, Phys. Rev. A **93**, 021604(R) (2016)
[3] J. L. Helm, T. P. Billam, and S. A. Gardiner, Phys. Rev. A **85**, 053621 (2012)
[4] A. D. Cronin, J. Schmiedmayer, and D. E. Pritchard, Rev. Mod. Phys. **81**, 1051 (2009)
[5] J. L. Helm, S. L. Cornish, and S. A. Gardiner, Phys. Rev. Lett. **114**, 134101 (2015)
[6] C. Weiss and Y. Castin, Phys. Rev. Lett. **102**, 010403 (2009)
[7] A. I. Streltsov, O. E. Alon, and L. S. Cederbaum, Phys. Rev. A **80**, 043616 (2009)
[8] S. L. Cornish, N. G Parker, A. M. Martin, T. E. Judd, R. G. Scott, T. M. Fromhold, and C. S. Adams, Physica D **238**, 1299 (2009)

*Corresponding author: ana.rakonjac@durham.ac.uk
†Corresponding author: s.l.cornish@durham.ac.uk

To the list of contents

Improved sensitivity to the electron's electric dipole moment using YbF molecules

Isabel M. Rabey[*1], **J. A. Devlin**[1], **C. Ho**[1], **B. E. Sauer**[1], **M. R. Tarbutt**[1], **E. A. Hinds**[1]
1. Centre for Cold Matter (CCM), The Blackett Laboratory, Imperial College London
Prince Consort Road, London SW7 2AZ, UK

It is well known that the electron has a magnetic dipole moment. This property has been measured with exquisite precision and provides one of the most successful comparisons between experiment and theory. However, no one has ever been able to detect the analogous *electric* dipole moment (EDM), d_e. In principle, there is no reason why an electron should not have an electric dipole moment, but a non-zero value of d_e will violate time reversal symmetry T. The standard model of particle physics does contain some T-violation, but the value of d_e it predicts is almost vanishingly small ($|d_e| < 10^{-38}$ e.cm) — the displacement of the electron's charge from its centre of mass is predicted to be less than a Planck length. This is many orders of magnitude smaller than current experiments could ever measure. However, theories that extend the Standard Model, such as supersymmetry, will typically include additional sources of T-violation to help explain the matter-antimatter imbalance we see in the universe today. If these theoretical predictions are correct, we expect to measure an EDM between the current experimental upper limit $|d_e| < 8.7 \times 10^{-29}$ e.cm (90% confidence) [1] and the lower theoretical limit $|d_e| > 1 \times 10^{-30}$ e.cm [2].

We measure the electron EDM by performing a spin precsession measurement on a beam of supersonic ytterbium fluoride (YbF) molecules [3]. Recently, we have developed a series of improvements to the state preparation and detection of the molecules [4] [5] which has increased the flux of useful molecules by two orders of magnitude. This has significantly improved the statistical sensitivity of our machine and will allow EDMs of a few 10^{-29} e.cm to be measured.

Noise and systematic effects also need to be under good control below the level of the improved sensitivity. With the leading concern being flucuating magnetic fields, we have also improved our measurement and control of these unwanted fields [6]. With this upgraded apparatus, we are now able to search for evidence of new T-violating physics with even higher precision.

References

[1] The ACME Collaboration, Science **343**, 269 (2014).
[2] I. B. Khriplovich and S. K. Lamoreaux, *CP Violation Without Strangeness* (Springer, New York, 1997).
[3] J. J. Hudson, D. M. Kara, I. J. Smallman, B. E. Sauer, M. R. Tarbutt, and E. A. Hinds, Nature **473**, 493 (2011).
[4] J. A. Devlin, PhD Thesis, Imperial College London, 2015.
[5] I. M. Rabey, PhD Thesis, Imperial College London, 2017.
[6] I. M. Rabey, J. A. Devlin, E. A. Hinds, and B. E. Sauer, Rev. Sci. Instrum. **87**, 115110 (2016).

[*]Corresponding author: isabel.rabey08@imperial.ac.uk

To the list of contents

Quantum gas in a box

Z.Hadzibabic[*1]
1. Cavendish Laboratory, University of Cambridge, J J Thomson Avenue, Cambridge, CB3 0HE, United Kingdom

For the past two decades ultracold Bose and Fermi atomic gases have been used with great success to study fundamental many-body physics. While traditionally they were produced in harmonic electromagnetic traps, it recently also became possible to create them in the uniform potential of an optical box trap. This has opened even more possibilities for fundamental studies, allowing closer connections with other many-body systems and the theories that rely on the translational symmetry of the system. Research topics for which the homogeneous, box-trapped quantum gases offer distinct advantages include critical phenomena near phase transitions, quantum turbulence, and searches for exotic states of matter in strongly interacting (unitary) gases. I will give an overview of our recent progress in this growing field.

[*]Corresponding author: zh10001@cam.ac.uk

To the list of contents

Exploring Quantum Antiferromagnets with single-site resolution

D. Greif[*1]
1. Department of Physics, Harvard University, Cambridge, Massachusetts, USA

Strongly correlated electron systems such as high-temperature superconductors and pseudo-gap states are a cornerstone of modern condensed matter research. A complementary approach to studying solid-state systems is to build an experimentally tunable quantum system governed by the Hubbard model, which is thought to qualitatively describe these systems but is difficult to understand theoretically. Ultracold fermionic quantum gases in optical lattices provide a clean and tunable implementation of the Hubbard model. At the same time, optical microscopy in these systems gives access to single-site observables and correlation functions, and provides dynamic control of the potential landscape at the single-site level. But so far ultracold atom experiments have not been able to reach the low-temperature regime of the Hubbard model, which becomes particularly interesting when doped.

I will report on the observation of antiferromagnetic long-range order in a repulsively interacting Fermi gas of Li-6 atoms on a 2D square lattice containing about 80 sites. The ordered state is directly detected from a peak in the spin structure factor and a diverging correlation length of the spin correlation function. When doping away from half-filling into a numerically intractable regime, we find that long-range order extends to doping concentrations of about 15%. Our results open the path for a controlled study of the low-temperature phase diagram of the Hubbard model.

[*]Corresponding author: greif@g.harvard.edu

To the list of contents

Single atom- and momentum-resolved investigation of thermal and quantum depletion in metastable Helium Bose condensates

H. Cayla[1], **C. Carcy**[1], **Q. Bouton**[1], **R. Chang**[1], **C. I. Westbrook**[1], **A. Aspect**[1], **M. Mancini**[1], **D. Clément***[1]
1. Laboratoire Charles Fabry, Institut d'Optique, CNRS, Univ. Paris Sud, 2 Avenue Augustin Fresnel 91127 PALAISEAU cedex, France

The interplay of quantum fluctuations and interaction is at the core of intriguing phenomena of quantum many-body physics. An emblematic example, conceptually rather simple, of such a manifestation is the quantum depletion of a Bose condensate occurring at zero temperature. The resulting many-body ground-state, a vacuum of quasi-particles [1], is composed of single-particle excitations on top of the condensate, for which a direct observation has been missing.

We will report on the single-atom-resolved measurement of the momentum distribution in interacting Bose gases of metastable Helium after a 330 ms Time-Of-Flight (TOF). We produce Bose-Einstein condensates of Helium-4 atoms in a metastable state [2], whose internal energy (20 eV) is large enough to allow for an electronic detection of individual atoms in three dimensions [3][4]. We investigate two different potentials where atoms are trapped before being released: a 3D harmonic trap and a 3D optical lattice.

We monitor the TOF distribution of Bose-Einstein condensates produced in a 3D harmonic at various temperatures. It allows us to clearly separate and identify, by their k-dependence, two distinct contributions to the depletion of the condensate: the thermal depletion and the quantum depletion [5]. This observation is illustrated in Fig. 1 where the different scalings of the momentum distribution with momentum k are shown in log-log scale.

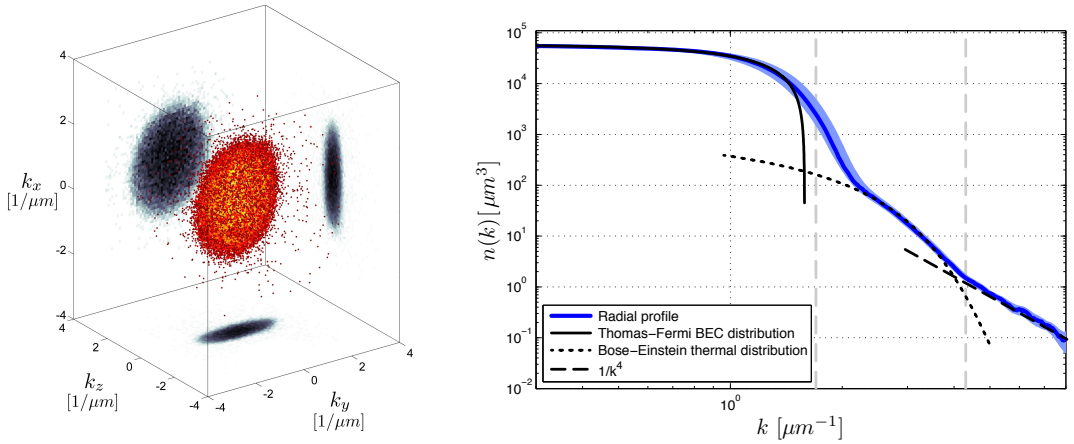

Fig. 1: Left: 3D momentum distribution of a Bose-Einstein condensate released from a 3D harmonic trap. Each red dot is a single atom. We also show the 2D projections of the 3D distribution along each axis.
Right: Cut through the asymptotic momentum density of the 3D condensate (log-log scale). Our detection method yields a large dynamics in atomic density which allows us to identify: (i) the Bose-Einstein condensate, (ii) the thermal depletion and (iii) the quantum depletion (k^{-4} scaling).

When released from a 3D optical lattice, we show that the measured TOF distributions are in the far-field regime of expansion where the density can be precisely mapped onto the in-trap momentum distribution. The far-field condition along with the absence of integration along a line of sight (as done in usual absorption imaging) provide us with novel signals. For instance, we can precisely determine the thermal fraction (and the temperature) as well as the condensed fraction of lattice superfluids, paving the way to establishing finite-temperature phase diagrams with our original approach.

References

[1] N. N. Bogoliubov, J. Phys. (USSR) **11**, 23 (1947).
[2] Q. Bouton, R. Chang, L. Hoendervanger, F. Nogrette, A. Aspect, C. I. Westbrook and D. Clément, Phys. Rev. A **91** 061402(R) (2015).
[3] M. Schellekens, R. Hoppeler, A. Perrin, J. Viana Gomes, D. Boiron, A. Aspect, and C. I.Westbrook, Science **310**, 648 (2005).
[4] F. Nogrette, D. Heurteau, R. Chang, Q. Bouton, C. I. Westbrook, R. Sellem and D. Clément, Rev. Scient. Intrum. **86**, 113105 (2015).
[5] R. Chang, Q. Bouton, H. Cayla, C. Qu, A. Aspect, C. I. Westbrook and D. Clément, Phys. Rev. Lett. **117**, 235303 (2016).

*Corresponding author: david.clement@institutoptique.fr

To the list of contents

Supersolidity with Bose-Einstein condensates

A.Morales[1], **J. Leonard**[1], **P.Zupancic** [1], **T.Esslinger***[1], **T.Donner**[1]
1. ETH Zuerich, Department of Physics, Institute for Quantum Electronics, Otto Stern Weg 1, Zuerich, Switzerland

Supersolidity is a paradoxical state of matter featuring both the crystalline order of a solid and the dissipationless flow typical of a superfluid. The realization of this state of matter requires the breaking of two continuous symmetries, the phase invariance of a superfluid and the translational invariance to form the crystal [1]. Proposed for Helium almost 50 years ago [2], experimental verification of supersolidity remained elusive [3].
Here we report on the realization of such a supersolid state of matter [4]. This state is realized by coupling a Bose-Einstein condensate (BEC) to the modes of two crossed optical cavities. Self-organization to individual cavities only breaks a discrete spatial symmetry and realizes a 'lattice supersolid'. By equally coupling the BEC to both modes we enhance the symmetry of the system to a continuous one and observe simultaneous self-organization to the two cavities. We reveal the high ground state degeneracy of the new supersolid state by measuring the crystal position over many realizations through the light fields leaking from the cavities (Fig.1a).
Using cavity-enhanced Bragg-spectroscopy we measure the excitation spectrum at the superfluid to supersolid phase transition (Fig.1b). In the supersolid phase we detect a Higgs (gapped) and a Goldstone (gapless) branch.

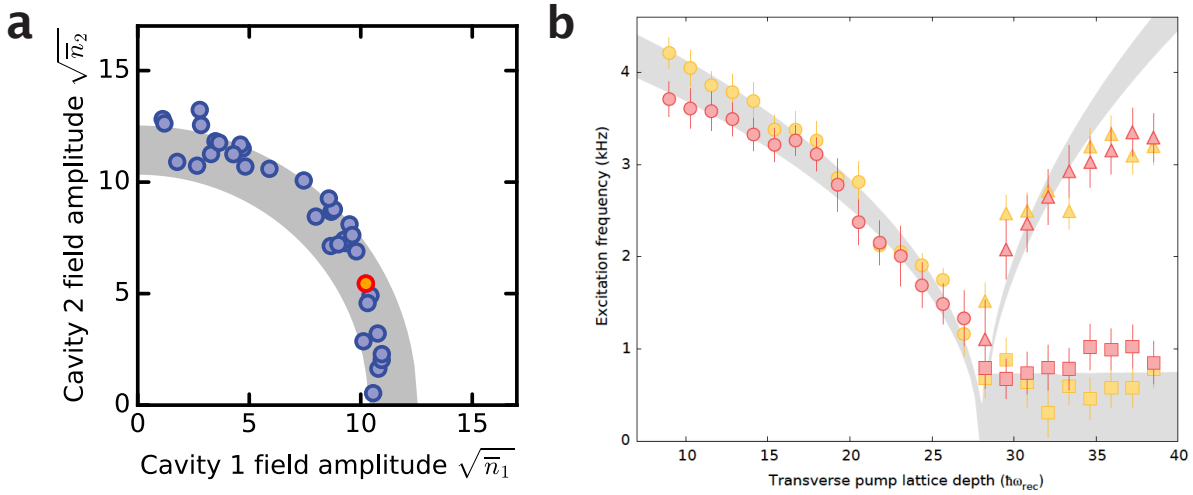

Fig. 1: **a** Measurement of the high ground state degeneracy of the two cavities self-organized ground state as measured from their light field amplitudes upon multiple realizations. **b** Excitation spectrum of the system across the superfluid to supersolid phase transition. After a critical transverse pump power we enter the supersolid phase, where we observe a Higgs and a Goldstone branch.

References

[1] Boninsegni, M. Prokof'ev, N. V. Supersolids: what and where are they? (2012)
[2] Morales, A. Can a solid be superfluid?, SIF-Società Italiana di Fisica, Prima Pagina, (2017).
[3] Kim, D.Y. and Chan, M.H.W. Absence of supersolidity in solid helium in porous Vycor glass. Phys. Rev. Lett. **109**, 155301 (2012).
[4] Leonard, J. Morales, A. Zupancic, P. Esslinger, T. Donner, T., Supersolid formation in a quantum gas breaking a continuous translational symmetry. Nature **543**, 87-90 (2017).

*Corresponding author: esslinger@phys.ethz.ch

To the list of contents

Crossing Over from Attractive to Repulsive Interactions in a Tunneling Bosonic Josephson Junction

Giovanni Ferioli[*1], **G. Spagnolli**[2] **G. Semeghini**[2] **L. Masi**[1] **A. Trenkwalder**[,2] **S. Coop**[2] **M. Landini**[2] **L. Pezzé**[1,2] **G. Modugno**[1] **M. Inguscio**[2] **A. Smerzi**[1,2] **M. Fattori**[1,2]

1. LENS and Universitá di Firenze, 50019 Sesto Fiorentino, Italy

2. CNR Istituto Nazionale Ottica, 50019 Sesto Fiorentino, Italy

We study the dynamics of a spatial bosonic Josephson junction realized by an atomic BEC loaded in a double well optical potential [1]. We can tune both the tunneling energy, by controlling the height of the barrier between the two wells, and the interaction energy U using a magnetic Feshbach resonance. By preparing the system with a finite population imbalance $z \neq 0$, we observe the transition from Rabi to Josephson oscillations between the two wells when the interaction goes from zero to finite values. In particular we observe that the oscillation frequency increases for $U > 0$ and decreases on the negative side, until it vanishes in correspondence of a quantum phase transition that we studied in a previous work [2]. The exquisite control of tunneling and interactions in the system paves the way to the realization of a Mach-Zehnder interferometer (built with the two spatial modes of the double-well potential) with trapped atoms: with non interacting clouds we can perform the linear beam splitter operation, while interactions could be used to create many-body quantum-entangled states, improving the phase resolution of the device beyond the shot noise limit.

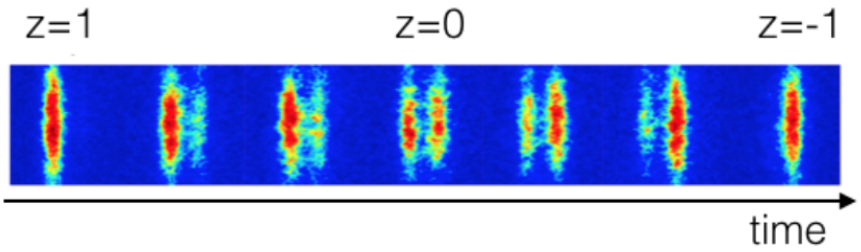

Fig. 1: Oscillation of population imbalance between the two spatial mode

References

[1] G. Spagnolli *et al.*. PRL accepted

[2] A. Trenkwalder *et al.*, Nature Physics (2016)

*Corresponding author: ferioli@lens.unifi.it

To the list of contents

Real-time dynamics of lattice gauge theories with a few-qubit quantum computer

E. Martinez[1], C. Muschik[*2,3], P. Schindler[1], D. Nigg[1], A. Erhard[1], M. Heyl[2,3], P. Hauke[2,3], M. Dalmonte[2,3], T. Monz[1], P. Zoller[2,3], and R. Blatt[1,2]

1. Institute for Experimental Physics, University of Innsbruck, 6020 Innsbruck, Austria
2. Institute for Quantum Optics and Quantum Information of the Austrian Academy of Sciences, 6020 Innsbruck, Austria
3. Institute for Theoretical Physics, University of Innsbruck, 6020 Innsbruck, Austria
4. Physik Department, Technical University Munich, 85747 Garching, Germany

Gauge theories are fundamental to our understanding of interactions between the elementary constituents of matter as mediated by gauge bosons. However, computing the real-time dynamics in gauge theories is a notorious challenge for classical computational methods. In the spirit of Feynman's vision of a quantum simulator, this has recently stimulated theoretical effort to devise schemes for simulating such theories on engineered quantum-mechanical devices, with the difficulty that gauge invariance and the associated local conservation laws (Gauss laws) need to be implemented. We report the first experimental demonstration of a digital quantum simulation of a lattice gauge theory[1], by realising 1+1-dimensional quantum electrodynamics (Schwinger model) on a few-qubit trapped-ion quantum computer. We are interested in the real-time evolution of the Schwinger mechanism, describing the instability of the bare vacuum due to quantum fluctuations, which manifests itself in the spontaneous creation of electron-positron pairs. To make efficient use of our quantum resources, we map the original problem to a spin model by eliminating the gauge fields in favour of exotic long-range interactions, which have a direct and efficient implementation on an ion trap architecture. We explore the Schwinger mechanism of particle-antiparticle generation by monitoring the mass production and the vacuum persistence amplitude. Moreover, we track the real-time evolution of entanglement in the system, which illustrates how particle creation and entanglement generation are directly related. Our work represents a first step towards quantum simulating high-energy theories with atomic physics experiments, the long-term vision being the extension to real-time quantum simulations of non-Abelian lattice gauge theories.

References

[1] E. A. Martinez, C. A. Muschik, P. Schindler, D. Nigg, A. Erhard, M. Heyl, P. Hauke, M. Dalmonte, T. Monz, P. Zoller, and R. Blatt, Nature 534, 516-519 (2016).

*Corresponding author: Christine.Muschik@uibk.ac.at

To the list of contents

Single organic molecule coupling to a hybrid plasmonic waveguide

S. Grandi[1], M. A. Nielsen[2], J. Cambiasso[2], S. Boissier[1], K. D. Major[1], C. Reardon[3], T. F. Krauss[3], R. F. Oulton[2], E. A. Hinds[1], A. S. Clark*[1]

1. Centre for Cold Matter, Blackett Laboratory, Imperial College London, South Kensington, SW7 2AZ, UK
2. Experimental Solid State Physics Group, Blackett Laboratory, Imperial College London, South Kensington, SW7 2AZ, UK
3. Department of Physics, University of York, York, YO10 5DD, UK

Efficient photon sources will enable many quantum technologies. Single dibenzoterrylene (DBT) molecules are promising photon sources, but often emit in an unknown direction making photon collection challenging. Dielectric structures redirect emission into single optical modes [1], but are relatively large due to the diffraction limit of light. Plasmonic devices, such as antennae, can concentrate the electromagnetic field at the site of an emitter on a surface in volumes below the diffraction limit and redirect emission into well-controlled directions, but often suffer from losses. Recently, planar dielectric antennae have shown promise for redirecting emission [2], however often they do not provide single mode operation or compatibility with integrated photonics.

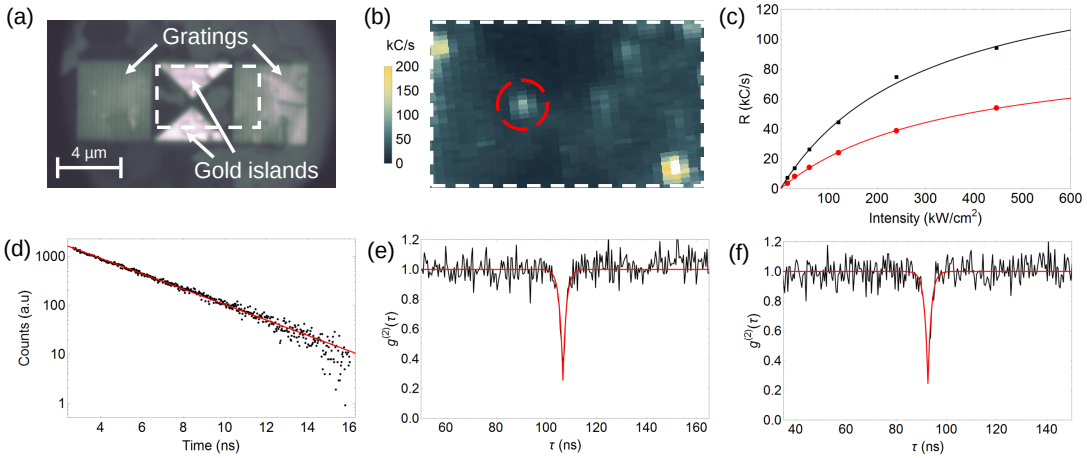

Fig. 1: (a) White-light image of a HPW showing input/output grating couplers and anthracene crystals on the surface. (b) Molecule fluorescence from the dashed box in (a). (c) Saturation curves for the molecule indicated with a red dashed circle in (b), showing count rates collected from the confocal microscope (black squares) and from a grating coupler (red circles). (d) Pulsed laser measurement of the molecule excited state lifetime. (e) $g^{(2)}(\tau)$ measured from the microscope only and (f) $g^{(2)}(\tau)$ measured from the grating and microscope.

Here we present a hybrid dielectric–metal approach in coupling a single molecule to an optical mode in an integrated planar device. We designed and fabricated a hybrid plasmonic waveguide (HPW) consisting of a dielectric slab with a nanoscale gap patterned in gold on the surface, as shown in Fig. 1(a). Replacing the silicon layer used in our previous work [3] with titanium dioxide (TiO_2) allows operation at ~ 785 nm, the emission wavelength of DBT. Light propagating in the TiO_2 layer passes through the gap between the islands of gold. The width of the gap controls mode confinement: when the gap is <100 nm the propagating mode is mainly in the gap providing strong confinement; but when the gap is wider the mode decouples from the gold and propagates mainly in the TiO_2 with low loss. We deposited DBT-doped anthracene crystals on the surface (Fig. 1(a)) using a supersaturated vapour growth technique [4]. Using confocal fluorescence microscopy we found a DBT molecule positioned near the gap (Fig. 1(b)). We then measured the saturation intensity of the molecule (Fig. 1(c)) to be $I_{sat} = 325(27)$ kW/cm^2. Illuminating the molecule with a pulsed laser (Fig. 1(d)) we measured the lifetime of the molecule to be 2.74(2) ns. Under CW excitation we measured the second-order correlation function $g^{(2)}(\tau)$ of the light emitted directly into the microscope. This shows clear anti-bunching (Fig. 1(e)) with $g^{(2)}(0) = 0.25(6)$ proving this to be a single molecule. By detecting photons simultaneously from the microscope and from the grating coupler we measured $g^{(2)}(0) = 0.24(6)$ (Fig. 1(f)), demonstrating that this single molecule was emitting into the waveguide mode. By measuring the optical losses in our setup we calculated the coupling efficiency from the molecule to the HPW to be $\sim 22\%$. This method provides a route to building waveguide sources of photons in planar integrated quantum photonic circuits for applications in quantum technology.

References

[1] S. Faez *et al.*, Phys. Rev. Lett. **113**, 213601 (2014).
[2] X. L. Chu *et al.*, Optica **5**, 203–208 (2014).
[3] M. A. Nielsen *et al.*, Nano. Lett. **16**, 1410–1414 (2016).
[4] C. Polisenni *et al.*, Opt. Express **24**, 5615–5627 (2016).

*Corresponding author: alex.clark@imperial.ac.uk

To the list of contents

Identifying optical transitions in highly charged ions with applications for metrology and searches of variation of the fine-structure constant

H. Bekker[*1], **A. Windberger** [1], **N. Potters** [1], **J. Rauch** [1], **J. Berengut** [2], **A. Borschevsky** [3], **J. R. Crespo López-Urrutia** [1]

1. Max-Planck-Institut für Kernphysik, Saupfercheckweg 1, 69117 Heidelberg, Germany
2. School of Physics, The University of New South Wales, Sydney NSW 2052, Australia
3. Van Swinderen Institute, Universiteit Groningen, Nijenborgh 4, 9747 AG Groningen, Netherlands

Many highly charged ions (HCI) have been proposed for use in next generation optical clocks for metrology purposes, see for example [1, 2]. Due to the compact size of their electronic cloud, HCI are less sensitive to external perturbations than the neutral and singly charged systems that are currently widely employed in metrology. Furthermore, increased relativistic effects in HCI lead to a strong sensitivity to variation of the fine-structure constant α. However, for these HCI, theory is not capable of predicting the energy level structures to the precision required for precision laser spectroscopy.

To address this issue, we investigated several of the proposed HCI, which we produced, trapped, and collisionally excited in the Heidelberg electron beam ion trap (HD-EBIT). The wavelengths of subsequent fluorescence light were determined at the ppm-level using a grating spectrometer. We present our latest results for Ir^{17+}, which features transitions with an extremely high sensitivity to variation of the fine-structure constant [1,3]. Identifying these transitions is cumbersome due to the uncertainties of the predictions, the large amount of observed transitions, and their low intensities. However, by observing their Zeeman splitting in the strong magnetic field of the HD-EBIT, many important lines could be identified, c.f. Fig. 1.

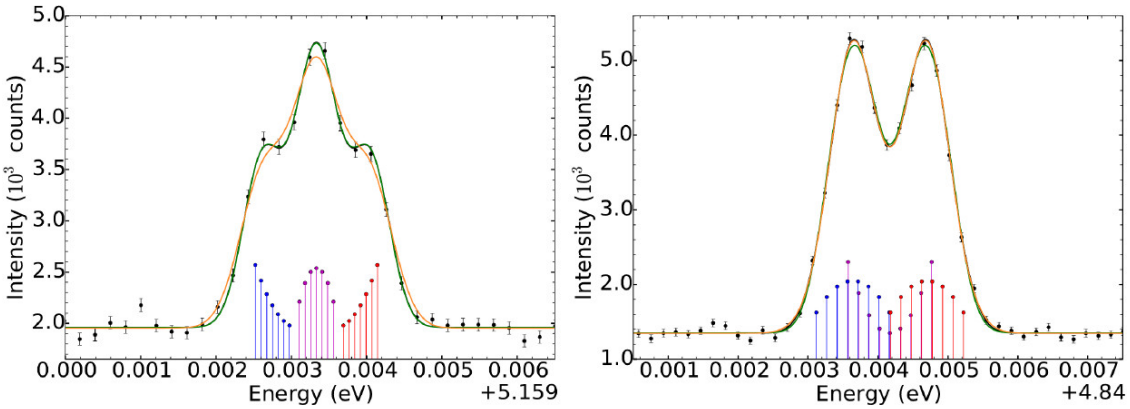

Fig. 1: Observed Zeeman splitting of two Ir^{17+} lines (black points), and fits to the data based on predicted line shapes (solid lines). The individual Zeeman components as determined by the fit, are shown by vertical lines.

Furthermore, our latest results for Pr^{9+} and Pr^{10+} are discussed. In addition to the previously mentioned advantageous properties of HCI, Pr^{9+} is predicted to have a metastable state with an extremely long lifetime of 21 megayears, which potentially makes it suitable as a quantum memory [2].

All the presented results are used to benchmark state-of-the-art atomic theory calculations. Our investigations aim to provide a deeper insight into the suitability of the proposed HCI for metrology purposes, and to pave the way for future laser spectroscopy.

References

[1] J. C. Berengut *et al.*, Phys. Rev. Lett. **106**, 210803 (2011)
[2] M. S. Safronova *et al.*, Phys. Rev. Lett. **113**, 030801 (2014)
[3] A. Windberger *et al.*, Phys. Rev. Lett. **114**, 150801 (2015)

*Corresponding author: bekker@mpi-hd.mpg.de

To the list of contents

Monochromatic electron beam from Rydberg atoms

E. Moufarej*[1], Z. Mazzotta[1], M. Vielle-Grosjean[1], F. Robicheaux[2], Y. J. Picard[1], D. Comparat[1]
1. Laboratoire Aimé Cotton, CNRS, Université Paris-Sud, ENS Paris-Saclay
Bât. 505, 91405 Orsay, France.
2. Department of Physics and Astronomy, Purdue University
West Lafayette, Indiana 47907, USA

We develop a source of focused electron and ion beams, through ionization of a high flux effusive atomic beam. The atomic (cesium) beam is obtained from an effusive oven. The low transverse temperature (sub-K range) and the relative density of the starting atomic sample ensure excellent initial conditions in order to obtain a bright and monochromatic (≈1 meV) charged source (Fig. 1(b)). Typically, by photo-ionizing the atomic beam, the energy spread of extracted electrons is limited by chromaticism created during the ionization process, related to the laser's waist. To overcome those effects, we use Rydberg atoms field ionization (Fig. 1(a)).

Here, we present an experimental and theoretical study of the photoexcitation and ionization of high quantum defect states, using excitation from the 7s state in cesium to Rydberg states in the presence of a uniform electric field [1]. Such states can exhibit complex ionization behavior, for instance, highly localized growth in the ionization rate due to interference effects. We observe that large changes in the Rydberg ionization rate from small changes in electric field are possible when a nearly stable state crosses a more unstable state (Fig. 1(c)). A fast variation of the ionization rate with electric field allows for the production of charged beams with very low energy spread.

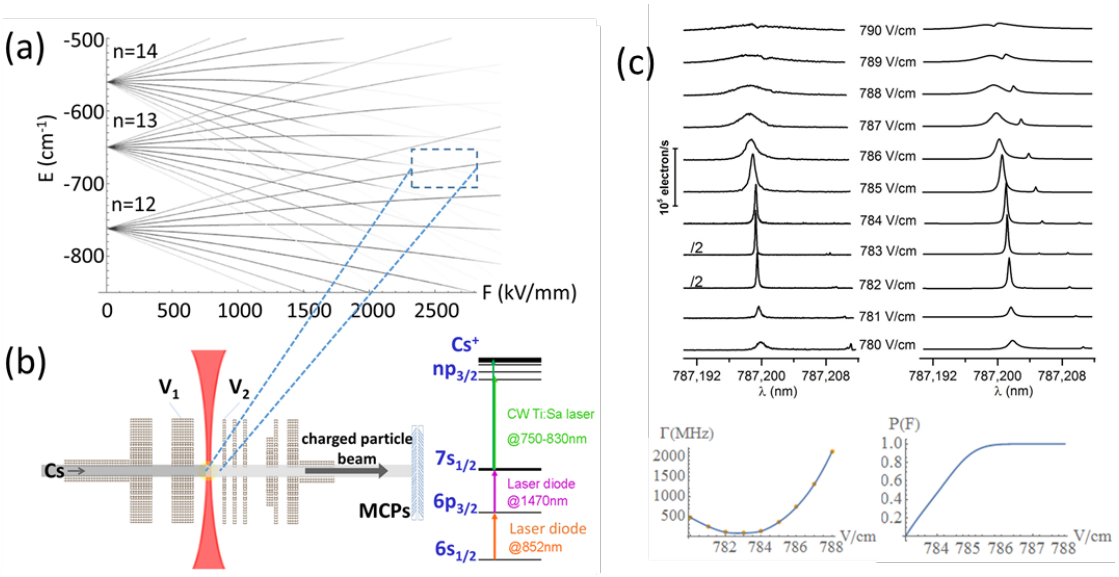

Fig. 1: (a) and (b) Principle of ion or electron beam production using sharp Rydberg forced field ionization. Electrons and ions are produced by laser excitation of Rydberg states that are then field ionized. (c) Scan of ionization rate versus wavelength for varying field, displaying interference narrowing.

References

[1] E. Moufarej *et. al.*, Physical Review A, **95**, 043409 (2017)

*Corresponding author: elias.moufarej@univ-paris13.fr

To the list of contents

Atomic clock and quantum many-body physics

Jun Ye[*1]
1. JILA, National Institute of Standards and Technology and University of Colorado Boulder, Colorado 80309-0440, USA

Quantum state engineering of ultracold atoms and precise control of laser coherence have revolutionized a new generation of atomic clocks with accuracy at the 18th digit. This progress has benefited greatly from microscopic understandings of atomic interactions in the quantum regime. In return, the unified front of precision metrology and quantum physics has enabled exploration of many-body quantum systems. Our next clock will have at its core a Sr Fermi degenerate gas configured as a band insulator in a three-dimensional optical lattice. The correlated, high-density atomic system provides a clear path for improving the clock performance to the next decimal point, and sets the stage to explore spin-orbit coupling and long-range interactions in a many-body spin system. These emerging quantum technologies will allow us to test the fundamental laws of nature and search for new physics.

[*]Corresponding author: Ye@jila.colorado.edu

To the list of contents

Observation of the 1*S*-2*S* transition in trapped antihydrogen

N. Madsen[*1]
1. Department of Physics, College of Science, Swansea University
Singleton Park, Swansea SA2 8PP, UK

Antihydrogen, the bound state of an antiproton and a positron and the antimatter counterpart of hydrogen, holds the promise of some of the most precise tests imaginable on the fundamental symmetry of matter and antimatter. We report the first observation of the 1*S*-2*S* transition in trapped antihydrogen[1], a milestone in the quest to use antihydrogen to do a precision test of the CPT Theorem, a cornerstone of the Standard Model. The 1*S*-2*S* transition is known to $\sim$15 decimal places in hydrogen[2]. We discuss how this first observation was made possible through a number of key advances in the ability to magnetically trap antihydrogen, that must be made from its constituents. We further discuss the crucial enhancement of the 243 nm laser light that excites the two-photon transition and the unique detection capabilities of the ALPHA apparatus necessary to probe the ultimately few anti-atoms available for these experiments. This first observation was consistent with the equivalent transition in hydrogen to $\sim 2\times10^{-10}$, and paves the way for measurements of the line shape in order to establish tight experimental bounds on the CPT symmetry of hydrogen and antihydrogen.

References

[1] ALPHA Collaboration, Nature **541**, 566 (2017)
[2] G. Parthey et al., Phys. Rev. Letts. **107**, 203001 (2011)

*Corresponding author: n.madsen@swansea.ac.uk

To the list of contents

An Improved Value of the Atomic Mass of the Proton

Florian Köhler-Langes[*1], **Fabian Heiße**[1,2,3], **Sascha Rau**[1,3], **Sven Junck**[4], **Andreas Mooser**[5], **Wolfgang Quint**[2], **Stefan Ulmer**[5], **Günter Werth**[4], **Klaus Blaum**[1], **Sven Sturm**[1]

1. Max Planck Institute for Nuclear Physics (MPIK), Saupfercheckweg 1, 69117 Heidelberg, Germany
2. GSI Helmholtzzentrum für Schwerionenforschung GmbH, Planckstraße 1, 64291 Darmstadt, Germany
3. Universität Heidelberg, Fakultät für Physik und Astronomie, Im Neuenheimer Feld 227, 69120 Heidelberg, Germany
4. Universität Mainz, Institut für Physik, Staudingerweg 7, 55099 Mainz, Germany
5. RIKEN, Ulmer Fundamental Symmetries Laboratory, Wako, Saitama 351-0198, Japan

The electron, the proton and the neutron are the basic building blocks of atomic matter. The precise knowledge of their properties, e.g. their masses, is of utmost importance for tests of fundamental physics and the current revision of the SI base units.
In this context an experiment dedicated to the determination of the atomic mass of the proton and the neutron has been designed, assembled and commissioned. It is based on the former g-factor experiment for highly charged ions, which provided most stringent tests of bound-state QED by studying the bound-electron g-factors of $^{28}Si^{13+}$ [1], $^{28}Si^{11+}$ [2] and the g-factors of the calcium isotopes $^{40}Ca^{17+}$ and $^{48}Ca^{17+}$ [3]. Moreover, it delivered the most precise value of the atomic mass of the electron [4]. The new experiment consists of a stack of five individual cylindrical Penning traps, enclosed in a vacuum vessel operated at liquid helium temperature. Various single ions can be trapped at different locations for months.
For the high-precision measurement of the atomic mass of the proton the cyclotron frequency ratio of a single proton, $\nu_c(H^+)$, and a single highly-charged carbon ion, $\nu_c(^{12}C^{6+})$, is measured:

$$m(H^+) = \frac{1}{6}\frac{\nu_c(^{12}C^{6+})}{\nu_c(H^+)} m(^{12}C^{6+}),$$

where the relative uncertainty of $m(^{12}C^{6+})$ due to the missing electrons and their binding energies is sufficiently small ($\delta m/m = 9 \cdot 10^{-14}$).
In order to measure both cyclotron frequencies in the same electric and magnetic field configuration, both ions are transported alternately into a Penning trap, the Measurement Trap (MT), consisting of seven cylindrical electrodes. These electrodes serve to produce an extremely harmonic quadrupole trapping field by cancelling out to a large extent higher orders electric field contributions by properly chosen voltages. By applying exactly the same electric field configuration for both ions with different charge/mass ratio, requires two separate, precisely tuned axial resonators for non-destructive frequency detection. The modified cyclotron frequency is detected via the phase sensitive measurement technique PnA [5].
Aiming for relative precisions of less than $1 \cdot 10^{-11}$, magnetic field fluctuations which limit the statistical uncertainty have to be overcome. For this purpose, the simultaneous PnA technique has been developed. Here, the modified cyclotron frequency of a highly-charged ion, $\nu_+(HCI)$, placed in an adjacent Penning trap, the Reference Trap (RT), and the modified cyclotron frequency of the ion of interest in the MT, e.g. of the proton or the carbon ion, are measured simultaneously, which enables dramatically longer phase evolution times. Thus, the two ultra-precise cyclotron frequency ratios: $R_1 = \nu_c(H^+)/\nu_+(HCI)$ and $R_2 = \nu_c(^{12}C^{6+})/\nu_+(HCI)$ can be determined and combined to finally derive the desired frequency ratio: $R_1/R_2 = \nu_c(H^+)/\nu_c(^{12}C^{6+})$.
At this conference, the new setup will be introduced and the latest results on the atomic mass of the proton will be discussed [6].

References

[1] S. Sturm *et al.*, Phys. Rev. Lett. **107**, 023002 (2011).
[2] A. Wagner *et al.*, Phys. Rev. Lett. **110**, 033003 (2013).
[3] F. Köhler-Langes *et al.*, Nat. Commun. **7**, 10246 (2016).
[4] S. Sturm *et al.*, Nature **506**, 13026 (2014).
[5] S. Sturm *et al.*, Phys. Rev. Lett. **107**, 143003 (2011).
[6] F. Heiße *et al.*, unpublished.

*Corresponding author: florian.koehler@mpi-hd.mpg.de

To the list of contents

Precision spectroscopy on the $2\,^3S \rightarrow 2\,^1S$ transition in ultracold helium inside a magic wavelength trap

R.J. Rengelink[*1], **R.P.M.J.W. Notermans**[1], **W. Vassen**[1]
1. LaserLaB, Department of Physics and astronomy, Vrije Universiteit
De Boelelaan 1081, 1081 HV Amsterdam, NL

Atomic level energies experience minute shifts caused by the finite size of the nucleus. When this shift was measured in muonic hydrogen a 5σ discrepancy was found with the then most recent CODATA recommended value for the proton radius [1]. Since then this discrepancy has only increased and has been extended to the deuteron as well [2]. The discrepancy has become known as the proton radius problem. Does this problem exist for other atoms as well? To answer this question new measurements on the helium nucleus, both in muonic and electronic systems, are underway. We are aiming for an improved measurement of the doubly forbidden $2^3S \rightarrow 2^1S$ transition in neutral helium. By combining frequency metrology with ab initio QED calculations the ^{3}He to ^{4}He nuclear charge radius difference can be determined with sub-attometer accuracy, competitive with current measurements in muonic He^+ [3].

In order to reach this goal we need to improve our previous measurement, which was done in a Bose-Einstein condensate of ^{4}He and a degenerate Fermi gas of ^{3}He trapped in a 1557 nm optical dipole trap (ODT) and was accurate to 2.3 kHz [4], by an order of magnitude. To entirely eliminate the largest term in the uncertainty budget, the ac-Stark shift induced by the ODT, we have implemented a magic wavelength ODT.

Previously, we calculated polarizabilities of the $2\,^3S$ and $2\,^1S$ levels and found a magic wavelength candidate at 319.815 nm [5]. We built a laser system at this wavelength, producing over 2 W of power, and used it to trap ^{4}He atoms [6]. Currently, we have implemented a full ODT with this laser system and are using it for spectrosopy. By varying the wavelength of the laser we have now verified our calculations within their accuracy and we have found the precise position of the magic wavelength at 319.816 nm, accurate enough that the uncertainty in the Stark shift is no longer significant compared to other errors. Finally, we have made a number of other improvements to the set-up and measurement scheme to better deal with other systematics, most notably an improved linewidth of the spectroscopy laser to better deal with the mean-field shift [7] and we hope to present a more accurate determation of the transition frequency in ^{4}He at the conference.

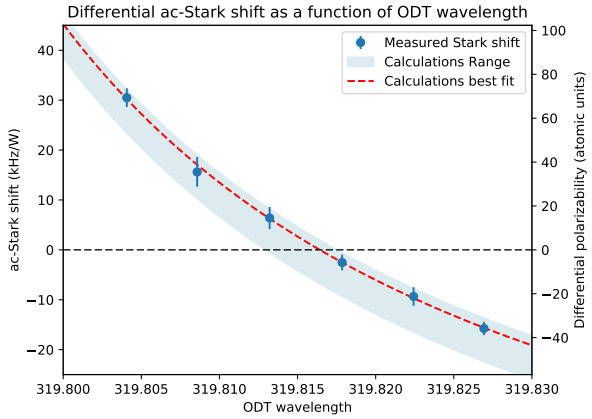

Fig. 1: (Preliminary) ac-Stark shift as a function of trap laser wavelength. The blue band is the calculated differential polarizability from reference [5] with its uncertainty range (rescaled to the data). The leading uncertainty in this calculation is a constant offset caused by the continuum contribution to the polarizability. The dashed line is the calculation with this offset fitted to the data.

References

[1] R. Pohl *et al.*, Nature **466**, 213-216 (2010)
[2] R. Pohl *et al.*, Science **353**, 669-673 (2016)
[3] A. Antognini *et al.*, Can. J. Phys. **89**, 47-57 (2011)
[4] R. van Rooij, J.S. Borbely, J. Simonet, M.D. Hoogerland, K.S.E. Eikema, R.A. Rozendaal, and W. Vassen, Science **333**, 196-198 (2011)
[5] R.P.M.J.W. Notermans, R.J. Rengelink, and W. Vassen *et al.*, Phys. Rev. A, **90**, 052508 (2014)
[6] R.J. Rengelink, R.P.M.J.W. Notermans, and W. Vassen *et al.*, Appl. Phys. B **122**, 122 (2016)
[7] R.P.M.J.W. Notermans, R.J. Rengelink, and W. Vassen *et al.* Phys. Rev, Lett. **117**, 123001 (2016)

*Corresponding author: r.j.rengelink@vu.nl

To the list of contents

Vector Correlations in Molecular Photodissociation: Production of Spin-Polarized H-Atoms and Femtosecond Stereodynamics

O. S. Vasyutinskii*
1. Ioffe Institute, 26 Polytechnicheskaya, 194021 St.Petersburg, Russia

The talk presents recent achievements in the rapidly growing field of angular momentum polarization in reactive collisions and molecular photodissociation. The outstanding role of angular momentum in chemical reactions has been realized many years ago. Molecules always interact with each other by anisotropic forces, giving rise to anisotropic angular momentum distributions which may have relation to approach direction, scattering direction, photon polarization, etc [1].

Although the production of spin-polarized hydrogen atoms in molecular photodissociation by circularly polarized photolysis laser was considered theoretically more than thirty years ago [2], it has been directly experimentally observed only recently, by detection of the polarized fluorescence in the H atoms excited by circularly polarized Lyman-alpha radiation [3]. More recently, a new and more practically convenient experimental techniques have been realized [4-6] allowing for direct measurement of the velocity dependence of hydrogen atom spin polarization with high resolution and sensitivity. The strategy was a two-color high-n Rydberg excitation of hydrogen atoms by a linearly polarized Lyman-α laser and a circularly polarized UV tagging laser combined either with Rydberg time-of-flight approach, or with slice imaging, followed in both cases by a pulsed-field ionization. The techniques allow for experimental determination of all three anisotropy parameters α_1 γ_1, and γ_1' [1] which contain important information on the photodissociation dynamics (excited state symmetry, nonadiabatic and long-range interactions, quantum mechanical scattering phase shifts, ets.). The techniques were realized in photodissociation of HCl, HBr, and DBr molecules and can be used for production of dense highly polarized atomic and nuclear targets and beams for high-energy collision and surface scattering experiments. Moreover, the method can be applied for the study of dissociation of polyatomic molecules and reactive scattering and promises a wealth of new detail concerning these elementary processes.

The talk also presents the results of experimental and theoretical study of time-resolved vector correlations in the femtosecond photolysis of polyatomic molecules by predissociation and direct dissociation mechanisms. Experimentally, the photolysis of methyl iodide (CH_3I) by linearly polarized laser beam via the B-band at 201.2 nm has been studied [7-8]. Time-dependent anisotropy parameters β has been determined from fragment angular distributions using the pump-probe technique coupled with the velocity map imaging detection of the dissociation products CH_3(v=0) and $I^*(^2P_{1/2})$. The results obtained were theoretically interpreted with a quantum mechanical quasiclassical theory which took into account the alignment of CH_3 photofragments orbital momentum, nonadiabatic interaction between the $^3R_1$ and $^3A_1$(E) excited states, excited state symmetries, the parent molecule rotation during dissociation, and the CH_3 fragment rotation after the bond break. The time-dependent vector correlations were described by a set of anisotropy parameters [1]. The results obtained demonstrate an important role of the molecular orbital angular momentum alignment and molecular rotation on the time-dependent photolysis. Comparison between the photolysis via the predissociative $^3R_1$ and direct dissociative $^3A_1$(E) excited states showed the profound role of the predissociation mechanism. The $^3R_1$ and $^3A_1$(E) excited state lifetimes, anisotropy transforming coefficients, parent molecule beam temperature, and molecular rotation angles were determined from the experimental data.

References

[1] A. G. Suits and O. S. Vasyutinskii, Chem. Rev. **108**, 3706 (2008).
[2] O. S. Vasyutinskii, Sov. Phys. JETP **54**, 855 (1981).
[3] D. Sofikitis *et al.*, J. Chem. Phys. **129**, 144302 (2008).
[4] B. M. Broderick *et al.*, J. Phys. Chem. Lett. **4**, 3489 (2013).
[5] B. M. Broderick *et al.*, Chem. Phys. Lett. **635**, 350 (2015).
[6] B. M. Broderick *et al.*, 2014 Rev. Sci. Instr. **85**, 053103 (2014).
[7] M. G. Gonzalez *et al.*, J. Chem. Phys. **135**, 021102 (2011).
[8] M. E. Corrales *et al.*, J. Phys. Chem. Lett. **7**, 4458 (2016).

*Corresponding author: osv@pms.ioffe.ru

To the list of contents

Electron-Nuclear Coupling through Autoionizing States after Strong-Field Excitation of H_2 Molecules

Yonghao Mi*, **Nicolas Camus, Lutz Fechner, Martin Laux, Robert Moshammer, Thomas Pfeifer**†

Max-Planck-Institut für Kernphysik
Saupfercheckweg 1, 69117 Heidelberg, Germany

When an H_2 molecule is exposed to a strong laser field, the following two single ionization channels may occur:

$$H_2 \xrightarrow{IR} H_2^+ + e^- \tag{1}$$

$$H_2 \xrightarrow{IR} H^+ + H + e^- \tag{2}$$

The first channel is called bound ionization, in which one electron is freed by the laser field and the molecule ends up as a bound molecular ion H_2^+ and a free electron. The second channel is named dissociative ionization, where the H_2 molecule breaks up into a proton, a hydrogen atom and a free electron.

By using a Reaction Microscope (REMI) [1] and ultrashort laser pulses, we investigated channel-selective electron emission from strong-field ionization of H_2 [2]. Measuring of electrons and ions in coincidence, we distinguished the bound and dissociative ionization channels and extracted electron momenta for the two channels. According to the two-step mechanism [3], the laser-induced dissociation of H_2 molecules is described as follows: the molecule is ionized by the laser field in the first step and then dissociates as the vibrational wave packet is excited from the bound $1s\sigma_g$ state to the repulsive $2p\sigma_u$ state in most cases, which means that the dissociative ionization process is independent from the bound ionization process. On first approximation, the electrons from the two channels should thus be the same. As shown in Fig. 1, the fanlike stripes and the above-threshold ionization rings appear for both channels, as expected from the two-step mechanism. However, an enhancement of the photoelectron yield in the low-energy region for the bound ionization channel can be clearly observed.

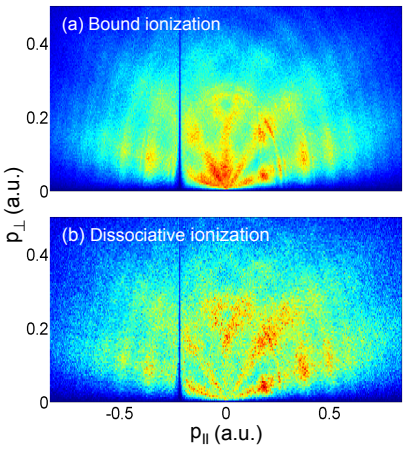

Fig. 1: Electron momentum distribution for (a) bound ionization and (b) dissociative ionization.

We interpret the low-energy enhancement in the electron yield for bound ionization as being due to the population and subsequent decay of autoionizing states. For H_2 molecules, the autoionzing states represent a series of high-lying Rydberg states and are characterized by a simultaneous electronic and vibrational excitation. Instead of populating the H_2^+ bound state and being excited to the repulsive state for dissociation, the molecule can be excited to the above-mentioned autoionizing state located above the ionization limit. Therefore, an autoionization process occurs, in which the vibrational energy of the nuclei is transferred to the excited electron, which becomes free and appears in the photoelectron momentum spectra.

References

[1] J. Ullrich, R. Moshammer, A. Dorn, R. Dörner, L. P. H. Schmidt, and H. Schmidt-Böcking, Rep. Prog. Phys. **66**, 1463 (2003)
[2] Y. Mi, N. Camus, L. Fechner, M. Laux, R. Moshammer, and T. Pfeifer, Phys. Rev. Lett. (2017), in press
[3] M. F. Kling, C. Siedschlag, A. J. Verhoef, J. I. Khan, M. Schultze, T. Uphues, Y. Ni, M. Uiberacker, M. Drescher, F. Krausz, and M. J. J. Vrakking, Science **312**, 246 (2006)

*Corresponding author: yonghao.mi@mpi-hd.mpg.de
†Corresponding author: thomas.pfeifer@mpi-hd.mpg.de

To the list of contents

Control of 3D photoelectron wavepackets using single beam bichromatic and polarization shaped ultrashort laser pulses

D. Pengel[*1], **S. Kerbstadt**[1], **D. Johannmeyer**[1], **L. Englert**[1], **T. Bayer**[1], **M. Wollenhaupt**[1]
1. Ultrafast Coherent Dynamics, Institute of Physics, Carl von Ossietzky Universität Oldenburg
Carl-von-Ossietzky-Str. 9-11, 26129 Oldenburg, Germany

We report on the generation and control of complex shaped, three dimensional (3D) wave packets using single beam bichromatic and polarization shaped laser pulses. Coherent control is based on the interference of multiple quantum pathways connecting the initial system state with a preselected target channel. In our approach the interplay of selection rules and intra pulse frequency mixing disentangles different quantum pathways. In the experiment we use polarization-tailored bichromatic fields produced by our novel 4f polarization shaper setup [1][2]. It provides full control over all bichromatic pulse parameters such as the frequency and amplitude ratio, the spectral phase profile (including CEP and relative phase) and the polarization state of both colors. Using bichromatic polarization shaped laser fields we observe complex shaped 3D electron wavepackets measured by velocity map imaging and retrieved by tomographic reconstruction [3].

In the first experiment we study sequences of two counter rotating, circular polarized laser pulses. These pulse sequences generate vortex shaped electron wavepackets with different rotational symmetries, relying on the quantum paths selected. In general, the coherent superposition of two continuum electron wavepackets with quantum numbers m_1 and m_2 of different sign leads to electron vortices with $c_{|m_1-m_2|}$ rotational symmetries. We present measurements of perturbative electron vortices with c_6 symmetry and nonperturbative electron vortices with c_4 symmetry created from multi photon ionization of potassium atoms [4]. In addition, creation of electron vortices with ultra-broadband few-cycle laser pulses is discussed. Secondly, we show the creation of unusual superposition states using bichromatic, orthogonal linear laser pulses. Finally, we show how the combination of bichromatic fields with polarization control permits selective detection of single $|l,m\rangle$-states.

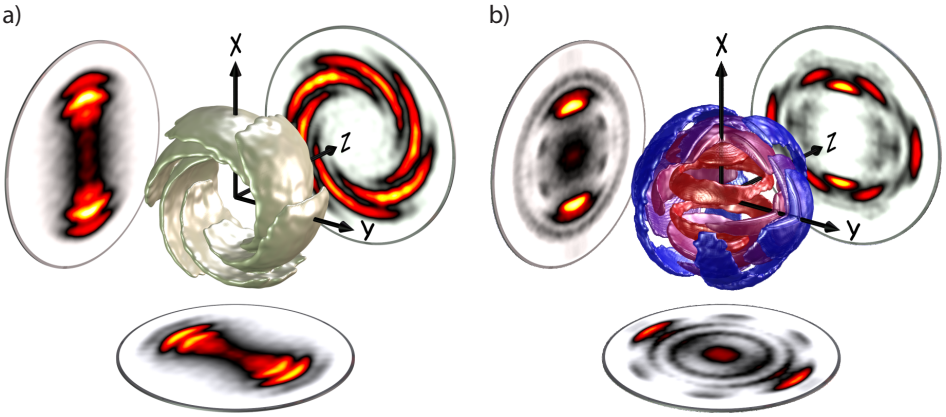

Fig. 1: Measured 3D electron wavepackets using velocitiy map imaging and tomographic reconstruction. **a)** Measured 3D electron vortex with retrieved projections. A sequence of two counter rotating circular polarized laser pulses interacts with gaseous potassium and produces an electron vortex in the continuum. **b)** Measured 3D electron wavepacket generated from interaction between orthogonal linear polarized bichromatic laser pulses and gaseous potassium.

References

[1] S. Kerbstadt, L. Englert, T. Bayer, M. Wollenhaupt, Opt. Express, *accepted* (2017)
[2] S. Kerbstadt, L. Englert, T. Bayer, M. Wollenhaupt, J. Mod. Opt. DOI: 10.1080/09500340.2016.1271151 (2016)
[3] M. Wollenhaupt, M. Krug, J. Köhler, T. Bayer, C. Sarpe Tudoran, and T. Baumert, Appl. Phys. B **95**, 647 (2009)
[4] D. Pengel, S. Kerbstadt, D. Johannmeyer, L. Englert, T. Bayer, M. Wollenhaupt, Phys. Rev. Lett. **118**, 053003 (2017)

*Corresponding author: dominik.pengel@uni-oldenburg.de

To the list of contents

Dipolar quantum gases and liquids

Tilman Pfau[*1]
1. 5. Physikalisches Institut and Center for Integrated Quantum Science and Technology (IQST), Universität Stuttgart, Germany

Dipolar interactions are fundamentally different from the usual van der Waals forces in real gases. Besides the anisotropy the dipolar interaction is nonlocal and as such allows for self organized structure formation. Candidates for dipolar species are polar molecules, Rydberg atoms and magnetic atoms. More than ten years ago the first dipolar effects in a quantum gas were observed in an ultracold Chromium gas. By the use of a Feshbach resonance a purely dipolar quantum gas was observed three years after [1]. By now dipolar interaction effects have been observed in lattices and also for polar molecules. Recently it became possible to study degenerate gases of lanthanide atoms among which one finds the most magnetic atoms. The recent observation of their collisional properties includes the emergence of quantum chaos and very broad resonances [2][3]. Similar to the Rosensweig instability in classical magnetic ferrofluids self-organized structure formation was expected. In our experiments with quantum gases of Dysprosium atoms we could recently observe the formation of a droplet crystal [4]. In contrast to theoretical mean field based predictions the super-fluid droplets did not collapse. We find that this unexpected stability is due to beyond meanfield quantum corrections of the Lee-Huang-Yang type [5][6]. We observe and study self-bound droplets [7] which can interfere with each other. These droplets are 100 million times less dense than liquid helium droplets and open new perspectives as a truly isolated quantum system.

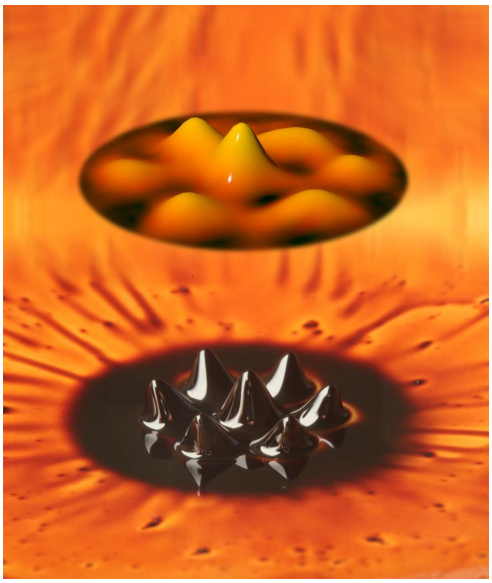

Fig. 1: Insitu image of a quantum droplet arrangement (shown above where the distance between droplets is about 3 microns) in comparison to a ferrofluid showing a Rosensweig Instability (shown below).

References

[1] T. Lahaye, C. Menotti, L. Santos, M. Lewenstein, and T. Pfau, Rep. Prog. Phys. **72**, 126401 (2009)
[2] T. Maier, I. Ferrier-Barbut, H. Kadau, M. Schmitt, M. Wenzel, C. Wink, T. Pfau, K. Jachymski, P. S. Julienne, Phys. Rev. A **92**, 060702(R) (2015)
[3] T. Maier, H. Kadau, M. Schmitt, M. Wenzel, I. Ferrier-Barbut, T. Pfau, A. Frisch, S. Baier, K. Aikawa, L. Chomaz, M. J. Mark, F. Ferlaino, C. Makrides, E. Tiesinga, A. Petrov, S. Kotochigova, Phys. Rev. X **5**, 041029 (2015).
[4] H. Kadau, M. Schmitt, M. Wenzel, C. Wink, T. Maier, I. Ferrier-Barbut, T. Pfau, Nature **530**, 194 (2016).
[5] T. D. Lee, K. Huang, and C. N. Yang, Phys. Rev. **106**, 1135 (1957). D.S. Petrov, Phys. Rev. Lett. **115**, 155302 (2015).
[6] I. Ferrier-Barbut, H. Kadau, M. Schmitt, M. Wenzel, T. Pfau, Phys. Rev. Lett. **116**, 215301 (2016).
[7] M. Schmitt, M. Wenzel, F. Böttcher, I. Ferrier-Barbut, and T. Pfau, "Self-bound droplets of a dilute magnetic quantum liquid", Nature **539**, 259 (2016).

*Corresponding author: t.pfau@physik.uni-stuttgart.de

To the list of contents

Ultracold Dipolar Fermi Gas of NaK Molecules

Martin Zwierlein[*1]

1. Department of Physics, Massachusetts Institute of Technology, MIT Harvard Center for Ultracold Atoms, and Research Laboratory of Electronics, MIT, Cambridge, MA 02139, USA

Strongly interacting dipolar gases of molecules hold great promise for precision measurements, high-speed quantum simulation and the creation of novel many-body systems. I will describe the creation of an ultracold dipolar gas of fermionic NaK molecules in their absolute rovibrational and hyperfine ground state. The NaK molecule is chemically stable and features a large electric dipole moment of up to 2.7 Debye. We observe lifetimes exceeding four seconds, even in rotationally excited states of the molecule. We demonstrate coherent microwave control of rotational and hyperfine states and observe second-long nuclear spin coherence times even without spin-echo techniques. To induce large dipole moments, we explore microwave dressing of molecules, a technique that has been proposed for shielding of inelastic collisions and the realization of topological superfluids.

[*]Corresponding author: zwierlei@mit.edu

To the list of contents

Two-dimensional arrays of single Rydberg atoms for the quantum simulation of spin systems

T. Lahaye[*1], **S. de Léséleuc,**[1] **V. Lienhard,**[1] **D. Barredo,**[1] **A. Browaeys**[1]
1. Laboratoire Charles Fabry, Institut d'Optique and CNRS, Palaiseau, France

In our experiments, we generate arrays of up to 50 optical tweezers arranged in arbitrary two-dimensional geometries, each containing a single cold atom, and separated by distances of a few micrometers (Fig. 1). This is achieved by active sorting of atoms in larger arrays that are initially loaded stochastically [1]. By exciting the atoms to Rydberg states (with principal quantum numbers in the range 50–100), we can induce strong, tunable dipolar interactions between the atoms [2].

This system is an ideal platform for the quantum simulation of spin Hamiltonians. By using van der Waals interactions we can implement the quantum Ising model in a transverse field and observe the dynamics of the magnetization and of correlation functions following a quantum quench [3]. Using resonant dipole-dipole interactions, we observed the propagation of a spin excitation in a minimalistic spin chain of three atoms governed by the XY Hamiltonian [4].

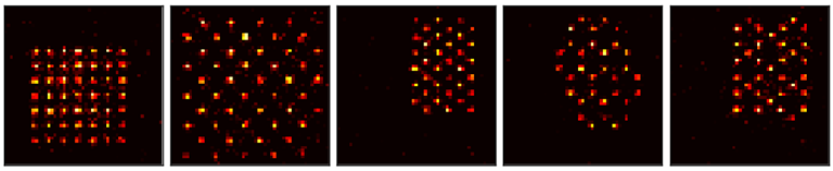

Fig. 1: Examples of fully loaded, two-dimensional arrays of individual atoms with various geometries that are relevant for quantum simulation of spin Hamiltonians. The typical distance between nearest-neighbour atoms is 4 μm.

References

[1] D. Barredo *et al.*, Science **354**, 1021 (2016).
[2] A. Browaeys, D. Barredo, and T. Lahaye, J. Phys. B **49**, 152001 (2016).
[3] H. Labuhn *et al.*, Nature **534**, 667 (2016).
[4] D. Barredo *et al.*, Phys. Rev. Lett. **114**, 113002 (2015).

*Corresponding author: thierry.lahaye@institutoptique.fr

To the list of contents

Nondestructive detection of polar molecules via Rydberg atoms

M. Zeppenfeld[*1], **F. Jarisch**[1]
1. MPI für Quantenoptik, Hans-Kopfermann Str. 1, 85748 Garching, Germany

A quantum hybrid system combining polar molecules with Rydberg atoms provides fascinating opportunities for research in quantum physics. Thus, the strong dipole-dipole interactions between polar molecules and Rydberg atoms have been proposed for quantum information processing [1]. Moreover, the long-range interactions might be used for efficient cooling of molecules to ultracold temperatures [2-3].

Here, we discuss using Rydberg atoms to efficiently and nondestructively detect polar molecules [4] and show first experimental results. Förster resonant energy transfer between molecules and Rydberg atoms imprints the presence of a molecule on a Rydberg atom. This allows detection of the molecule by subsequent state sensitive field ionization of the Rydberg atom. Huge molecule-Rydberg-atom interaction cross sections on the order of $10^{-6}\,\mathrm{cm}^2$ for sufficiently low collision energies allows for efficient detection [4].

We show experimental results for the detection of ammonia molecules in a room temperature thermal gas. For Rubidium atoms initially excited to an nP state with $n \sim 46$, Förster resonant energy transfer induced transitions to the $n-1$D state. No population transfer to other nearby n'S or n'D Rydberg states is observed, indicating the necessity for a transition which is resonant to a molecular transition (in our case the inversion splitting of ammonia), as expected for Förster resonant energy transfer. Changing the resonance condition for energy transfer using electric fields to tune the Rydberg transition changes the amount of population transfer, indicating the observation of electric field dependent collisions.

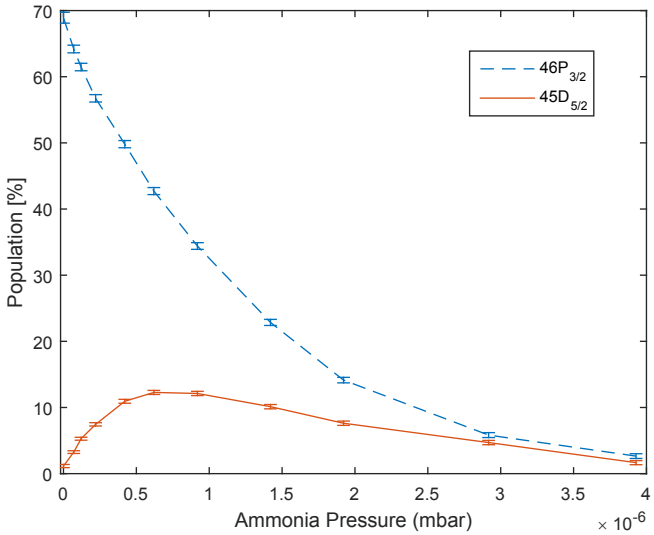

Fig. 1: Population in states $46P_{3/2}$ and $45D_{5/2}$ as a function of ammonia pressure. Rubidium atoms are initially excited to the 46P state with a pulsed UV laser and detected by field ionization after $10\,\mu$s interaction time. Actual populations are slightly higher due to imperfect state detection.

References

[1] E. Kuznetsova, S.T. Rittenhouse, H.R. Sadeghpour, and S.F. Yelin, Phys. Chem. Chem. Phys. **13**, 17115 (2011).
[2] S.D. Huber and H.P. Büchler, Phys. Rev. Lett. **108**, 193006 (2012).
[3] B. Zhao, A.W. Glaetzle, G. Pupillo and P. Zoller, Phys. Rev. Lett. **108**, 193007 (2012).
[4] M. Zeppenfeld, arXiv:1611.08893 [physics.atom-ph] (2016).

*Corresponding author: martin.zeppenfeld@mpq.mpg.de

To the list of contents

Three-Body Förster Resonances in a Few Interacting Rb Rydberg Atoms

I.I. Ryabtsev[*1,2], **D.B. Tretyakov**[1,2], **I.I. Beterov**[1,2], **E.A. Yakshina**[1,2], **V.M. Entin**[1,2], **P. Cheinet**[3], **P. Pillet**[3]

1. Rzhanov Institute of Semiconductor Physics SB RAS, pr.Lavrentyeva 13, 630090 Novosibirsk, Russia

2. Novosibirsk State University, 630090 Novosibirsk, Russia

3. Laboratoire Aime Cotton, CNRS, Univ. Paris-Sud, ENS Paris-Saclay, Bat. 505, 91405 Orsay, France

Three-body Förster resonances at long-range interactions of Rydberg atoms were first predicted and observed in Cs atoms [1]. In these resonances, one of the atoms carries away an energy excess preventing the two-body resonance, leading thus to a Borromean type of Förster energy transfer. The experiment in [1] was done with an ensemble of $\sim 10^5$ Cs atoms in an interaction volume of $\sim$200 μm in size. Therefore, the three-body Förster resonance was in fact observed as the average signal for the large number of atoms $N \gg 1$.

In this report we present the first experimental observation of the three-body Förster resonance $\mathrm{Rb}(nP_{3/2}) + \mathrm{Rb}(nP_{3/2}) \rightarrow \mathrm{Rb}(nS_{1/2}) + \mathrm{Rb}([n+1]S_{1/2})$ for a few Rb Rydberg atoms with n=36, 37. In our experiment, N=2-5 Rydberg atoms in the initial $nP_{3/2}$ Rydberg state interact in a single volume of $\sim$20-30 μm in size. This volume is formed at the intersection of the two tightly focused laser beams that excite Rydberg states at the center of the cold Rb atom cloud in a magneto-optical trap [2]. Using the selective field ionization technique with the detection efficiency of 70%, the measured Förster resonance spectra are post-selected over the number of the detected Rydberg atoms N=1-5 [3] and then additionally processed to extract the true multi-atom spectra taking into account finite detection efficiency. The spectra represent the measured dependence of the fraction of atoms in the final $nS_{1/2}$ state on the applied dc electric field, which controls the Förster resonance detuning, for various N.

Figure 1 shows the Stark-tuned Förster resonance in Rb atoms observed for N=2-5. In Fig.1(a) the atoms are in the initial state $37P_{3/2}(|M_J| = 1/2)$. The main peak at 1.79 V/cm is the ordinary two-body resonance that occurs for all N=2-5 [2-4]. The additional peak at 1.71 V/cm is the three-body resonance that is absent for N=2 and appears only for N=3-5.

The feature at 1.71 V/cm can in principle be caused by the imperfection of the electric-field pulses used to control the Förster resonance [4]. In order to check for this effect, the resonance has also been recorded for the atoms in the initial state $37P_{3/2}(|M_J| = 3/2)$, as shown in Fig.1(b). Here we see again that the main peak at 2.0 V/cm is the ordinary two-body resonance that occurs for all N=2-5. The additional peak at 2.14 V/cm is the three-body resonance that is absent for N=2 and appears only for N=3-5. We conclude that the three-body resonances really take place, as their positions and behavior well agree with theoretical calculations.

As a result, we have found clear evidence that there is no signature of the three-body Förster resonances for exactly two interacting Rydberg atoms, while it is present for the larger number of atoms. As the observed three-body resonance appears at the different dc electric field with respect to the two-body resonance (the difference increases for the lower n [1], and we have checked for it at n=36), it represents an effective three-body operator, which can be used to directly control the three-body interactions. This can be especially useful in quantum simulations and quantum information processing with neutral atoms in optical lattices.

This work was supported by the RFBR Grants No. 16-02-00383 and 17-02-00987, the Russian Science Foundation Grant No. 16-12-00028, the Novosibirsk State University, the public Grant CYRAQS from Labex PALM (ANR-10-LABX-0039) and the EU H2020 FET Proactive project RySQ (Grant No. 640378).

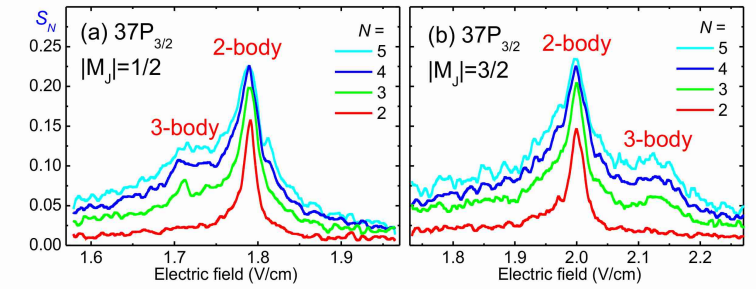

Fig. 1: Förster resonance in Rb Rydberg atoms observed for various numbers of atoms N=2-5: (a) in the initial state $37P_{3/2}(|M_J| = 1/2)$; (b) in the initial state $37P_{3/2}(|M_J| = 3/2)$.

References

[1] R.Faoro, B.Pelle, A.Zuliani, P.Cheinet, E.Arimondo, P.Pillet, Nature Comm. **6**, 8173 (2015).
[2] I.I.Ryabtsev, D.B.Tretyakov, I.I.Beterov, V.M.Entin, Phys. Rev. Lett. **104**, 073003 (2010).
[3] D.B.Tretyakov, V.M.Entin, E.A.Yakshina, I.I.Beterov, C.Andreeva, I.I.Ryabtsev, Phys. Rev. A **90**, 041403(R) (2014).
[4] E.A.Yakshina, D.B.Tretyakov, I.I.Beterov, V.M.Entin, C.Andreeva et al., Phys. Rev. A **94**, 043417 (2016).

*Corresponding author: ryabtsev@isp.nsc.ru

To the list of contents

Coherent Control and Trapping of Ultracold ^{87}Rb^{133}Cs Molecules

Philip D. Gregory[*1], **Jacob A. Blackmore**[1], **Elizabeth M. Bridge**[1], **Jesus Aldegunde**[2], **Jeremy M. Hutson**[3], **and Simon L. Cornish**[1],

1. Joint Quantum Centre (JQC) Durham–Newcastle, Department of Physics, Durham University, South Road, Durham DH1 3LE, UK
2. Departmento de Quimica Fisica, Universidad de Salamanca, 37008 Salamanca, Spain
3. Joint Quantum Centre (JQC) Durham–Newcastle, Department of Chemistry, Durham University, South Road, Durham DH1 3LE, UK

The formation of ultracold heteronuclear molecules opens many exciting areas of research, spanning precision measurement, quantum computation, quantum simulation, ultracold chemistry, and fundamental studies of quantum matter. The large electric dipole moments of such molecules allow long-range interactions tunable over length scales similar to the spacing between sites in an optical lattice. Long-lived, trapped samples of molecules with full quantum control of the molecular internal state are crucial to realising many of their applications.

In this work, a sample of up to 4000 ^{87}Rb^{133}Cs molecules in their electronic, vibrational, rotational, and hyperfine ground state are created at ultracold temperatures in a two-step process. Initially, weakly-bound molecules are formed by magnetoassociation on a Feshbach resonance from a pre-cooled atomic mixture [1]. These molecules are then transferred to their rovibronic and hyperfine ground state by stimulated Raman adiabatic passage (STIRAP) [2]. The transfer is characterised by a precision measurement of the binding energy of the molecule with reference to an offset-free optical frequency comb; we find $D_0 = h \times 114\,268\,135.25(3)$ MHz [3].

We demonstrate coherent control of the rotational and hyperfine state using external microwave fields (see Fig. 1). Spectroscopy of the hyperfine structure of the first excited rotational state $N = 1$ allows us to determine accurate values of rotational and hyperfine coupling constants that agree well with previous calculations. We find that there is significant mixing between hyperfine states principally due to the scalar spin-spin coupling in $N = 0$, and nuclear quadrupole coupling in $N = 1$. Complete population transfer between selected hyperfine levels of the ground, first and second rotational states is performed using one- and two-photon π-pulses [4].

We investigate the interaction between the far-off-resonant light of our optical trap on the molecules. Through high-resolution microwave spectroscopy, we measure the AC Stark shift of the hyperfine states of the ground and first excited rotational states. We demonstrate that the trapping light can couple neighbouring hyperfine states, yielding rich and complex structure with many avoided crossings. This coupling is due to the anisotropic component of the real part of the AC polarizability. We show that this coupling can be tuned by varying the angle of the laser polarization to broaden or narrow select avoided crossings as required and to allow access to previously dark transitions between hyperfine states. This leads to our conclusion where we will be looking towards our future work, where we hope to investigate collisions between our bosonic molecules confined in a 3D optical trap.

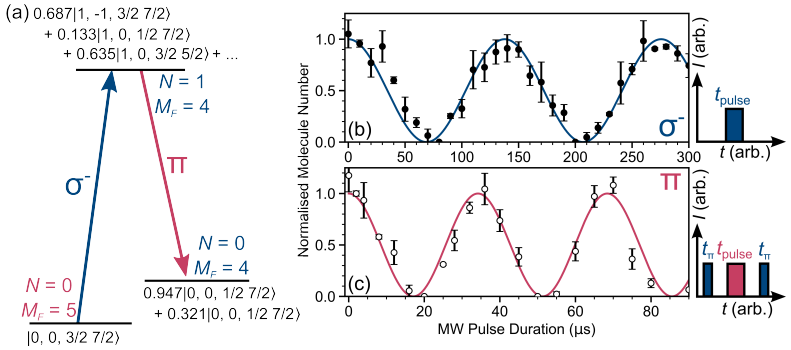

Fig. 1: Coherent population transfer of molecules between specific hyperfine states in rotational levels $N = 0$ and $N = 1$. (a) Transfer scheme followed in this work, where molecules begin in the lowest hyperfine state $M_F = 5$ of $N = 0$. States are described in the uncoupled basis set $|N, M_N, m_I^{\mathrm{Rb}}, m_I^{\mathrm{Cs}}\rangle$. (b) Rabi oscillations in one-photon transfer of molecules to the single hyperfine level of $N = 1$ shown in (a). (c) Rabi oscillations in two-photon transfer, using a π-pulse on the first transition and a second microwave pulse with different frequency and polarization to drive transitions to the $M_F = 4$ hyperfine state of $N = 0$ shown in (a). Figure reproduced from [4].

References

[1] M. P. Köppinger *et al.*, Phys. Rev. A. **89**, 033604 (2014).
[2] P. K. Molony *et al.*, Phys. Rev. Lett. **113**, 255301 (2014).
[3] P. K. Molony *et al.*, Phys. Rev. A **94**, 022507 (2016).
[4] P. D. Gregory *et al.*, Phys. Rev. A **94**, 041403(R) (2016).

*Corresponding author: p.d.gregory@durham.ac.uk

To the list of contents

Towards conductivity imaging of biological tissues with atomic magnetometers

Cameron Deans[*1], **Luca Marmugi**[1], **Ferruccio Renzoni**[1]
1. Department of Physics & Astronomy, University College London, GowerStreet, London, UK, WC1E 6BT.

The ability to map the conductivity of biological samples would aid the diagnosis and treatment of diseases and conditions where a change in conductivity plays, or is expected to play, an important role. Examples include the detection and diagnosis of cardiac arrhythmias and malignant tumours [1,2]. Currently deployed technologies, such as magnetocardiography and electrocardiography, do not provide any direct information regarding the local conductivity of tissue.

We identify Magnetic Induction Tomography (MIT) [3] as the ideal solution for mapping the conductivity of living tissues. MIT is an attractive method of medical imaging as it is non-invasive and no direct contact with the patient is required. In MIT, an AC magnetic field induces eddy currents in a target object. These eddy currents generate an additional oscillating magnetic field component. The detection of this field gives access to the electromagnetic properties of the object, without requiring direct physical contact. In particular, it allows the direct mapping of all three passive dielectric properties; the conductivity σ, the permittivity ϵ, and the permeability μ. As such, MIT represents a promising solution for non-invasively addressing the conductivity of biological tissues. Conductivity maps can be obtained by taking spatially resolved MIT measurements. Tomographic measurements can be constructed by taking measurements at various excitation field frequencies, thus varying the penetration into the sample.

Our novel approach to MIT measurements is based on atomic magnetometers (AMs) [4,5,6]. This overcomes the performance limitations of classical systems which use inductive pick-up coil sensors. AMs offer extreme sensitivity over a wide frequency range, from Hz to tens of MHz. This allows simple tuning of the operation frequency in MIT measurements and overcomes the poor low-frequency sensitivity of pick-up coils. AMs offer robust operation in unshielded environments providing flexibility for applications and miniaturised AMs could offer excellent imaging resolution.

Here, we report on the progress towards mapping the conductivity of biological tissues using AMs. We experimentally demonstrate the use of radio-frequency optical atomic magnetometers (RF-AM) for MIT imaging. The RF-AM records the changes in the magnetic field's properties due to eddy current excitation. We build images of target properties in real-time and without background subtraction. We demonstrate the imaging of dummy targets placed in the proximity of the sensor. These scans include of a range of materials with a wide range in conductivities. We show the progression towards low-conductivity biological targets by successfully imaging non-metallic samples, for the first time. Our results show the wide range of operation frequencies available and the ease with which the operating frequency is adapted. We also show that it is possible to image different parameters of the oscillating field, each of these equates to the mapping of different electromagnetic properties of the target. Finally, we present simulations validating the application of this approach to imaging biological samples.

Our results demonstrate the feasibility of an instrument based on AMs for MIT measurements of biological tissues. The system is shown to perform over a wide frequency range facilitating the imaging of targets with a wide range in conductivities. We envisage an instrument capable of ultra-sensitive high-resolution imaging, using arrays of atomic magnetometers operating in a MIT modality. Such a device could find important applications in the diagnosis and treatment of cardiac arrhythmias such as atrial fibrillation. This sustained arrhythmia affects more than 10% of the population over 70. A conductivity map of the heart would shed light on both the fundamental causes of fibrillation, aid diagnosis, and help guide effective clinical treatments.

References

[1] L. Marmugi and F. Renzoni. *Scientific reports* **6**, (2016).
[2] C. Deans, L. Marmugi, S. Hussain, and F. Renzoni. *Proc. SPIE 9900*, 99000F (2016).
[3] H. Griffiths. *Measurement science and technology* **12**(8), 1126 (2001).
[4] D. Budker and M. Romalis. *Nature Physics* **3**(4), 227-234 (2007).
[5] A. Wickenbrock, S. Jurgilas, A. Dow, L. Marmugi, and F. Renzoni. *Optics Letters* **39**(22), 6367-6370 (2014).
[6] C. Deans, L. Marmugi, S. Hussain, and F. Renzoni. *Applied Physics Letters* **108**(10), 103503 (2016).

*Corresponding author: cameron.deans.14@ucl.ac.uk

To the list of contents

Moddeling LMT Atom Interferometry in Optical Cavities

M. Dovale[1], **Aaron Jones**[*1], **D. Brown**[1], **H. Miao**[1], **A. Freise**[1]
1. Institute of Gravitational Waves, School of Physics and Astronomy, University of Birmingham
Edgebaston Park Road, Birmingham B15 2TT, UK

We present work modelling atom interferometry in optical cavities, based on our optical modelling experience for gravitational wave detectors. The python based modelling activity will be an open source framework to benefit the atom interferometry community. We are using this model to investigate Large Momentum Transfer (LMT) atom optics in an optical cavity.

We have developed models for both Bragg and Raman transitions and verified these against both analytic solutions and literature[1][2]. In the case of an analytic solution being available, we were limited only by double width floating point precision errors.

Optical cavities offer an effective laser power increase, and cleaning of the laser wave-front distortions, reducing noise in the interferometer. However, for the short pulses needed in the quasi-Bragg regime, the cavity may cause a deformation and elongation of the temporal envelope of the pulse.

We are working towards the definition of safe parameters ranges for the cavity length and finesse in order to avoid the problem of the temporal envelope elongation.

For short cavities ($\sim 1m$), we found that short π pulses are still achievable even at large finesse (> 1000). The effect becomes very severe for long cavities ($\geq 100m$), such as that proposed for MIGA[3], for which the width of the shortest pi-pulses increases considerably even at low finesse (~ 100). These conclusions provide a quantitative understanding of the ability of the interferometer to operate in this regime.

Our latest work explores the effect of mirror misalignment, astigmatism, beam clipping, mode mismatches and mirror surface imperfections on the transition probabilities of the atoms.

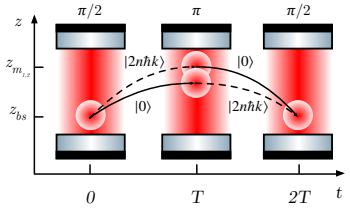

Fig. 1: Depiction of an interferometer sequence using cavity-assisted large momentum beam splitters. A cloud of atoms is coherently split ($t = 0,\ z = z_{bs}$), deflected ($t = T,\ z = z_m$) and recombined ($t = 2T,\ z = z_{bs}$) using light pulses that resonate in the cavity.

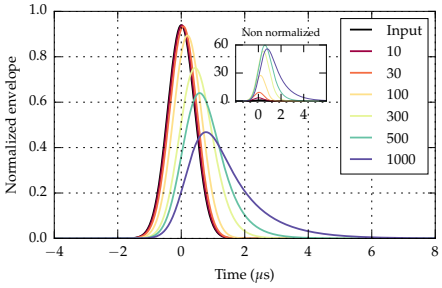

Fig. 2: Envelope functions of the intracavity field for a 1 m cavity injected with a 1 μs pulse for different cavity finesses. All areas normalized to the input pulse area for comparison. Inset: envelopes without the normalization.

References [1] P. R. Berman, L. Yan, and K Chiam, *Nonadiabatic transitions in a two-level quantum system: Pulse-shape dependence of the transition probability for a two-level atom driven by a pulsed radiation field*, Phys. Rev. A, Vol. **57** (Jan 1998)
[2] Müller, Holger and Chiow, Sheng-wey and Long, Quan and Herrmann, Sven and Chu, Steven, *Atom interferometry with up to 24-photon-momentum-transfer beam splitters*, Physical Review Letters, 2008
[3] B. Canuel et. al., *Exploring gravity with the MIGA large scale atom interferometer*, *in prep.* (2017)

*Corresponding author: ajones@star.sr.bham.ac.uk

To the list of contents

Application of cavity ring-down spectroscopy for diagnostics of low temperature N_2H^+ dominated afterglow plasmas

Ábel Kálosi[1], **P. Dohnal**[*1], **D. Shapko**[1], **R. Plašil**[1], **J. Glosík**[1]
1. Department of Surface and Plasma Science, Faculty of Mathematics and Physics, Charles University
V Holešovičkách 2, 18000 Prague, Czech Republic

A cavity ring down spectrometer (CRDS) in conjunction with a stationary afterglow (SA) apparatus has been employed to extend the measurements of Sasada and Amano [1] on the $2\nu_1$ vibrational band of N_2H^+. The observed transition frequencies were fitted to experimental accuracy. Improved molecular parameters for the upper vibrational state have been obtained. The ground state molecular parameters have been fixed to the high precision values obtained by terahertz absorption spectroscopy [2]. The new measurements reported here will be employed in a plasma afterglow study of the recombination of N_2H^+ ions with electrons at low temperatures.

Sasada and Amano using a single distributed feedback (DFB) laser diode in their experiments observed only the R-branch with rotational quantum number (J) values higher than 14. The relatively high output power and low noise of this type of lasers and the integrated intensity of absorption of the $2\nu_1$ band which is comparable with that of the ν_3 fundamental band made the observations available in their multipass absorption experiment. The aim of our ongoing experimental effort is to extend the observations towards transitions with lower-J values in the lower ro-vibrational state which have higher intensities at temperatures below 300 K or can be used to evaluate the rotational temperature of the ions in a wider range of temperatures.

According to absorption intensities predicted by Botschwina [3] the main limiting factor of our experimental setup is the wavelength coverage of the DFB laser diodes available in our laboratory. We can also make use of a fiber-coupled optical switch to utilize the wavelength range of a chosen pair of laser diodes in a set of recombination measurements. The N_2H^+ ions are produced abundantly in a pulsed microwave discharge in a mixture of H_2 and N_2 with typical number densities: $10^{16}\,\mathrm{cm}^{-3}$ and $10^{15}\,\mathrm{cm}^{-3}$, respectively. For technical details of the employed laser absorption spectrometer and SA apparatus with the exceptions of the optical switch and the modified solid-state microwave source see Ref. [4]. Examples of measured absorption lines are shown in Fig. 1.

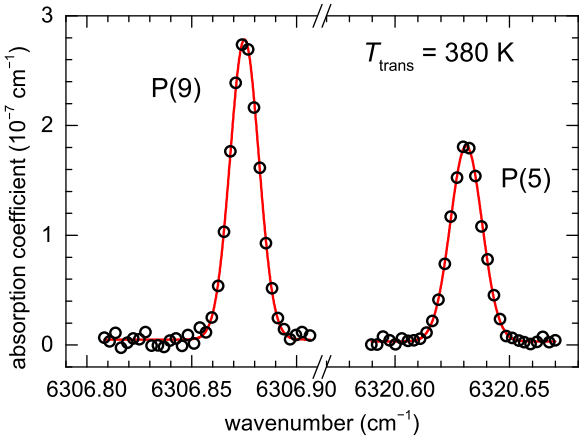

Fig. 1: An example of the recorded absorption spectrum of N_2H^+. The figure shows typical absorption lines of the newly observed P-branch in the $2\nu_1$ vibrational band. The lines are labeled by the rotational transition as $\Delta J(J)$, where J is the lower state rotational quantum number. Experimental conditions were: $[H_2] = 6\times10^{16}\,\mathrm{cm}^{-3}$, $[N_2] = 1\times10^{15}\,\mathrm{cm}^{-3}$ and discharge tube temperature $T = 230\,\mathrm{K}$

In a different set of experiments we calibrated the wavelength readings by comparing the center wavelength of known carbon monoxide second overtone absorption lines [5] with our measured values. The wavelength of the active laser is measured absolutely by a Michelson interferometer-based wavemeter (WA-1650). The differences were on the order of our statistical uncertainty and within the guaranteed absolute accuracy of the wavemeter ($\pm0.3\,\mathrm{pm}$) after taking into account the acousto-optic modulator induced frequency shift.

References

[1] H. Sasada and T. Amano, J. Chem. Phys. **92**, 2248 (1990).
[2] S. Yu, J. C. Pearson, B. J. Drouin, T. Crawford, A. M. Daly, B. Elliott, and T. Amano, J. Mol. Spectrosc. **314**, 19 (2015).
[3] P. Botschwina, Chem. Phys. Lett. **107**, 535 (1984).
[4] P. Macko, G. Bánó, P. Hlavenka, R. Plašil, V. Poterya, A. Pysanenko, O. Votava, R. Johnsen, and J. Glosík, Int. J. Mass Spectrom. **233**, 299 (2004).
[5] D. Mondelain, T. Sala, S. Kassi, D. Romanini, M. Marangoni, and A. Campargue, J. Quant. Spectrosc. Rad. Trans. **154**, 35 (2015).

*Corresponding author: Petr.Dohnal@mff.cuni.cz

To the list of contents

Multichannel optical atomic magnetometer operating in unshielded environment

V.Biancalana[*1], **Antonio Vigilante**[†2], **G.Bevilacqua**[1], **Y.Dancheva**[2], **E.Mariotti**[2], **C.Rossi**[3]

1. DIISM, University of Siena, Italy
2. DSFTA, University of Siena, Italy
3. DBCF, University of Siena, Italy

We present a multichannel optical magnetometer operating in an unshielded environment, which is characterized by high sensitivity, cost efficiency and robustness.
The scalar magnetometer is mostly sensitive to magnetic field variations along to a bias field's direction. The bias field ranges from hundreds of nT to tens of μT. The ultimate sensitivity, in gradiometric regime, is of the order of $100 fT/cm\sqrt{Hz}$.

The system contains two diode lasers differently tuned to pump and probe two Cs cells (atomic sensors). The atomic precession signal is detected is such a way that two different channels are distinguished for each sensor. The multichannel nature of the apparatus is exploited to perform various order magnetic field gradient measurements [1]. The unshielded nature makes it necessary to perform a preliminary field and gradient field compensation. A field tracking system is implemented to follow the environment magnetic variations and to cancel actively external disturbances.
The magnetometer has been exploited to detect Zero-to-Ultra-Low Field (ZULF) NMR signals [2]. The experiment is based on remote premagnetization with permanent magnets, shuttling of the nuclear sample, and detecting the nuclear precession signal in the same highly homogenous low field where atoms precess. Compared to traditional NMR, ZULF-NMR enables the study of nuclear spin coupling in conditions where it is a dominant term in the nuclear Hamiltonian. Among several investigated substances, trimethyl-phosphate has been thoroughly analyzed. ZULF-NMR spectral structures dictated by P-H J-coupling have been recorded and studied as a function of the magnetic field (Fig. 1) [3].

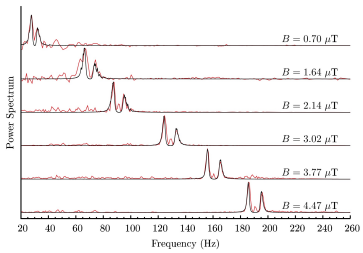

Fig. 1: Trimethyl-phosphate experimental and theoretical NMR spectra recorded at different bias magnetic fields.

Our perspectives for the next future concern to perform new ZULF-NMR studies and to improve the experimental apparatus in terms of sensitivity and active compensation. Among possible investigation fields we foresee the study of relaxation and diffusion processes in ZULF regime, of solvent dynamics and the characterization of heterogeneous materials and spins in porous media. The experimental apparatus improvements consist of the increase the number of sensors to achieve a better sample coupling and ambient noise rejection. The gradient and field compensation will be upgraded through a real time embedded board which analyses and actively correct the field through using numeric control methods. Novel experimental campaigns will be devoted to the detection and characterization of samples polarized by alternative methods (for example hyperpolarization) and to the MRI of remotely magnetized samples.

References

[1] G.Bevilacqua, V.Biancalana, P.Chessa and Y.Dancheva, Appl. Phys. B **122** (2016) no.4, 103 doi:10.1007/s00340-016-6375-2
[2] M.P. Ledbetter, C.W. Crawford, A. Pines, D.E. Wemmer, S. Knappe, J. Kitching, D. Budker, Journal of Magnetic Resonance, Volume 199, Issue 1, July 2009, Pages 25-29, ISSN 1090-7807, https://doi.org/10.1016/j.jmr.2009.03.008
[3] G.Bevilacqua, V.Biancalana, A.Baranga, Y.Dancheva and C.Rossi. Journal of Magnetic Resonance, Volume 263, February 2016, Pages 65-70, ISSN 1090-7807, http://doi.org/10.1016/j.jmr.2015.12.018.

[*]Corresponding author: valerio.biancalana@unisi.it
[†]Corresponding author: antonio.vigilante@student.unisi.it

To the list of contents

Real-time Monitoring of Breath Acetone in Diabetic Patients

Arin Mizouri[1], **Nada Al Taisan**[2], **Eckart Wrede**[1], **N. Hendrik Nahler**[3] **and David Carty**[*1,2]
1. Department of Chemistry, Durham University, South Road, Durham DH1 3LE, UK
2. Department of Physics, Durham University, South Road, Durham DH1 3LE, UK
3. School of Engineering and Physical Sciences, Heriot-Watt University, Edinburgh, EH14 4AS, UK

Diabetic ketoacidosis (DKA) is a life threatening complication of type-1 diabetes (T1D). In DKA, the body breaks up fatty acids as an alternative energy source producing poisonous ketones, including acetone, as a by-product. Normally, DKA is treated by intravenous insulin infusion. A ”guess” insulin dosage is administrated following untimely blood analysis. There is, therefore, a timely translational opportunity to develop a non-invasive, bedside ketone-monitoring device. We are currently building a sensor prototype that can measure the concentration of acetone in breath, non-invasively and passively in real time. The sensor is based on the proven technique cavity-enhanced laser-induced fluorescence (CELIF).

CELIF combines the sensitivity of laser induced fluorescence (LIF) and the absolute measurement capabilities of cavity ring-down spectroscopy (CRDS) into one cross-correlated technique. A gas sample dense enough to be measured by CRDS enters the sensor's detection volume via a controlled flow system. Simultaneous CRDS and LIF measurements measure the proportionality constant between the LIF intensity and the number of acetone molecules in the sample that created it. This is then used for measurements at concentration levels where measurements cannot be made by CRDS but can be made by LIF.

The instrument was validated by comparing measurements with the gold-standard measuring technique, gas chromatography. The linear fitting suggests that the obtained acetone concentrations via both methods are consistent.

References

[1] C. Wang *et al.*, *IEEE Sensors J.* **10**, (2010).
[2] C. Jiang *et al.*, *Sensors* **16**, (2016).
[3] S. E. Sanders *et al.*, *arXiv: 1308.1989*, (2013).

[*]Corresponding author: david.carty@durham.ac.uk

To the list of contents

Dynamical Studies in Electron Impact Ionization of Atoms and Molecules

S. Houamer[*,1], M. Chinoune[1,2] and C. Dal Cappello[3]

[1]LPQSD, Department of Physics, Faculty of Sciences, University Sétif1, Sétif 19000, Algeria

[2] USTHB, Faculty of Physics, Department of theoretical physics, Algiers 16111, Algeria

[3]SRSMC, UMR CNRS 7565, University of Lorraine, BP 70239, 54506 Vandoeuvre-les-Nancy, France

Ionization of matter by electron impact is a fundamental process in collision theory which plays a significant role in many fields such as plasma physics and astrophysics. The triply differential cross section (TDCS) obtained in (e,2e) coincidence experiments where the two outgoing electrons are detected simultaneously represents the most detailed description of the ionization process.

In this paper we study the electron impact ionization of some atomic and molecular targets using non first order models. We use the BBK and BBKDW models which have been very recently investigated [1] and where the interaction between the projectile and the target is purely Coulombic. We also apply the BBKSR model where further to the Coulombic interaction, the short range potential is included [2]. The one active electron approximation is made to study (e,2e) processes in the present work. Results are compared with recent results [3].

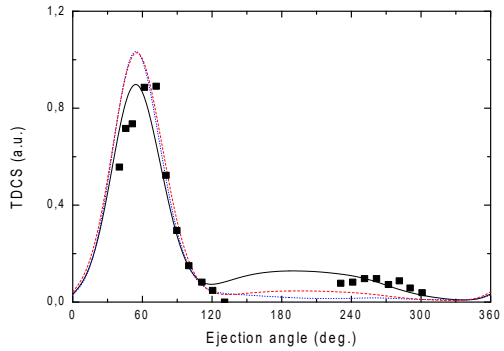

Fig1. TDCS of CH_4 molecule in its ground state under kinematics $E_0 = 250\ eV$, $E_e = 50\ eV$ and $\theta_s = 10°$. Comparison is made between experiments [3] and the theoretical models: (i) the BBKSR model (solid line), (ii) the BBK model (dashed line), (iii) the BBKDW model (dotted line).

References

[1] M. Chinoune, S. Houamer, C. Dal Cappello and A. Galstyan, J. Phys B **49,** 205201 (2016).

[2] S. Houamer, M. Chinoune and C. Dal Cappello, Eur. Phys. J. D **71, 17** (2017).

[3] N. Isik, M. Dogan and S. Bahceli, J. Phys B **49,** 065203 (2016).

s_houamer@univ-setif.dz

To the list of contents

The filleted atom revisited - a new dynamical description

H. Agueny, M. Chovancova, M. Førre and J. P. Hansen*

Department of Physics and Technology, Allegt. 55, University of Bergen, N-5007 Bergen, Norway

Significant recent advances and progress of attosecond technology have led to the generation of extremely short, increasingly intense pulses compressed towards a single optical cycle [1]. The emergence of these pulses have been applied to study electron motion inside atoms, molecules and solids in real-time scale [3]. Extensive theoretical and experimental studies of atoms in strong attosecond pulses have also led to a seemingly complete picture of the induced electron dynamics [4].

In this context a most intriguing phenomenon induced by a single cycle attosecond pulse was discussed few years ago by J. S. Briggs et al. [5]. They showed that it is possible to create atoms without nuclei, a "filleted atom", by a suitable attosecond laser pulse. Their theoretical work, based on the first order Magnus approximation and where each half cycle is modeled by an instantaneous Dirac function, provides insight into the feasibility of stripping the nucleus from the atom, without distorting the electronic bound state wavefunction. The phenomenon was confirmed by numerical solutions of the time-dependent Scrhödinger Equation.

In this presentation we will give an alternative description of the process based on a translated moving coordinate system and derive a precise criterion for a clean and complete filleting [6]. Under this criterion the process is very robust which indicates that it may be the basis of new imaging technology of structure as well as time-dependent electronic processes [7]. During the conference, we shall present our results stemming from the time-dependent Schrödinger equation, and show that by tailored short pulses one can transport a coherent superposition of quantum states in a specific region in momentum and position spaces, and steer their motion. An extension to a diatomic molecule will also be addressed in observing the wavefunction of a double-slit process as the electron emerges at the same time from both slits.

References

[1] T. J. Hammond *et al.*, Nature Photonics **10**, 171-175 (2016).
[2] M. Chini *et al.*, Nature Photonics **8**, 178-186 (2014).
[3] E. Goulielmakis *et al.*, Science **320**, 1614 (2008).
[4] F Calegari, G Sansone, S Stagira, C Vozzi, and M Nisoli, J. Phys. B: At. Mol. Opt. Phys. **49**, 062001 (2016).
[5] J. S. Briggs and D. Dimitrovski, New Journal of Physics **10**, 025013 (2008).
[6] H . Agueny, M. Chovankova, M. Førre and J. P. Hansen, Subm. to Journal of Optics, (2017).
[7] M. Hentschel *et al.*, Nature (london) **414**, 509 (2001).

*Corresponding author: jan.hansen@uib.no

To the list of contents

Phase Properties of the Cutoff High-Order Harmonics

M. Khokhlova[*1], **V. Strelkov**[2,3]

1. Quantum Optics and Laser Science Group (QOLS), Department of Physics, Faculty of Natural Sciences, Imperial College London South Kensington Campus, London SW7 2AZ, UK

2. Theory Department, Prokhorov General Physics Institute, Russian Academy of Sciences 38 Vavilov str., 119991 Moscow, Russia

3. Moscow Institute of Physics and Technology (State University) 141700 Dolgoprudny, Moscow Region, Russia

One of the most characteristic features of the high-order harmonic generation (HHG) by atoms, molecules and ions in intense laser field is the plateau in the spectrum, namely the region where the harmonic intensity almost does not depend on the harmonic order. The high-frequency part of the plateau ends up with a sharp decrease known as the cut-off of the harmonic spectrum [1]. The number of harmonics in the plateau increases with the fundamental intensity [2]. When the fundamental intensity increases the given harmonic first is generated at the cut-off and then within the plateau. At first glance, the former stage can be understood just as a sudden "turning on" of the generation, thus providing negligible contribution to the total signal. Using quantum mechanical calculations we show that this is not the case. The cut-off regime can be attributed to a *range* of fundamental intensities and provides an important impact on the generation under typical experimental conditions. The dependence of the harmonic phase on the laser intensity substantially defines the phase-matching of the generation [3], spectral shift and the harmonic line broadening [4], coherence [5] and the spatial properties of the harmonic beam [6]. Thus, the cut-off high harmonic phase behavior has a pronounced effect on these properties. Moreover, the cut-off xuv is used to generate an isolated attosecond pulse via amplitude gating technique [7]. Studying the phase properties of these harmonics allows us to suggest the spectral range which should be used in this method to provide the shortest attosecond pulse for given pump intensity and frequency.

We find that the cut-off regime can be defined as the one having regular linear dependence of the harmonic phase φ on the fundamental intensity I. The phase coefficient α ($\alpha = -\frac{\partial \varphi}{\partial I}$) in the cut-off regime is well approximated with equation $\alpha \approx \frac{3.309}{4\omega^3}$. The phase coefficient grows as the cube of the fundamental wavelength, therefore this dependence becomes very important for the HHG by mid-infrared fields. The value of the phase coefficient is much higher than that for the short trajectory in the plateau regime. We show that HHG takes place in the cut-off regime for a *range* of intensities and that the xuv intensity within this range is comparable or even higher than in the plateau regime. This makes the studies of the cut-off regime rather important from the practical viewpoint. Moreover, for rather high harmonics the generation occurs mainly within this range because the medium ionization practically limits the fundamental intensity for which the HHG takes place.

The change of the harmonic phase-locking when HHG evolves from the cut-off to the plateau regime determines the optimal bandwidth of the spectral region which should be used for the attosecond pulse production via amplitude gating technique. We find that the minimal pulse duration which can be obtained with this technique using argon as generating medium without utilizing dispersion elements is approximately 0.08 – 0.1 of the laser cycle; this result is found for different laser intensities and for frequencies of the fundamental from $0.5\omega_{Ti:Sapp}$ to $2\omega_{Ti:Sapp}$. Using filters with proper dispersion [8] or chirped multilayer mirrors [9] is necessary to obtain shorter attosecond pulses.

References

[1] A. McPherson, G. Gibson, H. Jara, U. Johann, T. S. Luk, I. A. McIntyre, K. Boyer, and C. K. Rhodes, *J. Opt. Soc. Am. B* **4**, 595 (1987).

[2] J. L. Krause, K. J. Schafer, K. C. Kulander, *Phys. Rev. Lett.* **6**8, 3535 (1992).

[3] M. Lewenstein, P. Salieres, and A. L'Huillier, *Phys. Rev. A* **5**2, 4747 (1995); J. Peatross, M. V. Fedorov, and K. C. Kulander, *J. Opt. Soc. Am. B* **1**2, 863 (1995).

[4] Zhou J., Peatross J., Murnane M.M., Kapteyn H.C., Christov I.P., *Phys.Rev.Lett.* **7**6, 752 (1996); Platonenko V.T., Strelkov V.V., Ferrante G., Miceli V., Fiordilino E., *Laser Phys.* **6**, 1164 (1996); A. Dubrouil, O. Hort, F. Catoire, D. Descamps, S. Petit, E. Mevel, V.V. Strelkov, and E. Constant, *Nature Communications* **5**, 4637 (2014).

[5] M. Bellini, C. Lynga, A. Tozzi, M. B. Gaarde, T. W. Hansch, A. L'Huillier, and C.-G. Wahlstrom, *Phys. Rev. Lett.* **8**1, 297 (1998).

[6] J. Peatross and D. D. Meyerhofer, *Phys. Rev. A* **5**1, R906(R) (1995); M. B. Gaarde, F. Salin, E. Constant, Ph. Balcou, K. J. Schafer, K. C. Kulander, and A. L'Huillier, *Phys. Rev. A* **5**9, 1367 (1999).

[7] I. P. Christov, M. M. Murnane, and H. C. Kapteyn, *Phys. Rev. Lett.* **7**8, 1251 (1997); V. T. Platonenko, V. V. Strelkov, *Quantum Electronics* **2**8 (7), 564 (1998); G. G. Paulus, F. Grasbon, H. Walther, P. Villoresi, M. Nisoli, S. Stagira, E. Priori, and S. De Silvestri, *Nature* **4**14, 182 (2001); M. Hentschel, R. Kienberger, Ch. Spielmann, G. A. Reider, N. Milosevic, T. Brabec, P. Corkum, U. Heinzmann, M. Drescher, and F. Krausz, *Nature* **4**14, 509 (2001).

[8] R. Lopez-Martens, , *Phys. Rev. Lett.* **9**4, 033001 (2005).

[9] E. Goulielmakis, M. Schultze, M. Hofstetter, V. S. Yakovlev, J. Gagnon, M. Uiberacker, A. L. Aquila, E. M. Gullikson, D. T. Attwood, R. Kienberger, F. Krausz, U. Kleineberg, *Science* **3**20, 1614 (2008).

*Corresponding author: m.khokhlova@imperial.ac.uk

To the list of contents

Study of atomic delays in negative ions

E. Lindroth[*1], **Marcus Dahlström**[1,2]
1. Department of Physics Stockholm University
SE-106 91 Stockholm, Sweden
2. Mathematical Physics, Lund University
SE-221 00 Lund, Sweden

Attosecond pulses are traditionally characterized by methods based on laser-assisted photoionization. Further experimental work with these methods have shown that new insight into the photoionization process can be achieved by performing relative delay measurements between different bands in solids [1], atomic orbitals [2],[3], atomic species [4] or angle of photoemission [5]. Theoretically, it has been found that the atomic delay ($\tau_A \approx \tau_W + \tau_{cc}$) can be interpreted as a sum of the photoelectron Wigner delay (τ_W) and a contribution from the laser–ion interaction (τ_{cc})[6]. The τ_{cc} depends on the effective charge Z of the photoionized target. In the special case of photodetechment from negative ions τ_{cc} is expected to vanish because the electron leaves a neutral target with $Z_{eff} = 0$. Here, we present work on laser-assisted photoionization of negative ions with the aim to answer the question if it is possible to measure directly the photoelectron delay τ_W from targets that lack long-range interaction.

We have chosen to study the negative ions of fluorine and chlorine for two reasons (i) they both have large affinities and (ii) they are isoelectronic to the much studied rare gases atoms neon and argon. One important difference is that there are no bound excited states in most negative ions and few autodetaching resonances as well. This is good news because it is understood that Fano resonances in laser-assisted photoionization will invalidate the atomic delay relation when the laser photon is larger than the resonance width [7]. In this work ionization from the outermost shell is performed using the Random Phase approximation with Exchange (RPAE) with a computer program that has been used in earlier studies to compute the atomic delay in noble gas atoms [8]. In Fig. 1 we present the difference $\tau_A - \tau_W$ for both negative ions and noble gas atoms. As expected, we find that the delay difference associted with negative ions are small at high kinetic energy of the photoelectron, so that $\tau_A \approx \tau_W$. However, below 8 eV the delay difference is increasing, thus making it impossible to directly extract τ_W from τ_A by laser-assisted photoionization. Finally, we have studied the effect of reversed time-order processes (IR+XUV). While the dominant process remains the XUV+IR process, the IR+XUV process is not negligible for negative ions. As an example, we find that the reversed process induces a delay of ∼5 as in F^- close to the affinity threshold, while in the noble gas atoms this effect is less than 1 as.

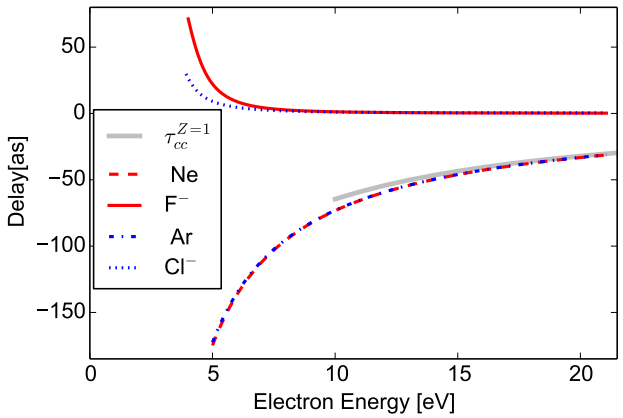

Fig. 1: The difference between atomic delay and Wigner delay ($\tau_A - \tau_W$) is computed for negative ions and noble gas atoms.

References

[1] A L Cavalieri *et al.* 2007 *Nature*, **449** 1029
[2] M Schultze *et al.* 2010 *Science*, **328** 1658
[3] K Klünder *et al.* 2011 *Phys. Rev. Lett.* **106** 143002
[4] D Guénot *et al.* 2014 *J. Phys. B* **47** 245602
[5] S Heuser *et al.* 2016 *Phys. Rev. A* **94** 063409
[6] J M Dahlström *et al.* 2012 *J. of Physics B* **45** 183001
[7] M Kotur *et al.* 2016 *Nat. Comm.* **7** 10566
[8] J M Dahlström *et al.* 2012 Phys. Rev. A **86** 061402

*Corresponding author: Eva.Lindroth@fysik.su.se

To the list of contents

Relativistic ionization dynamics for a hydrogen atom exposed to superintense XUV laser pulses

E. Lindroth[*1], **Tor Kjellsson**[1], **Sølve Selstø**[2], **Morten Førre**[3]
1. Department of Physics Stockholm University
SE-106 91 Stockholm, Sweden
2. Faculty of Technology, Art and Design, Oslo and Akershus University College of Applied Sciences
NO-0130 Oslo, Norway
3. Department of Physics and Technology, University of Bergen
NO-5007 Bergen, Norway

With the high laser intensities, available already now, or expected in the near future, the description of light-matter interaction in a relativistic framework is of growing importance. The ionization dynamics initiated with few cycle laser pulses calls further for a time-dependent treatment. Several attempts have consequently been made to solve the time-dependent Dirac equation, see e.g. Ref. [1], [2], but it has been proven a hard task to explore the true relativistic region while simultaneously account for the spatial dependence of the electromagnetic field and the full dimensionality of the problem. In a recent attempt [3], we did account for high orders of the multipole expansion of the electromagnetic field (well beyond the dipole approximation), and treated intensities that can drive electrons ionized from hydrogen to velocities $\sim 20\%$ of the speed of light. We could also show a shift from the non-relativistic results of expected magnitude. However, the study also underlines some important problems that appear when the time-dependent Dirac equation is tackled with the usual velocity-gauge minimal-coupling Hamiltonian, leading to slow convergence and exploding requirements on computing time and space. In the poster we will demonstrate the reason for these inherit problems and show how they can be avoided by a gauge transformation, originally proposed for the Schrödinger equations in Ref. [4]. Non-relativistically it replaces the diamagnetic term with new terms that depend explicitly on the momentum in the direction of the laser propagation. The gauge was consequently coined the *propagation gauge*. We will show that a corresponding gauge choice for the Dirac equation is even more advantageous, and further takes a much simpler form.

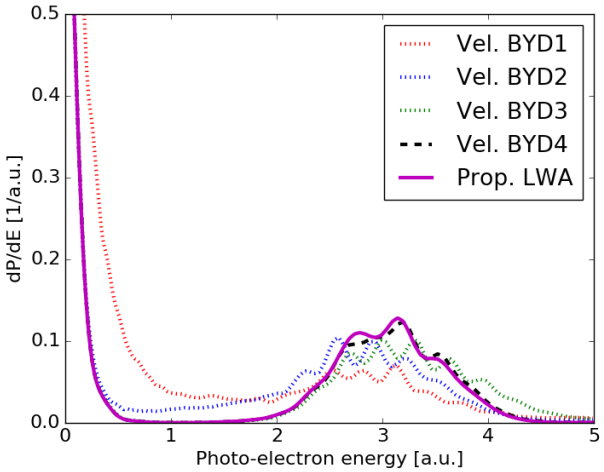

Fig. 1: Photo-electron spectrum from hydrogen exposed to a 15 cycle laser pulse, $\hbar\omega = 3.5$ a.u.(~ 95 eV) and a field strength of 45 a.u. ($\sim 7 \cdot 10^{19}$ W/cm^2). The results labelled BYD show successive higher orders of effects beyond the dipole interaction. This expansion is slowly converging when calculated in velocity gauge. The purple line shows the results within the so-called propagation gauge which is converged already in lowest order.

References

[1] S . Selstø *et al.*, Phys. Rev. A 79, 043418 (2009)
[2] Y . V. Vanne *et al.*, Phys. Rev. A 85, 033411 (2012)
[3] T . Kjellsson *et al.*, Phys. Rev. A 95, 043403 (2017)
[4] M . Førre *et al.*, Phys. Rev. A 93, 013423 (2016)

*Corresponding author: Eva.Lindroth@fysik.su.se

To the list of contents

XUV-initiated High-harmonic Generation in Ar^+

Daniel D. A. Clarke[1]*, **H. W. van der Hart**[1], **A. C. Brown**[1]
1. Centre for Theoretical Atomic, Molecular and Optical Physics, School of Mathematics and Physics, Queen's University Belfast, University Road, Belfast, BT7 1NN, UK

High-harmonic generation (HHG) has emerged as the canonical representative for non-linear and ultrafast optical effects. The process has become a cornerstone of attosecond physics [1], wherein its innately ultrafast nature has enabled the synthesis of coherent extreme-ultraviolet (XUV) and soft-X-ray light pulses, with ever-shortening durations [2-4]. The semiclassical three-step model [5] captures well the gross features of the phenomenon. Here, an electron (i) tunnels through the laser-suppressed Coulomb barrier, (ii) is accelerated by the field, and (iii) radiatively recombines with the parent ion, all within a single cycle of the driving laser field.

In more recent years, research in HHG has diversified beyond the development of light sources, acquiring new leitmotivs that reflect its potential as a sensitive probe of structure and dynamics. Concomitant with this growth of interest in so-called high-harmonic spectroscopy [6-7] has been a demand for enhanced control and optimisation of the process, especially at the single-atom level. In particular, tunnel ionisation from the initial state, traditionally recognised as the first step, yields only poor temporal control and a low conversion efficiency, being both confined to a fixed time interval during the laser pulse evolution, as well as restricted to the emission of an electron from the outermost atomic shell. Acknowledging these limitations, several authors have advocated schemes based on two-colour laser fields [8-10], whereby the target is subject to a strong visible or infrared (IR) driving pulse, as well as a short-duration, often somewhat weaker, XUV pulse. The HHG process can then be initiated by direct photoionization, rather than tunnelling. This has the advantage of being significantly more efficient, and also admits the possibility of driving more deeply bound electrons for an investigation of their real-time dynamics [11-13].

The potential of this XUV-initiated HHG (XIHHG), both as a more efficient mode of single-atom HHG, and as a spectroscopic tool, merits further disquisition of its features in general atomic systems. Importantly, the process remains largely unexplored in atomic ions, whose attraction as HHG sources has been highlighted in several experimental studies [14-15]. Only a limited number of theoretical techniques, however, possess the predictive capacity needed to explore multielectron and multichannel effects in XIHHG, and thereby to inform, and impart directionality to, experimental endeavours. Among them, the R-matrix with time-dependence (RMT) methodology holds considerable promise, enabling the description of laser-driven, ultrafast dynamics in both open- and closed-shell multielectron systems [16-18]. In this contribution, and following recent work on XIHHG in neutral atoms [18], we report on an application of the RMT method to XIHHG from the Ar^+ ion. We address the consequences of direct XUV-mediated photoionisation, from the outer $3p$ subshell, for the HHG process, and discuss the dependence of the harmonic yield on both the peak intensity, and time delay, of the XUV pulse with respect to the IR pulse. Moreover, we highlight the manifestation of electronic structure effects in the two-colour harmonic spectrum, assuming the form of a pronounced Cooper minimum. Finally, we demonstrate the consequences of interference amongst the outer-valence $3p$ and inner-valence $3s$ electrons for the harmonic response.

References

[1] F. Krausz and M. Ivanov, *Rev. Mod. Phys.* **81**, 163 (2009).
[2] E. Goulielmakis *et al.*, *Science* **320**, 1614 (2008).
[3] K. Zhao, Q. Zhang, M. Chini, Y. Wu, X. Wang and Z. Chang, *Opt. Lett.* **37**, 3891 (2012).
[4] T. Popmintchev *et al.*, *Science* **336**, 1287 (2012).
[5] P. B. Corkum, *Phys. Rev. Lett.* **71**, 1994 (1993).
[6] O. Smirnova *et al.*, *Nature* **460**, 972 (2009).
[7] A. D. Shiner *et al.*, *Nat. Phys.* **7**, 464 (2011).
[8] M. B. Gaarde, K. J. Schafer, A. Heinrich, J. Biegert and U. Keller, *Phys. Rev. A* **72**, 013411 (2005).
[9] E. J. Takahashi, T. Kanai, K. L. Ishikawa, Y. Nabekawa and K. Midorikawa, *Phys. Rev. Lett.* **99**, 053904 (2007).
[10] M. Tudorovskaya and M. Lein, *J. Mod. Opt.* **61**, 845 (2014).
[11] J. Biegert *et al.*, *J. Mod. Opt.* **53**, 87 (2006).
[12] G. Gademann *et al.*, *New J. Phys.* **13**, 033002 (2011).
[13] J. Leeuwenburgh, B. Cooper, V. Averbukh, J. P. Marangos and M. Ivanov, *Phys. Rev. Lett.* **111**, 123002 (2013).
[14] E. A. Gibson *et al.*, *Phys. Rev. Lett.* **92**, 033001 (2004).
[15] D. M. Gaudiosi *et* al., *Phys. Rev. Lett.* **96**, 203001 (2006).
[16] L. R. Moore *et al.*, *J. Mod. Opt.* **58**, 1132 (2011).
[17] T. Ding *et al.*, *Opt. Lett.* **41**, 709 (2016).
[18] A. C. Brown and H. W. van der Hart, *Phys. Rev. Lett.* **117**, 093201 (2016).

*Corresponding author: dclarke23@qub.ac.uk

To the list of contents

Rydberg excitations of cold atoms inside a hollow-core fiber

Maria Langbecker[1], **Mohammad Noaman**[1], **Chantal Voss**[1], **Patrick Windpassinger**[*1]
1. Institut für Physik, Johannes Gutenberg-Universität Mainz, Staudingerweg 7, 55128 Mainz, Germany

Cold atoms inside hollow-core fibers ([1] - [4]) present a promising candidate to study strongly coupled light-matter systems. Combined with the long range Rydberg interaction which is controlled through an EIT process, a corresponding experimental setup should allow for the generation of a strong and tunable polariton interaction. Using this scheme, novel photonic states can be generated and studied with possible applications in quantum information and simulation (e.g. [5], [6]).

In our experimental setup, laser cooled Rubidium atoms are transported into a hollow-core fiber fiber using an optical conveyor belt (compare Fig. 1). We explain the details of our transport procedure of the cold atoms into the fiber. Further, we show characterizations of Kagomé-type hollow-core fibers, whose properties allow for two-photon Rydberg excitation, and use them to study Rydberg EIT in a hot atom setup. Finally, we present the first measurements of cold Rydberg excitations inside a hollow-core fiber and discuss our progress towards Rydberg quantum optics in a quasi-one-dimensional geometry.

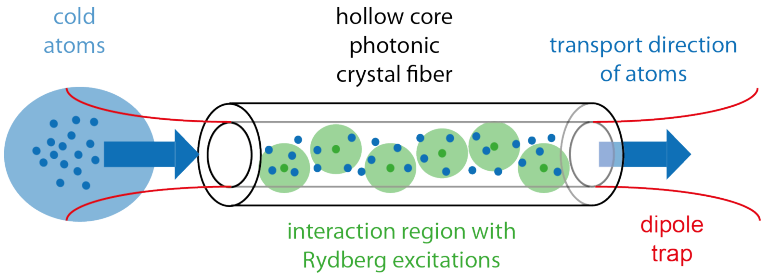

Fig. 1: Schematic sketch of the experimental setup. In front of the hollow-core fiber, cold atoms are produced in a MOT (blue). They are then transported into the fiber using an optical conveyor belt (red). Inside of the fiber, the atoms are excited into Rydberg states (green).

References

[1] S. Vorrath, S. A. Möller, P. Windpassinger, K. Bongs, and K. Sengstock, New J. Phys. **12**, 123015 (2010).
[2] M. Bajcsy, S. Hofferberth, T. Peyronel, V. Balic, Q. Liang, A. S. Zibrov, V. Vuletic, and M. D. Lukin, Phys. Rev. A **83**, 063830 (2011).
[3] F. Blatt, T. Halfmann, and T. Peters, Opt. Lett. **39**, 446-449 (2014).
[4] S. Okaba, T. Takano, F. Benabid, T. Bradley, L. Vincetti, Z. Maizelis, V. Yampol'skii, F. Nori, and H. Katori, Nat. Commun. **5**, 4096 (2014).
[5] J. Otterbach, M. Moos, D. Muth, and M. Fleischhauer, Phys. Rev. Lett. **111**, 113001 (2013).
[6] M. Moos, M. Höning, R. Unanyan, and M. Fleischhauer, Phys. Rev. A **92**, 053846 (2015).

[*]Corresponding author: windpass@uni-mainz.de

To the list of contents

Species-Selective Confinement of Atoms Dressed With Multiple Radiofrequencies

E. Bentine[*1], **T. L. Harte**[1], **K. Luksch**[1], **A. Barker**[1], **J. Mur-Petit**[1], **B. Yuen**[1], **C. J. Foot**[1]
1. Clarendon Laboratory, Department of Physics, University of Oxford, OX1 3PU

Radiofrequency-dressed adiabatic potentials confine atoms using a combination of static and oscillating magnetic fields, and provide a means to create smooth, anisotropic traps with low heating rates [1]. The versatility of these potentials is greatly increased by using multiple radiofrequencies to dress the atoms, enabling for example the creation of multiple individually controllable wells [2]. We have recently demonstrated this approach on a ^{87}Rb apparatus, where control over the amplitudes of each frequency component in the dressing field permits the dynamical modification of a double well potential that confines the atoms [3].

We extend this work to propose a method of species-selective confinement that is suitable for mixtures in which the Landé g_F-factors of the constituent atomic species differ [4]. We describe a mixture dressed with two radiofrequencies, which confines each species in an independently controllable harmonic well. Adjustment of the dressing field allows the two atomic species to be spatially overlapped or separated. This is further developed into a four radiofrequency scheme, in which a double well for one species is overlaid with a single well for the other, while maintaining the ability to dynamically adjust the individual potentials. The discussion is framed with parameters that are suitable for a ^{85}Rb and ^{87}Rb mixture, but is readily generalised to other combinations. We report on progress towards the implementation of this method on our rubidium BEC apparatus, where atoms of ^{85}Rb will play the role of impurities immersed in a ^{87}Rb condensate.

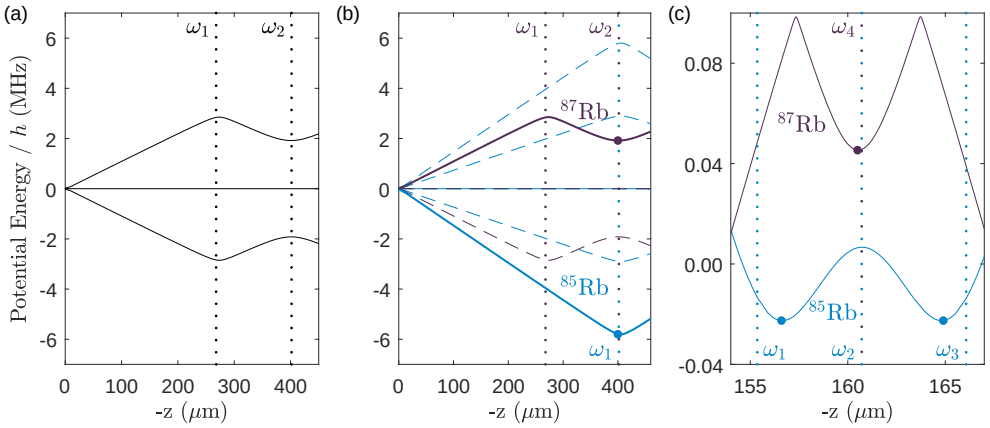

Fig. 1: Adiabatic energy levels for atoms confined in a spherical magnetic quadrupole field and dressed with a homogeneous multiple-radiofrequency field. Energies are plotted as a function of displacement $(-z)$ below the center of the static quadrupole field. **(a)** Eigenenergies of $^{87}\mathrm{Rb}, |F=1\rangle$ atoms dressed with two frequencies $\omega_{1,2} = 2\pi \times 3.0,\ 4.5$ MHz. Avoided crossings occur at locations where the applied radiofrequencies are resonant with the Zeeman splitting (dotted lines). **(b)** An applied radiofrequency is resonant at different locations for $^{85}\mathrm{Rb}, |F=2\rangle$ and $^{87}\mathrm{Rb}, |F=1\rangle$ because of the different magnitude of their Landé g-factors. Atoms are trapped on the eigenstates depicted by solid lines at the filled circles; other eigenstates are shown as dashed lines. Each species is manipulated by controlling the relevant radiofrequency field component. The quadrupole gradient along $\hat{z}$ is 160 Gauss cm^{-1} for the first two subfigures (a) and (b). **(c)** Extending the scheme to four radiofrequencies enables a double well for one species to be overlapped with a single well for the other. The ^{85}Rb is confined in a double well by three frequencies $\omega_{1,2,3} = 2\pi \times 2.9,\ 3.0,\ 3.1$ MHz while the ^{87}Rb experiences a single well potential formed by dressing at $\omega_4 = 2\pi \times 4.5$ MHz. The quadrupole gradient in this subfigure is 400 Gauss cm^{-1}.

References

[1] K. Merloti *et al.* New J. Phys. **15**, 033007 (2013)
[2] P. W. Courteille *et al.*, J. Phys. B: At. Mol. Opt. Phys. **39**, 1055 (2006)
[3] T. L. Harte, E. Bentine, K. Luksch, A. Barker, D. Trypogeorgos, B. Yuen and C. J. Foot, in preparation.
[4] E. Bentine *et al.*, J. Phys. B: At. Mol. Opt. Phys. **50**, 094002 (2017)

*Corresponding author: elliot.bentine@physics.ox.ac.uk

To the list of contents

An ε-pseudoclassical model for quantum resonances in a cold dilute atomic gas periodically driven by finite-duration standing-wave laser pulses

B. T. Beswick[*1], **S. A. Gardiner**[†1], **I. G. Hughes**[1], **H. P. A. G. Astier**[2] **M. F. Andersen**[3], **B. Daszuta**[4],

1. Joint Quantum Centre (JQC) Durham–Newcastle, Department of Physics, Durham University
South Road, Durham DH1 3LE, UK
2. Department of Physics, Cavendish Laboratory
Cambridge, CB3 0HE, United Kingdom
3. Dodd–Walls Centre for Photonics and Quantum Technologies, Department of Physics, University of Otago
Dunedin 9016, New Zealand
4. Department of Mathematics and Statistics, University of Otago
Dunedin 9054, New Zealand

Atom interferometers are a useful tool for precision measurements of fundamental physical phenomena, ranging from local gravitational field strength to the atomic fine structure constant [1]. In such experiments, it is desirable to implement a high momentum transfer "beam-splitter," which may be achieved by inducing quantum resonance in a finite-temperature laser-driven atomic gas [2]. We use Monte Carlo simulations to investigate these quantum resonances in the regime where the gas receives laser pulses of finite duration, and derive an ε-classical model for the dynamics of the gas atoms, conceptually similar to that introduced to describe quantum accelerator modes by Fishman, Guarneri and Rebbuzzini [3]. This model is attractive due to its mathematical simplicity and the minimal computational complexity of the numerics. We show that the ε-classical model is capable of reproducing quantum resonant behavior for both zero-temperature and finite-temperature non-interacting gases, see Fig. 1. We show that this model agrees well with the fully quantum treatment of the system over a time-scale set by the choice of experimental parameters. We also show that this model is capable of correctly treating the time-reversal mechanism necessary for implementing an interferometer with this physical configuration, and that it explains an unexpected universality in the dynamics [4].

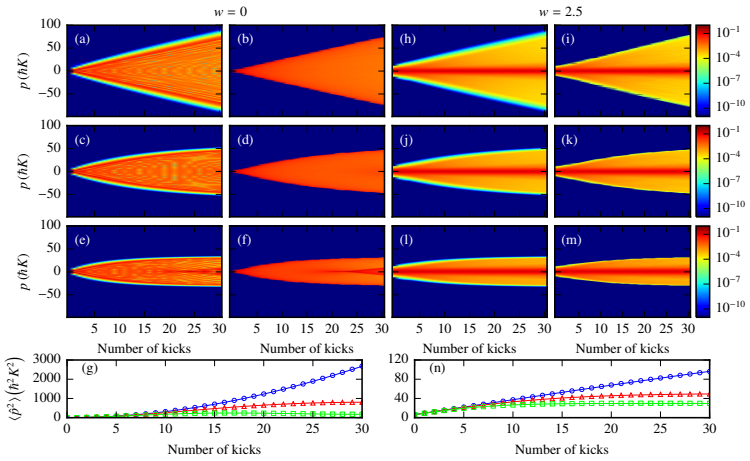

Fig. 1: Comparison between the dynamics of the momentum distributions of the gas population, computed by the fully quantum model, and the pseudoclassical model for zero ($w = 0$) and finite temperature gases ($w = 2.5$), for differing values of the scaled pulse duration ε. The first and second columns show momentum distributions for a zero temperature gas ($w = 0$) as computed by the quantum [(a), (c), (e)] and pseudoclassical models [(b), (d), (f)] respectively. Columns 3 and 4 give the momentum distributions computed by the quantum [(h), (j), (l)] and effective classical models [(i), (k), (m)] respectively, for $w = 2.5$. In each row, the distribution dynamics are computed for a different value of ε: row 1 [(a), (b), (h), (i)] has $\varepsilon = 0.02$, row 2 [(c), (d), (j), (k)] has $\varepsilon = 0.11$, and row 3 [(e), (f), (l), (m)] has $\varepsilon = 0.2$. To accommodate the logarithmic color scale, we have chosen a cutoff value of $C = 10^{-11}$. The corresponding time-evolution of $\langle \hat{p}^2 \rangle$ [in units of $\hbar^2 K^2$] is given in (g), for $w = 0$ and (n) for $w = 2.5$; solid lines represent results of quantum calculations, and symbols those of the effective classical model (squares correspond to $\varepsilon = 0.2$, triangles to $\varepsilon = 0.11$, and circles to $\varepsilon = 0.02$).

References

[1] A. Miffre, M. Jacquey, M. büchner, G. Trénec and J. Vigué, arXiv:quant-ph/0605055v1 (2006)
[2] B. Daszuta and M. Andersen, Physical Review A **86**, 043604 (2012)
[3] Shmuel Fishman, Italo Guarneri and Laura Rebuzzini, Phys. Rev. Lett. **89**, 084101 (2002) ,
[4] B. T. Beswick, H. P. A. G. Astier, S. A Gardiner, I. G Hughes, M. F. Andersen, B. Daszuta, Phys. Rev. A **94**, 063604 (2016)

[*]Corresponding author: b.t.beswick@durham.ac.uk
[†]Corresponding author: s.a.gardiner@durham.ac.uk

To the list of contents

Fibonacci anyon excitations of one-dimensional dipolar lattice bosons

Tanja Đurić[1], **Krzysztof Biedroń**[*1], **Jakub Zakrzewski**[1,2]
1. Instytut Fizyki im. M. Smoluchowskiego, Uniwersytet Jagielloński, Łojasiewicza 11, 30-348 Kraków, Poland
2. Mark Kac Complex Systems Research Center, Jagiellonian University, Łojasiewicza 11, 30-348 Kraków, Poland

Recent research on topological order in quantum systems has lead to greater understanding of some fundamental physical phenomena (such as Fractional Quantum Hall (FQH) effect), as well as provided new perspectives on realising exotic states of matter, such as Majorana fermions. All of this may prove to be beneficial in the development of quantum computation, as topologically protected states are a promising candidates for building blocks of quantum computers, which need to stay coherent and error free for long periods of time. It turns out that non-Abelian states of matter (whoose lowest excitations can combine - braid - in noncommutative ways) are enough to perform universal quantum computation. Studies suggest that it should be possible to create such uncommon systems using optical lattices, e.g. 1D optical lattices described by extended Bose-Hubbard model, where the lowest excitations correspond to some of the FQH states in the limit of zero tunneling[1]. We have done extensive exact diagonalization and DMRG calculations in order to provide clearer picture of the system in question[2]. For small, finite values of tunneling we have found that overlaps of the exact wavefunctions with, non-Abelian by design, ansatz wave functions are still close to 1. We have also analyzed quantum phase transitions in the system.

References

[1] E. Wikberg, J. Larson, E. J. Bergholtz, and A. Karlhede, Phys. Rev. A **85**, 033607 (2012).
[2] T. Đurić, K. Biedroń, and J. Zakrzewski, Phys. Rev. B **95**, 085102 (2017).

[*]Corresponding author: krzysztof.biedron@doctoral.uj.edu.pl

To the list of contents

Laser cooling of molecules to below the Doppler limit

L. Caldwell*, **S. Truppe, M.Hambach, H. J. Williams, N. J. Fitch, E. A. Hinds, B. E. Sauer, M. R. Tarbutt**
1. Centre for Cold Matter, Blackett Laboratory, Prince Consort Road, Imperial College London, London SW7 2AB, UK.

The use of lasers to magneto-optically trap atoms and cool them to temperatures below the Doppler limit has been essential to progress in many branches of physics in the last 30 years. Ensembles of ultracold atoms have been utilised in precision measurements of fundamental physics, production of quantum degenerate gases and the study of a range of phenomena in quantum optics and many body physics. A broad set of new applications await ultracold molecules [1]. We will present our recent work with CaF molecules. We slow CaF molecules produced from a pulsed cryogenic buffer gas source [2] and then load them into a magneto-optical trap (MOT). We lower the temperature of the trapped molecules to <1 mK by reducing the intensity of the trapping light before loading them into a blue detuned "grey molasses" where we are able to further reduce the temperature to 50 μK, well below the doppler limit [3]. These ultracold molecules are suitable for loading into optical tweezers for quantum simulation, launching in a molecular fountain for testing fundamental physics or for use in the study of ultracold collisions and ultracold chemistry.

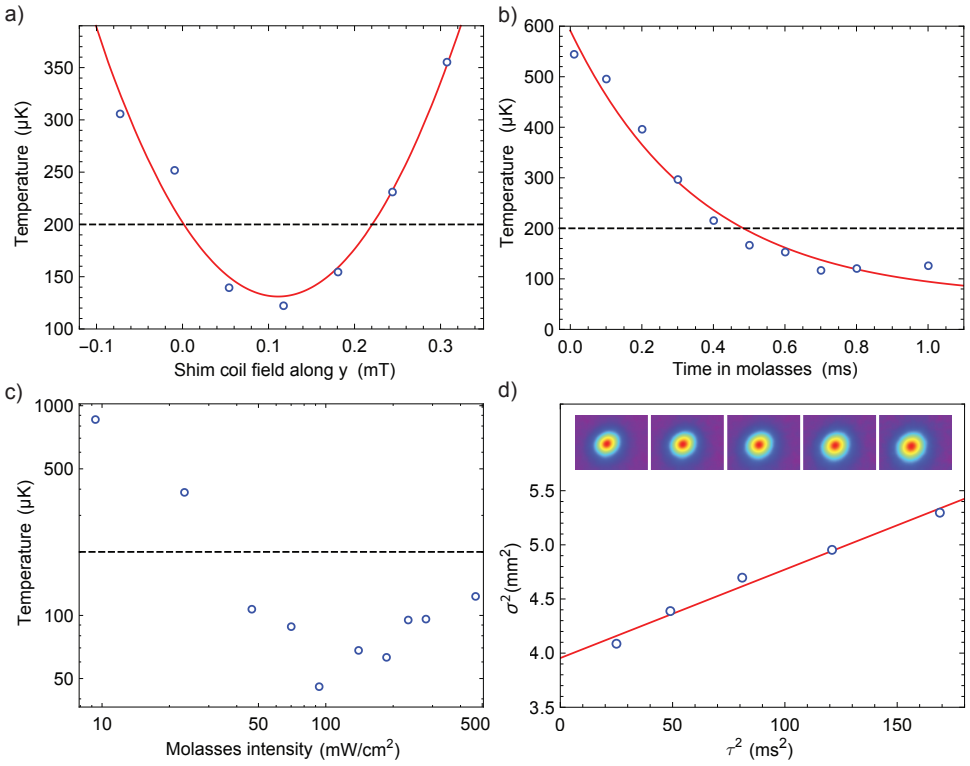

Fig. 1: Sub-Doppler cooling of molecules. (a) Temperature versus magnetic field produced at the cloud by external coil. The intensity of the molasses light is 460 mW/cm^2 and the molecules are held in molasses for 5 ms. (b) Temperature versus time in the molasses. The intensity of the molasses light is 460 mW/cm^2. (c) Temperature versus light intensity for 5 ms molasses. (d) Free expansion temperature measurement of molecule cloud at 52(2) μK.

References

[1] L. D. Carr *et al.* Cold and ultracold molecules: science, technology and applications. *New J. Phys.*, **11**, 055049 (2009).
[2] S. Truppe *et al.* An intense, cold, velocity-controlled molecular beam by frequency-chirped laser slowing. *New J. Phys.*, **19**, 022001 (2017).
[3] S. Truppe *et al.* Molecules cooled below the doppler limit. (2017) *arXiv:1703.00580.*

*Corresponding author: l.caldwell@imperial.ac.uk

To the list of contents

The long-range behavior of ab initio transition dipole moments and spin-orbit coupling matrix elements between the low-lying electronic states of LiRb and KRb molecules

E. A. Bormotova[*1], **S. V. Kozlov**[†1], **E. A. Pazyuk**[1], **A. V. Stolyarov**[1]
1. Chemistry Department, Moscow State University, Moscow 119991, Russia

Both spin allowed transition dipole moments (TDM) and spin-orbit coupling (SOC) matrix elements are calculated using ab initio methods for a wide range of internuclear distances, R, for the electronic states converging to the lowest three dissociation limits of LiRb and KRb molecules. TDM and SOC functions are evaluated in the basis of the spin-averaged wavefunctions corresponding to pure Hund's coupling case (a) by means of effective core pseudopotentials (ECP). The electronic correlation is accounted for by applying the multi-reference configuration interaction (MR-CI) method to only two valence electrons. Core-polarization potentials (CPP) are used to take the core–valence effect into account.

The achieved accuracy allowed us to quantitatively demonstrate that the domonant asymptotic behavior of the TDM and SOC functions is $1/R^3$ and $1/R^6$, respectively. Furthermore, the asymptotic behavior of the resulting ab initio TDM functions is very close to their analytical counterparts obtained within the framework of the long range perturbation theory (LRPT) by Chu and Dalgarno [1]. The present correct long range TDM and SOC functions, together with the relevant potential energy curves [2,3], could be applied to the comprehensive coupled-channel (CC) treatment of the competitive radiative and predissociative dynamics of the mutually perturbed molecular states located in the vicinity of dissociation thresholds.

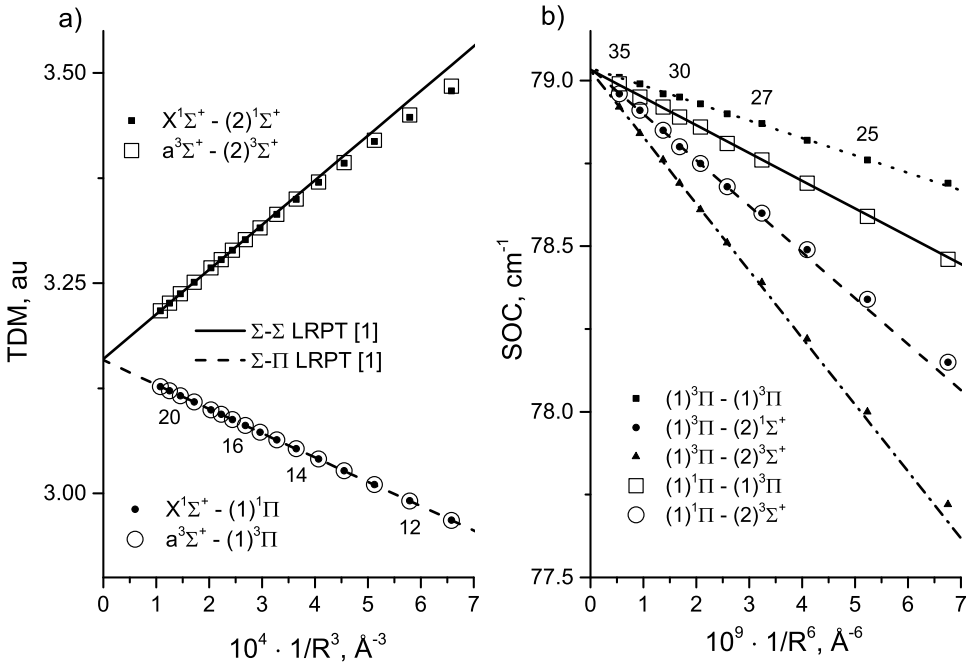

Fig. 1: a) Transition dipole moments (TDM) between electronic states converging to the first and second dissociation limits for LiRb; b) Spin-orbit coupling (SOC) functions between the electronic states converging to the second dissociation limit for KRb

The work was partly supported by the RFBR grant N 16-03-00529-a.

References

[1] X. Chu and A. Dalgarno, Phys. Rev. A, **66**, 024701 (2002).
[2] S. Rousseau, A.R. Allouche and M. Aubert-Frecon, J. Mol. Spectrosc. **203**, 235 (2000).
[3] M. Korek, A. R. Allouche, M. Kobeissi, A. Chaalan, M. Dagher, K. Fakherddin, M. Aubert-Frécon, Chem. Phys. **256**, 1 (2000)

[*]Corresponding author: bormotova@laser.chem.msu.ru
[†]Corresponding author: sevlakoz@phys.chem.msu.ru

To the list of contents

Prospects of the usage of the $A^1\Sigma^+ \sim b^3\Pi$ and $D^1\Pi \sim d^3\Pi$ complexes in ultracold LiRb molecule production

E. A. Bormotova[*1], **A.V. Stolyarov**[1]
1. Department of Chemistry, Moscow State University, ul. Leninskiye Gory 1/3, 119991 Moscow, Russia

Within the field of modern molecular physics laser synthesis and cooling has seen a surge of attention. Due to their attractive properties, heteronuclear alkali metal dimers have been singled out as especially advantageous diatomics. In particular, the LiRb molecule has a large permanent dipole moment in both ground and excited electronic states which not only allows for easy manipulation by external electric field but also makes it possible to use as a base material for quantum computers. Recently, few laser schemes for the assembly and cooling of the LiRb molecule have been proposed, found and probed. However, a systematical searching of the most efficient optical pathways for conversion of ultracold Li and Rb atoms into the stable ground molecular state, indispensably requires highly accurate term values, and radiative and electric properties of the "intermediate" excited states, especially possessing strong "mixed" singlet-triplet character.

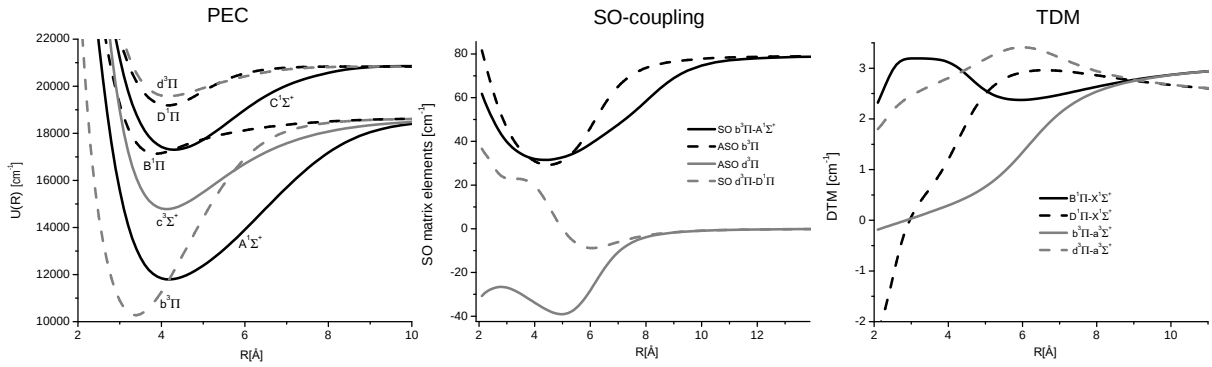

Fig. 1: (a) The schema of adiabatic potentials for the low-lying excited states of the LiRb molecule; (b) *ab initio* calculated spin-orbit functions of the $A^1\Sigma^+ \sim b^3\Pi$ and $D^1\Pi \sim d^3\Pi$ complex; c) selected transition dipole moments.

We accomplished a comprehensive deperturbation analysis of the spin-orbit coupled $A^1\Sigma^+ \sim b^3\Pi$ and $D^1\Pi \sim d^3\Pi$ complexes of the LiRb molecule exploiting the recent spectroscopic observations[1-3] and our own electronic structure estimates. The large scale *ab initio* calculations were performed within the framework of a pure Hund's coupling case "a" for both singlet and triplet state manifolds converging to the lowest three dissociation limits. The adiabatic potential energy curves (PECs), spin-orbit (SO) and angular coupling matrix elements as well as the permanent and transition dipole moments were calculated in a wide range of inter-atomic distances. Most obtained electronic matrix elements demonstrate a pronounced dependence on inter-atomic distance due to strong configuration interaction occurring in the chemical bond domain. The predicted SO splitting in the triplet $b^3\Pi$ and $d^3\Pi$ states are found to be in good agreement with their experimental counterparts [2]. The rigorous coupled-channel (CC) deperturbation model was used to describe the spin-orbit and spin-rotational interactions in mutually perturbed states of the $A^1\Sigma^+ \sim b^3\Pi$ and $D^1\Pi \sim d^3\Pi$ complexes of LiRb on the spectroscopic level (~ 0.01 cm^{-1}) of accuracy. The adjusted fitting parameters of the developed CC model (such as PECs and SO matrix elements) were then applied for the simulation of the stimulated Raman $a^3\Sigma^+ \rightarrow [A^1\Sigma^+ \sim b^3\Pi]/[D^1\Pi \sim d^3\Pi] \rightarrow X^1\Sigma^+$ processes which can lead to efficient formation of ultracold LiRb molecules in their absolute ground state $v_X = 0$; $J_X = 0$.

The work was supported by the RFBR grant Nr. 16-03-00529a.

References

[1] A. Altaf, S. Dutta, J. Lorenz, J. Perez-Rios, Y.P. Chen, D. S. Elliott, J. Chem. Phys. **142**, 114310, (2015).
[2] I. Stevenson, D. Blasing, A. Altaf, Y. P. Chen, D. S. Elliott, J. Chem. Phys., **145**, 224301, (2016).
[3] I. Stevenson, D. B. Blasing, A. Altaf, Y. P. Chen, D. S. Elliott, Phys. Rev. A **94**, 062503, (2016).

*Corresponding author: bormotova@laser.chem.msu.ru

To the list of contents

Towards non-destructive, real-time transport measurements of interacting Fermi Gas

Barbara Cilenti[*1], **K. Roux**[1], **O. Bettermann**[1], **V. Helson**[1], **J. Brantut**[1]
1. Institute of physics, École Polytechnique Fédérale de Lausanne, 1015 Lausanne, Switzerland

Over the last decades an intensive research has been conducted on ultracold atoms, inspired by their good isolation from the environment and ease in manipulation. As a result a very high degree of control is now accessible, including the tuning of inter-atomic interactions, the possibility to organize them in defined geometrical patterns or in lower dimensions. For these reasons, ultracold atoms can simulate a large variety of many-body quantum system that cannot be studied theoretically directly [1]. Among the open problems in many-body physics, the study of the transport properties has gained popularity in the past years, and several experiments have been realized to study the phenomenon under different perspectives. In particular, simulation of conductance in mesoscopic devices has been performed, by connecting two macroscopic reservoirs of ultracold fermions via a channel and observing the current induced by a controlled unbalance of the two reservoirs [2]. These experiments are usually limited in sensitivity by the noise associated to the preparation of a new sample after each measurement.
The aim of the experiment that is currently being setting up in Lausanne is to overcome this limitation to the sensitivity by integrating a high finesse cavity in the experimental set-up to perform non-destructive measurements [3]. This feature will allow us to observe the dynamics of the system in real time and, as a consequence, to reduce the preparation noise.
It can be shown that, for a fixed destructivity of the measurement, the signal to noise ratio increases like the square root of the Finesse, we thus planned a finesse of 50000, as a compromise between high signal to noise ration and experimental complexity. Our experimental setup will combine cavity assisted measurements with a tunable Fermi gas of ^{6}Li atoms.
In my poster, I will give a detailed description of the current status of the experimental setup and I will discuss the preliminary test that have been performed on a cavity prototype.

References

[1] I. Bloch, J. Dalibard, and W. Zwerger, Rev. Mod. Phys **80**, 885 (2008)
[2] J. Brantut, J. Meinke, D. Stadler, S. Kinner and T. Esslinger, Science **337**, 6098 (2012).
[3] J. E. Lye, J. J. Hope, and J. D. Close, Phys. Rev. A **67**, 043609 (2003)

*Corresponding author: barbara.cilenti@epfl.ch

To the list of contents

Towards the implementation of quantum probes in spin-dependent optical lattice potentials

Andrea Di Carli[1], **C.Colquhoun** [1], **E.Haller** [1]
1. University of Strathclyde, Department of Physics,
Scottish Universities Physics Alliance (SUPA), Glasgow G4 0NG, United Kingdom

Ultracold atomic gases in optical lattice potentials provide a powerful approach to simulate strongly correlated quantum systems [1] due to the possibility to tune almost any parameter of the system, such as the lattice geometry, the particle density and temperature, and interactions. In particular caesium atoms, unlike the other alkali atoms, provide very favorable scattering properties and a precise control of the interaction strength with magnetic Feshbach resonances at low magnetic fields strength. The study of a complex quantum system by means of a small, immersed quantum system (probe), with a reduced number of degrees of freedom, can provide new insight into global and local properties of the complex system. Properties such as phase, correlations, and temperature can change the decoherence and dissipation of the probe dramatically, and they can be determined by measuring the dynamics of the probe. I am going to report on our progress and future plans to realise such quantum probes with ultracold Cesium atoms in spin-dependent optical lattice potentials.

References

[1] I.Bloch, J. Dalibard, and S. Nascimbène, Nature. Phys. **8**, 267 (2012).

To the list of contents

Discovering new physics strategies with citizen science driven, human-computer hybrid optimization

Ottó Elíasson[*1], **Jacob Sherson**[†1] **the scienceathome.org team**[1]
1. Institute of Physics and Astronomy, Aarhus, Denmark

Problem solving is central to every scientific discipline. To solve a particular problem, we employ a certain /em strategy. New and novel strategies can lead to new insight to the nature of the problem. The formulation of such strategies is usually based on observations, intuition and theoretical assessment. For any given physical process, often several distinct strategies are identified. The question arises, are they truly distinct or simply low dimensional representations of a high dimensional continuum of possible solutions. Here, we investigate this question in two physical frameworks.

Our online citizen science platform scienceathome.org used by more than 200,000 people, recently enabled finding solutions to fast, 1D single atom transport [1]. Surprisingly, player trajectories of the quantum games were found to bunch into discrete solution strategies (clans) yielding clear, distinct physical insight. These solutions are locally optimal against perturbations along each of the roughly 1000 dimensions. However, searching along the high-dimensional vector in the direction of other local maxima, we locate /em bridges demonstrating a continuum of solutions with no clear physical interpretation exists. With this insight, we have developed a hybridized local search and evolutionary algorithm (Memetic Algorithm) outperforming current quantum optimal control (QOC) methods. This algorithm was not only tested on the single atom transport problem, but also in other systems relating to the creation of a two-qubit gate using controlled double well merger, optimal splitting of a condensate and condensate excitation.

In a second study, the experimental problem of creating atomic Bose-Einstein Condensates (BEC) was investigated. Four conventional trap configurations forming distinct strategies were identified. We find again, that bridges between the approaches can be identified by appropriate mixing of variables. In a novel approach, the problem was gamified and nearly 800 citizen scientists from all over the world contributed in real-time to the optimization of the experiment. The best player results yielded an improvement of about 50% in atom number [2].

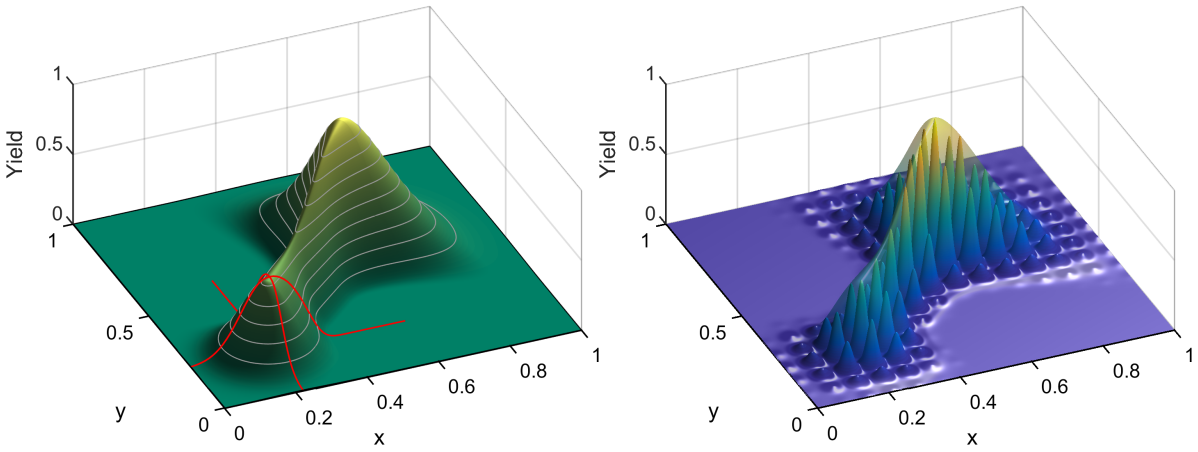

Fig. 1: The two figures illustrate control landscapes, with arbitrary control variables on the horizontal axes and the yield of the fitness function on the vertical axis. (left) The problem has an optimal solution with respect to 1D scans, depicted in red. By appropriate variable mixing, one climbs to the global optimum. (right) There exist many distinct seemingly locally optimal solutions. In a different parametrisation these are connected by a continuum of solutions (as the transparent envelope).

References

[1] Jens Jakob W. H. Sørensen et al., Nature, 532, 210–213 (2016).
[2] Robert Heck et al., in preparation.

[*]Corresponding author: ottoel@phys.au.dk
[†]Corresponding author: sherson@phys.au.dk

To the list of contents

Observing Metastability in a strongly-correlated many-body system

L. Hruby[*1], **N. Dogra**[1], **M. Landini**[1], **K. Kroeger**[1], **T. Donner**[1], **T. Esslinger**[1]
1. Institute for Quantum Electronics, Department of Physics, ETH Zurich
HPF, Otto-Stern-Weg 1, 8093 Zurich, Switzerland

Common assumptions at the basis of statistical mechanics often rely on interactions being sufficiently short-ranged [1]. The opposite limit where interactions do not decay with distance is less well studied. Such global-range interactions hinder the coexistence of phases and can result in the creation of long-lived metastable states [2]. These states are usually associated with first order phase transitions in strongly correlated matter, heralded via the observation of hysteresis.

Our system consists of a Bose-Einstein condensate exposed to a three-dimensional optical lattice to enhance short-range on-site interactions. The condensate is coupled to a single mode of an optical high-finesse cavity which mediates effective atom-atom interactions of global range [3], see Fig. 1A. We are able to tune the relative strength of short- and global range interaction independently which allows us to map out the phase diagram [4] sketched in Fig. 1B . Photons leaking from the cavity provide real-time information on the amount of a λ-periodic density modulation present in the system which we quantify by an even-odd particle imbalance.

We study the phase transition between two insulators, namely a Mott-insulator (MI) and a charge density wave (CDW). The CDW is characterized by a non-zero even-odd particle imbalance Θ, which is zero in the MI phase. Thus the imbalance Θ plays the role of an order parameter for the transition. We initialize the system in an MI state and sweep the cavity-detuning towards the CDW phase so as to increase the strength of global-range interactions. Proceeding the sweep we observe that the system ends up in either one of two distinct imbalance levels separated by a gap. We attribute the existence of these levels to two metastable many-body states present in the system and isolated from each other by an energy barrier. During the sweep from the MI to the CDW the imbalance jumps within about a single tunneling time signaling a correlated tunneling of several thousand atoms to their neighboring lattice sites. When approaching the transition from opposite directions we find hysteresis in the even-odd particle imbalance. Our results provide a unique real-time study of a first order phase transition between two strongly-correlated many-body phases.

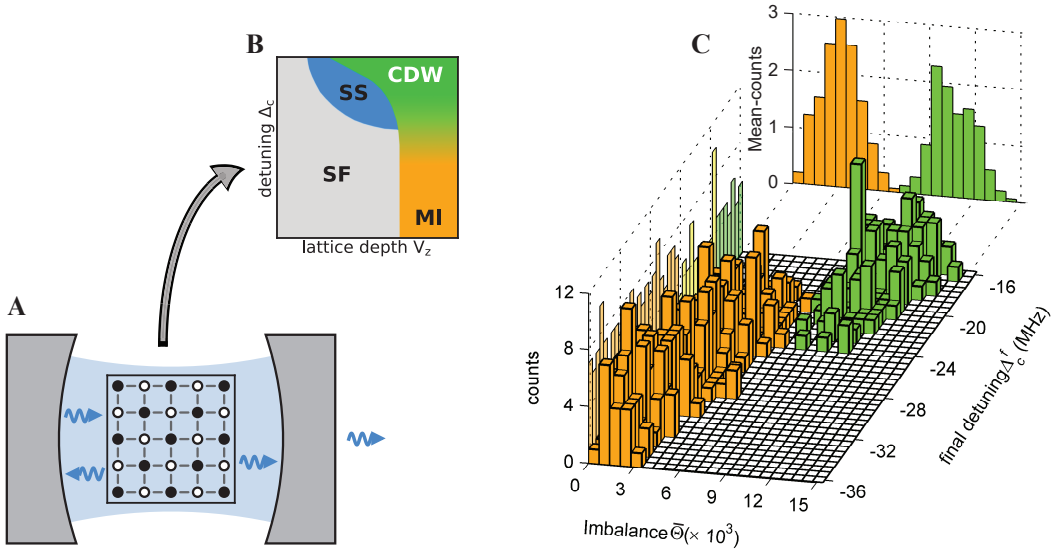

Fig. 1: **A:** Our experiment consists of a ^{87}Rb Bose-Einstein condensate coupled to a single mode of an optical resonator. It is exposed to a three-dimensional optical lattice. **B:** A sketch of the observed phase diagram of the system consisting of four phases: a superfluid (SF), a lattice supersolid (SS), a Mott-insulator (MI) and a charge-density wave (CDW). **C:** Metastable behavior of the imbalance when sweeping the cavity-detuning to cross from an MI to a CDW state. Two distinct imbalance levels are highlighted in orange and green. A gap in the imbalance is visible between them.

References

[1] A. Campa, T. Dauxois and S. Ruffo, Physics Reports **480** (3-6), 57-159 (2009).
[2] Y. Levin, R. Pakter, F. B. Rizzato, T. N. Teles and F. P. C. Benetti, Physics Reports **535** (1), 1-60 (2014).
[3] K. Baumann, C. Guerlin, F. Brennecke and T. Esslinger, *Nature* **464**, 1301-1306 (2010).
[4] R. Landig, L. Hruby, N. Dogra, M. Landini, T. Donner and T. Esslinger, *Nature* **532**, 476-479 (2016).

*Corresponding author: hruby@phys.ethz.ch

To the list of contents

Blue-Detuned Magneto Optical Trap

Kyle N. Jarvis[*1], **T. E. Wall, E. A. Hinds, B. E. Sauer, M. R. Tarbutt**
1. Centre for Cold Matter, Blackett Laboratory, Imperial College London, London SW72AZ, UK

The magneto optical trap (MOT) is an essential tool for a wealth of scientific and technological applications of ultra-cold atoms. The vast majority of atomic MOTs use a transition where the upper-state angular momentum, F', is larger than the ground-state angular momentum, F. These are known as type-I MOTs. Conversely, type-II MOTs have F' $\leq$ F. Molecular MOTs use type-II transitions to prevent rotational branching, and recent progress in forming molecular MOTs [1] has stimulated a renewed interest in this type of trap [2][3]. Atomic type-II MOTs have also been reported [4] but tend to produce relatively hot, low-density traps and so have not been used much. We show that it is possible to circumvent these limitations by making a simple, but counter-intuitive, modification to the trapping scheme: we use light that is blue-detuned from resonance. The temperature in the blue-detuned MOT is far below the Doppler limit because the cooling is due entirely to polarization gradient cooling. The atoms spend much of their time in dark states, and so the photon scattering rate is low. This reduces re-scattering within the MOT which normally limits the density [5], and as a result the density in the blue-detuned MOT is higher than in a type-I MOT. Our blue-detuned MOT has a phase-space density many orders of magnitude higher than reported for red-detuned type-II atomic MOTs, and is also higher than most type-I MOTs.

References

[1] J. F. Barry, D. J. McCarron, E. B. Norrgard, M. H. Steinecker, D. DeMille, Nature 512, 286 (2014).
[2] M. R. Tarbutt, New. J. Phys. 17, 015007 (2015).
[3] J. A. Devlin, M. R. Tarbutt, New J. Phys. 18, 123017 (2016).
[4] E. L. Raab, M. Prentiss, A. Cable, S. Chu, D. E. Pritchard, Phys. Rev. Lett. 59, 2631 (1987).
[5] T. Walker, D. Sesko, C. Wieman, Phys. Rev. Lett. 64, 408 (1990).

[*]Corresponding author: k.jarvis14@imperial.ac.uk

To the list of contents

Spin mixing and protection of ferromagnetism in a spinor dipolar condensate

Kaci Kechadi[*] [1], **Bruno Laburthe-Tolra**[†] [1], **Paolo Pedri**[1]
1. Laboratoire de Physique des Lasers (LPL), CNRS UMR 7538, Université Paris 13, Institut Galilée
99 Avenue J.-B. Clment, F-93430 Villetaneuse, France

Our work focuses on the study of Bose-Einstein condensates with internal spin degrees of freedom, commonly known as spinor BECs. We study out-of-equilibrium physics of spin-3 chromium dipolar BECs following an excitation of the spin degree of freedom. We describe in particular spin dynamics which, we find, results from an interplay between contact and dipolar interactions. Here we focus on the theoretical studies in contact with the experiment at Villetaneuse [1].

Starting from a fully polarized spin 3 chromium dipolar BEC in state $m=-3$, we numerically investigate spin mixing dynamics after rotation of the collective spin by an angle θ compared to the magnetic filed. For $\theta \neq \pi/2$ dynamics is triggered by dipolar interactions [2]. On the contrary, for $\theta = \pi/2$ dipolar interaction does not drive any dynamics and magnetic filed gradient is necessary to trigger dynamics.

Just after rotation, all spins are aligned and the sample therefore has a ferromagnetic character. One striking observation derived from our simulations of the spinor Gross-Pitaevskii equation, which are in good agreement with experimental results, is a protection of a local ferromagnetic character of the gas while dynamics proceeds. Indeed, the local spin length remains close to its maximum, 3. Surprisingly the spinor remains locally ferromagnetic, despite the fact that spin dependent interactions energetically favor depolarization.

To understand this effect, we have solved the spinor Gross-Pitaevskii equation for a homogeneous BEC in presence of magnetic field gradients. We find that the initial ferromagnetic character of the BEC is protected by spin exchange contact interactions, which provide self-rephasing of the spinor components. Taking the phenomenological assumption that the spinor remains ferromagnetic, we developed a simple analytical model based on spinor hydrodynamic approach [3] to investigate the short time dynamics induced by a magnetic field gradient b. We derive the following evolution of the fractional populations p_m of the Zeeman state m when taking an initial Gaussian ansatz of $1/e^2$ radius R:

$$p_m(t) = p_m(0)\left[1+\left(\frac{g\mu_B b}{2MR}\right)^2\left(m^2-\sum_{n=-3}^{3} n^2 p_n(0)\right)t^4\right] \qquad (m=-3,...,+3) \tag{1}$$

where M, g and μ_B are the mass, the gyromagnetic factor and the Bohr magneton respectively.

We find excellent agreement with simulations at short time when only contact interactions are taken into account (See Fig. 1). Then eq. (1) provides a time scale $(MR/g\mu_B b)^{1/2}$ for the spin dynamics. We stress that the resulting dynamics predicted in this model is independent of spin dependent interactions, which are in practice adiabatically eliminated. Large enough spin dependent contact interactions convey metastability to ferromagnetism.

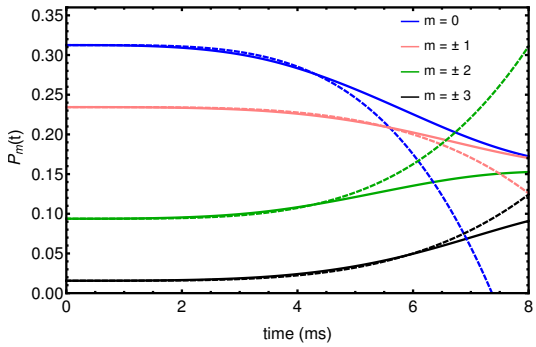

Fig. 1: Temporal evolution following an initial rotation of individual spins by an angle $\theta = \pi/2$ for $b = 35$mG/cm. Spin dynamics given by eq. (1) (dashed lines) are in good agreement with simulations at short time when only contact interactions are taken into account (full lines).

References

[1] S. Lepoutre, K. Kechadi *et al.*, unpublished.
[2] Y.Kawaguchi, H. Saito PRL and and M. Ueda **98**, 110406 (2007)
[3] K.Kudo,Y.Kawaguchi, Phys. Rev. A **82**,053614(2010)

[*]Corresponding author: kaci.kechadi@univ.paris13.fr
[†]Corresponding author: laburthe-tolra@univ-paris13.fr

To the list of contents

Nonlinear scattering of atomic bright solitons in disorder.

A. Boissé[1], **G. Berthet**[1], **T. Bourdel**[*1]
1. Laboratoire Charles Fabry (LCF), Institut d'Optique, CNRS, Univ Paris-Sud
2 Avenue Augustin Fresnel, 91127 Palaiseau Cedex, France

We observe nonlinear scattering of ^{39}K atomic bright solitons [1] launched in a one-dimensional (1D) speckle disorder. We directly compare it with the scattering of non-interacting particles in the same disorder. The atoms in the soliton tend to be collectively either reflected or transmitted, in contrast with the behavior of independent particles in the singlescattering regime, thus demonstrating a clear nonlinear effect in scattering. The observed strong fluctuations in the reflected fraction, between zero and 100%, are interpreted as a consequence of the strong sensitivity of the system to the experimental conditions and in particular to the soliton velocity [2]. This behavior is reproduced in a mean-field framework by Gross-Pitaevskii simulations, and mesoscopic quantum superpositions of the soliton being fully reflected and fully transmitted are not expected for our parameters. We discuss the conditions for observing such superpositions, which would find applications in atom interferometry beyond the standard quantum limit [3].

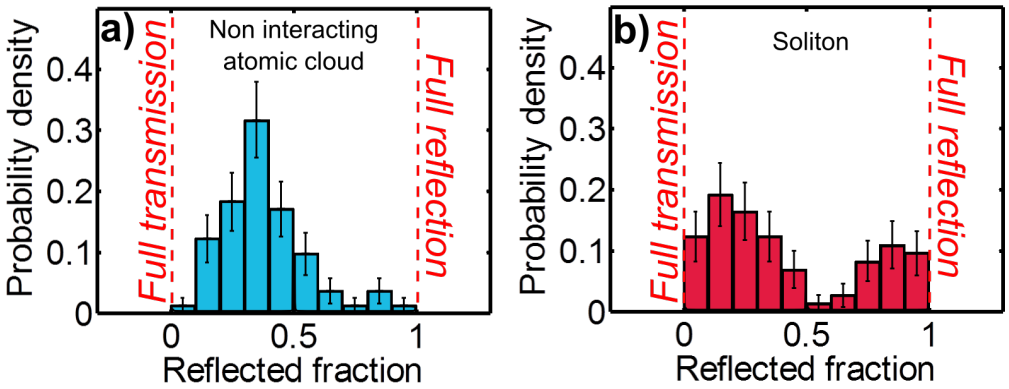

Fig. 1: (Color online) Histograms of the experimentally measured reflected fractions of non-interacting atoms ((a) in blue) and solitons ((b) in red). The double-peak structure in (b) is a clear signature of nonlinear scattering.

References

[1] S. Lepoutre, L. Fouché, A. Boissé, G. Berthet, G. Salomon, A. Aspect, and T. Bourdel, Phys. Rev. A **94**, 053626 (2016).
[2] A. Boissé, G. Berthet, L. Fouché, G. Salomon, A. Aspect, S. Lepoutre and T. Bourdel, EPL **117**, 10007 (2017).
[3] Alexej I. Streltsov, Ofir E. Alon, and Lorenz S. Cederbaum, Phys. Rev. A **80**, 043616 (2009).

[*]Corresponding author: thomas.bourdel@institutoptique.fr

To the list of contents

Towards Coherent splitting and recombination of bright solitary matter waves

A. Rakonjac*[1], O. J. Wales[1], T. P. Billam[2], J. L. Helm[3], S. A. Gardiner[1], and S. L. Cornish†[1]

1. Joint Quantum Centre (JQC) Durham–Newcastle, Department of Physics, Durham University South Road, Durham DH1 3LE, UK

2. Joint Quantum Centre (JQC) Durham–Newcastle, School of Mathematics and Statistics, Newcastle University Newcastle upon Tyne NE1 7RU, UK

3. Dodd-Walls Centre for Photonic and Quantum Technologies, Department of Physics, University of Otago 730 Cumberland Street, Dunedin 9016, New Zealand

We report on the controlled creation, splitting, and recombination of bright solitary matter waves formed from Bose-Einstein condensates of ^{85}Rb atoms. These solitary wavepackets, or solitons, are long-lived, with lifetimes of over 20 seconds, and can propagate without observable dispersion over macroscopic distances. Following our previous work on classical reflection of solitons from a broad repulsive barrier [1] and quantum reflection from a narrow attractive well [2], we extend our investigations to solitons incident on a narrow repulsive gaussian barrier [3]. When the kinetic energy of the soliton wavepacket is comparable to the barrier height, we observe controllable splitting of the soliton into two daughter solitons. The splitting proportion varies according to incident velocity and barrier height with good agreement with 1-D and 3-D Gross-Pitaevskii simulations. After allowing the daughter solitons to oscillate in a weak harmonic potential, they recombine on the barrier and continue propagating as an apparent single soliton, though the recombination is in this case the result of velocity filtering rather than a coherent process. Future experiments with a narrower barrier should allow us to reach the coherent recombination regime.

The coherent splitting and recombination of solitons as well as their long lifetime leads the way to using such a scheme for soliton-based interferometry in a variety of configurations [4]. In particular, the scheme can be utilised in a ring geometry for Sagnac interferometry [5]. Future work includes implementing a soliton Sagnac interferometer using a 2-D painted ring potential and further experimental studies of bright matter-wave soliton dynamics that can be used to elucidate the wealth of theoretical work in the field, as well as to explore, for example, the realisation of Schrödinger cat states [6, 7] and the study of short-range atom-surface potentials [8].

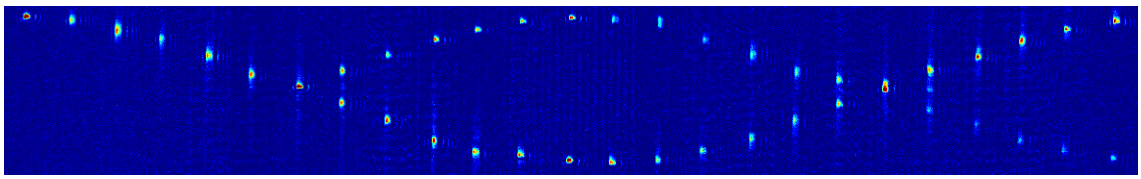

Fig. 1: A series of destructive absorption images at 30 ms time intervals showing splitting and apparent recombination of two equally populated daughter solitons on a narrow repulsive Gaussian barrier.

References

[1] A. L. Marchant, T. P. Billam, T. P. Wiles, M. M. H. Yu, S. A Gardiner, and S. L. Cornish, Nat. Commun. **4**, 1865 (2013)
[2] A. L. Marchant, T. P. Billam, M. M. H. Yu, A. Rakonjac, J. L. Helm, J. Polo, C. Weiss, S. A. Gardiner, and S. L. Cornish, Phys. Rev. A **93**, 021604(R) (2016)
[3] J. L. Helm, T. P. Billam, and S. A. Gardiner, Phys. Rev. A **85**, 053621 (2012)
[4] A. D. Cronin, J. Schmiedmayer, and D. E. Pritchard, Rev. Mod. Phys. **81**, 1051 (2009)
[5] J. L. Helm, S. L. Cornish, and S. A. Gardiner, Phys. Rev. Lett. **114**, 134101 (2015)
[6] C. Weiss and Y. Castin, Phys. Rev. Lett. **102**, 010403 (2009)
[7] A. I. Streltsov, O. E. Alon, and L. S. Cederbaum, Phys. Rev. A **80**, 043616 (2009)
[8] S. L. Cornish, N. G Parker, A. M. Martin, T. E. Judd, R. G. Scott, T. M. Fromhold, and C. S. Adams, Physica D **238**, 1299 (2009)

*Corresponding author: ana.rakonjac@durham.ac.uk
†Corresponding author: s.l.cornish@durham.ac.uk

To the list of contents

A multipurpose experiment for ultracold lanthanides

P. Ilzhöfer[1,2], **G. Durastante**[1,2], **A. Patscheider**[1,2], **M. Sohmen**[2], **A. Trautmann**[2], **M. J. Mark**[1,2], **F. Ferlaino**[1,2],

1. Institut für Experimentalphysik, Universität Innsbruck, Technikerstraße 25, 6020 Innsbruck, Austria
2. Institut für Quantenoptik und Quanteninformation, Österreichische Akademie der Wissenschaften, 6020 Innsbruck, Austria

In recent years experiments with highly magnetic lanthanide atoms have attracted great attention due to their rich interaction properties. We will present the latest status of our new experimental apparatus on ultracold Er-Dy mixtures.
Here, we will also focus on Rydberg physics with multi-electron atoms. Unlike in alkali or alkaline earth metals, where only electrons from the outer s-shell can be excited to Rydberg states, for lanthanides with their complex electronic structure also electrons from the open anisotropic 4f-shell are addressable. Thus, s-, p-, d-, f- or h-Rydberg states can be excited via a simple two-photon excitation scheme utilizing either a broad- or narrow-line transition in the first excitation step. This allows for the investigation of Rydberg-Rydberg or Rydberg-ground state atom interaction for a larger set of parameters compared to the cases of alkali or alkaline earth metals. A further noteworthy feature of lanthanide Rydberg atoms is an optically active core, which might allow optical manipulation, cooling or even trapping of these Rydberg atoms.
We will present our first spectroscopy results utilizing a hollow-cathode lamp as well as the technical aspects of our planned electric field control and ion detection for more sophisticated experiments on Rydberg physics in ultracold samples of lanthanides in the near future.

To the list of contents

Reflection of noble gas endohedral structure in electron and positron scattering cross-sections

Miron Amusia[*1,2], **L. V. Chernysheva**[†2]
1. Racah Institute of Physics, Hebrew University, Jerusalem 91904, Israel
2. Ioffe Physical-Technical Institute, St. Petersburg 194021, Russian Federation

We demonstrate in this talk, that by studying the low-energy elastic scattering cross-sections of electrons and positrons upon endohedrals it is possible to disclose some specific features of their inner structure. An endohedral $A@C_N$ consists of a fullerene C_N "stuffed" inside by an atom A. We demonstrate that the scattering cross-sections are strongly affected not only by static potentials of both A and C_N, but also by their polarizabilities as well as by mutual influence of these polarizabilities upon each other.

We have found a number of minima and maxima, for example, like the Ramsauer minima in partial wave contributions to the total cross-section, and demonstrated their reflection in the differential cross-section at a given angle, etc. We show that completely new structures appear in the cross-sections of electron and positron scattering upon $A@C_N$ that originate due to the presence of a single relatively small atom A inside a big fullerene. This is a strong evidence of the quantum nature of the considered scattering process [1]. In classical physics the scattering cross-sections, at least in the low-energy limit, is entirely determined by the size of the target and the radius of the projectile-target interaction.

The concrete calculations for electron scattering were performed for all noble gas atoms, from He to Xe, and a big metal atom Ba [2]. As a fullerene, we consider almost ideally spherically symmetric C_{60}. This choice permits to simplify the calculations considerably, since the atom A can be treated as located at the very center of C_{60}. We found that the presence of atom A prominently modifies the $e^- + A@C_N$ scattering cross-sections, adding to them new resonances. We have also predicted the appearance of additional bound states, it is formation of negative ions $A@C_{60}^-$. In the generation of new structures the role of interference of A and C_{60} polarizabilities proved to be essential.

At first glance, the positron e^+ scattering upon $A@C_N$ is an easier object of investigation than the electron e^- scattering, since for e^+ there is no exchange between the projectile and target constituencies. However, this is not the case, since in the process of collision the projectile e^+ and a virtually excited target electron form a temporal bound state that we call *virtual positronium*. We took this effect into account shifting the energy of virtual excitations by the positronium Ps binding energy value, I_{Ps}. This shift increases considerably the value of both A and C_{60} polarizabilities. It can also chance sign of polarizabilities, thus leading to a paradoxical situation of repulsive polarization potential, contrary to the well-known from textbooks statement that polarization potential has to be attractive for any sign of the projectile charge.

Concrete results were obtained for all noble gas endohedrals [3]. The cross-sections for e^+ and e^- are essentially different and are strongly affected by the energy shift in polarizabilities. The results for the case of $e^\pm + He@C_N$ scattering are presented by the Fig. 1.

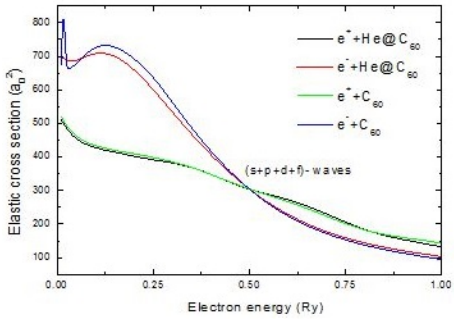

Fig. 1: Elastic scattering cross-section of an electron and positron upon He and $He@C_{60}$.

References

[1] M. Ya. Amusia and L. V. Chernysheva, JETP Letters, **103**, 4, 260 (2016).
[2] V. K. Dolmatov, M. Ya. Amusia, and L. V. Chernysheva, Phys. Rev. A **95**, 012709 (2016).
[3] M. Ya. Amusia and L. V. Chernysheva, in preparation.

[*]Corresponding author: amusia@vms.huji.ac.il
[†]Corresponding author: Larissa.Chernysheva@mail.ioffe.ru

To the list of contents

Quantitative modeling of coherent atom-light interactions in 2, 3 and 4-level systems in the hyperfine Paschen-Back (HPB) regime

J. Keaveney[1], **D. J. Whiting**[1], **R. Mathew**[1], **C. S. Adams**[1], **I. G. Hughes**[*1]
1. Joint Quantum Centre (JQC) Durham–Newcastle, Department of Physics, Durham University
South Road, Durham DH1 3LE, UK

The study of light propagation through thermal atomic vapours subject to external magnetic fields is a flourishing area of research [1]. At Durham we have spent 15 years studying the quantitative spectroscopy of alkali-metal vapours, culminating in the publication of our electric susceptibility code *ElecSus* [2]. We have extended our investigations to nondegenerate three-level ladder and four-level diamond schemes. Application of a sufficiently large magnetic fields (where the Zeeman splittings exceed the Doppler width) allows us to gain access to the hyperfine Paschen-Back (HPB) regime [3], [4]. In hot alkali-metal vapors we have demonstrated that it is possible to realise electromagnetically induced transparency (EIT) [5] and absorption (EIA) [6] in nondegenerate three-level systems.

Applications of the quantitative understanding of atom-light interactions in the presence of a magnetic field range from devices (a compact optical isolator [7], narrow-line filters [8], a Faraday laser [9]) to fundamental physics (single-photon interference due to motion in an atomic collective excitation [10], a possible new method to measure Boltzmann's constant).

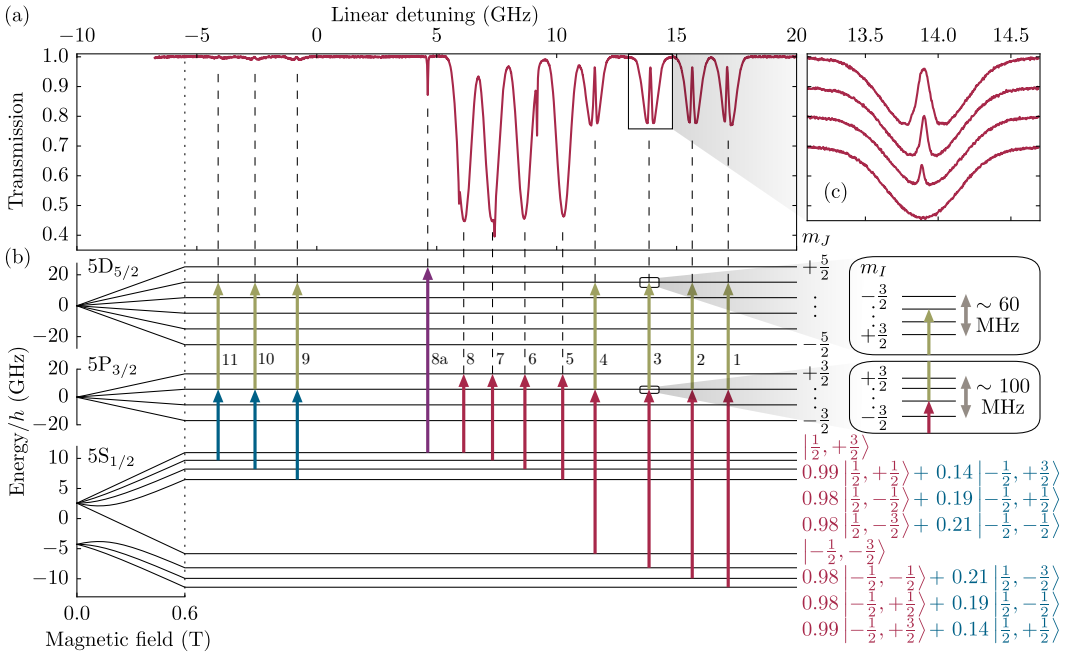

Fig. 1: EIT in isolated three-level systems in the hyperfine Paschen-Back regime. (a) shows a typical weak-probe transmission spectrum (red) and (b) a diagram of the transitions associated with the spectral features in (a). The eigenstates of the system in the $|m_J;m_I\rangle$ basis are shown to the right of the diagram for a magnetic field strength B = 0.6 T, where a significant admixture of states with opposite spin (blue text) in the $5S_{1/2}$ manifold remain; these result in the weak transitions indicated by the blue arrows. (c) shows an expanded view of one of the EIT resonances as a function of control-beam power. Zero detuning is the weighted D2 line centre of naturally abundant rubidium in zero-magnetic field [11].

References

[1] D. Budker *et al.*, Reviews of Modern Physics **74**, 1153 (2002)
[2] M. A. Zentile *et al.*, Computer Physics Communications **189**, 162–174 (2015)
[3] A Sargsyan *et al.*, Optics Letters **37**, 1379–1381 (2012)
[4] A Sargsyan *et al.*, Journal of the Optical Society of America B **31**, 1046–1053 (2014)
[5] D. J. Whiting *et al.*, Physical Review A **93**, 043854 (2016)
[6] D. J. Whiting *et al.*, Optics Letters **40**, 4289–4292 (2015)
[7] L. Weller *et al.*, Optics Letters **37**, 3405–3407 (2012)
[8] M. A. Zentile *et al.*, Optics Letters **40**, 2000-03 (2015)
[9] J. Keaveney *et al.*, Review of Scientific Instruments **87**, 095111 (2016)
[10] D. J. Whiting *et al.*, arXiv preprint arXiv:1612.05467 (2016)
[11] P. Siddons *et al.*, Journal of Physics B: Atomic, Molecular and Optical Physics **41** 155004 (2008)

*Corresponding author: i.g.hughes@durham.ac.uk

To the list of contents

Atom probing of thermally populated surface polaritons

J. C de Aquino Carvalho*, A. Laliotis, P. Chaves de Souza Segundo#, I. Maurin, M. Ducloy, D. Bloch
Laboratoire de Physique des Lasers, UMR 7538 du CNRS, Université Paris13-USPC, 93430 Villetaneuse France

The universal blackbody radiation, defined for the far-field, reveals not sufficient to account for the near-field effects of the thermal emission [1]. When matter is heated-up, its boundary, susceptible to bear surface polaritons, is thermally excited, and intense electromagnetic fields evanescently decay away from the surface. The population of these surface modes obeys a thermodynamic distribution, according to the local density of states in vacuum near the interface. In addition to this near-field extension of the fundamental thermal radiation, which is highly sensitive to the nature of the material, elevating the temperature is susceptible to modify phenomenologically the surface mode resonances themselves (broadening and/or shift). This genrates heavy uncertainties for the predictions of our experiments to test the resonant behavior of an atom in the vicinity with the hot surface, which uses the atom as a detector of the quantum thermal fluctuations.

Our group has already demonstrated, in the near-field van der Waals (vW) limit, that the Casimir-Polder surface-induced energy shift varies with temperature [2]. We use here the coincidence [3] between the surface mode of sapphire at ~ 24.6 THz (~ 12.2 µm), and the excited state transition (at 12.15 µm) of Cs $6D_{3/2} \rightarrow 7P_{1/2}$, known to lead to surface repulsion (instead of the standard vW attraction), and to a surface-induced quenching of the $6D_{3/2}$ level (Förster transfer). The experiments we report on are performed with selective reflection (SR) spectroscopy - probing the vapour at ~100 nm- on the second resonance line of Cs, at 459 nm and 455 nm, reaching Cs($7P_{1/2}$) and Cs($7P_{3/2}$) respectively (fig.1) The near coincidence between the sapphire resonance and the $7P_{1./2}$-$6D_{3/2}$ coupling is responsible for a very different temperature-dependence of the surface attraction for Cs($7P_{1/2}$) and for Cs($7P_{3/2}$) -*cf.* fig. 1a-. Indeed, the couplings for $7P_{3/2}$ (to $6D_{3/2}$ and $6D_{5/2}$) fall off the sapphire surface resonance (respectively at 15.6 and 14.6 µm).

We also aim to observe how the thermal emission of sapphire in a polariton mode sapphire can be absorbed by Cs($7P_{1/2}$), which would be a realization of a near-field heat transfer experiment, limited up to now to classical objects. For this purpose, we investigate the population induced in the $6D_{3/2}$ level close to the sapphire window through reflection spectroscopy on the 1.52 µm line (see fig. 1b). Aside from the observation of a (weak) thermal transfer through absorption in the volume (even for temperature as low as 500K), the frequency tuneability of the 459 nm excitation allows to address specific atomic velocities and hence interaction time with the vcininty of the surface, yielding varying selective reflection lineshapes (at 1.52 µm). The analysis of these first results is presently in progress.

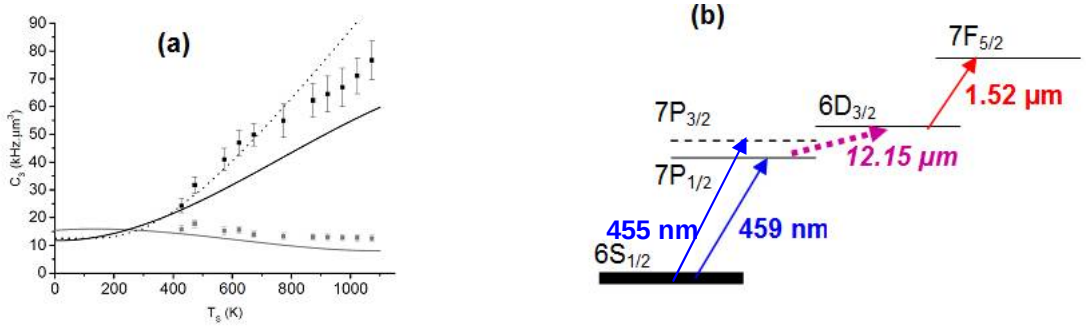

Fig. 1: (a) The measured C_3 coefficient of the C_3z^{-3} van der Waals surface potential, with z the atom-surface distance, for Cs($7P_{1/2}$) (black) and Cs($7P_{3/2}$) (grey) as a function of temperature. The theoretical predictions include (solid line), or negelect (dashed line) the temperature-dependence on the sapphire polariton itself; (b) Scheme of the Cs energy levels, showing how a surface-induced thermal transfer by sapphire from 7P population to 6D is probed by SR at 1.52 µm..

References

[1] J.-J. Greffet *et al.* ", Nature, **416**, 61-64 (2002).
[2] A. Laliotis *et al* " Nat. Commun., **5**, 4364 (2014).
[3] H. Failache *et al* Phys. Rev. Lett. **83**, 5467 (1999) and Phys. Rev. Lett. **88**, 243603 (2002).
[4] T.Passerat de Silans *et al* , J. Phys. Condensed Matter **21** 255902 (2009)

*Corresponding author: joao.carvalho@univ-paris13.fr

Permanent address Universidade Federal de Campina Grande, Cuité, PB, Brazil.

To the list of contents

Sub-Doppler features in the backward-emitted fluorescence of a dense vapor and analogies with thin-cell spectroscopy

J. C. de Aquino Carvalho[1], A. Laliotis[1], M. Chevrollier[2], M. Oriá[2], D. Bloch[1]

1.Laboratoire de Physique des Lasers, UMR 7538 du CNRS, Université Paris13-USPC, 93430 Villetaneuse France
2. Universidade Federale Rural de Pernambuco, UACSA, Cabo de Santo Agostinho, PE, Brazil

Literature has incidentally mentioned [1] a sub-Doppler contribution in the excitation spectrum of the backward fluorescence of a dense vapor, while the interpretation had assumed a metal layer in a boundary region close to the window of the (alkali-metal) vapor container. We confirm here the appearance of a sub-Doppler structure for the fluorescence emitted from a dense Cs vapor when tuning the frequency of normal incidence irradiation. Experiments are performed both on the strong D1 line (894 nm), or on the weaker second resonance at 459nm, with an IR wavelength filtering. A decrease of the fluorescence emission attributed to surface quenching had already been noted [2], but for high atomic densities so that the Doppler effect was negligible with respect to other broadenings. Here, we show that this surface-induced quenching appears in a regime compatible with velocity-selection, causing a decrease of fluorescence on the red side of the excitation spectrum. The velocity selection in the initial excitation process partly survives on the way to the quenching window, despite the redistributions occurring in an optically thick medium. Among atoms directed to the surface, only atoms moving slowly enough do not feel the surface quenching. The visibility of the corresponding sub-Doppler structure (fig.1) is here greatly improved by applying a frequency-modulation (FM) technique, which monitors the frequency-derivative of the lineshape through a lock-in detection, specifically sensitive to narrow features.

The specificity of this sub-Doppler signature when exciting fluorescence in an optically thick medium is that it combines surface quenching with the rapid spatial attenuation of the irradiation. This is in close analogy with the narrow spectroscopic features appearing in thin vapor cells [3]: here, the strong attenuation occurring on distances typically on the order of tens of μm is the equivalent of a "soft" window for the thin cell. We have developed a simple model, based upon the comparison between the velocity Λ/τ of atoms unaffected by the quenching in the window (Λ the attenuation length, τ the free decay time of atomic excitation into fluorescence) and the thermal velocity u. This model (fig.1) also justifies that a normal incidence irradiation is the key to find the sub-Doppler structure, which is independent of the geometry chosen to detect the fluorescence**.**

Despite the complexity naturally attached to an optically thick medium (radiation trapping, energy pooling collisions and other redistributions), our observation rules out previous interpretations based upon an interaction with a specific thin or intermediate metal layer. It may offer a diagnostics of the complex physics occurring specifically close to a surface. Specificities of the diagnostics may be improved by wavelength selection in the fluorescence process. The required quick attenuation can also be brought by a first pumping step on a strong resonance line, with the useful excitation reaching high-lying states brought by a second laser.

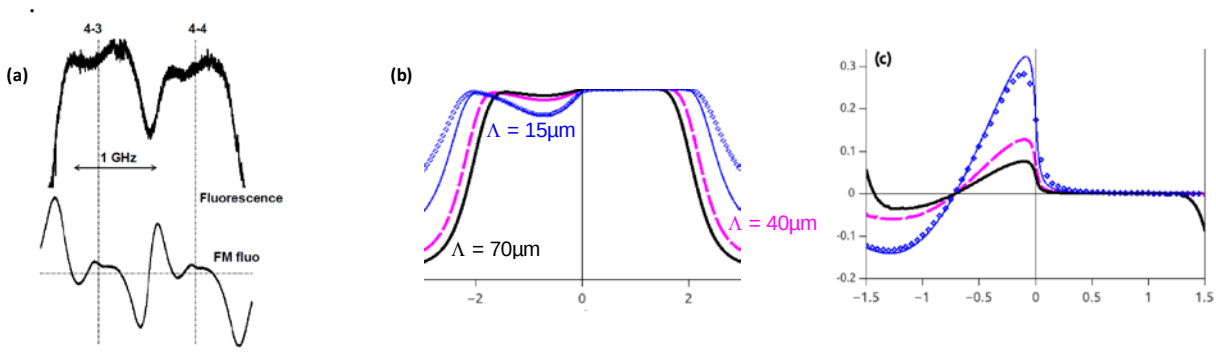

Fig. 1: (a) Excitation spectrum of fluorescence on the 894 nm line, in direct detection (top) or FM detection (bottom), with the markers of the Doppler-free resonance. The characteristic Doppler width ku is ~200 MHz ; (b) Simulation of the fluorescence with a frequency scale normalized in ku units. The calculation assumes here that the absorption maximal at line center (absorption length Λ), is governed by a Voigt profile (for u = 200 m/s and λ=1μm) with an optical width γ=10MHz (or γ=20MHz for diamonds). The fluorescence is integrated on a finite length 3mm, and the far wings appear when absorption becomes weak; (c) Frequency-derivative of the predictions in (b), corresponding to the FM detection of the fluorescence.

References

[1] K. Le Bris *et al*, JOSA B **18**,1701 (2001) and JM. Gagné *et al*, JOSA B **22**,2242 (2005).
[2] G Zajonc, and AV Phelps, PRA **23**, 2479 (1981) and H. van Kampen *et al*, PRA **56**, 3569 (1997).
[3] D Sarkisyan *et al*, PRA **69**, 065802 (2004).

To the list of contents

† Corresponding author: joao.carvalho@univ-paris13.fr

Slow molecular beams of heavy diatomic polar molecules

Kevin Esajas[*1], **Artem Zapara**[1], **Steven Hoekstra**[1]
1. Van Swinderen Institute for Particle Physics and Gravity, University of Groningen
Zernikelaan 25, 9747 AA Groningen, The Netherlands

Cold and slow beams of heavy diatomic polar molecules can be used to probe physics beyond the standard model. We aim to utilize slow BaF molecules in their ground state for a measurement of the electron-EDM, which is a test of CP violation. To produce intense beams of these molecules we are in the process of constructing a cryogenic buffer gas source that we will combine with a Stark decelerator. We have already constructed a 4 meter long Stark decelerator that we operate using SrF molecules. At the maximum deceleration strength we are able to reduce the velocity of the SrF molecules from 290 m/s to 120 m/s, thereby removing 85% of their initial kinetic energy[1]. With the cryogenic source we will produce BaF molecules with velocities around 180 m/s. In combination with the decelerator this enables production of intense and slow (30 m/s) molecular beams.

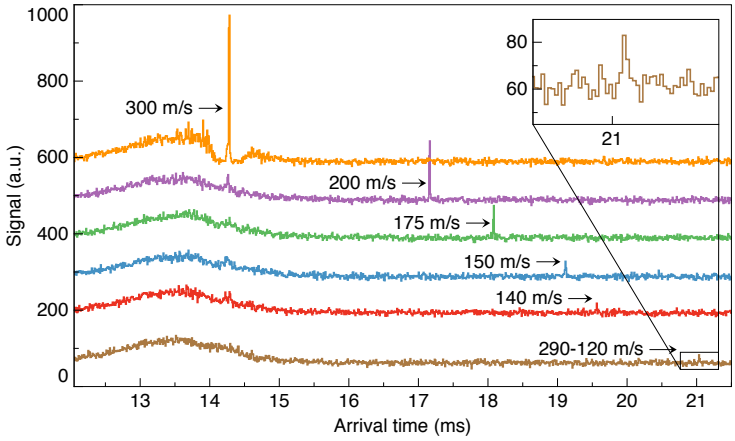

Fig. 1: Time of flight profiles showing the deceleration of SrF molecules from an initial velocity of 300 m/s to the indicated final velocities. The bottom curve shows deceleration from 290 m/s to 120 m/s.

References

[1] Mathavan S.C., Zapara A., Esajas Q., and Hoekstra S. (2016). Deceleration of a Supersonic Beam of SrF Molecules to 120 ms(-1). ChemPhysChem, 17(22), 3709-3713.

*Corresponding author: q.a.esajas@rug.nl

To the list of contents

Dielectric response of a particle embedded in media

Johannes Fiedler[*1], **Stefan Y. Buhmann**[1,2]
1. Albert-Ludwigs-Universität Freiburg, Physikalisches Institut, Hermann-Herder-Str. 3, 79104 Freiburg, Germany
2. Freiburg Institute for Advanced Studies, Albert-Ludwigs-Universität Freiburg, Albertstr. 19, 79104 Freiburg, Germany

To determine the electromagnet interaction between particles, such as the Coulomb force for charged particles or the van–der–Waals forces for neutral atoms or molecules, the electromagnetic responses of the involved particles are required. For particles embedded in media, e.g. in a solution, the surrounding medium may have a strong impact on its response. In general, each interaction between two particle depends on both the response of the particles and on the geometry surrounding them. The medium affects both - the local response and the geometry. The change of the local response is caused in additional electromagnetic boundary conditions for the solution of the Schrödinger equation describing the particle, which can be studied, e.g. by DFT simulations.

We present a theory based on the macroscopic quantum electrodynamics (QED) to describe both effects for neutral atoms or molecules. Due to Pauli blocking the particles create a vacuum cavity in the surrounding solvent medium which has two effects [1]: on the one hand, this cavity changes the electromagnetic scattering properties of the environment, which can be described via cavity QED [2]. On the other hand, the cavity leads to Casimir-Polder shifts in the particles' internal eigenenergies [2,3]. Both effects will be introduced using macroscopic QED and will be illustrated with a simple example.

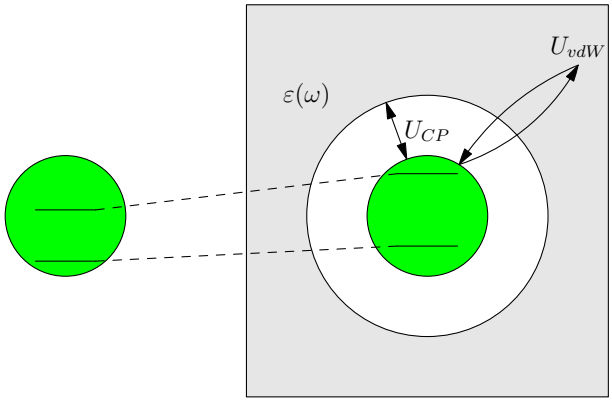

Figure 1: Sketch of particle in vacuum (left) and embedded in a medium with permittivity $\varepsilon(\omega)$ (right). The atomic states are shifted due to the Casimir–Polder interaction with the medium (U_{CP}). The change of the van–der–Waals interaction (U_{vdW}) is caused by the propagation through cavity.

References

[1] A. Held, and M. Walter, The Journal of Chemical Physics **141**, 174108 (2014).
[2] S.Y. Buhmann, *Dispersion Forces I: Macroscopic Quantum Electrodynamics and Ground-State Casimir, Casimir–Polder and van der Waals Forces* (Springer, Heidelberg, 2012).
[3] H.B.G. Casimir, and D. Polder, Phys. Rev. **73**, 360–372 (1948).

[*]Corresponding author: johannes.fiedler@physik.uni-freiburg.de

To the list of contents

A new general cooling technique for ions by autoresonance in an electrostatic ion beam trap

R. K. Gangwar*[1], K. Saha [1], O. Heber†[1], M. L. Rappaport[2] and D. Zajfman[1]

1. Department of particle Physics and Astrophysics, Weizmann Institute of Science, Rehovot, Israel 76100

2. Physics Core Facilities, Weizmann Institute of Science, Rehovot 7610001 Israel

In many fundamental studies in physics and chemistry, the essential basic requisite is the control of the kinematic and the internal degrees of freedom of ions. It also enables detailed experiments such as studies with merged beams where precise control of the kinetic energies of the two beams permits fine tuning of their relative velocities[1]. Many techniques have been developed that can cool molecular ions kinematically and/or internally, such as buffer-gas cooling [2], electron cooling (for molecular beams [3]), laser cooling [4], supersonic expansion [5] and many more.

Here we demonstrate an evaporative-like cooling scheme to reduce the initial relatively wide momentum distribution ($\Delta p/p$), of a trapped molecular ion bunch oscillating inside an electrostatic ion beam trap (EIBT). In this approach, by applying adiabatic autoresonance (AR) acceleration, we were able to eject the ions that are at the tail of the momentum distribution. Consequently, the momentum distribution of the adiabatic AR dragging force part of the bunch can be narrowed by at least an order of magnitude depending on AR drag force parameters (see Fig 1 (A)). This reduction corresponds to a velocity width about 6 m/s and the temperature well below 1 K, in the frame of reference of moving with the average speed of the ions.

In an EBIT, ion-ion collisions are expected mostly near the turning points in the mirrors, which serve to thermalize the distribution. To test this conjecture, further experiments were performed with time-dependent AR forces (linearly decreasing amplitude) and also by changing the injected ion density. Our results clearly indicate that sufficient ion-ion interactions occurred and can increase the phase space density of such an AR-accelerated bunch by at least an order of magnitude (see Fig 1 (B)). The technique is general in that it is applicable for all ions irrespective of their charge or mass.

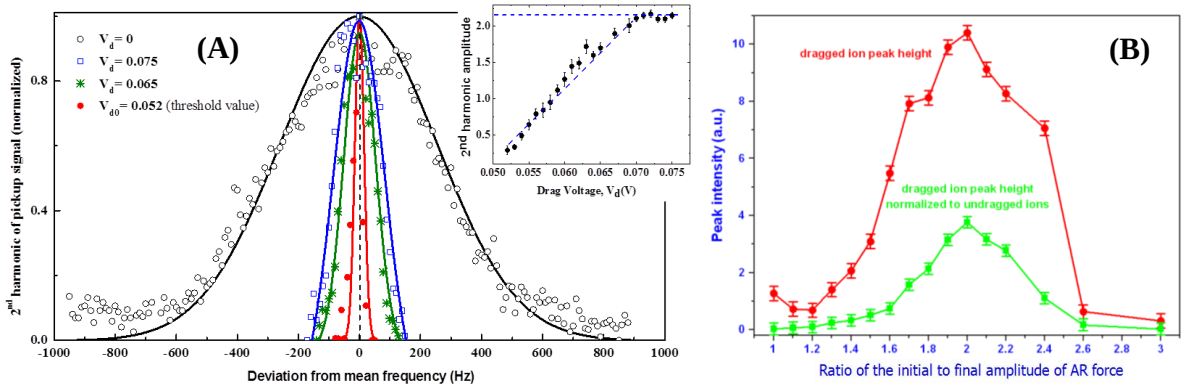

Fig. 1: (A) Normalized distribution of the second harmonic of the oscillation frequency plotted as the deviation from the mean frequency for different drag voltages (V_d). The inset shows the actual peak height vs. V_d. Note that for $V_d \geq 0.07$ V, the peak height is approximately constant, indicating that above this value the AR force dragged all the ions of the bunch (B) Dragged bunch height vs. ratio between initial and final values of V_d. The circles are the direct height measurements of the dragged ion intensity while the squares are the same normalized to the residual (not dragged) ions in the trap. The lines are a guide to the eye.

We have extended this technique further to explore whether ion-ion interactions can lead to control of ro-vibrational degrees of freedom of molecular ions. Our preliminary results are encouraging and further experiments are currently being conducted. Detailed results of the experiments conducted with SF_6^-, SF_5^+ ions and explanation of the technique shall be presented.

References

[1] A. B. Henson *et al.*, Science, **338**, 234, (2012).

[2] D. Gerlich, *Low temperatures and cold molecules* (World Scientific Publishing, ed. Ian W M Smith, 2008)

[3] K. Mølhave and M. Drewsen, Phys. Rev., **62**, 011401R, (2000).

[4] D. A. Orlov *et al.*, *Electron cooling with photocathode electron beams applied to slow ions at TSR and CSR" Proceedings of COOL 2007*, Bad Kreuznach, Germany, 230.

[5] C. Y. Lien *et al.*, Nat. Commun., **5**, 4873, (2014).

*Corresponding author: reetesh-kumar.gangwar@weizmann.ac.il

†Corresponding author: oded.heber@weizmann.ac.il

To the list of contents

Optical diagnostic of gas mixture plasmas with fine-structure resolved population-kinetic models

R. K. Gangwar[*1], **Priti** [2], **S. Gupta** [2], **Dipti** [3], **and R. Srivastava**[†2]

1. Department of particle Physics and Astrophysics, Weizmann Institute of Science, Rehovot, Israel 76100
2. Department of Physics, Indian Institute of Technology Roorkee, 247667, India
3. Atomic Spectroscopy Group, NIST, 100 Bureau Drive, Gaithersburg, MD 20899, USA

Non-equilibrium plasmas (NEP) have been found very suitable for developing multi-sectorial technologies such as synthesis of materials (dielectric, magnetic, smart layers, biomaterials, multifunctional materials, etc.), nanotechnology (production and functionalization of nanoparticles), biomedical (to deactivate pathogens, to stop bleeding without damaging healthy tissue, to disinfect wounds and accelerate wound healing etc.) and many more. The interest is rapidly growing as they offer wide range of reactive atomic/molecular species and photons. Often in these applications, the chemically-reactive radicals, such as reactive nitrogen species (RNS) $NO, N_2(A)$ or reactive oxygen species (ROS) O, O_3, OH etc. are required. Optical characterization (by coupling the spectroscopic measurements with population-kinetic models) of such reactive molecular gas (RMG) plasmas is very challengingDue to the increasing role of complex processes such as dissociation and recombination in the population balance equation of excited radiating states. In addition the corresponding cross-section data of these complex molecules are often not available.

However, alternatively sufficient yield of required radicals can be achieved by introducing the traces of RMG in the inert gas plasmas. Although this reduces the complexity of the needed models to analyze spectroscopic measurements but still require an appropriate extension of pure gas plasmas. Incorporating our calculated fully relativistic distorted wave electron-impact cross sections, we developed fine-structure resolved collisional-radiative (CR) models and successfully applied for the diagnostic of low-pressure pure Ar and Kr plasmas [1] [2] [3]. The most important feature of these CR models is that it can perform the diagnostic with the intensity of individual emission lines that are originated between fine-structure transitions. Moreover it uses all the data obtained from reliable theoretical approaches, contrary to most previous model which uses data from non/semi relativistic approaches when these are not available in the literature. We strongly believe that the extension of our fine-structure resolved model can provide very reliable diagnostic for gas mixture plasmas. In this context, our first effort for the diagnostic of Hydrogen-cesium plasma which is suitable for developing the negative ion sources was very successful [4]. Currently we are extending our models for the diagnostic of $Ar + N_2$, $Ar + O_2$ plasmas. The detailed results and comparision with previous avaliable results along with the overview of our models shall be presented.

References

[1] R. K. Gangwar *et al.*, J. Appl. Phys., **111**, 053307, (2012).
[2] Dipti *et al.*, European Physical Journal D, **67**, 203, (2013).
[3] R. K. Gangwar *et al.*, Plasma Sources Sci. Technol., **25**, 035025, (2016).
[4] Priti *et al.*,Journal of Quantitative Spectroscopy and Radiative Transfer, **187**, 426, (2017).

[*]Corresponding author: reetesh-kumar.gangwar@weizmann.ac.il
[†]Corresponding author: rajsefph@iitr.ac.in

To the list of contents

Single- and double-electron capture in the collisions of C^{4+} + He

J. W. Gao[1,2], Y. Wu[1], N. Sisourat[2], J. G. Wang[1] and A. Dubois*[2]
1. Institute of Applied Physics and Computational Mathematics, 100088, Beijing, China.
2. Sorbonne Universités, UPMC Univ Paris 06, CNRS, Laboratoire de Chimie Physique Matière et Rayonnement, 75005, Paris, France.

Electron capture processes by carbon ions colliding with atoms or molecules have attracted much attention because of their importance in astrophysics and in the treatment of thermonuclear fusion plasma. From an astrophysical perspective, electron capture processes between multiply-charged ions with neutral atoms can play an important role in determining ionization balance of the interstellar medium [1]. In fusion plasmas, carbon ions are important impurities since carbon is used in divertor target plate tiles [2], while helium is abundant as a product in the fusion reaction, and both of them appear at various impact energies in different ionization stages in the plasma. Therefore, comprehensive knowledge of electron capture processes between multiply-charged carbon ions and helium are important for the simulation and diagnostic of fusion plasmas.

In the conference, we shall present results for single- and double-electron capture processes occurring during the collisions of C^{4+} + He:

$$C^{4+}(1s^2) + He(1s^2) \rightarrow C^{3+} + He^{+}(SEC) \quad (1)$$

$$\rightarrow C^{2+} + He^{2+}(DEC). \quad (2)$$

The cross sections are calculated by using two-active-electron semi-classical atomic orbital close-coupling (SC-AOCC) method [3] with a large expansion basis. Our calculations shown in Fig.1 cover a wide energy domain $0.1 - 300$ keV/u overlapping most of the previous experimental [4-8] and theoretical [8-13] works for $E < 10$ keV/u, where our calculations are in good agreement with the previous works. For $E > 3$ keV/u, our present calculations are in better agreement with the experimental measurements of [8] than the theoretical calculations of [4, 5]. A detailed state-to-state comparison with previous works and further interpretations will also be presented during the conference.

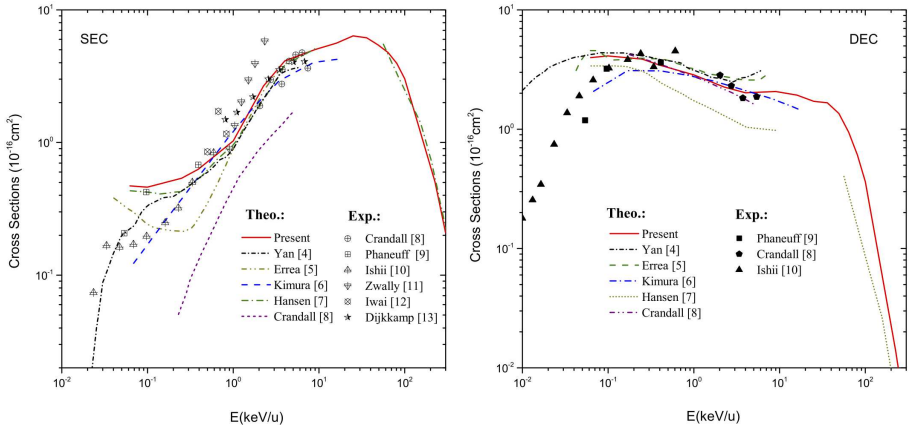

Fig. 1: Comparison between the present total SEC and DEC cross sections with different experimental and theoretical results.

References

[1] G. Steigman, Astrophys. J **199**, 642 (1975).
[2] J. N. Brooks, A. Kirschner, D. G. Whyte, D. N. Ruzic, and D. A. Alman, J. Nucl. Mater. **313**, 424 (2003).
[3] N. Sisourat, I. Pilskog, and A. Dubois, Phys. Rev. A **84**, 052722 (2011).
[4] L. L. Yan, Y. Wu,Y. Z. Qu, J. G. Wang, and R. J. Buenker, Phys. Rev. A **88**, 022706 (2013).
[5] L. F. Errea, B. Herrero, L. Méndez, and A. Riera, J. Phys. B **28**, 693 (1995).
[6] M. Kimura and R. E. Olson, J. Phys. B **17**, L713 (1984).
[7] J. P. Hansen, J. Phys. B **25**, L17 (1992).
[8] D. H. Crandall, R. E. Olson, E. J. Shipsey, and J. C. Browne, Phys. Rev. Lett. **36**, 858 (1976).
[9] R. A. Phaneuf and D. H. Crandall (unpublished).
[10] K. Ishii, A. Itoh, and K. Okuno, Phys. Rev. A **70**, 042716 (2004).
[11] H. J. Zwally, D. W. Koopman, and T. D. Wilkerson, Rev. Sci. Insrum. **40**, 1492 (1969).
[12] T. Iwai, Y. Kaneko, M. Kimura, N. Kobayashi, S. Ohtani, K. Okuno, S. Takagi, H. Tawara, and S. Tsurubuchi, Phys. Rev. A **26**, 105 (1982).
[13] D. Dijkkamp, D. Ciric, A. de Boer, F. J. De Heer, and E. Vlieg, J. Phys. B **18**, 4763 (1985).

*Corresponding author: alain.dubois@upmc.fr

To the list of contents

Effect of Gravity on Magnetobound States of Protonium

Elijah Goodrich[*1], **Carlos A. Ordonez**[†1]
1. Department of Physics, University of North Texas, Denton, Texas 76203, USA

A magnetobound state of protonium is a system of two pair particles (proton and antiproton) that become spatially correlated in a strong magnetic field [1,2]. The state forms adiabatically and dissociates spontaneously. This research uses classical trajectory simulations to determine the effect of gravity on these systems. The possibility of a gravity experiment involving antimatter is explored. This material is based upon work supported by the U.S. National Science Foundation under Grant No. PHY-1500427 and by the U.S.Department of Energy under Grant No. DE-FG02-06ER54883.

References

[1] F. F. Aguirre and C. A. Ordonez, Physical Review E 91 (2015) 033103.
[2] J. R. Correa and C. A. Ordonez, Physics of Plasmas 21 (2014) 082115.

∗Corresponding author: ElijahGoodrich@my.unt.edu
†Corresponding author: cao@unt.edu

To the list of contents

Experimental upgrades to measure the electron's electric dipole moment using YbF molecules

Chris J. Ho[1], **I. M. Rabey***[1], **J. A. Devlin**[1], **B. E. Sauer**[1], **M. R. Tarbutt**[1], **E. A. Hinds**[1]
1. Centre for Cold Matter (CCM), The Blackett Laboratory, Imperial College London
Prince Consort Road, London SW7 2AZ, UK

The existence of a permanent electric dipole moment (EDM) of the electron is intimately related to the violation of time-reversal symmetry in nature. The Standard Model of elementary particle physics, which includes a degree of time-reversal asymmetry, predicts an upper limit to the electron EDM ($|d_e| < 10^{-38} e$.cm) that is far below current experimental sensitivities [1]. However, modern extensions to the Standard Model predict EDM values in the range accessible to experiment, $|d_e| \sim 10^{-27} - 10^{-30} e$.cm [2]. In fact, these theories are now constrained by recent experiments that utilise cold molecules (YbF [3], ThO [4]), and trapped molecular ions (HfF^+ [5]). The current upper limit to the EDM is $|d_e| < 8.7 \times 10^{-29} e$.cm [4].

Here I present some improvements made to improve the sensitivity of the experiment to measure the electron's EDM using YbF molecules [6]. The initial population of YbF molecules in the ground state has been improved by a factor of 6 using a combination of repump lasers, microwaves and rf fields [7]. The detection of YbF molecules has been increased by a factor of 14 by by choosing laser-induced fluorescence transitions that have a lower decay rate to unaddressed dark states [7]. We are also now detecting on both quadratures of the interferometer, improving the sensitivity of the experiment by $\sqrt{2}$. These improvements have made it possible to reduce the shot noise by an order of magnitude, allowing for an EDM to be measured with a sensitivity at the $10^{-29} e$.cm level.

We have demonstrated that the magnetic shields used in the experiment can reduce the magnetic noise down to 100fT per block of data, which is much lower than the shot noise sensitivity. We have also characterised a vacuum-compatible SERF magnetometer [8] that can measure the fluctuating magnetic field *in situ*. This will allow us to tightly constrain any magnetic field that switches with reversing electric fields, which is a potential source of systematic error.

With the various experimental upgrades, we are now able to search for physics beyond the Standard Model with even greater precision.

References

[1] B. L. Roberts and W. J. Marciano, *Lepton Dipole Moments* (World Scientific Publishing Co. Pte. Ltd., 2010).
[2] I. B. Khriplovich and S. K. Lamoreaux, *CP Violation Without Strangeness* (Springer, New York, 1997).
[3] J. J. Hudson, D. M. Kara, I. J. Smallman, B. E. Sauer, M. R. Tarbutt, and E. A. Hinds, Nature **473**, 493 (2011).
[4] The ACME Collaboration, Science **343**, 269 (2014).
[5] W. B. Cairncross, D. N. Gresh, M. Grau, K. C. Cossel, T. S. Roussy, Y. Ni, Y. Zhou, J. Ye, and E. A. Cornell, arXiv:1704.07928v1 (2017).
[6] J. A. Devlin, Ph.D. Thesis, Imperial College London, 2015.
[7] I. M. Rabey, Ph.D. Thesis, Imperial College London, 2017.
[8] V. K. Shah and R. T. Wakai, Phys. Med. Biol. **58**, 8153 (2013).

*Corresponding author: isabel.rabey08@imperial.ac.uk

To the list of contents

Molecular frame (e, 2e + ion) studies of CH_4 and CF_4

Khokon Hossen [*1,2], **Xueguang Ren**[1], **and Alexander Dorn**[1]

1. Max Planck Institute for Nuclear Physics, 69117 Heidelberg, Germany
2. University of Santiago de Compostela (USC), 15782 Santiago de Compostela, Spain

Ionization and fragmentation of the tetrahedral molecules CF_4 and CH_4 is studied at low electron impact energies ranging from E_0 = 35 eV to 67 eV. In kinematically complete experiments, the momentum vectors of the two outgoing electrons and one fragment ion are detected in triple coincidence. Various fragmentation channels are analyzed according to the ionized orbital binding energy (BE) and kinetic energy release (KER). Furthermore, we find electron emission patterns which depend on the spatial molecular orientation in particular for CH_4.

Kinematically complete electron impact ionization studies on atoms and molecules give detailed insight into correlated few-body reactions. Both, CH_4 and CF_4 have tetrahedral symmetry and are relevant in a large range of scientific and practical areas [1-2].

Experimentally, we use a reaction microscope and a pulsed photoemission electron beam [3]. For the incoming beam energies E_0 between 35 eV and 67 eV were chosen. The momentum vectors of the two outgoing electrons (energies E_1, E_2) and one fragment ion are detected in triple coincidence. E.g., for CF_4 the fragment products CF_3^+, CF_2^+, CF^+, F^+ and C^+ are resolved and can be associated to ionized orbitals according to the observed binding energies (BE) (E_0-E_1-E_2) (see [4] for CH_4).

In a two-body molecular dissociation the detected fragment momentum can provide the spatial orientation of the broken bond and, as result, of the whole molecule at the instant of the collision. Thus, molecular orientation resolved (e, 2e) cross sections can be obtained and the influence of the anisotropic molecular potential and multiple scattering of the electrons within the molecule can be studied. In this respect we analyzed fully differential cross sections (FDCS) for the dissociation reactions $CX_4^+ \rightarrow CX_3^+ + X$ where X = H or F. In the illustration in Fig.1 the projectile is coming in from below ($\vec{p}_0$) and scattered to the left ($\vec{p}_1$). For the CH_4 target and one CH bond being aligned either along the positive or negative x-axis the electron emission patterns in the (grey shaded) xy-plane perpendicular to the incoming beam are shown in Fig. 2. Clearly, the cross section is orientation dependent and shows a maximum at 180° for one orientation only. More results and a detailed analysis will be presented at the conference.

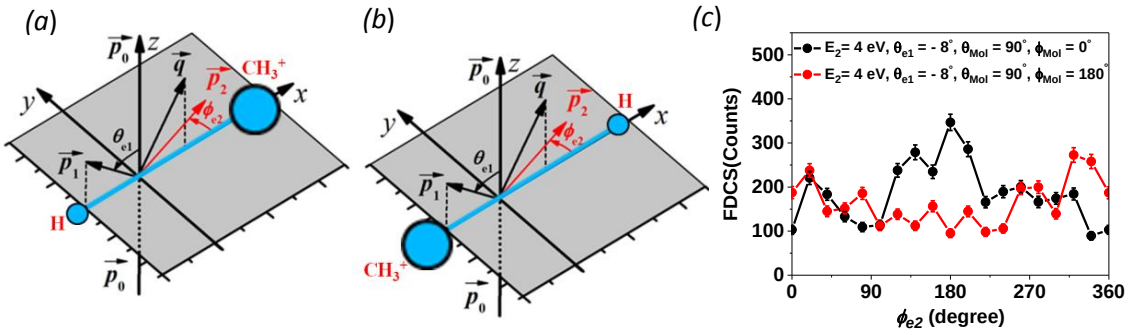

Fig. 1: Illustration of the collision kinematics (see main text). Incoming and scattered projectile momenta are p_0 and p_1. The ejected electron (p_2) is observed in the perpendicular xy-plane. (a) and (b) show CH_3^+ emission along positive and negative x-axis, respectively. Thus, one of the CH bonds of CH_4 is oriented along the x-axis. (c) The FDCS as a function of electron emission angle ϕ_{e2} in the perpendicular plane. Ejected electron energy E_2 = 4 eV, projectile scattering angle θ_{e1} = - 8°. The black and red solid circles refer to orientation as shown in Fig. (a) and (b), respectively.

References

[1] L. G. Christophorou, J. K. Olthoff and M. V. V. S. Rao, J. Phys. Chem. Ref. Data 25, 1341 (1996).
[2] S. L. Miller et al., Science 130, 245 (1959).
[3] X. Ren, T. Pflüger, M. Weyland, W. Y. Baek, H. Rabus, J. Ullrich, and A. Dorn, J. Chem. Phys. 141, 134314 (2014).
[4] X.Ren et al., J. Chem. Phys.142, 174313 (2015).

*Corresponding author: Khokon.Hossen@mpi-k.de

To the list of contents

Simultaneous magnetic trapping of O_2 molecules together with Li atoms

N.Akerman[*1], **Michael Karpov**[†2], **Y. Segev**[2], **S. Reitich**[2], **N. Bibelnik**[2], **J. Narevicius**[2], **and E. Narevicius**[2]

1. Department of Complex Systems, Weizmann Institute of Science, 234 Herzl st., Rehovot, Israel

2. Department of Chemical Physics, Weizmann Institute of Science, 234 Herzl st., Rehovot, Israel

During the last decades trapping and cooling of atoms became a workhorse of atomic physics with countless experiments, where atoms routinely cooled down to nano-Kelvin temperatures. On the other hand, cooling and trapping of molecules remains challenging, and far less progress has been made in generation of cold mixtures of atoms and molecules, even though it opens many possibilities in both physics and chemistry. Atom-molecule co-trapping can lead to orders of magnitude longer interrogation times compared to molecular crossed beam methods, which will enable the study of cold chemistry for especially slow processes. Particularly, inelastic collisions in such a setup have been already successfully studied by Parazzoli et al. [1] and the upper limit on reactive collisions between N and NH has been placed by Campbell et al. [2]. In addition, as in the production of cold alkali molecules, photoassociation or Feshbach resonances can be used to construct polyatomic cold molecules. We plan to implement/apply sympathetic cooling, one of the most exciting opportunities that cold atom-molecule mixtures enables, where cold atoms that are amenable to laser cooling can be used to collisionally cool molecules. Prospects of such a cooling scheme strongly depend on the collisional properties of atoms and molecules with several candidates identified [3] and cooling mechanism studied in detail [4].

The starting point of our experiment is a supersonic beam, generated by an Even - Lavie valve [5], which produces a cold plume of gas at temperatures of $\sim$1 K, moving at velocities of hundreds of m/s. In order to slow this beam we have constructed a 2.4 meter long moving-trap Zeeman decelerator, capable of slowing paramagnetic species to trappable velocities, which enables us to load them into a permanent-magnet quadrupole trap.

In order to achieve the highest possible trapped molecular density, we chose molecular Oxygen that can be easily seeded in a supersonic expansion and decelerated via Zeeman interaction, which has been demonstrated [6],[7]. As a first step, using our moving-trap Zeeman decelerator we have shown co-deceleration of molecular Oxygen together with metastable Argon atoms [8]. Subsequently, we replaced the Argon with Lithium, which has the advantages of lower reduced mass and is suitable for laser cooling, and demonstrated how the decelerated molecular ensemble together with the entrained Lithium atoms can be transferred into the permanent quadrupole trap [9]. We estimate 10^9 trapped O_2 molecules (with density of n=10^{10} cm^{-3}) at a temperature of 300 mK with a background limited lifetime of more than 600 ms, together with 10^5 Lithium atoms in the permanent trap. These results provide a pathway to further implementation of sympathetic cooling.

As a next step, we focus on a number of things: first, improving the entrainment of Lithium in order to increase the number of trapped atoms and increasing the initial molecular beam density. Recent results indicate that we can gain an order of magnitude in the density by cryo-cooling a skimmer placed between the supersonic nozzle and the decelerator entrance, as was shown by Y. Segev et. al. [10]. Second, we are designing a deep Ioffe-Pritchard trap, which will have a non-zero magnetic field minimum and will be able to confine a 300 mK ensemble of molecules and atoms, which will also enable to perform 1D Doppler cooling, as an important step towards sympathetic cooling.

References

[1] L. P. Parazzoli, N. J. Fitch, P. S. Zuchowski, J. M. Hutson, and H. J. Lewandowski, Phys. Rev. Lett. **106**, 193201 (2011).
[2] W. C. Campbell, E. Tsikata, Hsin-I Lu, L. D. van Buuren, and J. M. Doyle, Phys. Rev. Lett. **98**, 213001 (2007).
[3] A. O. G. Wallis and J. M. Hutson, Phys. Rev. Lett. **103**, 183201 (2009).
[4] J. Lim, M. D. Frye, J. M. Hutson, and M. R. Tarbutt, Phys. Rev. A **92**, 053419 (2015).
[5] U. Even, J. Jortner, D. Noy, and N. Lavie, J. Chem. Phys., Vol. 112, No. 18 (2000).
[6] E. Narevicius, A. Libson, C. G. Parthey, I. Chavez, J. Narevicius, U. Even and M. G. Raizen, Phys. Rev. Lett. **100**, 093003 (2008).
[7] A.W. Wiederkehr , H. Schmutz , M. Motsch and F. Merkt, Molecular Physics, Vol. 110, Nos. 15-16, 1807-1814 (2012).
[8] N. Akerman, M. Karpov, L. David, E. Lavert-Ofir, J. Narevicius and E. Narevicius, New J. Phys. **17**, 065015 (2015).
[9] N. Akerman, M. Karpov, Y. Segev, N. Bibelnik, J. Narevicius, E. Narevicius, arXiv:1611.00155v1.
[10] Y. Segev, N. Bibelnik, N. Akerman, Y. Shagam, A. Luski, M. Karpov, J. Narevicius, E. Narevicius, Sci. Adv. **3** : e1602258, (2017).

[*]Corresponding author: nitzan.akerman@weizmann.ac.il
[†]Corresponding author: michael.karpov@weizmann.ac.il

To the list of contents

The hyperfine structure Investigation of V I lines with Doppler Reduced Laser Spectroscopic Method

Gö. Başar*[1], I. K. Öztürk[1], F. Güzelçimen[1], Doğukan Bingöl[2], S. Kröger[3], Gü. Başar[4]

1. Faculty of Science, Physics Department, Istanbul University, Tr-34134, Istanbul, Turkey

2. Graduate School of Engineering and Sciences, Istanbul University, TR-34452 Beyazıt, Istanbul, Turkey

3. Hochschule für Technik und Wirtschaft Berlin, Wilhelminenhofstr. 75A, D-12459 Berlin, Germany

4. Faculty of Science and Letters, Physics Engineering Department, Istanbul Technical University, Tr-34469 Maslak, Istanbul, Turkey

This work is a continuation of our hyperfine structure investigation of Vanadium [1,2,3]. The aim of this work is to increase the accuracy of hyperfine structure data of atomic vanadium. Vanadium (V), with atomic number 23 is the third element of the iron group. Vanadium has one predominant stable isotope, ^{51}V, with a natural abundance of 99.75% and a nuclear spin of $I = 7/2$. ^{51}V has a large nuclear magnetic moment $\mu_I(^{51}\mathrm{V}) = 5.1574\ \mu_N$ [4], and the electric quadrupole moment $Q = -0.052$ barn [4].

Doppler-reduced intermodulated laser-induced fluorescence spectroscopy (IMLIF) with a tuneable single-mode cw Ti:Sa laser was applied to study the hyperfine structure of excited levels of Vanadium. The solid vanadium metal was transferred into the gas phase using a hollow cathode discharge. Eight transitions in the near infrared wavelength range between 760 nm and 850 nm have been investigated. In all our IMLIF spectra additional to the hyperfine structure components so-called cross-over peaks appear. As an example in Figure 1 the line at 811.932 nm is shown.

Precise values for the magnetic dipole hyperfine structure constants A as well as for the electric quadrupole hyperfine structure constants B of the isotope ^{51}V have been determined. Previously published values of magnetic dipole hyperfine structure constants A have been improved and new values of the electric quadrupole hyperfine structure constants B will be presented.

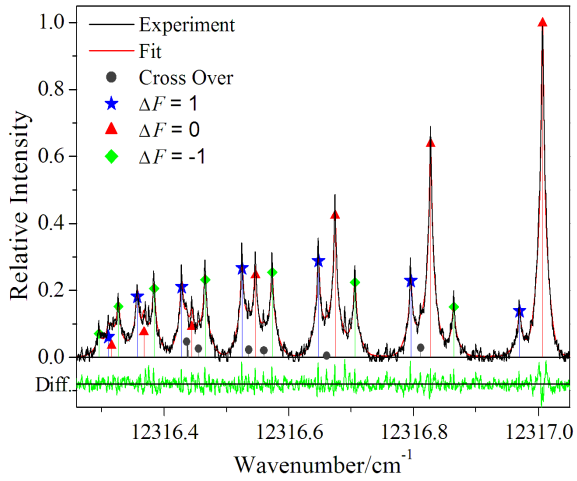

Fig. 1: Hyperfine structure spectrum measured with intermodulated laser-induced fluorescence spectroscopy together with the best fit curve for the line at 811.932 nm of atomic vanadium. The hyperfine structure components are marked by the difference ΔF of the total angular momenta of the lower and upper hyperfine structure levels. Cross-over signals are marked by a grey dot In the lower part of the figure the residuals between experimental and best fit curves are given.

References

[1] F. Güzelçimen, Gö. Başar, I. K. Öztürk, S. Kröger, R. Ferber, A. Jarmola, M. Tamanis and Gü. Başar, J of Physics B: At. Mol. Opt. Phys. **44**, 215001 (2011).

[2] F. Güzelçimen., B. Yapıcı, G. Demir, A. Er, I. K. Öztürk, Gö. Başar., S. Kröger, M. Tamanis, R. Ferber, D. Docenko, Gü. Başar, The Astrophysical Journal Supplement Series **214:9**, Doi: 10.1088/0067-0049/214/9 (2014).

[3] F. Güzelçimen, A. Er, I. K. Öztürk, Gö. Başar, S. Kröger, M. Tamanis, R. Ferber, Journal Of Physics B: At. Mol. Opt. Phys., **48** (11), 115005, Doi: 10.1088/0953-4075/48/11/115005 (2015).

[4] J. Emsley, *The Elements*, Oxford Chemistry Guides, New York: Oxford Univ. Press (1995).

*Corresponding author: gbasar@istanbul.edu.tr

To the list of contents

Identifying optical transitions in highly charged ions with applications for metrology and searches of variation of the fine-structure constant

H. Bekker[*1], **A. Windberger** [1], **N. Potters** [1], **J. Rauch** [1], **J. Berengut** [2], **A. Borschevsky** [3], **J. R. Crespo López-Urrutia** [1]

1. Max-Planck-Institut für Kernphysik, Saupfercheckweg 1, 69117 Heidelberg, Germany
2. School of Physics, The University of New South Wales, Sydney NSW 2052, Australia
3. Van Swinderen Institute, Universiteit Groningen, Nijenborgh 4, 9747 AG Groningen, Netherlands

Many highly charged ions (HCI) have been proposed for use in next generation optical clocks for metrology purposes, see for example [1, 2]. Due to the compact size of their electronic cloud, HCI are less sensitive to external perturbations than the neutral and singly charged systems that are currently widely employed in metrology. Furthermore, increased relativistic effects in HCI lead to a strong sensitivity to variation of the fine-structure constant α. However, for these HCI, theory is not capable of predicting the energy level structures to the precision required for precision laser spectroscopy.

To address this issue, we investigated several of the proposed HCI, which we produced, trapped, and collisionally excited in the Heidelberg electron beam ion trap (HD-EBIT). The wavelengths of subsequent fluorescence light were determined at the ppm-level using a grating spectrometer. We present our latest results for Ir^{17+}, which features transitions with an extremely high sensitivity to variation of the fine-structure constant [1,3]. Identifying these transitions is cumbersome due to the uncertainties of the predictions, the large amount of observed transitions, and their low intensities. However, by observing their Zeeman splitting in the strong magnetic field of the HD-EBIT, many important lines could be identified, c.f. Fig. 1.

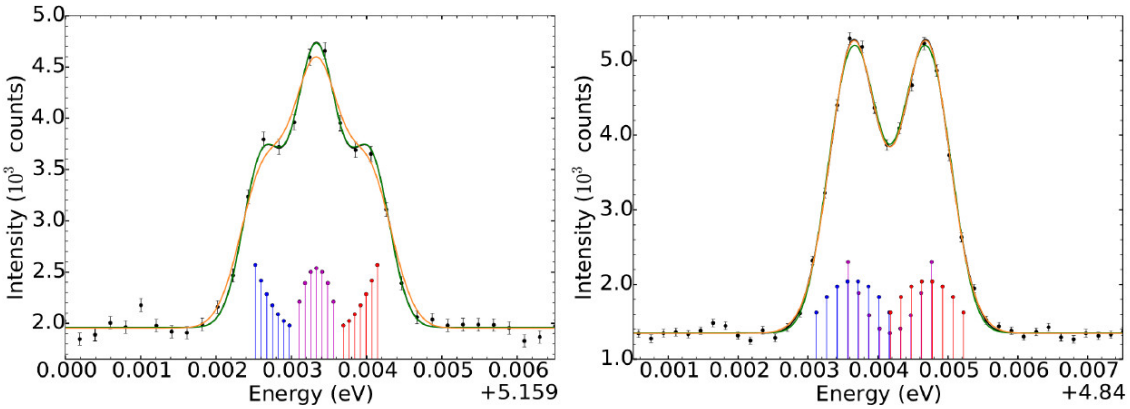

Fig. 1: Observed Zeeman splitting of two Ir^{17+} lines (black points), and fits to the data based on predicted line shapes (solid lines). The individual Zeeman components as determined by the fit, are shown by vertical lines.

Furthermore, our latest results for Pr^{9+} and Pr^{10+} are discussed. In addition to the previously mentioned advantageous properties of HCI, Pr^{9+} is predicted to have a metastable state with an extremely long lifetime of 21 megayears, which potentially makes it suitable as a quantum memory [2].

All the presented results are used to benchmark state-of-the-art atomic theory calculations. Our investigations aim to provide a deeper insight into the suitability of the proposed HCI for metrology purposes, and to pave the way for future laser spectroscopy.

References

[1] J. C. Berengut *et al.*, Phys. Rev. Lett. **106**, 210803 (2011)
[2] M. S. Safronova *et al.*, Phys. Rev. Lett. **113**, 030801 (2014)
[3] A. Windberger *et al.*, Phys. Rev. Lett. **114**, 150801 (2015)

*Corresponding author: bekker@mpi-hd.mpg.de

To the list of contents

Isotope shift of the $2p^4\,{}^3P_2 \rightarrow 2p^3 3p\,{}^3P_2$ two-photon transition of O I and the triplet energy levels of atomic Oxygen

Christophe Blondel[*1], **Daniil Marinov**[2], **Jean-Paul Booth**[2], **Cyril Drag**[1]

1. Laboratoire Aimé-Cotton, Centre national de la recherche scientifique, université Paris-sud, école normale supérieure de Cachan, Université Paris-Saclay, bâtiment 505, F-91405 Orsay, France

2. Laboratoire de Physique des plasmas, Centre national de la recherche scientifique, École polytechnique, université Paris-Sud, Université Paris-Saclay, Observatoire de Paris, Sorbonne Université, F-91128 Palaiseau, France

Two-photon induced fluorescence of atomic oxygen (TALIF), which is routinely used for plasma and flame diagnostics [1], is implemented with two counterpropagating laser beams of sufficient monochromaticity to permit Doppler-free spectroscopy. A single-mode injection-seeded pulsed Ti:sapphire laser has been frequency-doubled twice to produce narrow-band pulsed radiation at wavelengths around 225.6 nm, suitable to excite the ground-state-to-$2p^3[^4S^o_{3/2}]3p\,^3P$ two-photon resonance line of oxygen. Accurate measurement of the injection-seeding wavelength provides new data on the excitation energy of the $3p\,^3P$ states. The experiment was done both sequentially and simultaneously on ^{16}O and ^{18}O, which makes it possible to test recent calculations of the isotope shift. Those multiconfigurational Hartree-Fock (MCHF) and configuration interaction (CI) calculations predict a nearly exact compensation of the 33.7 m^{-1} normal mass shift by a similarly large specific mass shift of opposite sign, leading to a -326 MHz, or -1.1 m^{-1} isotope shift [2]. The nearly perfect agreement of the presently measured -0.8(2) m^{-1} with this value confirms it as one more noticeable success of MCHF+CI modelling.

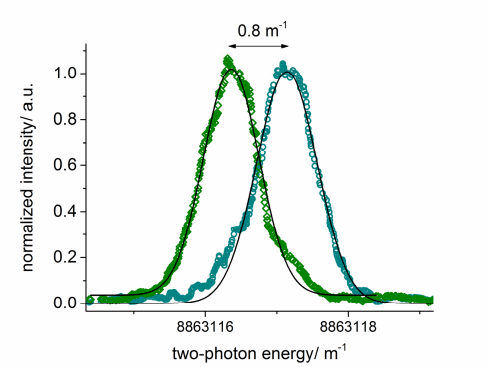

Fig. 1: Atomic-fluorescence response, inside a low-pressure DC discharge [1], as a function of the 2-photon excitation wavenumber of the $2p^3[^4S^o_{3/2}]3p\,^3P_2$ fine structure level, when the discharge tube is fed either with $^{16}O_2$ (higher energy) or $^{18}O_2$ (lower energy). The measured isotope shift is about $-0.8(2)\,\mathrm{m}^{-1}$.

Having an absolute measurement of the excitation wave-number from the ground level, which has been the case only twice in previous spectroscopic studies of O I, we can re-examine the energy levels of the subset of triplet states and present an updated set of optimized energy values that confirms and extends some proposals made after recent extreme-UV spectroscopic studies [3]. For instance, the energy of the upper level of the first ^3D term, $2p^3 3d\,^3D^o_3$, still given by the NIST table as being $9\,748\,853.8\,\mathrm{m}^{-1}$, was found by Ivanov *et al.* [3] to lie significantly lower, at $9\,748\,853.0(8)\,\mathrm{m}^{-1}$. We confirm this lower value and make it even a little lower and more accurate, recommending $9\,748\,852.6(5)\,\mathrm{m}^{-1}$ [4].

References

[1] D. Marinov, O. Guaitella, J.-P. Booth and A. Rousseau, J. Phys. D: Appl. Phys. **46**, 032001 (2013).
[2] P. Jönsson and M. R. Godefroid, Mol. Phys. **98**, 1141–9 (2000).
[3] T. I. Ivanov, E. J. Salumbides, M. O. Vieitez, P. C. Cacciani, C. A. De Lange and W. Ubachs, Mon. Not. R. Astron. Soc. **389**, L4–7 (2008).
[4] D. Marinov, J.-P. Booth, C. Drag and C. Blondel, J. Phys. B: At. Mol. Opt. Phys. **50**, 065003 (2017).

*Corresponding author: christophe.blondel@u-psud.fr

To the list of contents

Probing the size of helium droplets with Interatomic Coulombic Decay: A theoretical insight.

S. Kazandjian[*1], **T. Miteva**[1], **N. Sisourat**[1]

1. Sorbonne Universités, UPMC Univ Paris 06, CNRS, Laboratoire de Chimie Physique Matière et Rayonnement, F-75005, Paris, France

Cooling down a chemical system at the kelvin scale can be useful in order to perform high-resolution spectroscopy or to isolate unstable species. This can be achieved by trapping a molecule in a helium droplet. Making and doping helium droplets is commonly performed, but controlling their size proved to be very difficult [1].

In this work, we investigate how Interatomic Coulombic Decay (ICD) can be used as a tool to probe the size of helium clusters. ICD is an ultrafast non-radiative electronic decay process [2] which occurs in a variety of polyatomic systems such as rare gas clusters [3] or hydrogen bonded clusters [4-5]. In the case of helium clusters, one atom is simultaneously excited and ionized and its excess energy is transferred to a neighboring atom, ionizing it, as shown on **Fig. 1** for the case of helium dimer. After the decay, the cluster contains two He^+ ions, and dissociates due to Coulombic repulsion.

We have developed a diatomics-in-molecules [6,7] approach for the description of ICD in rare-gas clusters [8]. Combined with a semiclassical algorithm specifically designed for ICD [9], this method is used to compute the nuclear dynamics during the process. Our results, obtained for cluster sizes from 2 to 6 atoms, provide the first complete description of ICD in small helium clusters. In particular, the kinetic energy gained by the ions during the Coulombic explosion strongly depends on the initial geometry of the cluster, and, therefore, on the number of atoms constituting it. This is mainly due to charges hopping during the relaxation, which dramatically affects the relative kinetic energy of the two ions. We benchmarked the probability of such charge hopping for each cluster size, and concluded that the size of experimental clusters can be estimated by measuring only the final kinetic energy of the ions. This was successfully applied to recent experimental results [10].

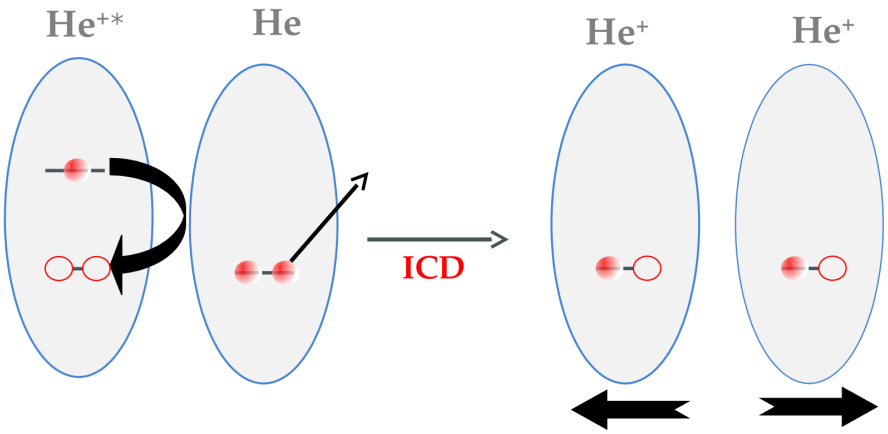

Fig. 1: ICD in helium dimer. After simultaneous ionization and excitation of one helium atom, this excited ion relaxes and transfers its excess energy to a neighboring helium atom, ionizing it. Due to Coulombic repulsion, the system fragments.

References

[1] S. Yang, A. M. Ellis, Chem. Soc. Rev. **42**, 472-484 (2013).
[2] L. S. Cederbaum et al, Phys. Rev. Lett. **79**, 4778 (1997).
[3] V. Averbukh et al., in *Dynamical Processes in Atomic and Molecular Physics* **29**, Bentham Science Publishers (2012).
[4] M. Mucke et al., Nat. Phys. **6**, 143 (2010).
[5] T. Jahnke et al., Nat. Phys. **6**, 139 (2010).
[6] F. O. Ellison, J. Am. Chem. Soc. **85**, 3540 (1963).
[7] P. J. Kuntz and J. Valldorf, Z. Phys. D - Atoms, Molecules and Clusters **8**, 185 (1988).
[8] N. Sisourat, S. Kazandjian, A. Randimbiarisolo and P. Kolorenč, J. Chem. Phys. **144**, 084111 (2016).
[9] N. Sisourat, J. Chem. Phys. **139**, 074111 (2013).
[10] R. Dörner, T. Jahnke, T. Miteva, S. Kazandjian and N. Sisourat, in preparation

*Corresponding author: sevan.kazandjian@upmc.fr

To the list of contents

E2 transitions between hyperfine structure components of the H_2^+ molecular ion

P. Danev[*1], **D. Bakalov**[1], **V. I. Korobov**[2], **S. Shiller**[3]
1. Institute for Nuclear Research and Nuclear Energy, Bulgarian Academy of Sciences, blvd. Tsarigradsko ch. 72, Sofia 1142, Bulgaria
2. Joint Institute for Nuclear Research, 141980, Dubna, Russia
3. Institut fur Experimentalphysik, Heinrich-Heine-Universit at Dusseldorf, 40225 Dusseldorf, Germany

Hydrogen molecular ions, due to the possibility of precise theoretical evaluation of their spectrum, transitions, and external effect shifts [1], are shown [2] to be of metrological relevance.
In the present work we have calculated the intensity of the electric quadrupole transitions between arbitrary Zeeman splitted components of the hydrogen molecular ion H_2^+ hyperfine structure stimulated by laser. The dependence of the induced transition rates on the laser polarization is thoroughly analyzed. In comparison with earlier results of Pilon and Baye [3] and Karr [4] our work covers the case of arbitrary laser beam polarization and takes into account all the details of H_2^+ hyperfine structure.

References

[1] D. Bakalov, V. I. Korobov and S. Schiller, Phys. B: At. Mol. Opt. Phys. **44** 025003 (2011).
[2] S. Schiller, D. Bakalov, and V. I. Korobov, PRL **113**, 023004 (2014).
[3] H. O. Pilón and D.l Baye,J. Phys. B: At. Mol. Opt. Phys. **45** 065101 (2012).
[4] J.-Ph. Karr, J. of Molecular Spectroscopy **300**, 37–43 (2014).

*Corresponding author: *petar_danev@abv.bg*

To the list of contents

Photodetachment of O^- from the $O(^3P)$ to the $O(^1S)$ threshold

M. Génévriez[*1], **A. Dochain**[1] **X. Urbain**[1]
1. Institute of Condensed Matter and Nanosciences, Université catholique de Louvain
Chemin du Cyclotron, 2, 1348 Louvain-la-Neuve, Belgium

Although photodetachment of atomic negative ions has been widely studied, experimental work is very often limited to a few photon energies and targets a specific quantity, either the asymmetry parameter β or the total photodetachment cross section σ. With the advent of widely tunable laser sources, measurements over much broader photon energy ranges are now feasible. In parallel, the development of the animated-crossed-beam technique for photodetachment [1] has opened the way to systematic, accurate and absolute cross section measurements, while the well-established velocity map imaging (VMI) technique is particularly powerful for the determination of asymmetry parameters and branching ratios. We have combined these techniques to study the photodetachment of O^- in full detail.

In a first experiment, we used the animated-crossed-beam technique, together with a pulsed laser, to measure the total absolute photodetachment cross section for photon energies ranging from threshold (1.46 eV) to 5.5 eV. The animated crossed beam technique eliminates the need for estimating the interaction volume, which often introduces inaccuracies in experimental results, leaving only integrated fluxes to be measured and thus providing us with a robust and reliable method for absolute measurements. The results, displayed in Fig. 1, confirm the trends observed in our previous measurement [1]: pronounced disagreements exist with the calculation of Zatsarinny and Bartschat [2], and with some other absolute experiments [3 – 4].

In a second step, we have constructed a VMI spectrometer in order to measure asymmetry parameters and final-state branching ratios. The instrument is devised to detect photoelectrons detached from a fast (several keVs) anion beam entering the VMI perpendicularly to the detection axis. The issues brought by the use of a fast beam and the perpendicular geometry have been tackled by modifying the original VMI design of León *et al.* [5] in order to accommodate a deflector and re-referencing unit. Our setup provides an energy resolution of about 2% and an accuracy of about 5% for β. We have taken VMI images for photon energies ranging, again, from threshold to 5.5 eV, and the analysis of the data is currently under way. Preliminary results for the asymmetry parameter β already show good overall agreement with previous works [6].

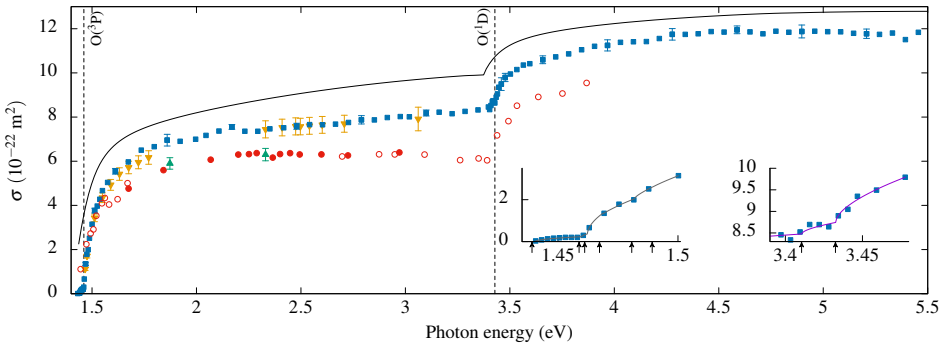

Fig. 1: Absolute photodetachment cross section of O^-. Squares: present results, circles: Branscomb *et al.* and Smith (see [3] and references therein), triangles: Hlavenka *et al.* [4], inverted triangles: Genevriez *et al.* [1], full line: Zatsarinny and Bartschat [2]. Error bars represent the 2σ statistical uncertainty. The insets show the present results near the $O(^3P)$ and $O(^1D)$ thresholds, fitted with the Wigner threshold law (solid line) and with arrows indicating the position of the various fine structure thresholds.

The present results offer a complete picture of the photodetachment of O^- in terms of *absolute* total, partial and differential cross sections, and over an unprecedented range of photon energies. Discrepancies with some theoretical calculations and some other experiments certainly call for further studies. The present work also stands as a methodological development paving the way to complete studies of the photodetachment of other atomic and molecular anions, and of other photoinduced processes.

References

[1] M . Genevriez *et al.* 2016 *Phys. Rev. A* **94** 023407
[2] O . Zatsarinny and K. Bartschat 2006 *Phys. Rev. A* **73** 022714
[3] L . M. Branscomb *et al.* 1965 *J. Chem. Phys.* **43** 2906
[4] P . Hlavenka *et al.* 2009 *J. Chem. Phys.* **130** 061105
[5] I . León *et al.* 2014 *Rev. Sci. Instr.* **85** 083106
[6] S . J. Cavanagh *et al.* 2010 *J. Phys. Conf. Ser.* **212** 012034

*Corresponding author: matthieu.genevriez@uclouvain.be

To the list of contents

Resonant Faraday rotation effect in Rb atoms with the use of a nano-cell: impact of cell thicknesses on observed spectra

A. Amiryan[*1,2], **A. Sargsyan**[1], **E. Klinger**[1,2], **S. Cartaleva**[3], **C. Leroy**[2], **D. Sarkisyan**[1]

1. Institute for Physical Research, National Academy of Sciences of Armenia,Ashtarak-2, 0203, Armenia
2. Laboratoire Interdisciplinaire Carnot de Bourgogne, UMR CNRS 6303, Université Bourgogne - Franche-Comté, BP 47870, 21078 Dijon Cedex, France
3. Institute of Electronics, Bulgarian Academy of Sciences 1784, Sofia, Bulgaria

Magneto-optical processes occur once the light interacts with a medium placed in a magnetic field. These effects are observed in usual cm length cells and are widely used in metrology, atomic spectroscopy, quantum information, etc. [1]. Among these processes the rotation of plane of polarization of the light, also known as Faraday Rotation (FR) was studied with use of a Rb atomic vapor contained in a nano-cell placed in a longitudinal magnetic field.

The cell is placed in a special vacuum chamber and the thickness $L = 140 - 1700$ nm is controlled by varying the internal pressure inside the chamber. This new technique allows one to measure cell thickness with better accuracy than it was done up to now.

Recently, the study [2] showed that the spectral width of absorption spectra takes its minimum value for thicknesses $L = (2n+1)\lambda/2$ ($\lambda = 795$ nm being the resonant wavelenght of the laser tuned to ^{85}Rb D_1 line), where n is an integer, while for the thickness $L = n\lambda$ the spectral width of absorption spectra reaches its maximum value, which is close to the Doppler width (several hundreds of MHz), as it presented in Fig. 1(a). This is called revival and collapse of coherent Dicke narrowing. Due to these effects the cell thicknesses $L = \lambda/2$ and $L = 3\lambda/2$ are of special interest since the obtained width of FR spectra is also several times narrower (~ 60 MHz) than in case of $L = \lambda$ and $L = 2\lambda$, is shown in Fig. 1(b). For the thicknesses $L = \lambda$ and $L = 2\lambda$ the signal decreases and gets enlarged as presented in [3]. Such dependence on L is absent in centimeter-length cells.

In comparison: the absorption spectra also have oscillating behavior which is less pronounced than in case of FR. Fluorescence spectra with the same experimental conditions are also observed. It is important to note that in contrast to the absorption spectra the amplitude and the line-width of the fluorescence spectra increases monotonically versus L, without oscillations of the line-width. The possible applications are presented [4].

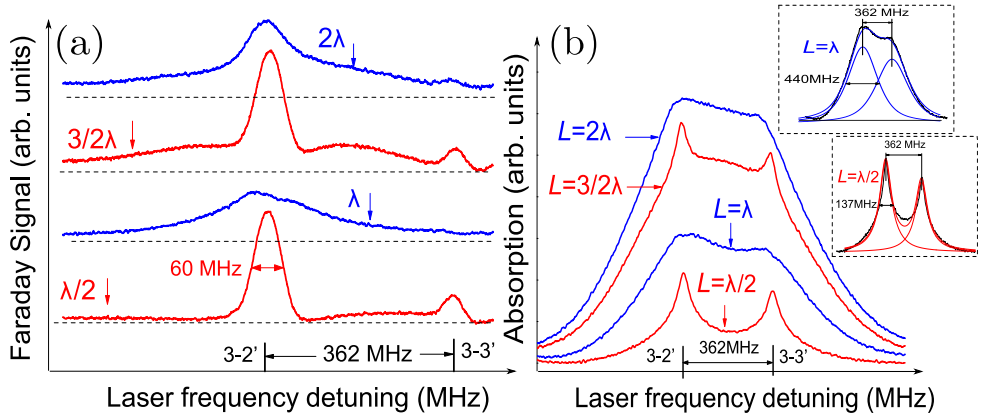

Fig. 1: Experimental spectra of Faraday Rotation (a) and absorption (b) of ^{85}Rb D_1 line atomic transitions recorded for the thicknesses $\lambda/2 \leqslant L \leqslant 2\lambda$ of the nano-cell, with the following experimental conditions $P = 10$ μW, $T = 120$ °C and $B = 10$ G.

References

[1] D. Budker, W. Gawlik, D. F. Kimball, S. M. Rochester, V. V. Yashchuk and A. Weis, Reviews of modern physics. **74**(4), 1153 (2002).
[2] A. Sargsyan, Y. Pashayan-Leroy, C. Leroy, and D. Sarkisyan, Journal of Experimental and Theoretical Physics, **123**(3), 395–402 (2016).
[3] A. Sargsyan, A. Amiryan, S. Cartaleva, and D. Sarkisyan, Journal of Experimental and Theoretical Physics, **151**(6), 1-8 (2017).
[4] Research conducted in the scope of the International Associated Laboratory IRMAS (CNRS France - SCS Armenia) and SCS MES of Armenia N 15T-1C040.

*Corresponding author: arevamiryan@gmail.com

To the list of contents

Selective Reflection monitoring of forbidden at zero B-field atomic transitions of a Rb vapor nanocell

Emmanuel Klinger[*1,2], **A. Sargsyan**[1], **A. Tonoyan**[1], **G. Hakhumyan**[1], **A. Amiryan**[1,2], **A. Papoyan**[1], **C. Leroy**[2], **D. Sarkisyan**[1]

1. Institute for Physical Research, NAS of Armenia, Ashtarak-2, 0203, Armenia

2. Laboratoire Interdisciplinaire Carnot de Bourgogne, UMR CNRS 6303, Université Bourgogne - Franche-Comté, BP 47870, 21078 Dijon Cedex, France

In the recent work [1] it was demonstrated that the Derivative Selective Reflection (DSR) technique from a cell having a thickness $L \approx \lambda/2$ (λ being the resonant wavelength of the laser radiation), allows the achievement of strong spectral line narrowing. Another advantage of the DSR is the proportionality of the recorded signal to the atomic transition probability. These benefits make the DSR-method convenient for the study of closely-spaced individual atomic transition components in a magnetic field [2].

It is known from the past decades that atomic levels undergo a frequency shift under the influence of a magnetic field. Besides, the coupling between hyperfine levels lead to a strong modification of the transition probabilities. A theoretical model covering all B-field range of the Zeeman effect for alkali atoms was proposed in [3], where they even noted that, due to the coupling, one can expect to detect transitions obeying to the selection rule $\Delta F = \pm 2$, *i.e.* transitions forbidden at zero magnetic field.

Using the DSR advantages, we have analyzed the Rb D_2 line in a wide range of magnetic field (200 – 1000 G), with a σ^+-polarized cw laser. We demonstrate that the amplitude of 8 initially forbidden transitions (5 for ^{85}Rb, 3 for ^{87}Rb) become the largest among the 17 transitions of ^{85}Rb $F_g = 2 \to F_e = 1,2,3,4$ group, and the 9 transitions of ^{87}Rb $F_g = 1 \to F_e = 0,1,2,3$ group, respectively. The theoretical model is perfectly consistent with the experimental results as it can be seen from Fig. 1 [4].

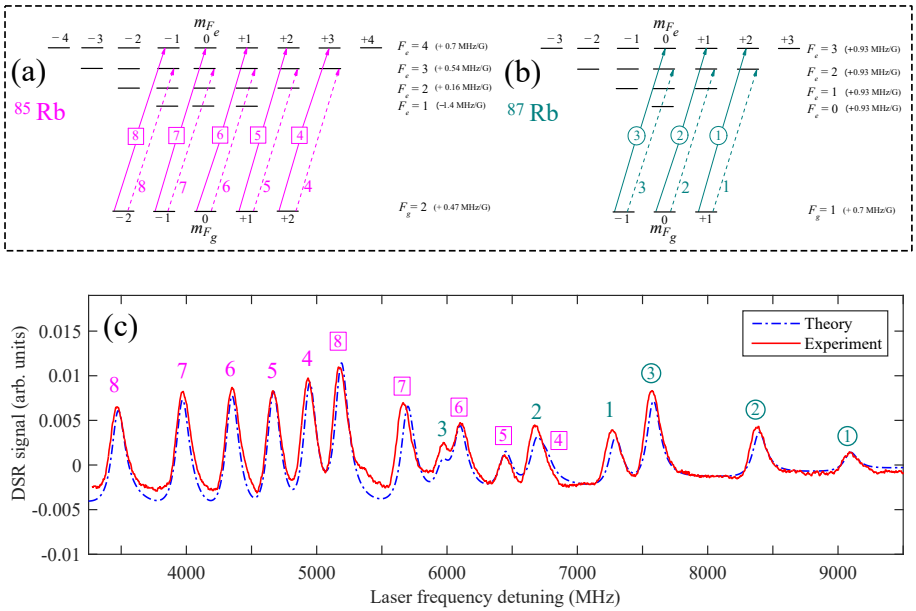

Fig. 1: (a), (b): Diagram of the relevant transitions between the Zeeman sublevels of Rb D_2 line with σ^+ (left-circular) laser excitation respectively for the case of ^{85}Rb (nuclear spin $I = 5/2$), and ^{87}Rb (nuclear spin $I = 3/2$). Transitions labeled in square (for ^{85}Rb) and in circle (for ^{87}Rb) obey to the selection rule $\Delta F = +2$. (c): experimentally recorded (red solid line) and calculated (dashed blue line) DSR spectra for the Rb nanocell with the thickness $L \approx \lambda/2$ for σ^+ laser excitation ($P_L = 10$ μW) and $B \approx 950$ G.

Among the possible applications of the DSR technique, we can emphasize the following: *(i)* optical magnetometry and metrology, *(ii)* laser technologies, *(iii)* thanks to a small divergence of selective reflection radiation beam, the DSR signal can be easily detected at large distance (~ 10 m away from the nanocell), which can be used for the remote optical monitoring of magnetic field.

References

[1] A. Sargsyan, E. Klinger, Y. Pashayan-Leroy, C. Leroy, A. Papoyan and D. Sarkisyan, JETP Letters **104**, (2016).
[2] A. Sargsyan, E. Klinger, G. Hakhumyan, A. Tonoyan, A. Papoyan, C. Leroy and D. Sarkisyan, J. Opt. Soc. Am. B **34**(4), (2017).
[3] P. Tremblay, A. Michaud, M. Levesque, S. Thériault, M. Breton, J. Beaubien and N. Cyr, Phys. Rev. A **42**, (1990).
[4] Research conducted in the scope of the International Associated Laboratory IRMAS (CNRS France - SCS Armenia).

*Corresponding author: emmanuel.klinger@u-bourgogne.fr

To the list of contents

Algebraic order and quench dynamics in Exciton-Polariton Condensates

P. Comaron[*1], **G. Dagvadorj**[†2], **A. Zamora**[‡2], **I. Carusotto**[§3], **N. Proukakis**[¶1], **M. H. Szymańska**[‖2]
1. Joint Quantum Centre (JQC) Durham–Newcastle, School of Mathematics and Statistics, Newcastle University Newcastle upon Tyne NE1 7RU, UK
2. Department of Physics and Astronomy, University College of London London, UK
3. INO-CNR BEC Center and Dipartimento di Fisica, Universita' di Trento Trento, Italy

The properties and dynamics of exciton-polariton condensates can, in certain regimes, be described by a stochastic driven-dissipative Langevin equation [1] (complex Ginzbug-Landau equation with noise), as already applied to the Berezinskii-Kosterlitz-Thouless transition [2]. Motivated by our related earlier work in the context of trapped cold atoms [3], we undertake a characterisation of the properties of an incoherently-pumped 2d condensate (focussing on densities and correlation functions) in terms of appropriate physical system parameters, extending our analysis to non-equilibrium regimes of experimental relevance [4]. We focus our studies on the out of equilibrium dynamics of a exciton-polariton condensate when cooled through the Berezinskii-Kosterlitz-Thouless phase transition; here bound and free vortices and phonons play a role in the change of the first-order correlation function and characterize the transition from a disordered to ordered state. Then, we discuss dynamical scaling of defects and characteristic length of the system when quenched across the transition and finally we present some preliminary results on Kibble-Zurek mechanism in a 2d geometry [5] in which the disordered state is plague with topological defects, and density of topological defects is related to the cooling rate.

Our work has been conducted with I. Carusotto, in collaboration with A. Zamora, G. Dagvadorj and M. Szymanska, with EPSRC funding.

References

[1] A. Chiocchetta, I. Carusotto, EPL (Europhysics Letters) **102**, 67007 (2013)
[2] G. Dagvadorj, J.M. Fellows, S. Matyjaakiewicz, F. M. Marchetti, I. Carusotto, M.H. Szymanska, [arXiv:1412.7361v1]
[3] S. P. Cockburn, N. P. Proukakis, PRA **86**, 033610 (2012)
[4] W. H. Nitsche et. al., Phys. Rev. B **90**, 205430 (2014)
[5] A. Jelic and L. F. Cugliandolo, J. Stat. Mech., P02032 (2011)

[*]Corresponding author: p.comaron@ncl.ac.uk
[†]Corresponding author: G.Dagvadorj@warwick.ac.uk
[‡]Corresponding author: alex.zamora.soto@gmail.com
[§]Corresponding author: iacopo.carusotto@unitn.it
[¶]Corresponding author: nikolaos.proukakis@newcastle.ac.uk
[‖]Corresponding author: m.szymaska@ucl.ac.uk

To the list of contents

Charge-state-resolved spectroscopy of highly charged tin ions for laser-plasma-based nanolithography EUV-light sources

F. Torretti*[1], J. Scheers[1], A. Windberger[1], W. Ubachs[1], R. Hoekstra[1], A. Ryabtsev[2], A. Borschevsky[3], J. Berengut[4], J. R. Crespo López-Urrutia†[5], O. O. Versolato[1]

1. Advanced Research Center for NanoLithography, Science Park 110, 1098 XG Amsterdam, Netherlands
2. Molecular Spectroscopy, Institute of Spectroscopy, Fizicheskaya Str. 5, Troitsk, Moscow, 108840 Russia
3. Van Swinderen Institute, Universiteit Groningen, Nijenborgh 4, 9747 AG Groningen, Netherlands
4. School of Physics, The University of New South Wales, Sydney NSW 2052, Australia
5. Max-Planck-Institut für Kernphysik, Saupfercheckweg 1, 69117 Heidelberg, Germany

Laser-produced tin plasmas are used in nanolithography applications for the generation of extreme ultraviolet (EUV) light around 13.5 nm. Radiation in this wavelength band is primarily generated by electronic transitions in highly charged tins ions in the charge states Sn^{8+}-Sn^{14+}. Due to the complex couplings present in the various excited electronic configurations of those ions, thousands of atomic lines cluster around 13.5 nm in a so-called unresolved transition array (UTA). While this makes accurate line identification in the EUV extremely difficult, optical forbidden transitions, which basically arise within the respective ground state configurations of those ions, are far less numerous. In those configurations, with far fewer electronic states involved, only from a few up to tens of optical lines appear. Additionally, the instrumental spectral resolution can also be made much higher. Therefore, we have systematically investigated such optical emission lines using an electron beam ion trap (EBIT) at MPIK. We separate the various charge states by stepwise raising the electron energy to selectively produce them, while simultaneously collecting series of EUV and optical spectra (see Fig. 1). Based on these data as well as on level-structure calculations obtained with various *ab-initio* methods, the optical lines found in the spectra were reliably assigned [1][2]. As a conclusion, earlier assignments of EUV transitions from the literature are found to require substantial corrections. Comparing the EUV and optical spectra obtained under controlled conditions in the EBIT with the laser-produced plasma thus provides essential information on the contribution of tin charge states to the EUV emission in this region of strong technical interest.

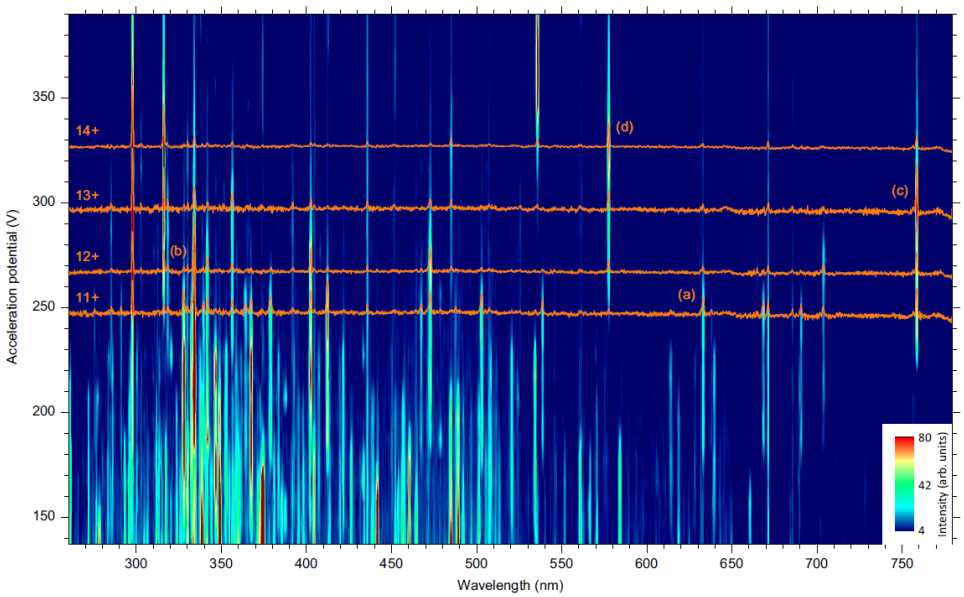

Fig. 1: Composite spectral map of Sn ions obtained at discrete acceleration potential in an electron beam ion trap (from Windberger *et al.* [1]). The superimposed curves show the spectra of Sn^{11+}–Sn^{14+} at their respective maximum fluorescence yield. Symbols (a), (b), (c), and (d) mark the most characteristic lines of specific charge states.

References

[1] A. Windberger, F. Torretti, A. Borschevsky, A. Ryabtsev, S. Dobrodey, H. Bekker, E. Eliav, U. Kaldor, W. Ubachs, R. Hoekstra, J. R. Crespo López-Urrutia, O. O. Versolato, Phys. Rev. A **94**, 012506 (2016).
[2] F. Torretti, A. Windberger, A. Ryabtsev, S. Dobrodey, H. Bekker, W. Ubachs, R. Hoekstra, E.V. Kahl, J.C. Berengut, J. R. Crespo López-Urrutia, O. O. Versolato, Phys. Rev. A **95**, 042503 (2017).

*Corresponding author: f.torretti@arncl.nl
†Corresponding author: crespojr@mpi-hd.mpg.de

To the list of contents

High-Helicity Vortex Conversion in a Rubidium Vapor

Aurélien Chopinaud[*1], **Marion Jacquey** [1], **Bruno Viaris de Lesegno** [1] **and Laurence Pruvost**[†1]
1. Laboratoire Aimé Cotton, CNRS, Univ Paris-Sud, ENS Paris-Saclay, Univ Paris-Saclay
batiment 505, 91405 Orsay, France

An optical vortex is a light beam with a helically-shaped wavefront. Such a beam carries an orbital angular momentum (OAM), which is quantized with a signed integer ℓ related to the helix period. This quantum variable of light is also called the third momentum of light and is exchanged with matter via quantum rules.

Vortex conversion from a red optical vortex at 776 *nm* to a blue one at 420 *nm* is demonstrated for high values of ℓ ranging -30 to +30. The vortex-conversion uses the 5S-5D two-photon transition in a rubidium vapor cell, monitored with a Gaussian beam at 780 nm transition plus a vortex beam at 776 nm with helicity ℓ. The 5D level emission creates a pair of photons, i.e. 5.2 μm and 420 *nm* With a parallel co-propagating beam configuration, we obtain a high-helicity transfer, which respects the OAM conservation as shown in Fig.1.

This process is a promising way for quantum variable transfer in the context of quantum technology.

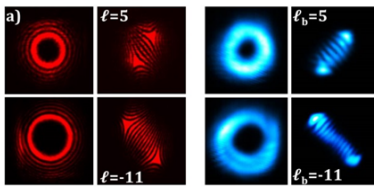

Fig. 1: Input red vortex (on the left) and generated blue one (on the right). For each ℓ value ($\ell = 5$ and -11) we show the vortex intensity (donut shape) and the measurement of its OAM by auto-interference through an astigmatic system (patterns with ℓ dark fringes).

[*]Corresponding author: aurelien.chopinaud@u-psud.fr
[†]Corresponding author: laurence.pruvost@u-psud.fr

To the list of contents

Colliding laser produced plasmas analysis: fast imaging and spectroscopic study

Domagoj Kos[*1,2], **O. Maguire**[1], **F. O'Reilly**[1], **P. Dunne**[1], **E. Sokell**[1]
1. School of Physics, University College Dublin, Belfield, Dublin 4, Ireland
2. Faculty of Nuclear Sciences and Physical Engineering, Czech Technical University in Prague, Brehova 7,511519 Praha 1, Czech Republic

The ablation of a target material with a focused high power laser creates a plasma, a mixture of ions, electrons and atoms. The plasma absorbs significantly more energy than the solid target, creating high ion stages and a very dynamic system. As the laser pulse ends, the plasma continues to expand into the surrounding space and cools down.

Creating two laser produced plasmas in close proximity can lead to their collision as they expand. Depending on the separation between the plasmas and the ion-ion mean free path, the two plasmas can interpenetrate or collide and form a stagnation layer [1]. The collision causes kinetic to thermal energy transfer [2], and the formed stagnation layer shows different properties than those of the original plasma, with a longer life time and nearly isothermal temperature distribution along the cylindrical shape [3]. As such, the stagnation layer has shown to be a very suitable target for the laser reheat of a plasma [4], a method used in the EUV lithography industry to increase emission from the plasma in the 13.5 nm region.

In this work we present the evolution of the colliding plasmas and the stagnation layer of a light element (Si, Z=14) and a heavy element (Pb, Z=82). We view the time resolved expansion of the plasma in the visible region of the spectrum, viewed at 90° angle with respect to the expansion direction of the two seed plasmas. The integration time was 10 ns and the time step was 10 ns. An example of an image is shown in Fig. 1. We also present a time resolved spectroscopic study of the stagnation layer of Si and Pb in the near ultraviolet region (360-415 nm) and compare the spectrum of single plasma and the stagnation layer.

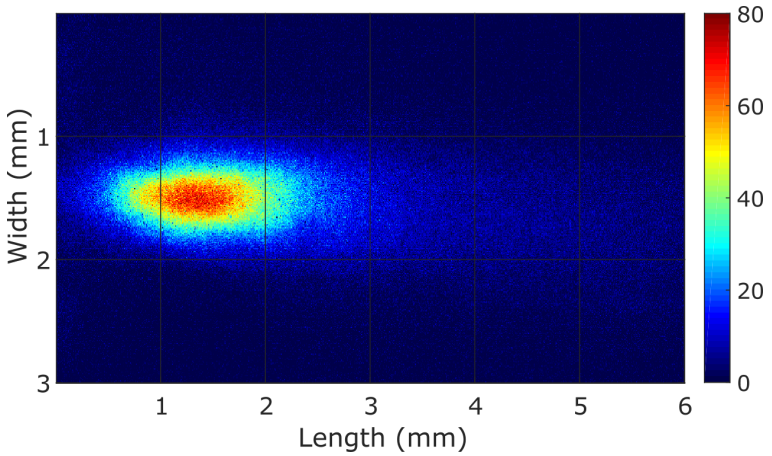

Fig. 1: Stagnation layer of Si colliding plasmas 150 ns after the laser pulse, 10 ns integration time, spectral region 350-800 nm. Plasma expands away from the target on the left edge of the figure.

References

[1] P.W. Rambo and J. Denavit, *J. Comput. Phys.* **98**, 317 (1992)
[2] C. Chenais-Popovics, P. Renaudin, O. Rancu, F. Gilleron, J.-C. Gauthier, O. Larroche, O. Peyrusse,M. Dirksmöller, P. Sondhauss, T. Missalla, I. Uschmann, E. Förster, O. Renner and E. Krousky, *Physics of Plasmas* **4**, 190 (1997)
[3] H. Luna, K. D. Kavanagh and J. T. Costello, *J. Appl. Phys.* **101**, 033302 (2007)
[4] T. Cummins, C. O'Gorman, P. Dunne, E. Sokell, G. O'Sullivan and P. Hayden, *Appl. Phys. Lett.* **105**, 044101 (2014)

*Corresponding author: domagoj.kos@ucdconnect.ie

To the list of contents

A novel off-axis electron gun for electron beam ion traps

S. Kühn[*1], **Sven Bernitt**[1,2], **Peter Micke**[3], **Thomas Stöhlker**[2], **José R. Crespo López-Urrutia**[1]
1. Max-Planck-Institut für Kernphysik, Heidelberg, Germany
2. IOQ, Friedrich-Schiller-Universität Jena, Germany
3. Physikalisch-Technische Bundesanstalt, Braunschweig, Germany

In an electron beam ion trap (EBIT) highly charged ions (HCIs) are produced using an electron beam compressed to very high densities, which sequentially ionizes atoms. EBITs usually employ on-axis electron guns blocking the view along the trap axis, which can constitute a limitation for certain applications, like laser spectroscopy, where the external photon beam is lost by hitting the gun. A novel off-axis gun (OAG) was built with its cathode displaced from the central axis, which is therefore free of any obstacles and thus the photon beam is available for further experiments downstream. One of the envisaged applications is using HCIs as a new in situ calibration standard for high energy photon beams as provided e.g. by synchrotrons. First measurements of dielectronic recombinations on argon ions in a compact 0.86 T permanent magnet EBIT have shown stable operations of the OAG with a 25 mA electron beam and up to 8 keV beam energy. A high energy beam resolution of $\Delta E = 2.6(1)$ eV could be achieved using low beam currents.

*Corresponding author: steffen.kuehn@mpi-hd.mpg.de

To the list of contents

Observing the Effect of Wavefront Aberrations in an Atom Interferometer by Modulating the Diameter of Raman Beams

Qin Luo, Le-le Chen, Xiao-Chun Duan, Min-kang Zhou, Zhong-kun Hu*

1. Ministry of Education Key Laboratory of Fundamental Physical Quantities Measurements, School of Physics, Huazhong University of Science and Technology, Wuhan 430074,People's Republic of China

Over the last two decades, atom interferometry technique has rapidly developed and was widely used. The gravity measurement is one of the most successful applications of this technology. Atom interferometry gravimeters have reached sub-μGal resolution [1-4] (1 $\mu Gal = 1 \times 10^{-8} m/s^2$), but the accuracy is limited by wavefront aberrations effect to several μGal [5-6].

The effect of wavefront aberrations in atom interferometers has been observed by some different methods. In this work [7], a new method observing this effect has been proposed and demonstrated by experiments. Firstly, the principle of atom interferometry and wavefront aberrations will be briefly described, furthermore, for observing the effect of wavefront aberrations in atom interferometer, we proposed to modulate the diameter of Raman beams, and some calculations and results will be displayed. Last but not least, some experiments have been carried out, and conspicuous variation of gravity measurement has been observed by using this novel method in our atom interferometry gravimeter.

References

[1] A. Peters, K. Y. Chung and S. Chu, "High-precision gravity measurements using atom interferometry", Metrologia **38**, 25-61 (2001).
[2] J. Le Gouet, T. Mehlstaubler, F. Pereira Dos Santos *et al.*, Limits to the sensitivity of a low noise compact atomic gravimeter, Appl. Phys. B: Lasers Opt. **92**, 133 (2008).
[3] M. Schmidt, A. Senger, A. Peters *et al.*, "A Mobile High-Precision Absolute Gravimeter Based on Atom Interferometry", Gyroscopy and Navigation **2**, 170-177 (2011).
[4] Zhong-Kun Hu, Bu-Liang Sun, Jun Luo *et al.*, "Demonstration of an ultrahigh-sensitivity atom-interferometry absolute gravimeter", Phys. Rev. A **88**, 043610 (2013).
[5] A. Louchet-Chauvet, T. Farah, F. P. Dos Santos *et al.*, "The influence of transverse motion within an atomic gravimeter", New J. Phys. **13**, 065025 (2011).
[6] V. Schkolnik, B. Leykauf, A. Peters *et al.*, "The effect of wavefront aberrations in atom interferometry", Appl. Phys. B: Lasers Opt. **120**, 311 (2015).
[7] Min-kang Zhou, Qin Luo, Le-le Chen *et al.*, "Observing the effect of wave-front aberrations in an atom interferometer by modulating the diameter of Raman beams", Phys. Rev. A **93**, 043610 (2016).

*Corresponding author: zkhu@hust.edu.cn

To the list of contents

Transmission Diffraction Gratings for ultrasensitive biosensors and atomic physics

A. Sierant[*1], **B. Jany**[1], **D. Bartoszek-Bober**[1], **J. Fiutowski**[2], **J. Adam**[2], **T. Kawalec**[1]
1. Marian Smoluchowski Institute of Physics
Łojasiewicza 11, 30-348 Cracow, Poland
2. NanoSyd, Mads Clausen Institute, University of Southern Denmark
Alsion 2, DK-6400 Sønderborg, Denmark

Transmission diffraction gratings are submicron structures with a variety of applications, from OLED light out-coupling and color filtering to surface plasmon polaritions (SPPs) excitation.

SPPs are collective electron oscillations confined at a metal-dielectric interface, which may be tailored with subwavelength resolution [1]. This phenomenon is widely used in highly sensitive refractive index sensing [2] and optical dipole mirrors for cold atoms [3,4,5]. In order to obtain a successful SPPs excitation one needs a strong photon-to-SPP coupling. The prism-based coupling is classically used, but this method prevents the miniaturized and compact systems application. An alternative realization is given by the use of a metallic diffraction grating, where the diffracted light couples to the SPPs.

Here, we propose a metallic transmission diffraction grating with precisely calculated and optimized grating parameters. The transmission structure is milled in a plain gold deposited on a glass substrate by means of focused ion beam (FIB) microscope. Subsequently, the grating is investigated with near-field scanning optical microscope (NSOM) and goniometric far field measurements (Fig. 1 a, b). We support the evidence of our analyses with numerical calculations done by rigorous coupled wave analysis (RCWA) and finite-difference in time-domain (FDTD) (Fig. 1 c).

Subsequently, such a structure can be applied in a plasmonic sensor setup and optical dipole mirror for ultracold atoms.

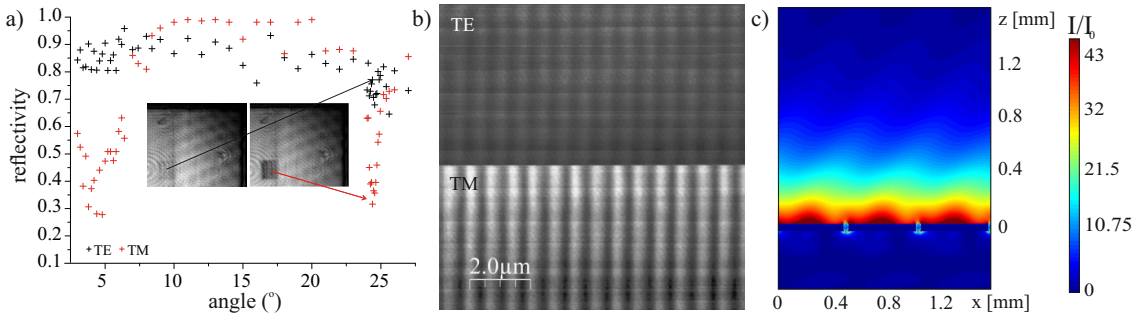

Fig. 1: a) Experimental results for transmission grating and CCD images for TE and TM polarized light. b) NSOM image for both polarizations. c) RCWA simulations for SPPs excitation.

References

[1] W. L. Barnes, A. Dereux, T. W. Ebbesen, Nature **424**, 824-830 (2003)
[2] X. D. Hoa, A. G. Kirk, M. Tabrizian, Biosens. Bioelectron., **23**, 151-160 (2007)
[3] T. Kawalec et al., Opt. Lett. **39**, 2932 (2014)
[4] T. Kawalec et al., Surface Plasmon Polaritons Probed with Cold Atoms, Plasmonics (2017)
[5] T. Esslinger et al., Opt. Lett. **18**, 450 (1992)

*Corresponding author: aleksandra.plawecka@doctoral.uj.edu.pl

To the list of contents

Effect of the Raman beams' alignment in four-pulse atom gyroscope

W. J. Xu[*1], **M. K. Zhou**[1], **X. C. Duan**[1], **M. M. Zhao**[1],**K. Zhang**[1], **Z. K. Hu**[†1]
1. MOE Key Laboratory of Fundamental Physical Quantities Measurements, School of Physics, Huazhong University of Science and Technology, Wuhan 430074, People's Republic of China

Since the demonstration of the first atom interferometer gyroscope was reported in 1991[1], Sagnac gyroscope based on Atom interferometry is highly concerned for the reason of high potential sensitivity and small dimension [2-5]. The alignment of the Raman beams should be carefully adjusted in large area atom gyroscope [6]. Here we theoretically analyze and experimentally demonstrate the effect of the parallel misalignment of the two Raman beams in four-pulse atom interferometer, what's more, the influence of space asymmetry of the four-pulse atom interferometer is also shown coupled with the misalignment of the two Raman beams. With this method, a four-pulse atom gyroscope with T=54.25 ms is achieved, the current sensitivity of the atom gyroscope is $1.5\times10^{-6}\mathrm{rad/s/Hz^{1/2}}$ by the means of vibration compensation.do not include acknowledgments in your abstract.

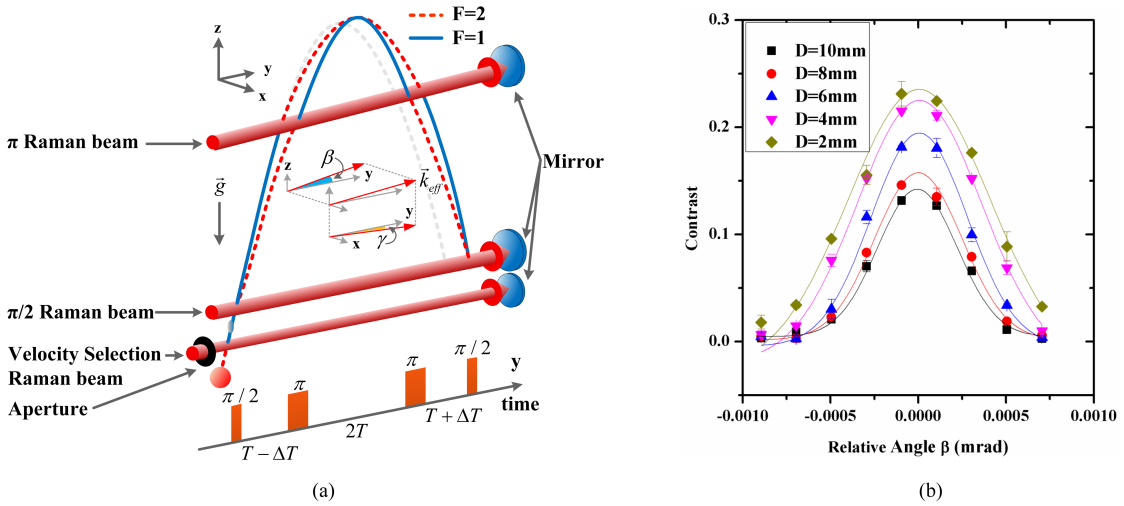

(a) (b)

Fig. 1: Fig. 1: (a) The configuration of the Raman beams. (b) Contrast measurement for different diameter of the velocity selection aperture as a function of the angle of the Raman beam in y-z plane.

References

[1] F. Riehle, T. Kisters, A. Witte, J. Helmcke, and C. J. Bordé, Phys. Rev. Lett. **67**, 177 (1991).
[2] D. S. Durfee, Y. K. Shaham, and M. A. Kasevich, Phys. Rev. Lett. **97**, 240801 (2006).
[3] J. K. Stockton, K. Takase, and M. A. Kasevich, Phys. Rev. Lett. **107**, 133001 (2011).
[4] P. Berg, S. Abend, G. Tackmann, C. Schubert, E. Giese, W. P. Schleich, F. A. Narducci, W. Ertmer, and E. M. Rasel, Phys. Rev. Lett. **114**, 063002 (2015).
[5] I. Dutta, D. Savoie, B. Fang, B. Venon, C. L. Garrido Alzar, R. Geiger, and A. Landragin, Phys. Rev. Lett. **116**, 183003 (2016).
[6] G. Tackmann, P. Berg, C. Schubert, S. Abend, M. Gilowski, W. Ertmer, and E. M. Rasel, New J. Phys. **14**, 015002 (2012).

[*]Corresponding author: wenjiexu@hust.edu.cn
[†]Corresponding author: zkhu@mail.hust.edu.cn

To the list of contents

Dielectronic-recombination processes in highly-charged heavy ions observed in ion traps

A. Borovik, Jr.[*1,2,3], **J. Dreiling**[1], **R. Silwal**[1,4], **Dipti**[1], **E. Takács**[1,4], **J. Gillaspy**[1,5], **R. Lomsadze**[3,6], **V. Ovsyannikov**[3], **K. Huber**[3], **A. Müller**[3], **and Yu. Ralchenko**[1]

1. Quantum Measurement Division, National Institute of Standards and Technology
100 Bureau Road, Gaithersburg, MD 20899, USA
2. I. Physikalisches Institut, Justus-Liebig-Universität Gießen
Leihgesterner Weg 217, 35392 Giessen, Germany
3. Institut für Atom- und Molekülphysik, Justus-Liebig-Universität Gießen
Leihgesterner Weg 217, 35392 Giessen, Germany
4. Department of Physics and Astronomy, Clemson University
118 Kinard Laboratory, Clemson, SC 29634-0978
5. Division of Physics, National Science Foundation
4201 Wilson Boulevard, Arlington, VA 22230, USA
6. Department of Physics, Ivane Javakhishvili Tbilisi State University
1 Chavchavadze Avenue, T'bilisi 0179, Georgia

Correct understanding of ionized-matter environments ranging from plasmas in small laboratory devices to ionized gas in interstellar clouds in far outer space requires reliable data on elementary atomic processes. Such data include parameters for numerous mechanisms in wide energy ranges and can, therefore, exclusively be obtained theoretically. However, for many atomic systems, the accuracy of theoretical approaches generally used for such purposes is limited. This is especially the case for plasmas including ensembles of highly-charged many-electron ions of heavy elements. In such cases, experimental data serving as a guiding light for theoretical calculations are highly desirable.

We report on the X-ray spectra of highly-charged tungsten and iridium ions measured employing the Electron-beam Ion Trap (EBIT) at National Institute of Standards and Technology [1] and the Main Magnetic Focus Ion Trap (MaMFIT) at Justus-Liebig Universität Gießen [2], respectively. The data are shown in Fig. 1. The NIST EBIT spectra (*a*), measured from 6.44 through 11.27 keV, reveal series of resonances corresponding to dielectronic-recombination (DR) processes involving transitions $2\ell - 3\ell'$ and $2\ell - 4\ell'$ subshells in Ne-like through Mn-like tungsten. The spectra from the MaMFIT (*b*), measured at energies 7.1 through 8.65 keV, show resonances corresponding to DR processes involving transitions between $2p - 3d$ subshells in K-like through Ni-like iridium. The detailed modeling of the observed spectra has been performed employing the non-Maxwellian collisional radiative code NOMAD [3] with the atomic data produced by the Flexible Atomic Code. Comparison of the experimental and theoretical results has revealed a good agreement for both cases of W^{q+} and Ir^{q+} spectra.

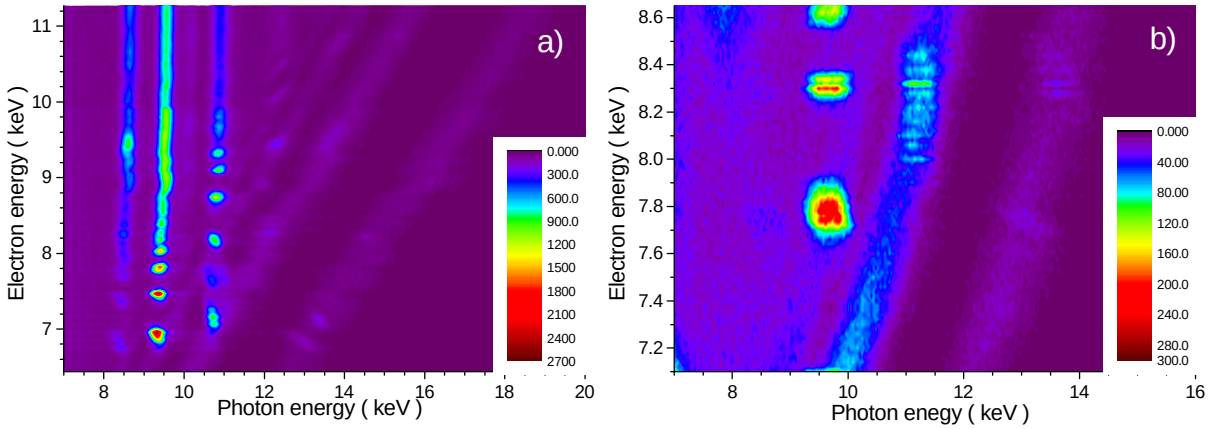

Fig. 1: X-ray spectra from EBIT at NIST a) and MaMFIT in Giessen b).

References

[1] J. D. Gillaspy, AIP Conf. Proc. **1438**, 97 (2012)
[2] V. P. Ovsyannikov, arXiv:1403.2168 (2014)
[3] Yu. V.Ralchenko and Yi. Maron, J. Quant. Spec. and Rad. Trans. **71** 609 (2001)

*Corresponding author: Alexander.Borovik@physik.uni-giessen.de

To the list of contents

Developments towards a transverse free-electron target for the storage ring CRYRING@ESR

C. Brandau*[1,2], A. Borovik, Jr[1], B. M. Döhring[1], B. Ebinger[1], C. Kozhuharov[2], T. Molkentin[1], A. Müller[3], Th. Stöhlker[2,4,5], and S. Schippers†[1], for the SPARC working group "Electron Targets"

1. I. Physikalisches Institut, Justus-Liebig-Universität Gießen
Leihgesterner Weg 217, 35392 Giessen, Germany
2. GSI Helmholtzzentrum für Schwerionenforschung
Planckstrasse 1, 64291 Darmstadt, Germany
3. Institut für Atom- und Molekülphysik, Justus-Liebig-Universität Gießen
Leihgesterner Weg 217, 35392 Giessen, Germany
4. Institut für Optik und Quantenoptik, Friedrich-Schiller-Universität Jena
Max-Wien-Platz 1, 07743 Jena, Germany
5. Helmholtz-Institut Jena
Fröbelstieg 3, 07743 Jena, Germany

The storage ring CRYRING@ESR will be one of the first operational devices at the upcoming antiproton and heavy-ion accelerator facility FAIR. As a part of the program of the SPARC collaboration it is intended to install a dedicated sheet-beam free-electron target at CRYRING@ESR [1]. Electron-ion collision studies with transverse electron targets were conducted at low-energy single-pass beam lines since the 1960s [2] but a crossed-beams setup has never been realized at a heavy-ion storage ring, yet. Currently, a new electron gun is being developed (Fig. 1) that advances previous multi-electrode arrangements [3,4,5] with adaptations to the special requirements at CRYRING@ESR, namely, free space for the circulating ion beam and stringent vacuum conditions with residual gas pressures of the order of 10^{11} mbar. The multi-electrode layout enables a detailed control of electron-beam parameters such as beam size, electron density and electron energy. Maximum electron energies up to 12.5 keV are envisaged. The typical beam-size in the interaction region is 8×80 mm^2 at an electron density of up to 109 cm^3.

The set-up is optimized for spectroscopy of photons thus enabling many new opportunities for experimental access to fundamental electron-ion collision processes including excitation, recombination, elastic scattering and ionization. In contrast to collision studies at a gas-jet target, no target nucleus is present. Hence, observations of electron-impact excitation or electron-ion recombination are not obscured by competing processes like proton-impact excitation or non-radiative capture. A further advantage is that the electron-ion collision energy can easily be changed over a wide range without changing the ion energy.

This work is supported by German Federal Ministry of Education and Research BMBF (contract 05P15RGFAA), and the Helmholtz International Center for FAIR, a Hessian state funded Center of Excellence.

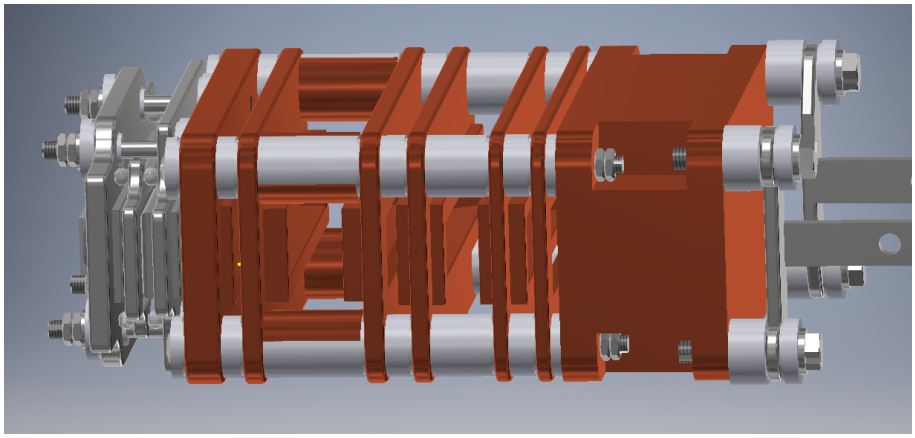

Fig. 1: Current design of the new electron gun, which is still being optimized. The electron beam is directed left to right.

References

[1] M. Lestinsky et al., Eur. Phys. J. **ST 225** 797 (2016)
[2] A. Müller, Adv. At. Mol. Opt. Phys. **55** 293 (2008)
[3] W. Shi et al., Nucl. Instrum. Meth. B **205** 201 (2003)
[4] S. Geyer et al., Phys. Scr. **T156** 014093 (2013)
[5] A. Borovik Jr. et al., J. Phys.: Conf. Ser. **488** 142007 (2014)

*Corresponding author: c.brandau@gsi.de
†Corresponding author: Stefan.Schippers@physik.uni-giessen.de

To the list of contents

Simulating strong control fields in nuclear quantum optics

K. P. Heeg*[1], A. Kaldun[1], C. Strohm[2], P. Reiser[1], C. Ott[1], S. Rajagopalan[1], D. Lentrodt[1], J. Haber[2], H.-C. Wille[2], S. Goerttler[1], R. Rüffer[3], C. H. Keitel[1], R. Röhlsberger[2], T. Pfeifer[1], J. Evers[1]

1. Max-Planck-Institut für Kernphysik, Saupfercheckweg 1, D-69117 Heidelberg, Germany
2. Deutsches Elektronen-Synchrotron DESY, Notkestraße 85, 22607 Hamburg, Germany
3. ESRF-The European Synchrotron, CS40220, 38043 Grenoble Cedex 9, France

X-ray quantum optics has gained considerable momentum during the last few years and opens up an avenue to study the light–matter interaction beyond the visible regime [1]. While x-rays can in principle interact with the transitions of atomic inner-shell electrons, driving nuclear resonances forms an interesting alternative [2-4]. In particular, Mössbauer nuclei with their narrow line widths offer some unique features. The light–matter interaction can be boosted by cooperative effects between the atoms [2] and systems with complex quantum superpositions can be operated essentially decoherence-free [3].

However, severe practical limitations arise from the fact that suitable strong control laser fields are generally not available. Even x-ray free electron lasers are expected to have only a moderate impact on the nuclei, mostly due to their narrow line width as compared to the bandwidth of typical x-ray pulses. Additionally, coherent multi-color x-ray sources are not routinely available in the lab. To circumvent this problem, we aim to develop methods which simulate the effect of strong control fields without actually applying an electromagnetic field.

Our approach is based on fast mechanical motion of the resonant target [4]. In certain configurations, such mechanical motions on tiny distance and short time scales take the role of the desired control fields and facilitate manipulations in the temporal as well as the spectral domain. Since our method is compatible with existing and upcoming x-ray sources, we anticipate that it will fuel new applications in particular with ultra-narrow x-ray resonances.

In this contribution, I will report on our recent theoretical and experimental results in this direction.

References

[1] B. W. Adams, *et al.*, J. Mod. Opt. **60**, 2 (2013).
[2] R. Röhlsberger, K. Schlage, B. Sahoo, S. Couet, R. Rüffer, Science **328**, 1248 (2010).
[3] K. P. Heeg, *et al.*, Phys. Rev. Lett. **111**, 073601 (2013).
[4] F. Vagizov, V. Antonov, Y. V. Radeonychev, R. N. Shakhmuratov, O. Kocharovskaya, Nature **508**, 80 (2014).

*Corresponding author: kilian.heeg@mpi-hd.mpg.de

To the list of contents

X-ray laser spectroscopy with highly charged ions using radiation from synchrotrons and free-electron lasers

S. Bernitt[*1,2,3], **R. Steinbrügge**[4,2], **S. Dobrodey**[2], **S. Kühn**[2], **P. Micke**[5,2], **J. K. Rudolph**[6,2], **S. W. Epp**[7], **T. Stöhlker**[3,1], **J. R. Crespo López-Urrutia**[2],

1. Institut für Optik und Quantenelektronik, Friedrich-Schiller-Universität, Max-Wien-Platz 1, 07743 Jena, Germany
2. Max-Planck-Institut für Kernphysik, Saupfercheckweg 1, 69117 Heidelberg, Germany
3. Helmholtz-Institut Jena, Fröbelstieg 3, 07743 Jena, Germany
4. TRIUMF, 4004 Wesbrook Mall, Vancouver, BC V6T 2A3, Canada
5. QUEST-Institut, Physikalisch-Technische Bundesanstalt, Bundesallee 100, 38116 Braunschweig, Germany
6. Institut für Atom- und Molekülphysik, Justus-Liebig-Universität, Leihgesterner Weg 217, 35392 Giessen, Germany
7. Max-Planck-Institut für die Struktur und Dynamik der Materie, Luruper Chaussee 149, 22761 Hamburg, Germany

By resonantly exciting electronic transitions with monochromatic light and recording the induced fluorescence as a function of the light wavelength, it is possible to directly probe the electronic structures of atoms, molecules and ions. This technique, commonly known as laser spectroscopy, is widely used in physics and chemistry, yielding highly accurate spectroscopic data. In recent years, the advent of the newest generation of ultrabrilliant light sources – synchrotrons with undulators and free-electron lasers – has enabled its application in the previously unaccessible x-ray regime.

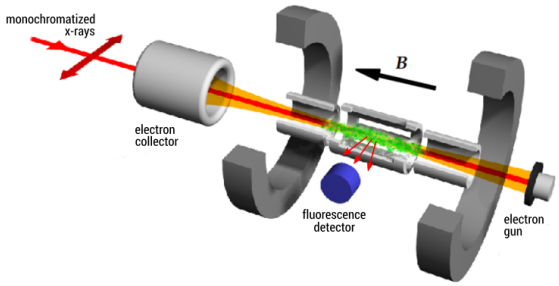

Fig. 1: X-ray laser spectroscopy with an electron beam ion trap (EBIT). Highly charged ions are produced by repeated electron impact ionization, and trapped radially by the negative space charge of the electron beam as well as axially by potentials applied to a set of cylindrical electrodes. An x-ray beam is overlapped with the cloud of trapped ions. Resonantly excited fluorescence is detected and recorded as a function of the x-ray wavelength.

The transportable electron beam ion trap FLASH-EBIT has been used in a number of experiments to provide targets of trapped highly charged ions for VUV and x-ray radiation from FLASH [1,2], LCLS [3], BESSY II [4] and PETRA III [5,6,7]. Our measurements have yielded accurate transition energies [1,2,5,7], natural line widths [5,6], and relative oscillator strengths [3]. By detecting changes of ion charge states we were also able to detect resonant photoionization [4] and deduce branching ratios as well as absolute radiative and Auger decay rates [6].

The atomic data obtained is valuable for the interpretation of astrophysical x-ray spectra [3], such as the ones expected from future satellite missions like the JAXA/NASA X-ray Astrophysics Recovery Mission (XARM) or ESA's ATHENA, where a lack of high accuracy spectroscopic data still limits the possible scientific gain. Furthermore, the study of high-Z few-electron systems provides benchmarks of atomic theory [5,7]. We present first results of recent experiments with helium-like and lithium-like Ge, Se, Br, and Kr, testing calculations on the level of QED contributions.

We also present a new compact electron beam ion trap based on permanent magnets, called PolarX-EBIT. It has been developed to investigate the possible use of electronic transitions in highly charged ions as future x-ray wavelength standards, and explore new applications for spectroscopy, metrology and polarimetry.

References

[1] S. W. Epp *et al.*, Phys. Rev. Lett. **98**, 183001 (2007).
[2] S. W. Epp *et al.*, J. Phys. B: At. Mol. Opt. Phys. **43**, 194008 (2010).
[3] S. Bernitt *et al.*, Nature **492**, 225-228 (2012).
[4] M. C. Simon *et al.*, Phys. Rev. Lett. **105**, 183001 (2010).
[5] J. K. Rudolph *et al.*, Phys. Rev. Lett. **111**, 103002 (2013).
[6] R. Steinbrügge *et al.*, Phys. Rev. A **91**, 032502 (2015).
[7] S. W. Epp *et al.*, Phys. Rev. A **92**, 020502(R) (2015).

*Corresponding author: sven.bernitt@mpi-hd.mpg.de

To the list of contents

Theoretical Studies of Dipole Blockade Parameters using Förster Resonances in Rb Atoms

Teodora Kirova[*1], **Arturs Cinins**[1], **Marcis Auzinsh**[2], **Ite A. Yu**[3]
1. Institute of Atomic Physics and Spectroscopy, University of Latvia, Riga, LV-1586, Latvia
2. Laser Centre, University of Latvia, LV-1002, Riga, Latvia
3. Department of Physics, National Tsing Hua University, Hsinchu 30013, Taiwan

Rydberg atoms [1] are characterized by a large separation between the electron and the ion core, which leads to their strong polarizability and extreme long-range dipolar interactions. At short distances the strong resonant dipole-dipole (DD) interaction is of $1/R^3$ dependence, while the long range interaction is of van der Waals $1/R^6$ type.

In the phenomenon of dipole blockade [2], the DD interaction causes the applied laser excitations to be off-resonant, as a result of which only a single atom can be excited within the "blockade sphere" [3] while simultaneous excitation of two/multiple Rydberg atoms will be suppressed.

Our aim is to find the best experimental parameters necessary to achieve a large (around $50\mu m$) blockade radius. For that purpose we are deriving a general expression for the DD interaction strength for an arbitrary Förster resonance transition [4], which will allow us to automatically find the best candidates among the multiple possible Förster resonances in ^{87}Rb.

Following the procedure outlined in [5], the expression for the DD interaction matrix element between the initial and final states results in calculating products of two integrals in the solid angles. Due to the properties of the 3j-symbols [6], most of these integrals have zero values in the case of Förster transitions between states with definite m_j-sublevels, which leaves us with a simple expression for the DD interaction matrix element.

To check the validity of our calculations we compare our results with the magnitute of the dipole-dipole interaction strength obtained for a specific experimental arrangement [7]. In the latter case, the authors base their calculations of the DD interaction strength on the procedure outlined in [8].

Next, we derive a generalized expression for the DD interaction matrix element between initial and final states with arbitrary m_j-sublevels. The generalized expression is further summed over all possible Zeeman components of the initial and final states, which we implement using numerical techniques.

References

[1] T. F. Gallagher, *Rydberg Atoms*, (Cambridge University Press, Cambridge, England, 1994).
[2] M. D. Lukin *et al.*, Phys. Rev. Lett. **87**, 037901 (2001).
[3] D. Tong *et al.*, Phys. Rev. Lett. **93(6)**, 063001 (2004).
[4] T. Förster, Ann. Phys. **437**, 55 (1948).
[5] R. Faoro, Ph.D. Thesis, Université Paris-Saclay, 2015.
[6] R. N. Zare, *Angular Momentum: Understanding Spatial Aspects in Chemistry and Physics*, (John Wiley and Sons, New York, Chichester, Brisbane, Toronto, Singapore, 1988).
[7] A. Gaetan *et al.*, Nature Phys. **5**, 115 (2009).
[8] T. G. Walker and M. Saffman, Phys. Rev. A **787**, 032723 (2008).

[*]Corresponding author: teo@lu.lv

To the list of contents

Single- and multi-layer platform of individually addressable atomic qubits for quantum simulation and quantum computation

M. Schlosser[*1], **D. Ohl de Mello**[1], **D. Schäffner**[1], **T. Preuschoff**[1], **L. Kohfahl**[1], **and G. Birkl**[†1]
1. Institut für Angewandte Physik, TU Darmstadt, Schlossgartenstraße 7, 64289 Darmstadt, Germany

Efficient quantum simulation and quantum information processing requires scalable architectures that guarantee the allocation of large-scale qubit resources. In our work, we focus on the implementation of multi-site geometries based on microoptical systems. This approach allows us to develop flexible, integrable and scalable configurations of multi-site focused beam traps for the storage and manipulation of single-atom qubits and their interactions [1]. The application of microfabricated optical elements, such as arrays of microlenses, as the core enabling technology enhances conventional focused beam trap setups for laser cooled neutral atoms to a scalable architecture [2]. It transfers the extensive versatility of lithographic fabrication techniques to the light fields generated for atom manipulation without introducing additional complexity. The use of microlens arrays allows for the creation of massive multi-site trap arrays with structure sizes approaching the wavelength of the light applied, yet the geometry is decoupled from the trapping laser wavelength and therefore customizable. Large scale quantum computing, quantum simulation and quantum error correction will be accessible [3].

We give an overview on the investigation of ^{85}Rb atoms in two-dimensional arrays of more than 400 individually addressable dipole traps featuring trap sizes and a tunable site-separation in the single micrometer regime. Furthermore, we report on a novel technique for the optical creation of 3D multi-layer configurations of 2D periodic quantum registers based on the Talbot effect and demonstrate the trapping and imaging of individual atoms in integer and fractional Talbot planes [4]. We prepare exactly one atom per site in more than 150 sites of a selected 2D register utilizing light assisted collisions and present single-site resolved addressing in a reconfigurable fashion.

We will discuss progress in introducing Rydberg based interactions and present prospects of our platform for the investigation of many-body physics. Controllable interatomic distances lead to tunable Rydberg-mediated dipolar or van der Waals type interactions. Our work is aiming towards the utilization of Rydberg interactions in the blockade regime for two-qubit gates and in the unblocked regime for the implementation of many-body spin Hamiltonians, e. g. for the study of topological phenomena.

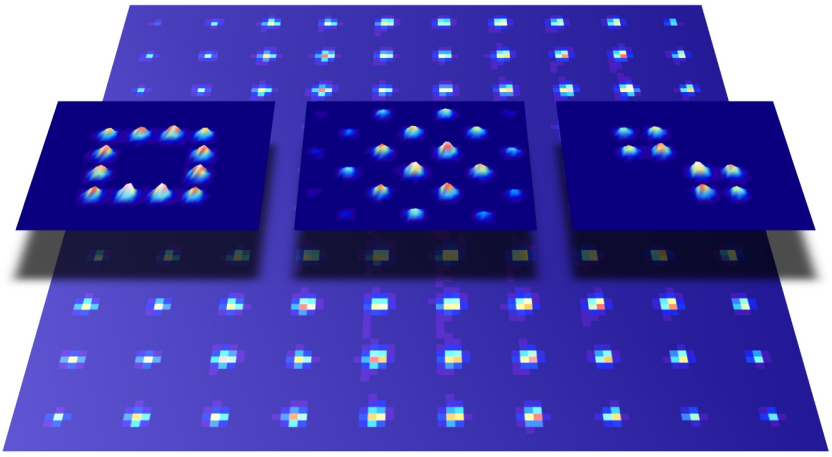

Fig. 1: Fluorescence images of rubidium atoms stored in a reconfigurable two-dimensional architecture of focused beam traps. The underlying configuration (background) reflects the 2D-periodic geometry of the microlens array. The pattern of trapped atoms is subject to external control via a spatial light modulator which is used to selectively illuminate the corresponding microlenses.

References

[1] For an overview see: M. Schlosser, S. Tichelmann, J. Kruse, and G. Birkl, Quant. Inf. Proc. **10**, 907 (2011).
[2] G. Birkl, F. B. J. Buchkremer, R. Dumke, and W. Ertmer, Opt. Commun. **191**, 67 – 81 (2001).
[3] R. Dumke et. al., J. Opt. **18**, 093001 (2016).
[4] M. Schlosser et. al., unpublished.

[*]Corresponding author: malte.schlosser@physik.tu-darmstadt.de
[†]Corresponding author: gerhard.birkl@physik.tu-darmstadt.de

To the list of contents

Ionization spectra of highly Stark shifted rubidium Rydberg states

J. Grimmel[*1], **M. Stecker**[1], **M. Kaiser**[1], **F. Karlewski**[1], **L. Torralbo-Campo**[1], **A. Günther**[1], **J. Fortágh**[†1]
1. Center for Quantum Science, Physikalisches Institut, Eberhard-Karls-Universität Tübingen, Auf der Morgenstelle 14, D-72076 Tübingen, Germany

Stark spectra of alkali Rydberg states above the classical ionization threshold exhibit an intricate energy level structure with strongly varying ionization behaviour, including rapidly ionizing states as well as the extreme of narrow resonances where ionization is almost suppressed. The latter feature is clearly distinct from hydrogen, where the ionization rate of a given state grows exponentially with the applied external electric field [1]. The study of these ionization spectra of non-hydrogenic atoms is therefore of particular interest not only from a fundamental point of view but also for the prospect of improved control over the ionization process in Rydberg gases.

For the theoretical treatment of such ionization processes a complex absorbing potential (CAP) can be employed to create a non-Hermitian Hamiltonian [2], leading to complex eigenvalues of the Hamiltonian which can be used to obtain the energy levels and linewidths, i.e. the ionization rates in the present case. The CAP is added to the original Hamiltonian in the form $-i\eta W(\vec{r})$. The free parameter η is usually determined for every single resonance of the system by a variational method.

In a previous work [3] we have calculated Stark shifted energy levels including the corresponding dipole matrix elements by diagonalization of a matrix representation of the Hamiltonian [4]. Here, we combine these calculations with an adaptive CAP method by choosing a potential that is adjusted to the external electric field. This removes the need to determine the free parameter η for each resonance separately and thereby greatly reduces the computational effort for the numerical calculation. We calculate ionization spectra near the unperturbed $43S_{1/2}$ and $70S_{1/2}$ Rydberg states for electric fields far beyond the classical ionization threshold. Furthermore, we present an experiment in which rubidium atoms in a magneto-optical trap (MOT) are excited to Rydberg states in the presence of an external electric field. When the atoms ionize from these Stark shifted Rydberg states, the ions are guided to a detector by an ion-optical system [5]. We have measured ionization spectra by ramping up the external electric field and scanning the excitation laser frequency near the aforementioned states.

The methods we present here can be used to search for resonances from the ionization spectra, like highly Stark shifted states which have a desirable ionization rate or sensitivity to the external electric field across a certain range. Furthermore, this opens up the possibility to tune a coupling between ionizing and non-ionizing states by the external electric field. This way of tailoring the ionization process is highly useful for the design of sources of cold ions and electrons for microscopy purposes [6]. Moreover, a precise knowledge of these ionization spectra opens new perspectives for experiments incorporating Rydberg atoms near surfaces, where static electric fields arise due to adsorbates [7].

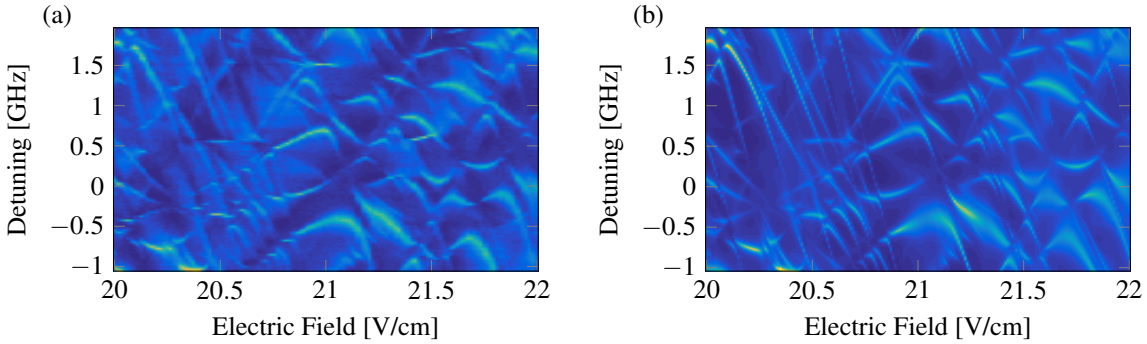

Fig. 1: Ionization Stark spectrum above the classical ionization threshold with a detuning given relative to the unperturbed state $70S_{1/2}$. (a) Detected ion signal from the experiment. (b) Results from the numerical calculations.

References

[1] R. J. Damburg and V. V. Kolosov, J. Phys. B **12**, 2637 (1979).
[2] R. Kosloff and D. Kosloff, J. Comput. Phys. **63**, 363 (1986).
[3] J. Grimmel, M. Mack, F. Karlewski, F. Jessen, M. Reinschmidt, N. Sándor and J. Fortágh, New J. Phys. **17**, 053005 (2015).
[4] M. L. Zimmerman, M. G. Littman, M. M. Kash, and D. Kleppner, Phys. Rev. A 20, 2251 (1979).
[5] M. Stecker, H. Schefzyk, J. Fortágh, and A. Günther, New J. Phys. **19**, 043020 (2017).
[6] D. J. Thompson, D. Murphy, R. W. Speirs, R. M. W. van Bijnen, A. J. McCulloch, R. E. Scholten, and B. M. Sparkes, Phys. Rev. Lett. **117**, 193202 (2016).
[7] H. Hattermann, M. Mack, F. Karlewski, F. Jessen, D. Cano, and J. Fortágh, Phys. Rev. A **86**, 022511 (2012).

[*]Corresponding author: jens.grimmel@uni-tuebingen.de
[†]Corresponding author: fortagh@uni-tuebingen.de

To the list of contents

Efficient preparation of circular states in He with $n \geq 70$ using a modified version of the crossed-fields method

A. Morgan, V. Zhelyazkova, S. D. Hogan
Department of Physics and Astronomy, University College London, Gower Street London WC1E 6BT, United Kingdom

Atomic helium is particularly appealing for use in the development of hybrid approaches to cavity quantum electrodynamics (cavity QED) with Rydberg atoms coupled to superconducting microwave circuits. This is because in cryogenic environments it does not easily adsorb onto surfaces minimising the detrimental effects that can arise with alkali metal adsorbates [1]. The low mass of helium means that when excited to Rydberg states it can be efficiently transported and manipulated using chip-based guides [2], decelerators [3], and traps [4]. Helium can also be laser cooled in the metastable $1s2s\ ^3S_1$ level [5, 6] and the laser radiation required for efficient two-photon excitation to Rydberg states from the $1s2s\ ^3S_1$ level is readily generated using commercially available diode laser systems.

For many hybrid cavity QED experiments it is desirable to use circular Rydberg states (with $\ell = m_\ell = n-1$, where ℓ and $|m_\ell|$ are the orbital angular momentum and azimuthal quantum numbers, respectively). This is because, circular states exhibit no first-order Stark shift, resulting in low sensitivity to stray electric fields and hence longer coherence times. Due to the selection rules for electric dipole transitions a system consisting of two consecutive circular states (where $\Delta n = 1$) represents a quasi two-level system, in that the only allowed transitions out of the two-level system is from the lower energy state, and these are weak. This leads to long radiative lifetimes (e.g. 46 ms for the $|n = 55, \ell = 54, m_\ell = +54\rangle$ state, scaling with n^5). At large values of n, $\Delta n = +1$, $\Delta m_\ell = +1$, circular-to-circular transitions are in the microwave domain, with transition frequencies $\nu \leq 40$ GHz for $n \geq 50$, and $\nu \leq 20$ GHz for $n \geq 69$. Lower transition frequencies are particularly desirable for hybrid cavity QED experiments as they impose fewer restrictions on the microwave circuitry, allow for longer microwave resonators which leads to longer atom-resonator interaction times, and permit interfacing with superconducting qubits which typically have transition frequencies in the 5-10 GHz range [7].

Efficient preparation of $n = 55$ circular states has recently been demonstrated using the crossed-fields method [8]. However, for larger values of n the efficiency of this method is limited by effects of electric field noise at the time of laser photo-excitation. Here, we present a modified version of the crossed-fields method which overcomes this problem. To prepare the $|n, n-1, +(n-1)\rangle$ circular state, this first involves exciting the atoms from the $1s2s\ ^3S_1$ level to the $1s(n+2)s\ ^3S_1$ Rydberg state in zero electric field. An electric field is then slowly turned on causing the atoms to adiabatically evolve through the first avoided crossing with the Stark states of the $n+1$ manifold, and switching it from a high-field-seeking to a low-field-seeking state. A resonant microwave pulse then transfers the population in this state to the outermost, low-field-seeking Stark state of the n manifold which has a similar static electric dipole moment. Finally, the electric field is adiabatically switched off causing the state to evolve into the n circular state in the perpendicular magnetic field. The circular states are then detected by ramped electric field ionisation and probed using microwave spectroscopy.

References

[1] H. Hattermann, M. Mack, F. Karlewski, F. Jessen, D. Cano, and J. Fortágh. Phys. Rev. A **86**, 022511 (2012)
[2] P. Lancuba and S. D. Hogan. Phys. Rev. A **88**, 043427 (2013)
[3] P. Lancuba and S. D. Hogan. Phys. Rev. A **90**, 053420 (2014)
[4] P. Lancuba and S. D. Hogan. J. Phys. B: At., Mol., Opt. Phys. **49**, 074006 (2016)
[5] W Rooijakkers, W Hogervorst, W Vassen. Opt. Commun. **123**, 321 (1996).
[6] R. Chang, A. L. Hoendervanger, Q. Bouton, Y. Fang, T. Klafka, K. Audo, A. Aspect, C. I. Westbrook, and D. Clément. Phys. Rev. A **90**, 063407 (2014)
[7] Ze-Liang Xiang, Sahel Ashhab, J. Q. You, and Franco Nori. Rev. Mod. Phys. **85**, 623 (2013)
[8] V. Zhelyazkova and S. D. Hogan. Phys. Rev. A **94**, 023415 (2016)

To the list of contents

A Rydberg-atom beam splitter

J. Palmer[*1] **and S. D. Hogan**[1]
1. Department of Physics and Astronomy, University College London, Gower Street, London WC1E 6BT, U.K.

The very large static electric dipole moments of high Rydberg states of atoms and molecules ($>$ 10000 D for states with principle quantum numbers $n > 51$) can be utilized to control the motion of gas-phase samples using inhomogeneous electric fields [1]. This has led to the development of sets of chip-based devices to guide [2][3], decelerate [3][4][5] and trap [4][5][7] Rydberg atoms and molecules. To further realise a complete Rydberg-laboratory-on-a-chip the development of Rydberg-atom beam splitters with similar electrode geometries is particularly valuable. Such devices will be useful in a wide range of experiments including (i) splitting Rydberg atom beams to distribute atoms among arrays of superconducting resonators, (ii) the development of Rydberg-atom interferometers, and (iii) using one part of a split beam as an intensity reference in collision and spectroscopy measurements.

The design and experimental implementation of a Rydberg-atom beam splitter will be presented. In this work beams of helium Rydberg atoms were split into pairs of components using static electric fields and separated by up to 15.6 mm. The operation of the beam splitter was characterised by position sensitive electric field ionisation of the Rydberg atoms. The interpretation of the experimental data was aided by comparison with the results of numerical particle trajectory simulations.

References

[1] S. D. Hogan, EJP Techniques and Inst. **3**, 1 (2016).
[2] P. Lancuba and S. D. Hogan, Phys. Rev. A **88**, 043427 (2013).
[3] P. Allmendinger, J. Deiglmayr, J. A. Agner, H. Schmutz, and F. Merkt, Phys. Rev. A **90**, 043403 (2014).
[4] P. Lancuba and S. D. Hogan, Phys. Rev. A **90**, 053420 (2014).
[5] S. D. Hogan, P. Allmendinger, H. Saßmannshausen, H. Schmutz, and F. Merkt, Phys. Rev. Lett. **108**, 063008 (2012).
[6] P. Allmendinger, J.A. Agner, H. Schmutz, and F. Merkt, (2013), Phys. Rev. A., **88**, 043433 (2013).
[7] P. Lancuba and S. D. Hogan, J. Phys. B: At. Mol. Opt. Phys. **49**, 074006 (2016) .

*Corresponding author: ucapjep@ucl.ac.uk

To the list of contents

Rydberg-mediated long-range interactions between stored optical photons

Hannes Busche[*1], **Paul Huillery**[1], **Simon W. Ball**[1], **Teodora Ilieva**[1], **Nicholas L. R. Spong**[1], **Matthew P. A. Jones**[1], **and Charles S. Adams**[1]

1. Joint Quantum Centre (JQC) Durham–Newcastle, Department of Physics, Durham University South Road, Durham DH1 3LE, UK

Rydberg non-linear optics [1] has emerged as a viable approach to induce strong effective photon-photon interactions, e.g. for applications in optical quantum information processing. Using electromagnetically induced transparency and photon storage, the μm-ranged dipolar interactions between collective Rydberg excitations, can be mapped onto photons. So far, experiments focused on observing Rydberg-mediated photon interactions between overlapping modes within a single cold atomic medium [1]. Recently however, we have demonstrated an effective 'contactless' interaction between photons stored as collective Rydberg excitations in two spatially separate atomic ensembles and propagating in non-overlapping modes [2].

During storage, van-der-Waals interactions between the excitations alter the phase relation between the individual atoms that contribute to the collective states. As the phase shifts are not spatially uniform, retrieval of the photons in their original modes is suppressed. The effect of the interactions can be observed as an anti-correlation in the statistics of the light retrieved in the original modes. We observe how the interaction varies while changing the distance between the clouds (see Fig. 1), the Rydberg state employed for storage, and the interaction time.

The stored photons can be coherently controlled using an additional microwave field which drives transitions between Rydberg states. Interfacing with microwaves allows to drive high-fidelity Rabi oscillations while the photons are stored and to shape the retrieved pulse [3]. The degrees of freedom provided by contactless, long-range effective interactions between stored photons combined with microwave control of their state and phase may lead towards a Rydberg-based all-optical quantum gate [4] and applications in quantum simulation.

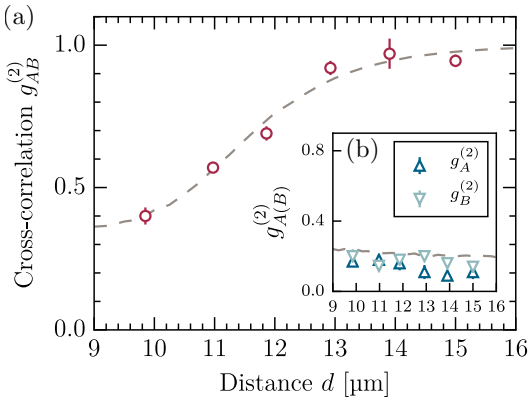

Fig. 1: (a) The effect of 'contactless', Rydberg-mediated photon interactions can be observed as an anti-correlation ($g^{(2)}_{AB} < 1$) between channels A and B in the retrieval. It emerges as the distance between the individual storage media and optical modes is reduced. (b) Rydberg-mediated interactions also lead to the retrieval of highly non-classical light in the individual channels as indicated by the suppression of the single channel correlation functions $g^2_{A(B)} < 1$. The results are in good agreement with a theoretical phase-shift model (grey lines).

References

[1] O. Firstenberg, C. S. Adams, and S. Hofferberth, J. Phys. B: At. Mol. Opt. Phys. **49**, 15 (2016).
[2] H. Busche, P. Huillery, S. W. Ball, T. Ilieva, M. P. A. Jones, and C. S. Adams, Nat. Phys. advance online publication (2017).
[3] S. W. Ball *et al.*, in preparation.
[4] D. Paredes-Barato and C. S. Adams, Phys. Rev. Lett. **112**, 040501 (2014).

*Corresponding author: hannes.busche@durham.ac.uk

To the list of contents

The coupled-channel deperturbation analysis of the mixed $(1 \sim 2)^1\Pi$, $1^3\Pi$, $2^1\Sigma^+$ and $2^3\Sigma^+$ states of KRb molecule

Sergei V. Kozlov[*1], **E. A. Pazyuk**[1], **A. V. Stolyarov**[1]
1. Chemistry Department, Moscow State University, Moscow 119991, Russia

The stimulated Raman adiabatic passage (STIRAP) [1] is widely used to create alkali diatomic molecules in their absolute ground state. This two step optical process involves intermediate excited rovibronic states which should be singlet-triplet mixed to provide an appropriate efficiency of nominally forbidden singlet-triplet transitions from the uppermost levels of both singlet $X^1\Sigma^+$ and triplet $a^3\Sigma^+$ ground states [1]. In the case of alkali diatomics containing heavy atoms (such as Rb or Cs) spin-orbit coupling indeed leads to pronounced mutual perturbation of low-lying excited states. Moreover, due to the vicinity of atomic energies of the first excited 4^2P(K) and 5^2P(Rb) states electronic the structure of the KRb molecule is additionally perturbed by a strong radial coupling effect between states possessing the same spatial and spin symmetry [2].

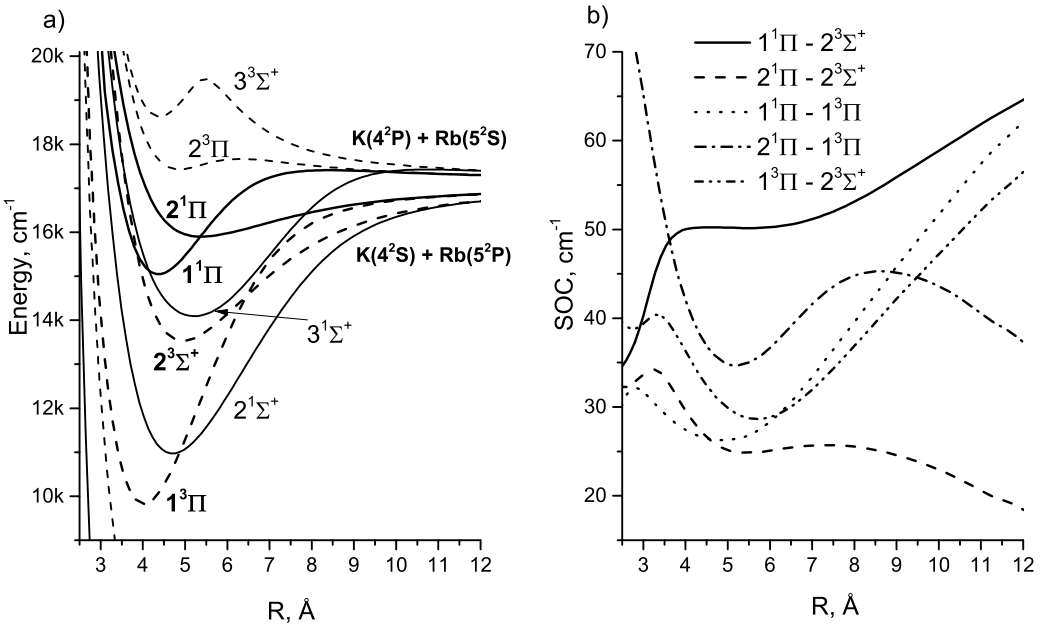

Fig. 1: a) Potential energy curves of the electronic states converging to the second and third dissociation limits; b) Spin-orbit coupling (SOC) functions between the electronic states converging to the second and third dissociation limits [2].

Recently, we performed a local deperturbation analysis of the experimental rovibronic term values mainly belonging to the $(1 \sim 2)^1\Pi$ and $2^1\Sigma^+ \sim 1^3\Pi$ complex of KRb [2,3]. In the present, work we significantly expand the examined energy manifold by involving the close-lying $(1,2)^1\Pi$, $1^3\Pi$, $2^1\Sigma^+$ and $2^3\Sigma^+$ states in the explicit coupled-channel (CC) deperturbation treatment simultaneously. Potential energy curves for isolated states of the $(1 \sim 2)^1\Pi$ complex and relevant spin-orbit coupling (SOC) matrix elements were presented in a diabatic basis [2] to simplify the numerical solution of the CC equations. The corresponding non-adiabatic eigenvalues and multi-channel eigenfunctions were found using a finite-difference scheme combined with a Richrdson extrapolation to the zeroth step. Analytical mapping was applied to improve the efficiency of the solution [4]. Using predicted rovibronic energies, as well as radiative lifetimes and linewidths, calculated from high level *ab initio* transition dipole moments, we further reanalyzed transition probabilities of the optical cycle $a^3\Sigma^+(v, J=0) \rightarrow [1^1\Pi \sim 2^1\Pi \sim 2^1\Sigma^+ \sim 2^3\Sigma^+ \sim 1^3\Pi](v^*, J=1) \rightarrow X^1\Sigma^+(v=0, J=0)$ for a wide range of the vibronic excitations.

The work was partly supported by the RFBR grant N 16-03-00529-a.

References

[1] D. Borsalino, B. Londoño-Florèz, R. Vexiau, O. Dulieu, N. Bouloufa-Maafa, and E. Luc-Koenig, Phys. Rev. A, **90**, 033413 (2014).
[2] S.V. Kozlov, E.A. Pazyuk, and A.V. Stolyarov, Phys. Rev. A **94**, 042510 (2016).
[3] K. Alps, A. Kruzins, M. Tamanis, R. Ferber, E.A. Pazyuk, and A.V. Stolyarov, J. Chem. Phys. **144**, 144310 (2016).
[4] V.V. Meshkov, A.V. Stolyarov, and R.J. Le Roy Phys. Rev. A **78**, 052510 (2008).

*Corresponding author: sevlakoz@phys.chem.msu.ru

To the list of contents

A cold atoms platform for testing the computational power of discord

K. Krzyzanowska[*1], **R. Romain**[1], **M. Copley-May**[1], **A. Odufowora**[1], **C. MacCormick**[1], **S. Bergamini**[†1],
1. School of Physical Sciences, Faculty of Science, Technology, Engineering and Mathematics (STEM), The Open University Walton Hall, Milton Keynes MK7 6AA, UK

Quantum computing models are generally based on the manipulation of qubits in highly pure states and the exploitation of entanglement to implement logic gates. Even if these conditions are satisfied for few qubits, scalability remains a challenge and the computational power is limited by the system's architecture. Deterministic Quantum Computing with One Clean Qubit (DQC1) [1] is a novel class of algorithms where only one control qubit is required to be in an almost pure state, while the target ensemble of qubits is initially prepared in a mixed state. In this case, interactions between atoms enable nonclassical correlations other than entanglement, namely discord. In [2] it was proposed that discord would provide sufficient quantum enhancement to solve a particular class of classically intractable computations.

Our project is the first attempt to use atoms to demonstrate the scalability of the DQC1 protocol, since the first demonstrations of DQC1 concept using 2 photonic qubits [3], and four NMR-based qubits using carbon nuclei [4]. Cold atoms are a natural platform to perform DQC1 and scale it up, as it is possible to load micrometer-size dipole traps with a controllable number of atoms, ranging from one to many, by varying the trap's parameters and loading rate [5-7]. We aim to demonstrate the DQC1 protocol for just a few atoms in the target ensemble initially to verify the model's prediction from [8], using a scheme in which the information processing is realized through the CNOT gate based on Rydberg blockade [9]. The implementation of this protocol imposes very stringent requirements on the dipole trap: to perform CNOT gate with high fidelity it is required that a full Rydberg blockade is operating throughout the extent of the ensemble. Moreover, the loss rate of the atoms needs to be kept to a minimum, as the loss of one atom during the processing or readout stages would result in loss of information.

In this work we report on the progress of the development of a cold atoms platform to demonstrate DQC1. In our experimental setup a vapour of ^{87}Rb is first trapped in a MOT and cooled to sub-Doppler temperatures. Atoms are subsequently trapped in two adjacent dipole traps (Fig.1 (left)), to encode the qubits in the hyperfine structure of the ground ^{87}Rb state. Our experimental setup is based on using a high-N.A. lens to achieve a sub-micron trapping potential and simultaneously observe trapped atoms with a micrometre resolution (Fig.1 (center)). The trap lifetime is limited by the background collisions, therefore vacuum is maintained on the level of 10^{-10} Torr. Fig.1(right) shows the fluorescence from about 50 atoms held in the single dipole trap, characterized by a 2.5s lifetime and 5μm waist.

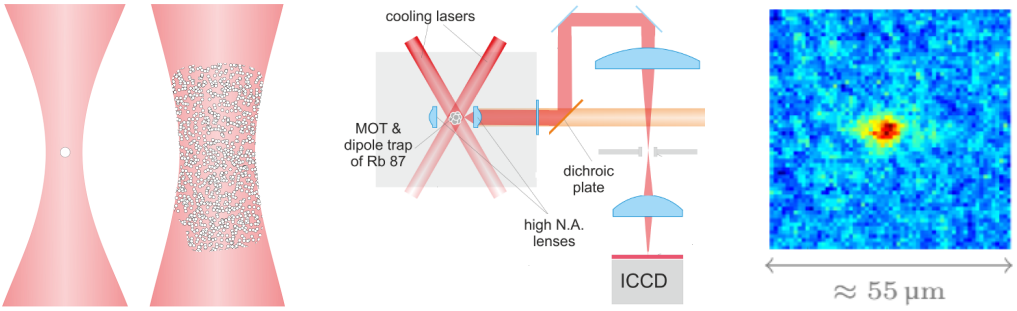

Fig. 1: (left) Two adjacent dipole traps, *control* and *target ensemble*, filled with a single and many atoms respectively. (center) Implementation of dipole trap with ^{87}Rb. A strong laser beam acts on the high N.A. lens and is focused in the center of the MOT. Fluorescence light is collected by the same lens and directed onto the ICCD. (right) The fluorescence image of 48 ± 6 ^{87}Rb atoms within dipole trap.

References

[1] A. Datta, S. T. Flammia, and C. M. Caves, Phys. Rev. A **72**, 042316 (2005)
[2] E. Knill and R. Laflamme, Phys. Rev. Lett. **81**, 5672 (1998).
[3] B. P. Lanyon, M. Barbieri, M.P. Almeida, and A. G. White, Phys. Rev. Lett. **101**, 1-4 (2008).
[4] G. Passante *et al*., Phys. Rev. Lett. **103**, 250501 (2009)
[5] Y. R. P. Sortais *et al*., Phys. Rev. A **75** 1-7 (2007)
[6] T. Grünzweig, A. Hilliard, M. McGovern and M. F. Andersen, Nature Physics, **6**, 951 (2010)
[7] N. Schlosser, G. Reymond, I. Protosenko and P. Grangier, Nature, **411**, 6841 (2001)
[8] C.W. Mansell, S. Bergamini, New J. Phys. **16** (2014)
[9] M.Muller, I. Lesanovsky, H.Weimer, H. P. Buchler, and P. Zoller, Phys. Rev. Lett. **102**, 170502 (2009)

[*]Corresponding author: katarzyna.krzyzanowska@open.ac.uk, katarzyna.a.krzyzanowska@gmail.com
[†]Corresponding author: silvia.bergamini@open.ac.uk

To the list of contents

Towards measuring the absolute frequency of Rydberg levels in ^{39}K.

Prosenjit Majumder[*1] **and Simon Cornish**[1]
1. Joint Quantum Centre (JQC) Durham–Newcastle, Department of Physics, Durham University
South Road, Durham DH1 3LE, UK

Since last few years atoms and molecules have been studied extensively for precision measurements for fundamental physics, such as exact measurement of Rydberg transition frequency [1], time, length, mass and the gravitation constant measurements [2-5]. Due to large dipole moments Rydberg atoms are attracting a large field of research, as their quantum states can be prepare and manipulate with large precision and can be controlled by electromagnetic fields. Due to large polarizability and dipole moments Rydberg atoms are responsive to the static and dynamic electric field with levels shifts and therefore sensitive to microscopic as we as macroscopic objective. For precision measurements of such interactions and accurate quantum state control is beneficial to know the unperturbed Rydberg energy levels that we trying to quantify in this present work with ^{39}K atoms.

In our work we are using $4S_{1/2} \rightarrow 5P_{1/2}$ as a probe to detect the EIT signal, which is locked using modulation transfer spectroscopy (MTS) technique [6]. And we use another coupling laser for $5P_{1/2} \rightarrow nS_{1/2}$ to populate the desired Rydberg levels and detect an electromagnetically induced transparency (EIT) signal. The signal is generated by a velocity selection scheme [7-9], which mitigates superposition of EIT by Doppler shifts for coupling wavelengths larger than the probe wavelength. In this scenario, a strong optical pumping beam, which is counter-propagating to the EIT probe beam, transfers atoms between hyperfine states. The transition frequencies between $5P_{1/2}$ and $nS_{1/2}$ states in ^{39}K are obtained via EIT spectroscopy in a 10 cm heated ^{39}K vapour cell. After calibration of the Rydberg transition $4S_{1/2} \rightarrow nS_{1/2}$, via the use of a wavelength meter and a frequency comb, we are able to measure the absolute frequency of Rydberg levels [1] for ^{39}K.

Currently, we measured the Doppler and Sub-Doppler features for the $4S_{1/2} \rightarrow 5P_{1/2}$ transition. After I identifying the atomic transitions we able to lock our laser at a specific atomic transition using MTS technique. Next step of our experiment is introduce coupling laser and perform the EIT spectroscopy.

References

[1] Mack, M., Karlewski, F., Hattermann, H., Höckh, S., Jessen, F., Cano, D., Fortágh, J. Physical Review A, **83(5)**, 052515 (2011).
[2] A. D. Ludlow, M. M. Boyd, J. Ye, E. Peik, and P. O. Schmidt, Rev. Mod. Phys. **87**, 637 (2015).
[3] A. D. Cronin, J. Schmiedmayer, and D. E. Pritchard, Rev. Mod. Phys **81**, 1051 (2009).
[4] G. Rosi, F. Sorrentino, L. Cacciapuoti, M. Prevedelli, and G. M. Tino, Nature **510**, 518 (2014).
[5] D. Weiss, B. Young, and S. Chu, Phys. Rev. Lett. **70**, 2706 (2013).
[6] McCarron, D. J., S. A. King, and S. L. Cornish, Meas. sci. and tech. **19.10**, 105601 (2010).
[7] A. K. Mohapatra, T. R. Jackson, and C. S. Adams, Phys. Rev. Lett. **98**, 113003 (2007).
[8] A. Urvoy, C. Carr, R. Ritter, C. Adams, K. Weatherill, and R. Löw, J. Phys. B **46**, 245001 (2013).
[9] Xu, Wenchao, and Brian DeMarco., Physical Review A **93.1**, 011801. (2016).

*Corresponding author: prosenjit.majumder@durham.ac.uk

To the list of contents

Creating Feshbach resonances for ultracold molecule formation with radiofrequency fields

Daniel J. Owens[*1], **Ting Xie, Jeremy M. Hutson**[†1]
1. Joint Quantum Centre (JQC) Durham-Newcastle, Department of Chemistry, Durham University
South Road, Durham DH1 3LE, UK

Polar molecules formed from ultracold atoms are opening up new possibilities for quantum-controlled chemistry [1], precision measurement [2-4], quantum computation [5], quantum phase transitions [6] and quantum simulation [7]. Molecules are first formed by magnetoassociation, in which atom pairs are converted into weakly bound molecules by ramping a magnetic field across a magnetically tunable Feshbach resonance. The resulting "Feshbach molecules" are then transferred to the polar ground state by stimulated Raman adiabatic passage (STIRAP).

A major problem in this field is that the magnetoassociation step is possible only if there is a Feshbach resonance of suitable width at a magnetic field where there is a lucky combination of intraspecies and interspecies scattering lengths. Ideally, all three scattering lengths have moderate positive values to allow cooling, condensate formation and mixing of the two atomic clouds. This is the so-called *one-field problem*, because a single field must be chosen to satisfy several different criteria, and such a field may not (often does not) exist.

Radiofrequency (RF) fields can be used to produce new Feshbach resonances that offer additional possibilities for magnetoassociation. In particular, they may be used to produce resonances at magnetic fields where the scattering lengths have desired properties. Formally similar resonances have been considered in homonuclear systems [8-11], and molecules have been formed by direct RF association [12-13]. We propose that rf-induced resonances may provide a solution to the one-field problem in heteronuclear systems.

We show that RF radiation may be used to create Feshbach resonances in ultra-cold gases of alkali-metal atoms at desired magnetic fields that are convenient for atomic cooling and degeneracy. For the case of ^{39}K+^{133}Cs, where there are no RF-free resonances in regions where Cs may be cooled to degeneracy, we show that a resonance may be created near 21 G with 69.2 MHz RF radiation. This resonance is almost lossless with circularly polarized RF, and the molecules created are long-lived even with plane-polarized RF.

References

[1] R. V. Krems, Phys. Chem. Chem. Phys., **10**, 4079 (2008)
[2] V. V. Flambaum and M. G. Kozlov, Phys. Rev. Lett., **99**, 150801 (2007)
[3] J. J. Hudson *et al.*, Nature London, **473**, 493 (2011)
[4] J Baron *et al.*, Science, **343**, 269 (2014)
[5] D. DeMille, Phys. Rev. Lett. **88**, 067901 (2002)
[6] M. L. Wall and L. D. Carr, Phys. Rev. A **82**, 013611 (2010)
[7] A. Micheli, G. K. Brennen, and P. Zoller, Nature Phys. 2, 341 (2006).
[8] T. V. Tscherbul *et al.*, Phys. Rev. A 81, 050701(R) (2010)
[9] T. M. Hanna, E. Tiesinga, and P. S. Julienne, New J. Phys. 12, 083031 (2010).
[10] D. H. Smith, Phys. Rev. Lett. 115, 193002 (2015).
[11] Y. Ding, J. P. D'Incao, and C. H. Greene, Phys. Rev. A, **95**, 022709 (2017)
[12] S. T. Thompson, E. Hodby, and C. E. Wieman, Phys. Rev. Lett. 95, 190404 (2005)
[13] J. J. Zirbel *et al.* Phys. Rev. A 78, 013416 (2008)

[*]Corresponding author: d.j.owens@durham.ac.uk
[†]Corresponding author: j.m.hutson@durham.ac.uk

To the list of contents

Inelastic losses in radiofrequency-dressed traps for ultracold atoms

Daniel J. Owens[*1] **and Jeremy M. Hutson**[†1]
1. Joint Quantum Centre (JQC) Durham-Newcastle, Department of Chemistry, Durham University
South Road, Durham DH1 3LE, UK

Radiofrequency-dressed traps [1-2] have been widely used [3] to confine ultracold atoms in complex geometries, including shells [4] and rings [5]. These geometries are valuable in many fields including atom interferometry [6] and the study of low-dimensional quantum systems [7]. The atoms are trapped using a combination of magnetic and radiofrequency (RF) fields, and are confined in an adiabatic potential obtained by diagonalizing a simple Hamiltonian in a basis set of rf-dressed atomic states.

Most experimental work with RF-dressed traps to date has used ^{87}Rb atoms. However, there is considerable interest in extending this to other atomic species. We use coupled-channel calculations to explore the rates of RF-induced inelastic collisions theoretically. We calculate the rates of losses due to RF-induced inelastic collisions for ultracold alkali-metal atoms in RF-dressed traps. By contrast to spin-relaxation collisions, RF-induced inelastic collisions are not suppressed by centrifugal barriers in the outgoing channel. We compare the rates of RF-induced collisions with those of spin-relaxation collisions. We find that ^{87}Rb is a special case, where RF-induced losses are slow compared to spin-relaxation losses. For most other alkali-metal pairs, RF-induced losses are expected to be much faster and may dominate.

References

[1] O. Zobay and B. M. Garraway, Phys. Rev. Lett., **86**, 1195 (2001)
[2] O. Zobay and B. M. Garraway, Phys. Rev. A, **69**, 23605 (2004)
[3] B. M. Garraway and H. Perrin, J. Phys. B, **49**, 172001 (2016)
[4] Y. Colombe, *et al.*, Europhys. Lett., **67**, 593 (2004)
[5] W. H. Heathcote *et al.*, New J. Phys., **10**, 043012 (2008)
[6] T. Schumm *et al.* Nature Physics, **1**, 57 (2005)
[7] N. Lundblad *et al.*, Phys. Rev. Lett., **100**, 150401 (2008)

[*]Corresponding author: d.j.owens@durham.ac.uk
[†]Corresponding author: j.m.hutson@durham.ac.uk

To the list of contents

Superstatistical energy distributions of an ion interacting with a neutral buffer gas

I. Rouse[*1], **S. Willitsch**[1],
1. Department of Physical Chemistry, University of Basel, 4056 Basel, Switzerland

An ion held in a radiofrequency (RF) trap interacting with an ultracold buffer gas allows for the study of two- and many-body physics in a regime of intermediate interaction strengths, notably including collisions and chemical reactions at very low energy [1]. The cross-section for these processes in this regime typically exhibits a complex dependency on the collision energy, requiring a thorough characterisation of the energy of the ion to make comparisons between theoretical and experimental results. This is complicated by the fact that during elastic ion-atom collisions energy is transferred between the thermal (secular) motion of the ion and the RF field, leading to multiplicative fluctuations of the ion's secular energy [2,3]. The resulting secular energy distribution exhibits a power-law tail and has frequently been described using Tsallis statistics, but thus far this has been a purely empirical choice [2,4].

Recently, we have used the formalism of superstatistics to show that a simplified model of the collision process leads to Tsallis statistics for the secular energy of the ion [5,6]. Through numerical simulations we have confirmed that the model correctly predicts the power-law exponent as a function of the ion-atom mass ratio and the trap parameters, paving the way for experimental control of the energy distribution. Furthermore, it is possible to map a superstatistical system onto a canonical ensemble at a fixed temperature, and hence our method provides a general framework to calculate the statistical mechanics and thermodynamic functions of an ion interacting with a buffer gas [7].

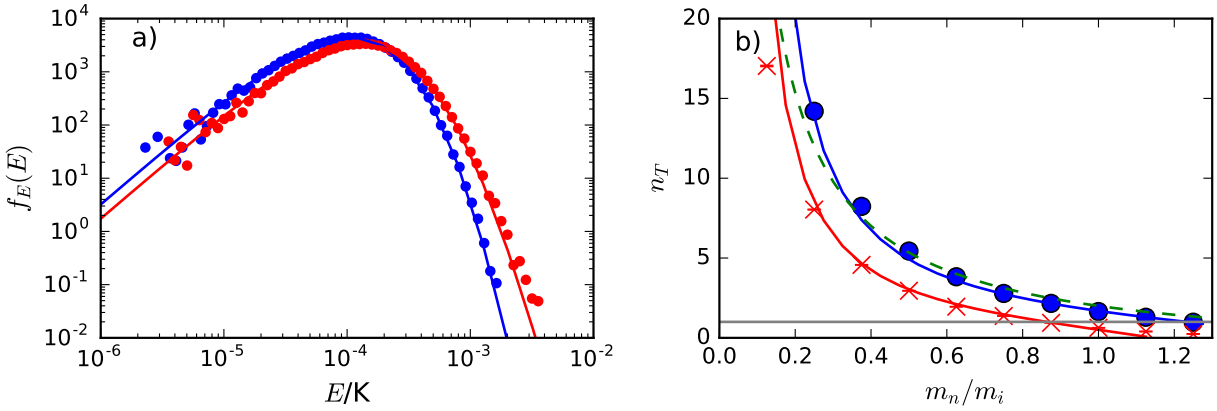

Fig. 1: a) Energy distribution of an ion in a radiofrequency ion trap interacting with a buffer gas from simulations (points) and the predicted distribution (solid lines) for Mathieu parameters $q = 0.1$ (blue) and $q = 0.5$ (red) at a mass ratio $m_n/m_i = 0.25$. b) The power-law exponent n_T over a range of mass ratios for Mathieu parameters $q = 0.1$ (blue) and $q = 0.5$ (red) found from simulations and compared to the predicted values. The green dashed line indicates the approximate exponent for $q < 0.4$ from [3].

We present an overview of the model and a comparison of the predicted power-law exponent to the results of numerical simulations, confirming the ability to fine-tune the energy distribution of the ion by altering experimental parameters. We also discuss the extensions to the model necessary to take into account an inhomogenous buffer gas and the effects of excess ion micromotion induced by stray electric fields to provide a comprehensive description of the dynamics of an ion in a hybrid ion-atom system [4,8].

References

[1] A. Härter and J. H. Denschlag, Contemp. Phys., **55** , 33, (2014).
[2] R. G. DeVoe, Phys. Rev. Lett. **102**, 063001 (2009).
[3] K. Chen, S. T. Sullivan, and E. R. Hudson, Phys. Rev. Lett. **112**, 143009 (2014).
[4] Z. Meir et al., Phys. Rev. Lett. **117**, 243401 (2016).
[5] C. Beck and E. Cohen, Physica (Amsterdam) **322A**, 267, (2003).
[6] I. Rouse and S. Willitsch, Phys. Rev. Lett., **118** 143401 (2017).
[7] C. Beck, Phil. Trans. R. Soc. A., **369**, 453 (2011).
[8] B. Höltkemeier et al., Phys. Rev. A **94**, 062703 (2016).

*Corresponding author: ian.rouse@unibas.ch

To the list of contents

An Optical Quasicrystal for Ultracold Atoms

Matteo Sbroscia[*1], **Konrad Viebahn**[1], **Edward Carter**[1], **and Ulrich Schneider**[1]
1. Cavendish Laboratory, AMOP group, J. J. Thomson Avenue, Cambridge CB3 0HE, UK

Ultracold atoms in optical lattices are a powerful tool to investigate many-body physics of interacting particles in periodic potentials. The main objective of our experiment is to extend this level of control to quasiperiodic potentials, by realising an optical quasicrystal. Quasicrystals are long-range ordered structures that display rotational symmetries forbidden for periodic crystals, resulting in a potential landscape described by an aperiodic arrangement of sites with more than one unit cell, similar to the well-known Penrose tiling. They were first observed in the 1980s by Dan Shechtman using diffraction experiments, where quasicrystals would still display sharp Bragg peaks, because of their long-range order, though in dense sets, tapering off into the continuum expected for an amorphous solid. This places them in an interesting middle ground between periodic and disordered systems and highlights their potential for novel many-body physics. For example, we expect novel transport phenomena, likely related to many-body localisation, as well as an intriguing link to higher-dimensional physics: a 2D quasicrystal can be derived from a periodic 4D "parent" crystal using the cut-and-project method, inheriting the edge states and topological properties of the parent. These systems might furthermore contain interesting novel phases at strong interactions. Our apparatus is almost completed; we have obtained a ^{87}Rb BEC at the end of April, and will likely start lattice experiment in the Summer.

*Corresponding author: ms2289@cam.ac.uk;http://www.manybody.phy.cam.ac.uk/

To the list of contents

Molecular beam brightening by shock-wave suppression

Yair Segev*, **N. Bibelnik, N. Akerman, Y. Shagam, A. Luski, M. Karpov, J. Narevicius and E. Narevicius**†
1. Department of Chemical Physics, Weizmann Institute of Science, Rehovot 7610001, Israel.

Supersonic beams are a prevalent source of cold atoms and molecules used in a wide variety of experiments. The triumph of this method emanates from the high densities produced in relation to other methods; however, beam densities have long been limited by interference with shock waves reflected from collimating surfaces. We show experimentally that this shock interaction can be reduced or even eliminated by cryocooling the interacting surface. An increase of nearly an order of magnitude in beam density was measured at the lowest surface temperature, with no further fundamental limitation reached. Visualization of the shock waves and reproduction with dilute gas simulations indicate that the suppression of the shock structure is caused by lowering the momentum flux of reflected particles. We observe that the scaling of beam density with source pressure is recovered, paving the way to order-of-magnitude brighter, cold molecular beams [1].

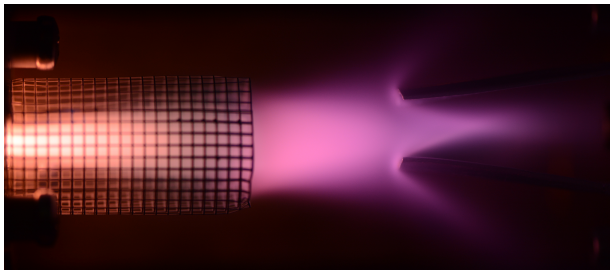

Fig. 1: Shock wave interference in a room-temperature skimmer, visualized using plasma discharge.

References

[1] Segev, Yair, et al. "Molecular beam brightening by shock-wave suppression." *Science Advances* 3.3 (2017): e1602258.

*Corresponding author: yair.segev@weizmann.ac.il
†Corresponding author: edn@weizmann.ac.il

To the list of contents

Many–body localization due to random interactions

Piotr Sierant *[1], **Dominique Delande**[3], **Jakub Zakrzewski**[1,2]
1. Marian Smoluchowski Institute of Physics Łojasiewicza 11, 30-348, Cracow, Poland
2. Mark Kac Complex Systems Research Center, Cracow, Poland
3. Laboratoire Kastler Brossel, UPMC-Sorbonne Universités, CNRS, ENS-PSL Research University, Collège de France; 4 Place Jussieu, 75005 Paris, France

Many-body localized (MBL) systems, i.e. systems that do not thermally equilibrate under their own dynamics but rather evolve in such a way that the memory about local features of the initial state is preserved, have recently received a lot of attention. MBL has been observed in a system of interacting fermions in one-dimensional quasi-random optical lattice [1]. We inquire whether a system, which posesses a fully delocalized eigenstates in absence of interactions can exhibit MBL.

A system of ultracold bosons in one-dimensional optical lattice with disordered on–site interparticle interactions is numerically investigated. Examination of level spacing distributions at various interaction strength amplitudes U (Fig. 1.) reveals a transition from statistics for Gaussian Orthogonal Ensemble of matrices characteristic for ergodic system to Poissonian statistics for large U which is a feature of localized system. Time evolution of initially prepared density–wave states explicitly shows that the system is non–ergodic: imbalance between occupations of even and odd sites of the lattice acquires a non–zero stationary value (Fig. 2.) in contrast to thermalizing systems for which one expects total decay of the initial density profile.

The two properties allow us to conclude that MBL occurs in the system as one increases the interactions [2]. The observed localization is an inherent effect of the interactions and thus a genuine many-body effect. Further calculations provide information about effects of Griffiths regions on MBL transition and mobility edge in the system.

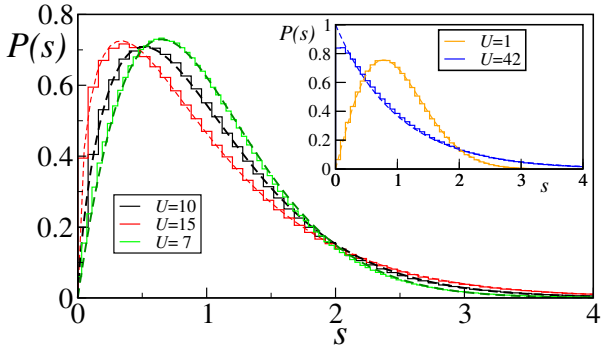

Fig. 1: Level spacing distributions during the transition between ergodic and many–body localized regimes. Limiting distributions are displayed in the inset, whereas the crossover region for intermediate values of interactions strength amplitude is shown in the main part of the figure.

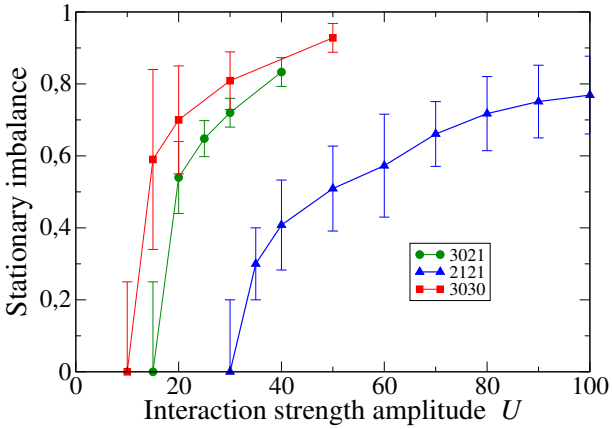

Fig. 2: Stationary value of difference between populations of even and odd lattice sites obtained during time evolution of various initial density wave states. Ergodicity breaking for different initial states at different U suggests presence of mobility edge in the system.

References

[1] M. Schreiber, S. S. Hodgman, P. Bordia, H. P. Lüschen, M. H. Fischer, R. Vosk, E. Altman, U. Schneider, and I. Bloch, Science **349**, 7432 (2015).
[2] P. Sierant, D. Delande, J. Zakrzewski, Phys. Rev. A **95**, 021601 (2017).

*Corresponding author: sierant.piotr@gmail.com

To the list of contents

Observation of Fano-Feshbach resonances in ultracold gas of thulium

Vladislav Tsyganok[*1,2], **E.T. Davletov**[1,2], **I.S. Cojocaru**[1,2,3] **and A.V. Akimov**[1,3,4]
1. Russian Quantum Center,
Business center "Ural", 100A Novaya str., Skolkovo, Moscow, 143025, Russia
2. Moscow Institute of Physics and Technology,
Institutskii per. 9, Dolgoprudny, Moscow region, 141700, Russia
3. Texas AM University,
4242 TAMU, College Station, Texas, 77843, USA
4. PN Lebedev Institute RAS,
Leninsky prospekt 53, Moscow, 119991, Russia

Fano-Feshbach resonances play extremely important role in controlling interaction between particles in ultracold quantum gasses and quantum simulators. These resonances provide a way to vary interaction strength between atoms in the cloud by changing scattering length of elastic collisions in wide range using magnetic field. While in alkaline atoms these resonances could only be observed in relatively high magnetic fields, in rare earth elements because of high orbital moment in the ground state one could expect number of low-field Fano-Feshbach at low (few Gauss) field. Indeed, such low field resonances been already observed in dysprosium and erbium [1], [2].
In this contribution, we report first observation of low-magnetic field Fano-Feshbach resonances in ultracold thulium (see Figure 1). Been on the resonance atoms experience strong modification of the scattering length, which also lead to increased rate of 3-body inelastic collisions and therefore enhanced loss of atoms from the optical dipole trap.

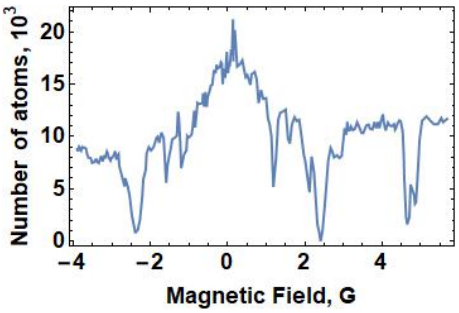

Fig. 1: Magnetic field depended losses were observed and clearly demonstrate number of low field Fano-Fieshbach resonances.

In our experiments, atoms were prepared in narrow transition magneto-optical trap (MOT) [3]. A cooling process consists of three stages: the first-stage cooling at a broad transition at wavelength 410.6 nm and natural linewidth 10 MHz. The second-stage cooling at weak transition at wavelength 530.7 nm and natural linewidth 350 kHz. This procedure allows us to obtain 10^7 atoms with a temperature about 18 μK in a MOT.
After that atoms were trapped into optical dipol trap (ODT) that is formed by two laser beam at wavelength 532 nm with a power up to 4 W focused into MOT region. To increase the efficiency of the overload into ODT we use oscillations of the horizontal beam which leads to increase the capture area. The oscillation frequency of 40 MHz is much higher than the characteristic frequencies of oscillations of atoms in a dipole trap. This allows us to avoid heating in ODT because atoms see only the time-averaged potential of the shaking beam. Thus, by controlling the intensity and the waist of the horizontal beam of optical dipol trap, we realized evaporative cooling. It allows us to cool the cloud to the temperature around 3 μK.
After preparing atoms in ODT we switch on a homogeneous magnetic field for 300 ms and then measure number of atoms stayed in the trap.

References

[1] Kristian Baumann, Nathaniel Q. Burdick, Mingwu Lu, and Benjamin L. Lev, Phys. Rev. A **89**, 020701(R) (2014)
[2] Albert Frisch, Michael Mark, Kiyotaka Aikawa, Francesca Ferlaino, John L. Bohn *et al.*, Nature **507**, 475479 (2014)
[3] I. S. Cojocaru, S. V. Pyatchenkov, S. A. Snigirev, A. V. Akimov *et al.*, Phys. Rev. A **95**, 012706 (2017)

*Corresponding author: tsyganokv22@gmail.com

To the list of contents

A new design of a high-flux Source of cold strontium atoms

Dongyang Xu*, **Rowan Moore, Christopher Foot**
1. Department of Physics, University of Oxford
Parks Road, Oxford OX1 3PU, UK

Strontium is an alkaline earth metal with two electrons in the outer shell giving it significantly different properties from other alkali metals. Key features relevant to quantum technology are i) the existence of very narrow transitions that are used for optical clocks (alkalis only have narrow microwave transitions, e.g. the hyperfine splitting of Cs), ii) two-stage laser cooling on strong then weak transitions gives very low temperatures quickly, and iii) some isotopes of strontium have a low sensitivity to inter-atomic collisions and magnetic fields which is a big advantage for clocks and interferometers. Typical apparatus for laser cooling of strontium is 50 to 100cm long with multiple stages: atomic oven, transverse collimation, slowing as the atoms pass along a tube through a magnetic solenoid, deflection (to avoid line of sight to the oven) and finally collection in a magneto- optical trap (MOT). Our proposed design is 15-25 cm long, which is design of a compact source of cold strontium atoms using a two-dimensional magneto-optical trap with a 'push' laser beam (a 2D+ MOT). We have designed and machined highly-efficient but small strontium oven, which can heat up to 700 °C.

*Corresponding author: dongyang.xu@physics.ox.ac.uk

To the list of contents

Collisions in ultracold polar bosonic RbCs molecules

Elizabeth M. Bridge[*1], **Jacob A. Blackmore**[1], **Philip D. Gregory**[1], **Jesus Aldegunde**[2], **Jeremy M. Hutson**[2], **Simon L. Cornish**[†1]

1. Joint Quantum Centre (JQC) Durham–Newcastle, Department of Physics, Durham University South Road, Durham DH1 3LE, UK

2. Joint Quantum Centre (JQC) Durham–Newcastle, Department of Chemistry, Durham University South Road, Durham DH1 3LE, UK

Experiments using ultracold molecules are a growing area of research, opening up a wide range of new and interesting research directions within the fields of ultracold chemistry, precision measurement, quantum simulation and quantum computation [1]. Heteronuclear molecules, such as RbCs, exhibit permanent electric dipole moments, providing tunable long-range anisotropic dipole-dipole interactions. Ultracold molecules also exhibit a rich internal structure of rotational and vibrational energy levels. This provides a vast array of energy levels to explore, with much scope for state manipulation and potential for applications such as long-term qubit storage [2][3][4] and the creation of pseudospins to simulate quantum magnetism [5][6]. The field of ultracold molecules is still in its experimental infancy, with only a small number of groups able to produce trapped samples of ultracold heteronuclear molecules in their rovibronic ground state [7][8][9][10][11].

At the Joint Quantum Centre in the Department of Physics, Durham University we have developed an apparatus capable of making samples of up to 4000 ultracold RbCs molecules in their rovibronic ground state [12]. We cool a mixture of Rb and Cs atoms, use Feshbach association to create RbCs molecules [13], and stimulated Raman adiabatic passage (STIRAP) to drive the molecules into their rovibronic ground state with $> 90\,\%$ efficiency [9][12]. We have demonstrated the use of microwave fields to control the rotational and hyperfine state, fully characterising the complex hyperfine structure in the process [14].

Although much progress has been made in the control and understanding of ultracold molecules, there are still many questions to be addressed, particularly in the realm of ultracold collisions. RbCs molecules are considered nonreactive due to the endothermic nature of the two-body process [15]. However, two molecules may stick together to form a long-lived four-body complex, these 'sticky collisions' may lead to trap loss if a third molecule collides with this complex during its lifetime [16]. We are working to understand and control the collision and loss mechanisms of RbCs molecules in optical lattice and dipole traps, including atom-molecule collisions and molecule-molecule collisions in a range of hyperfine and rotational states. We present our recent progress and findings.

References

[1] L. D. Carr, D. DeMille, R. V. Krems, and J. Ye, New J. Phys. **11**, 055049 (2009).
[2] D. DeMille, Phys. Rev. Lett. **88**, 067901 (2002).
[3] A. André, D. DeMille, J.M. Doyle,M. D. Lukin, S. E. Maxwell, P. Rabl, R. J. Schoelkopf, and P. Zoller, Nat. Phys. **2**, 636 (2006).
[4] J. W. Park, Z. Z. Yan, H. Loh, S. A. Will, and M. W. Zwierlein, arXiv:1606.04184 (2016).
[5] R. Barnett, D. Petrov, M. Lukin, and E. Demler, Phys. Rev. Lett. **96**, 190401 (2006).
[6] A. V. Gorshkov, S. R. Manmana, G. Chen, J. Ye, E. Demler, M. D. Lukin, and A. M. Rey, Phys. Rev. Lett. **107**, 115301 (2011).
[7] K.-K. Ni, S. Ospelkaus, M. H. G. de Miranda, A. Pe'er, B. Neyenhuis, J. J. Zirbel, S. Kotochigova, P. S. Julienne, D. S. Jin, J. Ye, Science **322**, 231-235 (2008).
[8] T. Takekoshi, L. Reichsöllner, A. Schindewolf, J. M. Hutson, C. R. Le Sueur, O. Dulieu, F. Ferlaino, R. Grimm, and H.-C. Nägerl, Phys. Rev. Lett. **113**, 205301 (2014).
[9] P. K. Molony, P. D. Gregory, Z. Ji, B. Lu, M. P. Köppinger, C. R. Le Sueur, C. L. Blackley, J. M. Hutson, and S. L. Cornish, Phys. Rev. Lett. **113**, 255301 (2014).
[10] J. W. Park, S. A. Will, and M. W. Zwierlein, Phys. Rev. Lett. **114**, 205302 (2015).
[11] M. Guo, B. Zhu, B. Lu, X. Ye, F.Wang, R. Vexiau, N. Bouloufa-Maafa, G. Quéméner, O. Dulieu, and D. Wang, Phys. Rev. Lett. **116**, 205303 (2016).
[12] P. K. Molony, P. D. Gregory, A. Kumar, C. R. Le Sueur, J. M. Hutson, and S. L. Cornish, Chem. Phys. Chem. **17** 3811-3817 (2016).
[13] M. P. Köppinger, D. J. McCarron, D. L. Jenkin, P. K. Molony, H.-W. Cho, and S. L. Cornish, Phys. Rev. A **89** 033604 (2014).
[14] P. D. Gregory, J. Aldegunde, J. M. Hutson, and S. L. Cornish, Phys. Rev. A **94** 041403(R) (2016).
[15] P. S. Żuchowski and J. M. Hutson, Phys. Rev. A **81** 060703 (2010).
[16] M. Mayle, G. Quéméner, B. P. Ruzic, and J. L. Bohn, Phys. Rev. A **87** 012709 (2013).

[*]Corresponding author: elizabeth.bridge@durham.ac.uk
[†]Corresponding author: s.l.cornish@durham.ac.uk

To the list of contents

Towards ultracold KCs molecules

Zhengkun Fu[*1], **Apichayaporn Ratkata**[1], **Danielle Boddy**[1], **Jesus Aldegunde**[2], **Jeremy M. Hutson**[2], **Simon L. Cornish**[†1]

1. Joint Quantum Centre (JQC) Durham–Newcastle, Department of Physics, Durham University South Road, Durham DH1 3LE, U.K.

2. Joint Quantum Centre (JQC) Durham–Newcastle, Department of Chemistry, Durham University South Road, Durham DH1 3LE, U.K.

Ultracold polar molecules offer a wide range of exciting research directions owing to their long-range anisotropic dipole-dipole interactions. In particular, ultracold heteronuclear molecules possess the long-range interactions needed to engineer an important class of problems relevant to condensed-matter physics [1] [2], with proposed applications spanning the fields of ultracold chemistry and precision measurement [3]. Additionally, the internal degrees of freedom of molecules can be used to encode quantum information and present new possibilities to engineer interparticle interactions when coupled to external electric and microwave fields [4].

We have developed an apparatus for producing ultracold mixtures of K and Cs, with the aim of producing trapped samples of ultracold fermionic KCs molecules in their rovibronic ground state. We have chosen to work with these atoms as KCs molecules are one of only a few bi-alkali molecules that are stable against reactive collisions of the form $2AB \rightarrow A_2 + B_2$ and $2AB \rightarrow A_2B + B$ [5]. Furthermore, Cs possesses a very rich spectrum of intraspecies Feshbach resonances allowing precise control of the intraspecies interactions, which is important for producing a miscible quantum-degenerate mixture.

We are working towards measuring the spectrum of interspecies Feshbach resonances for all K isotopes, similar to work in [6], and towards creating trapped samples of weakly bound ^{40}KCs Feshbach molecules. We present our recent research and findings.

References

[1] I. M. Georgescu, S. Ashhab, and F. Nori, Rev. Mod. Phys. **86**(1), 153–185 (2014).
[2] M. A. Baranov, M. Dalmonte, G. Pupillo, and P. Zoller, Chem. Rev., **112**(9), 5012–5061 (2012).
[3] L. D. Carr, D. DeMille, R. V. Krems, and J. Ye, New J. Phys. **11**, 055049 (2009).
[4] H. P. Büchler, E. Demler, M. Lukin, A. Micheli, N. Prokof'ev, G. Pupillo, and P. Zoller, Phys. Rev. Lett **98**(6), 060404 (2007).
[5] P. S. Żuchowski and J. M. Hutson, Phys. Rev. A, **81**(6), 060703 (2010).
[6] M. Gröbner, P. Weinmann, E. Kirilov, H-C Nägerl, P. S. Julienne, C. R. Le Sueur, J. M. Hutson, Phys. Rev. A, **95**(2), 022715, (2017).

[*]Corresponding author: zhengkun.fu@durham.ac.uk
[†]Corresponding author: s.l.cornish@durham.ac.uk

To the list of contents

Laser Cooling of YbF Molecules for Measuring the Electron's Electric Dipole Moment

M. A. Trigatzis[1] **J. Lim**[*1], **J. R. Almond** [1], **N. J. Fitch** [1], **B. E. Sauer** [1], **E. A. Hinds** [1], **M. R. Tarbutt** [1]
1. Centre for Cold Matter, Blackett Laboratory, Imperial College London, Prince Consort Road, London SW7 2AZ, UK

At the Centre for Cold Matter, we measure the electron's electric dipole moment (eEDM) by observing the electric-field induced spin precession of YbF molecules [1]. Theories that extend the Standard Model generally contain additional sources of CP violation and predict an eEDM that is large enough to measure by today's experiments. Indeed, recent measurements have already ruled out some such theories [1-3].

Laser cooling of a beam of diatomic molecules was first demonstrated in 2010 [4], and this new field promises a number of applications including cold chemistry, quantum simulations and quantum information, and precision measurements. A laser-cooled beam of YbF could increase the experiment's sensitivity by two orders of magnitude [5]. We recently observed 1D transverse laser cooling of our YbF cryogenic buffer gas beam, implementing the cooling scheme described in Ref. [6]. We observed evidence of both Doppler and Sisyphus cooling.

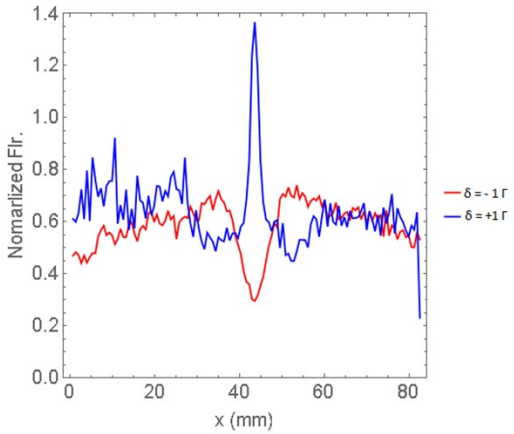

Fig. 1: A sample transverse position distribution of the molecular beam indicating evidence of Sisyphus cooling (blue curve) and heating (red curve). The signal at each point is divided by the signal measured when the cooling light is blocked.

References

[1] J. J. Hudson, D. M. Kara, I. J. Smallman, B. E. Sauer, M. R. Tarbutt, and E. A. Hinds, Nature 473, 493 (2011).
[2] J. Baron *et al.*, Science 343, 269 (2014).
[3] W. B. Cairncross, D. N. Gresh, M. Grau, K. C. Cossel, T. S. Roussy, Y. Ni, Y. Zhou, J. Ye, E. A. Cornell, arXiv:1704.07928.
[4] E. S. Shuman, J. F. Barry, and D. DeMille, Nature 467, 820 (2010).
[5] M. R. Tarbutt, B. E. Sauer, J. J. Hudson, and E. A. Hinds, New J. Phys. 15, 053034 (2013).
[6] I. Smallman, F. Wang, T. Steimle, M. R. Tarbutt, and E. Hinds, J. Mol. Spectrosc. 300, 3 (2014).

[*]Corresponding author: j.lim@imperial.ac.uk

To the list of contents

Retrieval of group refractive index in a dense atomic vapor helped by buffer gas-assisted radiation channeling

A. Papoyan [1], **S. Shmavonyan** [1], **Davit Khachatryan**[*1], **G. Grigoryan** [1]
1. Institute for Physical Research, NAS of Armenia
Ashtarak-2 0203, Armenia

Precise determination of dispersion and absorption properties of medium, notably on far wings of atomic resonance remains a challenge. We report on direct retrieval of the group refractive index in the spectral region of $\sim$ 30 GHz covering hyperfine structure of Rb D_2 line, exploiting reflection spectrum from the optical cell where rubidium atoms are buffered by a high-density cesium vapor [1].

In our experiment we use a vapor cell with non-parallel windows, which does not exhibit interference effects associated with multiply reflected light from cell's boundaries outside the resonance. Nevertheless, in the vicinity of resonance line the vapor cell behaves as a low-finesse Fabry–Pérot cavity. We attribute this behavior to fiber-type radiation channeling built up because of buffer gas-imprisonment of resonant atoms inside the laser beam. Group refractive index across the studied spectral region was determined from the frequency positions of interference oscillations of the reflected beam intensity.

The experimental results were compared with theoretical calculations based on the model presented in [2]. In this theory we consider one-dimensional problem with parallel boundaries, considering multiple reflection regime. The obtained results are fully consistent with experimental reflection spectra taken at different temperature conditions. Fig.1 presents the example of experimentally determined and calculated dispersion curves of group refractive index for the case of rubidium vapor density $N_{Rb} = 2.41\times10^{13}$ cm^{-3} and cesium vapor density $N_{Cs} = 9.27\times10^{15}$ cm^{-3}.

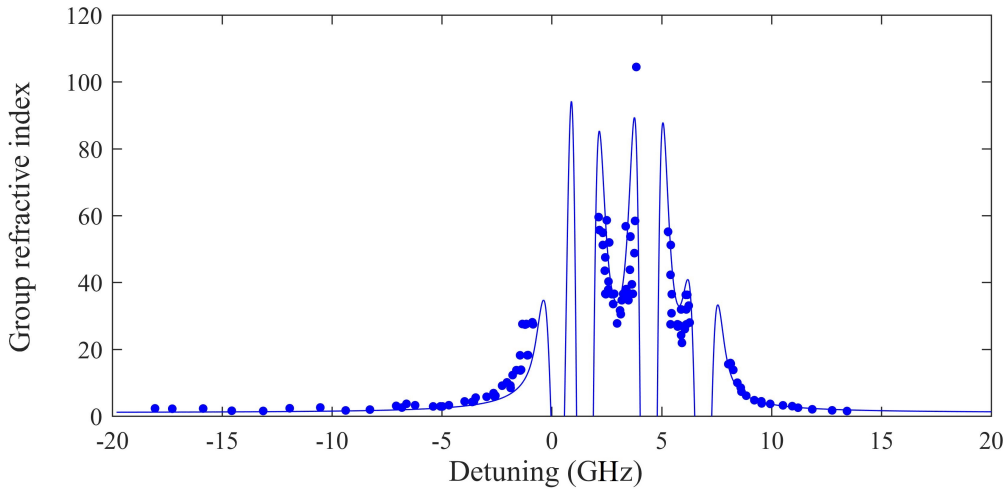

Fig. 1: Dependence of group refractive index on frequency retrieved from experimental reflection spectra (dots) and calculated from theory (solid lines) in the region of D_2 line of residual Rb. The zero detuning frequency is set to the F_g=2 $\rightarrow$ F_e=1 hyperfine transition of ^{87}Rb.

The presented technique can be used for dispersion measurements in dense buffered gases, quantitative studies of transition from dipole-dipole binary to multiparticle collisional regime, as well as for realization of optical effects in coherently driven hot atomic gases [3].

References

[1] A. Papoyan, S. Shmavonyan, D. Khachatryan, and G. Grigoryan, J. Opt. Soc. Am. B **34**, 877 (2017).
[2] A. Badalyan, V. Chaltykyan, G. Grigoryan, et al., Eur. Phys. J. D **37**, 157 (2006).
[3] D.J. Whiting, J. Keaveney, C.S. Adams, and I.G. Hughes, Phys. Rev. A **93**, 043854 (2016).

*Corresponding author: khachatryandavit333@gmail.com

To the list of contents

Two-dimensional Exciton Spectrum in GaAs Quantum Well in Tilted Magnetic Field

E.A.Koval[*1,2], **O.A.Koval**[1]
1. Bogoliubov Laboratory of Theoretical Physics, Joint Institute for Nuclear Research, Dubna, Moscow Region 141980, Russia
2. Department of fundamental problems of micro-world physics, Dubna University, Dubna, Moscow Region 141980, Russia

The main aspects of our report are devoted to the investigation of the properties of energy spectrum of such low-dimensional systems as a two-dimensional (2D) exciton in GaAs quantum well and a 2D hydrogen atom. From the physical point of view our results are interesting since they present for the first time the calculations of the nonlinear dependence of the energy spectrum of a two-dimensional hydrogen atom and of an exciton on the tilt angle α of the magnetic field $B = B\sin(\alpha)i + B\cos(\alpha)k$ in a wide range of the magnetic field strength B. The influence of the magnetic field tilt on the spectrum of the investigated systems is illustrated on the Fig. 1. In fact, this allows to regulate (substantially change) the energy spectrum of 2D Hydrogen and 2D exciton by varying the tilt angle. In this case, the Hamiltonian of the 2D hydrogen atom includes only the Coulomb interaction and interaction with the magnetic field, in contrast to problems with additional confinement in quantum dots in the works of other authors.

Our interesting result is that the dependence of the energy of the excited states of the 2D hydrogen atom and 2D exciton on the tilt angle α of the magnetic field is nonlinear and does not repeat the seemingly trivial cosine dependence. Moreover, at $\alpha = 90^\circ$ when the magnetic field lies in the atomic plane, the quadratic over magnetic field strength term of the Hamiltonian along the X axis disappears and potential does not lead to the formation of bound states in the positive region of the spectrum (interaction potential edge along Xaxis substantially weakens). Thus, at $\alpha = 90^\circ$ energy levels of excited states, rising with an increase in the magnetic field strength, do not exist at a certain critical (for them) value of the magnetic field.

We also found fascinating an accompanying effect of a quantum chaos initiation (turn on/turn off) by magnetic field tilt angle changing. The dynamics of the calculated electronic densities of the first three excited states of 2D Hydrogen atom on the magnetic field tilt angle is illustrative.

From the technical point of view, to discretize the Hamiltonian matrix, we used the wave function expansion, based on the discrete variable method,seven-point finite-difference approximation, whereas to solve the eigenvalue problem — the shifted inverse iteration method. In each iteration, the matrix equation was solved by matrix modification of the sweep algorithm. The details of the numerical algorithm used are given in our paper [1]. It was successfully verified for the 2D hydrogen atom in a magnetic field perpendicular to the atomic plane [1] and our results are in good agreement with the results of other authors [2-3].

The authors acknowledge the support by the Russian Foundation for Basic Research, Grant No. 16- 32-00865.

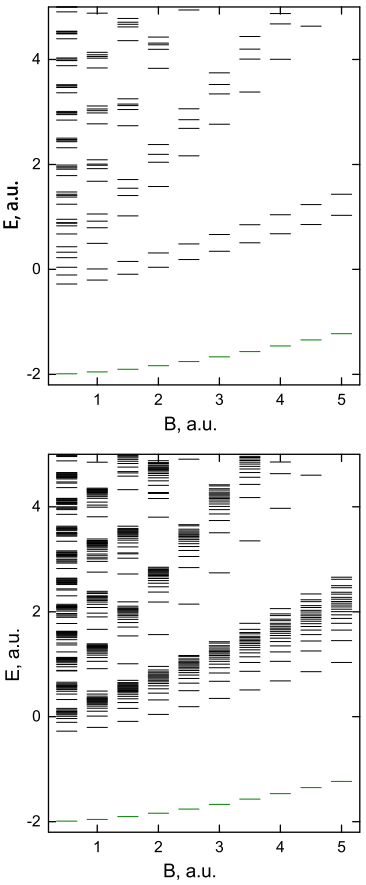

Fig. 1: The calculated spectra at different strengths of the magnetic field: perpendicular to the atomic plane (a), tilted to an angle $\alpha = 9^\circ$ with respect to the normal to the atomic plane (b). Ground state is indicated by green color. The tilting of the magnetic field leads to the splitting of the excited states of the considered systems.

References

[1] E.A. Koval and O.A. Koval, Zh. Eksperim. i. Teor. Fiz. **152** (2017) [In print, in Russian]; ArXiv quantph/1701.06235.
[2] A. Soylu, O. Bayrak and I. Boztosun, Int. J. Mod. Phys. E **15**, 1263 (2006).
[3] M. A. Escobar-Ruiz and A. V. Turbiner, Ann. Phys. (N. Y.) **340**, 37 (2014).
[4] A. Soylu and I. Boztosun, Physica B: Condens. Matter **396**, 150 (2007).
[5] C. Kallin, and B. I. Halperin, Phys. Rev. B **30**, 5655 (1984).
[6] D. G. W. Parfitt and M. E. Portnoi, J. Math. Phys. **43**, 4681 (2002).

*Corresponding author: e-cov@yandex.ru

To the list of contents

Cavity-enhanced frequency up-conversion in rubidium vapour

R. F. Offer[*1], **J. W. C. Conway**[1], **E. Riis**[1], **S. Franke-Arnold**[2], **A. S. Arnold**[†1]
1. Department of Physics, SUPA, University of Strathclyde
Glasgow G4 0NG, UK
2. School of Physics and Astronomy, SUPA, University of Glasgow
Glasgow G12 8QQ, UK

Atomic vapours are an experimentally simple system in which to study a wide variety of nonlinear phenomena. In particular, we investigate a resonantly enhanced four wave mixing (FWM) process within rubidium vapour, which allows for efficient frequency up-conversion of near-infrared light (780 and 776 nm) to blue light (420 nm) [1-4]. We have recently studied the effect of adding feedback to this already surprisingly rich system, showing that even a low finesse cavity both enhances the output power and dramatically narrows the linewidth of the generated light [5]. In addition, we investigate the transverse phase coherence of this process and the role of phase matching when shaped pump light, in particular light carrying orbital angular momentum (OAM), is used to pump the system.

Fig. 1 (a) compares the single pass and cavity-enhanced 420 nm output power as a function of pump laser detuning. Despite the low finesse of the cavity (12.8) the output power is dramatically increased when the blue light, which has a frequency that scans with the pump laser, is resonant with the cavity. The linewidth of the generated light was measured via a beat note with a separate 420 nm laser (Fig. 1 (b)). For a single pass the blue light has a power broadened linewidth of around 33 MHz, but with the cavity this is narrowed to < 1 MHz. The cavity thus allows both high output power and narrow linewidth to be achieved concurrently, suggesting this light source could have applications in ultracold atomic gases, for example in second-stage laser cooling of rubidium, or for enhanced resolution imaging.

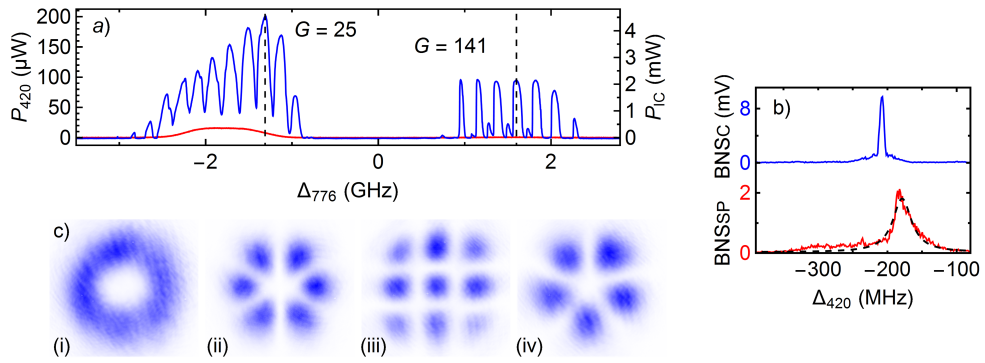

Fig. 1: (a) Blue output power as a function of 776 nm pump detuning. (b) Beat note measurement of the linewidth of the generated 420 nm light. Red curves are single pass FWM, blue curves are with the cavity. Offer *et al.* 2016 [5]. (c) Intensity profile of shaped 420 nm light generated via single pass FWM (i) $LG_{l=3,p=0}$ mode, (ii) $LG_{l=3,p=0}$ beam interfered with mirror image, (iii) $HG_{m=3,n=3}$ mode and (iv) $LG_{l=3,p=0} + LG_{l=2,p=0}$ superposition.

We also investigate, for single pass FWM, the effect of using shaped pump light on the phase and intensity profile of the generated 420 nm light. It has previously been shown that the transverse phase coherence of FWM allows OAM to be transferred from the near-IR pump fields to the 420 nm emission [6]. We explore the limits of this process, and also investigate the effect of shaping both pump beams independently. Fig. 1 (c) shows a selection of modes generated via appropriate shaping of one of the pump beams [7]. This process allows information transfer from one end of the visible spectrum to the other, which could be of use for applications such as higher dimensional quantum information processing.

References

[1] A. S. Zibrov, M. D. Lukin L. Hollberg, and M. O. Scully, Phys. Rev. A **65**, 051801 (2002).
[2] A. M. Akulshin, R. J. McLean, A. I. Sidorov, and P. Hannaford, Opt. Express **17**, 22861 (2009).
[3] T. Meijer, J. D. White, B. Smeets, M. Jeppesen, and R. E. Scholten, Opt. Lett. **31**, 1002 (2006).
[4] A. Vernier, S. Franke-Arnold, E. Riis, and A. S. Arnold, Opt. Express **18**, 17020 (2010).
[5] R. F. Offer, J. W. C. Conway, E. Riis, S. Franke-Arnold, and A. S. Arnold, Opt. Express. **41**, 2177 (2016).
[6] G. Walker, A. S. Arnold, and S. Franke-Arnold, Phys. Rev. Lett. **108**, 243601 (2012).
[7] T. W. Clark, R. F. Offer, S. Franke-Arnold, A. S. Arnold, and N. Radwell, Opt. Express **24**, 6249 (2016).

[*]Corresponding author: rachel.offer@strath.ac.uk
[†]Corresponding author: aidan.arnold@strath.ac.uk

To the list of contents

CPT Tests with Protons and Antiprotons

G. Schneider[*1,2], **Hiroki Nagahama**[2,3], **Mustafa Besirli**[2], **Matthew Bohman**[2,4], **Matthias Borchert**[2,5], **James Harrington**[4], **Takashi Higuchi**[2,3], **Andreas Mooser**[2], **Natalie Schön**[1], **Stefan Sellner**[2], **Christian Smorra**[2,6], **Toya Tanaka**[2,3], **Klaus Blaum**[4], **Yasuyuki Matsuda**[3], **Christian Ospelkaus**[5,7], **Wolfgang Quint**[8], **Jochen Walz**[1,9], **Yasunori Yamazaki**[10], **Stefan Ulmer**[2]

1. Institut für Physik, Johannes Gutenberg-Universität, 55099 Mainz, Germany.
2. RIKEN, Ulmer Initiative Research Unit, 2-1 Hirosawa, Wako, Saitama 351-0198, Japan.
3. Graduate School of Arts and Sciences, University of Tokyo, Tokyo 153-8902, Japan.
4. Max-Planck-Institut für Kernphysik, Saupfercheckweg 1, 69117 Heidelberg, Germany.
5. Institut für Quantenoptik, Leibniz Universität Hannover, Welfengarten 1, 30167 Hannover, Germany.
6. CERN, CH-1211 Geneva 23, Switzerland.
7. Physikalisch-Technische Bundesanstalt, QUEST, Bundesallee 100, 38116 Braunschweig, Germany.
8. GSI-Helmholtzzentrum für Schwerionenforschung GmbH, 64291 Darmstadt, Germany.
9. Helmholtz-Institut Mainz, Sektion MAM, 55099 Mainz, Germany.
10. RIKEN, Atomic Physics Research Unit, 2-1 Hirosawa, Wako, Saitama 351-0198, Japan.

Invariance under the combined transformation of charge (C), parity (P), and time (T) reversal is believed to be an exact symmetry of physics. The BASE collaboration at Mainz and CERN contributes to stringent tests of this symmetry by comparing the fundamental properties of protons and antiprotons, such as charge-to-mass ratios [1] and magnetic moments [2,3]. Recently we performed the most precise measurement of the antiproton magnetic moment $\mu_{\bar{p}}$ in units of the nuclear magneton μ_N with a relative uncertainty of 0.8×10^{-6} [3], an improvement by a factor of six [4]. By utilizing the continuous Stern-Gerlach effect [5] we measured the ratio $\mu_{\bar{p}}/\mu_N = g/2 = \nu_L/\nu_c$ of the Larmor frequency ν_L and the free cyclotron frequency ν_c of a single isolated antiproton stored in a cryogenic Penning trap with a superimposed magnetic inhomogeneity.

The presence of this strong inhomogeneity causes line broadening and thus ultimately limits the fractional precision achieved in such single trap experiments to the p.p.m. level [6]. To overcome this limitation the *double Penning-trap method* is applied. Hereby, precise frequency measurements are performed in the *precision trap* with a homogeneous magnetic field, whereas the spin state detection is carried out in a second spatially separated *analysis trap* with the superimposed magnetic inhomogeneity. This technique has already been demonstrated with protons with a measurement precision of 3.3×10^{-9} [2]. However, it was limited by magnetic field imperfections in the precision trap and saturation broadening of the g-factor resonance. With a considerably revised apparatus in Mainz we are currently conducting a measurement aiming at a tenfold improved fractional experimental uncertainty.

Our next step is to apply the double trap method also to the antiproton to improve the fractional precision of both g-factors to the 10^{-10} level and beyond. This will provide one of the most stringent tests of CPT symmetry in the baryon sector.

References

[1] S. Ulmer *et al., Nature* **524**, 196–199 (2015).
[2] A. Mooser *et al., Nature* **509**, 596–599 (2014).
[3] H. Nagahama *et al., Nature Communications* **8**, 14084 (2017).
[4] J. DiSciacca *et al., Phys. Rev. Lett.* **110**, 130801 (2013).
[5] H. Dehmelt and P. Ekstrom, *Bull. Am. Phys. Soc.* **18**, 727 (1973).
[6] S. Ulmer *et al., Phys. Rev. Lett.* **106**, 253001 (2011).

*Corresponding author: georg.schneider@uni-mainz.de

To the list of contents

Notes on non-relativistic QED and Bethe logarithm

D. Šimsa[1], **J. Zamastil**[*1] **and V. Patkóš**[1]
1. Department of Chemical Physics and Optics, Faculty of Mathematics and Physics, Charles University, Ke Karlovu 3, 121 16 Prague 2, Czech Republic

Quantum-electrodynamical (QED) effects have to be taken into account if accurate positions of the spectral lines are sought. QED effects shift the atomic spectral lines by an amount that is smaller only by the factor $Z\alpha\ln(Z\alpha)$ than the leading order of relativistic and magnetic effects, where Z is the charge of the nucleus.

Calculation of these effects is usually complicated because they belong to class of problems involving more than one significant scale (at least highly relativistic and non-relativistic regions). The Non-Relativistic Quantum Electrodynamics (NRQED) [1] is one of the ways to overcome the difficulties. The method is based on integrating out high energy degrees of freedom and constructing effective non-relativistic hamiltonian and corrections to this hamiltonian. Recently proposed relativistic multipole expansion (RME) [2] of the self-energy effect suggests some observations on the NRQED.

Firstly, nature of the series for the one-loop self-energy of an electron bound by the Coulomb field of the nucleus is clarified. It is customary to write the ground state energy shift caused by self-energy effect in the limit of infinitely massive nucleus in the form

$$\Delta E = m\frac{\alpha}{\pi}(Z\alpha)^4 F(Z\alpha)\,, \tag{1}$$

where $F(Z\alpha)$ is a dimensionless function which can be written in the form of series in $Z\alpha$. In [3] we show that the structure of the series is as follows

$$\begin{aligned} F(Z\alpha) = {} & A_{41}\ln(Z\alpha)^{-2} + A_{40} + A_{50}(Z\alpha) + (Z\alpha)^2\left[A_{62}\ln^2(Z\alpha)^{-2} + A_{61}\ln(Z\alpha)^{-2} + A_{60}\right] + \\ & + (Z\alpha)^3\left[\ln(Z\alpha)^{-2}A_{71} + A_{70}\right] + (Z\alpha)^4\left[\ln^3(Z\alpha)^{-2}A_{83} + \ln^2(Z\alpha)^{-2}A_{82} + \ln(Z\alpha)^{-2}A_{81} + A_{80}\right] + \\ & + (Z\alpha)^5\left[\ln^2(Z\alpha)^{-2}A_{92} + \ln(Z\alpha)^{-2}A_{91} + A_{90}\right] + \ldots \end{aligned} \tag{2}$$

Further, we show that for the coefficients A_{83}, A_{92} and so on it holds

$$\frac{A_{92}}{A_{50}} = \frac{1}{8}, \frac{A_{11,3}}{A_{50}} = \frac{1}{48}, \frac{A_{83}}{A_{62}} = \frac{1}{6}, \frac{A_{10,4}}{A_{62}} = \frac{1}{48}, \tag{3}$$

and so on. The origin of these terms is traced back to logarithmic divergence of the Dirac S-wave function at the origin. These terms eventually lead to breakdown of NRQED approach.

Secondly, the leading order of RME yields the self-energy effect of the bound particle in the form [2]

$$\Delta E = m\frac{\alpha}{\pi N^3}(Z\alpha)^4\left(\frac{m_r}{m}\right)^3 F(Z\alpha)\,, \quad F = F_{low} + F_{high}, \tag{4}$$

where

$$F_{low} = \langle\psi|p_i f\,(h-e_N)\,p_i|\psi\rangle\,, \qquad f(x) = N^3 x\int_0^1 dy\int_0^1 dw\frac{1-2w(1-w)}{y+w2(Z\alpha)^2\frac{m_r}{m}x}. \tag{5}$$

Here, h, p and e_N are non-relativistic hamilton operator, momentum operator and energy of the reference state ψ with the principal quantum number N in the atomic units. Further, m and m_r denote particle and reduced masses, respectively, and F_{low} is called here the extended Bethe logarithm (EBL). When expanded in series in $Z\alpha$, EBL reduces at the leading order to ordinary Bethe logarithm. However, it is argued that it is both more accurate and easier to calculate EBL than ordinary Bethe logarithm.

Finally, contribution of the combined self-energy vacuum polarization contribution to the Lamb shift in muonic hydrogen for the $1s-4s$ and $2p-4p$ states is calculated, see [3]. These results are more accurate than those reported before [4]. For the contribution of the effect considered here to the Lamb shift in muonic hydrogen we thus obtain

$$\Delta E(2p_{\frac{1}{2}}) - \Delta E(2s) \simeq -2.706\times10^{-6}\,eV.$$

References

[1] Proposed in W. E. Caswell and G. P. Lepage, Phys. Lett. **167B**, 437 (1986). For recent work see K. Pachucki, Phys. Rev. A **74**, 022512, (2006); K. Pachucki and V. A. Yerokhin Phys. Rev. A **79**, 062516 (2009); Errata *ibid* **80**, 019902 (2009); *ibid* **81**, 039903 (2010).
[2] V. Patkóš and J. Zamastil, Phys. Rev. A **91**, 062511 (2015). See also J. Zamastil and V. Patkóš, Phys. Rev. A **88**, 032501 (2013).
[3] V. Patkóš, D. Šimsa and J. Zamastil, Phys. Rev. A **95**, 012507 (2017).
[4] First reported in K. Pachucki, Phys. Rev. A, **53**, 2092 (1996) and later improved in U. D. Jentschura, Ann. Phys. **326**, 500 (2011).

[*]Corresponding author: zamastil@karlov.mff.cuni.cz

To the list of contents

Electron collisions with selected hydrocarbons: relation between total cross section and physical properties of molecule

Cz. Szmytkowski[1], **S. Stefanowska**[*1], **E. Ptasińska-Denga**[1], **P. Możejko**[1]
1. Department of Atomic, Molecular and Optical Physics, Faculty of Applied Physics and Mathematics, Gdańsk University of Technology ul. G. Narutowicza 11/12, 80-233 Gdańsk, Poland

Cross sections data concerning processes which occur during electron scattering from hydrocarbon molecules are of great importance in many fields of science and technology. For example, they apply in radiotherapy [1] and lithography technique FEBID [2]. Moreover, systematic studies of total cross section (TCS) for electron scattering from molecules allow to notice regularities and relationships between shape and magnitude of TCS energy dependence and some physical properties of target molecules. We have investigated several factors, which can affect on TCS energy curve: methylation, bond multiplicity, different geometrical arrangement of atoms in a molecule. Our research also confirms that simple additivity rule gives good agreement with experimental data in defined energy range.

We studied how the substitution of one hydrogen in hydrocarbon molecule with methyl group influences on TCS energy function, i.e. substitution effect. The research was carries out on alkynes [3], alkenes [4] and dienes [5]. Results for alkenes are shown in Fig. 1. For all studied targets we observed similar regularities. We have noticed that resonant structures appearing on TCS curve are shifted in energy and value of their amplitudes becomes smaller with increasing number of methyl groups [4].

Isomeric effect was also studied for some selected hydrocarbons series, e.g. C_4H_6 (1,2-butadiene, 1,3-butadiene, 1-butyne, 2-butyne) [6] and C_5H_{10} (1-pentene and 2-methyl-2-butene) [4]. Various geometric structures of isomeric molecules leads to changes in TCS energy dependence, due to different spatial charge distribution. Differences in the shape of the TCS curves are most evident in low energies. For intermediate and higher collision energy TCS curves for isomers practically overlap. This effect suggest, that simple additivity rule (TCS for a given molecule can be obtained as a sum of TCSs for atoms or smaller molecular fragments) can give quite good approximation of experimental data in this range of impact energies.

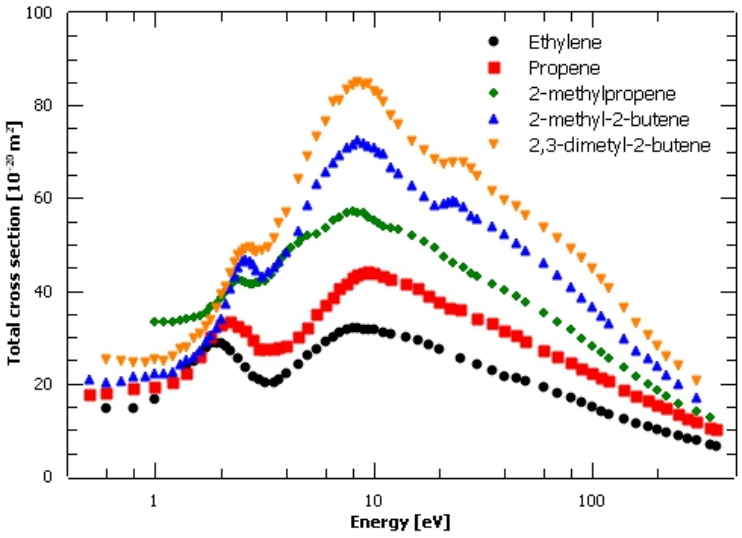

Fig. 1: Experimental total cross section from: ethylene; propene; 2-methylpropene; 2-methyl-2-butene and 2,3-dimethyl-2-butene [4].

Detailed discussion of above mentioned effects will be presented during the Conference.

References

[1] S. K. Sahbani, L. Sanche, P. Cloutier, A. D. Bass, D. J. Hunting, J. Phys. Chem. B **118**, 13123 (2014).
[2] R. M. Thorman, Ragesh Kumar T. P., D. H. Fairbrother and O. Ingólfsson, Beilstein J. Nanotechnol. **6**, 1904 (2015).
[3] Cz. Szmytkowski, P. Możejko, M. Zawadzki, K. Maciąg, E. Ptasińska-Denga, Phys. Rev. A**89**, 052702 (2014).
[4] Cz. Szmytkowski, S. Stefanowska, M. Zawadzki, E. Ptasińska-Denga, P. Możejko, J. Chem. Phys. **143**, 064306 (2015).
[5] Cz. Szmytkowski, S. Stefanowska, M. Zawadzki, E. Ptasińska-Denga, P. Możejko, Phys. Rev. A **94**, 042706 (2016).
[6] Cz. Szmytkowski, P. Możejko, M. Zawadzki, E. Ptasińska-Denga, J. Phys. B **48**, 025201 (2015).

*Corresponding author: sstefanowska@mif.pg.gda.pl

To the list of contents

Spectroscopy of trapped $^{138}Ba^{+}$ ions for atomic parity violation

E. A. Dijck*[1], N. Valappol†[1], A. Hofsteenge [1], T. Meijknecht [1], L. Willmann[1], K. Jungmann[1]
1. Van Swinderen Institute, FSE, University of Groningen, The Netherlands

Weak interactions manifest themselves in atomic spectra in electric dipole transition amplitudes and associated light shifts between states of the same parity. A quantitative measurement of the magnitude of these Atomic Parity Violation (APV) effects permits the extraction of $\sin^2\theta_W$, where θ_W is the weak mixing angle (Weinberg angle). This approach is complementary to the studies of weak interactions at high energies. The best measurement at the lowest accessible momentum transfer was performed in atomic Cs with a precision of 1.3% in $\sin^2\theta_W$ [1]. Single trapped heavy ions open the path to a new signature of APV by studying differential light shifts [2]. We investigate laser cooled Ba^+ and Ra^+ ions which have been identified as excellent candidates for this approach because APV effects scales with the atomic number as Z^3. The experimental setup is also suited for an ion based atomic clock promising a relative uncertainty in the range of 10^{-18}[3].
Measurements on a single trapped $^{138}Ba^+$ ion for the detailed understanding of atomic structure to a percent level are presented here. The lowest levels of Ba^+ form a Λ-configuration. The two major laser cooling transitions provide a coherent coupling between the $^2S_{1/2}$ and $^2D_{3/2}$ levels leading to Raman resonances in the spectrum. The one-photon and two-photon components of the line shape are extracted using an eight-level optical Bloch model. This results in an absolute accuracy of the transition frequency of the $^2S_{1/2}$ - $^2P_{1/2}$ transition of 200 kHz and for the $^2D_{3/2}$ - $^2P_{1/2}$ transition of 100 kHz which is an improvement by two orders of magnitude over previous determinations[4]. The spectrum shows the $5d^2D_{3/2} - 6p^2P_{1/2}$ transition of $^{138}Ba^+$ ion in excellent agreement with the calculations using the optical Bloch equations (Fig.(1a)). In order to extract matrix elements we determine the lifetime of the $5d^2D_{5/2}$ state employing quantum jump spectroscopy [5]. (Fig.(1b)). The rather long lifetime makes it sensitive to probe any effects that influence the long term performance of the experiment (i.e. several hours to days). Furthermore, light shifts permit the mapping of weak interaction effects onto the energy splitting between the magnetic sublevels (Fig.(1c)). They are well suited to determine the relevant matrix element in the Ba^+ system. The differential light shift of magnetic substates is proportional to square of the matrix element and the intensity of the laser. All of these measurements are required for the execution of an APV measurement in a single trapped ion.

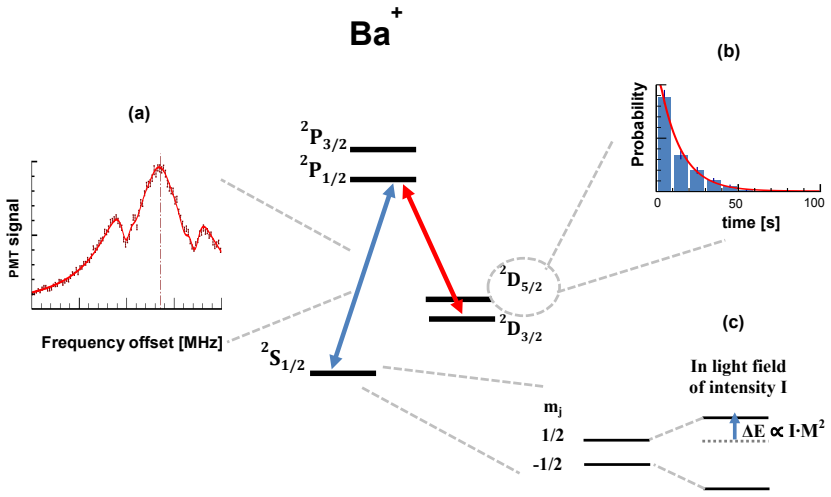

Fig. 1: Level scheme of Ba^+ with insets (a) Transition frequency measurement with Raman resonances (b) A typical lifetime measurement (c) Light shift measurement, M is matrix element.

References

[1] S. C. Bennett and C. E. Wieman, Phys. Rev. Lett. **82**, 2484 (1999).
[2] E. N. Fortson, Phy. Rev. Lett. **70**, 2383 (1993).
[3] M. Nuñez Portela *et al.*, Appl. Phys. B 114, 173 (2014).
[4] E. A. Dijck *et al.*, Phys. Rev. A 91, 060501(R) (2015).
[5] A. Mohanty *et al.*, Hyp. Int. 233, 113 (2015).

*Corresponding author: e.a.dijck@rug.nl
†Corresponding author: n.valappol@rug.nl

To the list of contents

Effect of confinement on the self-annihilation rate of positronium

A. R. Swann*, **D. G. Green, G. F. Gribakin**

School of Mathematics and Physics, Queen's University Belfast, University Road, Belfast BT7 1NN, UK

Positronium (Ps) is a hydrogen-like atom consisting of an electron and a positron. Free Ps annihilates into either two or three γ quanta with lifetimes $\tau = 0.125$ or 142 ns that are determined by QED and depend on its total spin ($S = 0$ for para-Ps or $S = 1$ for ortho-Ps) and on the electron-positron *contact density* η. Here we investigate how Ps confinement (e.g., by pores in condensed-matter systems) affects its contact density and self-annihilation rate.

Measurement of Ps lifetime provides rigorous tests of QED (see, e.g., Ref. [1]). In condensed-matter physics it is used to estimate pore sizes in nanoporous materials and study free volume in polymers; the underlying principle is that the lifetime of long-lived ortho-Ps is reduced by *pickoff* annihilation of the positron with an electron in the bulk [2]. Pore sizes are estimated using the Tao-Eldrup model and its extensions [3], which account for the pickoff annihilation but neglect the effect of confinement on the self annihilation of Ps.

The self-annihilation rate depends on η. For Ps in vacuum, $\eta = \eta_0 = 1/8\pi$ a.u. Ps confinement in pores tends to compress it, increasing η, while Ps interaction with the cavity walls polarizes it, reducing η. In experiment, η is determined by magnetic quenching, lifetime analysis, or three-gamma spectroscopy. In molecular solids with cavity radii $R_c < 1$ nm one typically finds $\eta < \eta_0$, though $\eta > \eta_0$ have also been observed [4].

Several models exist to predict values of η. Stepanov *et al.* [5] used a simple variational wave function for the electron-positron pair in a spherical cavity, with constant electron and positron potentials outside the cavity [equal to the negative of the electron (positron) work functions ϕ_e (ϕ_p), and assuming $\phi_p = \phi_e$]. Marlotti Tanzi *et al.* [6] considered the Ps centre-of-mass motion as free and constructed a crude internal wave function at the cavity wall. Both works showed sizeable lowering of η for $R_c < 1$ nm, but we believe these results are artefacts of the models.

Here we construct the Ps wave function in the cavity as an expansion $\Psi = \sum_{\mu,\nu} C_{\mu\nu}\psi_\nu^- \psi_\mu^+$, where ψ_ν^- (ψ_μ^+) are the electron (positron) states [7], and model the electron- and positron-wall interactions by the potentials $V_{e,p}(r) = -\phi_{e,p}/\{1+\exp[(R_c-r)/\Delta]\}$. To compare with the results of Ref. [6] we use $\phi_e = -0.5$ a.u., $\phi_p = 0.1$ a.u., $R_c = 10$ a.u., and $\Delta = 1$ a.u., so that the electron is repelled by the bulk, while the positron is attracted into it. The wave function $\Psi(\mathbf{r}_e, \mathbf{r}_p)$ is obtained by diagonalization of the Hamiltonian matrix (which includes the electron-positron Coulomb interaction). We calculate the annihilation density $\rho_{\rm ann}(\mathbf{r}) = |\Psi(\mathbf{r},\mathbf{r})|^2$, the Ps centre-of-mass density $\rho_{\rm cm}(\mathbf{r}) = \iint |\Psi(\mathbf{r}_e,\mathbf{r}_p)|^2 \delta[(\mathbf{r}_e+\mathbf{r}_p)/2 - \mathbf{r}]\, d^3\mathbf{r}_e\, d^3\mathbf{r}_p$, and the mean contact density $\langle\eta\rangle = \int \rho_{\rm ann}(\mathbf{r})\, d^3\mathbf{r}$.

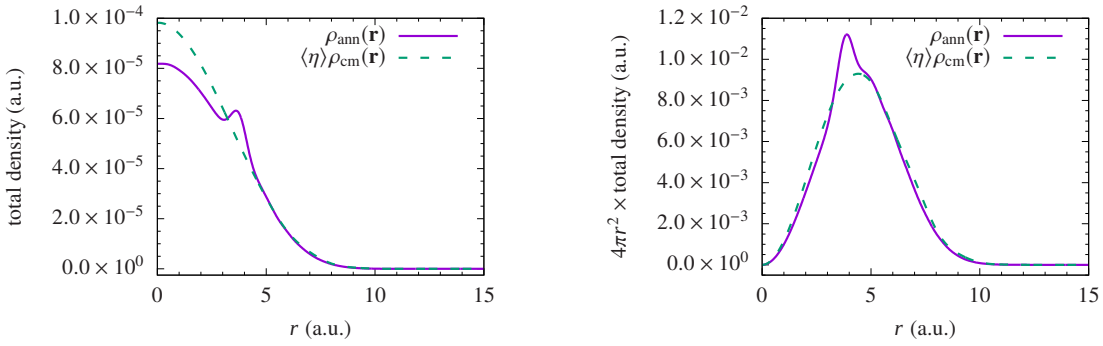

Fig. 1: Comparsion of the Ps annihilation density in the cavity of $R_c = 10$ a.u. with its centre-of-mass density.

We find that despite the attraction of the positron into the bulk, the overall effect of confinement on $\langle\eta\rangle$ is a 9% *increase* from its vacuum value, in contrast to the 15–20% reduction predicted by Ref. [6]. We also find that $\rho_{\rm ann}(\mathbf{r}) \approx \langle\eta\rangle\rho_{\mathbf{cm}}(\mathbf{r})$, which implies that the internal Ps wave function is almost unaffected by its centre-of-mass motion. The large reduction in $\langle\eta\rangle$ predicted by the model of Ref. [6] is due to their strict confinement of the electron inside the cavity. Explanation of the experimental data where $\eta < \eta_0$ thus requires further investigation.

References

[1] Y. Kataoka, S. Asai, and T. Kobayashi, Phys. Lett. B **671**, 219 (2009).
[2] D. W. Gidley, H.-G. Peng, and R. S. Vallery, Ann. Rev. Mat. Res. **36**, 49 (2006); V. P. Shantarovich *et al.*, Macromol. **33**, 7453 (2000).
[3] S. J. Tao, J. Chem. Phys. **56**, 5499 (1972); M. Eldrup, D. Lightbody, and J. N. Sherwood, Chem. Phys. **63**, 51 (1981); K. Wada and T. Hyodo, J. Phys.: Conf. Ser. **443**, 012003 (2013).
[4] G. Consolati and F. Quasso, Solid State Commun. **67**, 1113 (1988); G. Consolati, N. Gambara, and F. Quasso, Z. Phys. D **21**, 259 (1991).
[5] S. V. Stepanov, D. S. Zvezhinskiy, and V. M. Byakov, Mat. Sci. Forum **733**, 7 (2013).
[6] G. Marlotti Tanzi, F. Castelli, and G. Consolati, Phys. Rev. Lett. **116**, 033401 (2016).
[7] R. Brown, Q. Prigent, A. R. Swann, and G. F. Gribakin, Phys. Rev. A **95**, 032705 (2017).

*Corresponding author: aswann02@qub.ac.uk

To the list of contents

Many-body theory of positronium-atom scattering and pickoff annihilation

D. G. Green, A. R. Swann*, G. F. Gribakin

School of Mathematics and Physics, Queen's University Belfast, University Road, Belfast BT7 1NN, UK

Following the success of many-body theory calculations of positron scattering and annihilation rates [1] and γ-ray spectra [2] for noble-gas atoms, we have now developed the many-body theory approach to describe the interaction between an electron-positron pair (positronium, Ps) and many-electron atoms.

Recent experiments on Ps scattering on noble-gas atoms revealed some unexpected trends, e.g., that the scattering cross section becomes very small at low Ps energies [3]. Overall, there is a large uncertainty in Ps-atom scattering data. Theoretically, Ps collisions have been difficult to describe because of the composite nature of both the target and projectile and a significant cancellation between the repulsive static Ps-atom interaction and van-der-Waals-type attraction. An accurate calculation must account for virtual excitation of both objects during the collision, which until now has only been achieved for simple targets, e.g., hydrogen and helium.

In our approach, we confine the Ps-atom system within a hard-wall spherical cavity [4] with the atom at the centre. This allows an efficient discretization of the electron and positron continua. A B-spline basis is used to solve the Dyson equations $\left(H_0^{\pm}+\Sigma^{\pm}\right)\psi^{\pm}=\varepsilon^{\pm}\psi^{\pm}$ for the electron $(-)$ and positron $(+)$ in the field of the target atom. Here, $H_0^{\pm}$ is the Hamiltonian of the electron/positron in the static (Hartree-Fock) field of the atom and $\Sigma^{\pm}$ is the correlation potential. We calculate Σ^{-} in second order (which works well for the electrons [5]) and in Σ^{+} also add the electron-positron ladder series [1]. This yields the bases of electron/positron states $\psi^{\pm}$ with energies $\varepsilon^{\pm}$.

The Ps eigenstates $\Psi=\sum_{\mu,\nu}C_{\mu\nu}\psi_{\nu}^{-}\psi_{\mu}^{+}$ are found from $H\Psi=E\Psi$, where the total Hamiltonian includes the electron and positron parts $(H_0^{\pm}+\Sigma^{\pm})$ and the electron-positron interaction $V+\delta V$, V being the Coulomb interaction and δV the second-order screening contribution due to polarization of the atomic electrons. The boundary condition at the cavity wall enables the scattering phase shifts (and hence the cross section) to be found from the energies E. Figure 1 shows the cross section for Ar in the frozen-target approximation (i.e., without $\Sigma^{\pm}$ and δV) and with full many-body treatment. The origin of the disagreement with experiment is unclear, as our calculations are the most reliable to date and are expected to give the cross sections with $\leq$20% uncertainty.

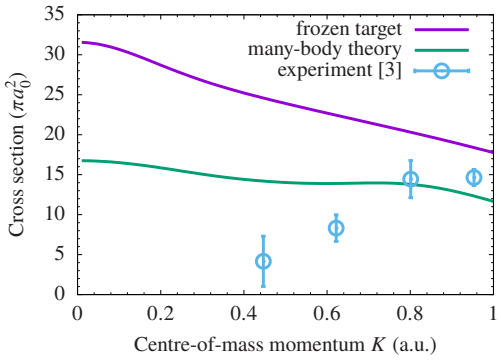

Fig. 1: Ps-Ar scattering cross section in the frozen-target approximation, using many-body theory, and from experiment.

The Ps wave function is also used to investigate *pickoff* annihilation, where the positron from Ps annihilates one of the atomic electrons. The pickoff annihilation rate λ is usually expressed in terms of the dimensionless quantity ${}^1Z_{\rm eff}$ defined by $\lambda=4\pi r_0^2 cn\,{}^1Z_{\rm eff}$, where r_0 is the classical electron radius, c is the speed of light, and n is the gas density. Previous calculations of ${}^1Z_{\rm eff}$ for noble gases [6] underestimated the experimental data [7] by as much as a factor of 10. By accounting for many-body corrections to the annihilation vertex, we obtain values of ${}^1Z_{\rm eff}$ in exact agreement with experiment for He and Ne and within a factor of 2 for Ar, Kr, and Xe.

References

[1] D. G. Green, J. A. Ludlow, and G. F. Gribakin, Phys. Rev. A **90**, 032712 (2014).
[2] D. G. Green and G. F. Gribakin, Phys. Rev. Lett. **114**, 093201 (2015).
[3] S. J. Brawley, S. E. Fayer, M. Shipman, and G. Laricchia, Phys. Rev. Lett. **115**, 223201 (2015).
[4] R. Brown, Q. Prigent, A. R. Swann, and G. F. Gribakin, Phys. Rev. A **95**, 032705 (2017).
[5] M. Ya. Amusia, N. A. Cherepkov, L. V. Chernysheva, D. M. Davidović, and V. Radojević, Phys. Rev. A **25**, 219 (1982).
[6] J. Mitroy and I. A. Ivanov, Phys. Rev. A **65**, 012509 (2001); J. Mitroy and M. W. J. Bromley, Phys. Rev. A **67**, 034502 (2003).
[7] M. Charlton, Rep. Prog. Phys. **48**, 737 (1985).

*Corresponding author: aswann02@qub.ac.uk

To the list of contents

Solution of Hartree-Fock Equations in the B-Spline Basis

David T. Waide*, **D. G. Green, G. F. Gribakin**

School of Mathematics and Physics, Queen's University Belfast, Belfast BT7 1NN, United Kingdom

The Hartree-Fock (HF) method provides a reliable and effective approach to the calculation of atomic structure. This self-consistent-field approximation treats each electron as if it were moving in the average field of all the electrons, providing a good compromise between treating the electron interaction exactly and ignoring it. The HF results can be sufficient in simple problems, but the corresponding electronic states can also be used a basis for higher-order calculations, e.g., using many-body theory.

The solutions to the HF equations may be represented in a B-spline basis, each solution a sum of piece-wise polynomials. In this representation the nonlinear integro-differential HF equations are reduced to a computationally simpler generalised eigenvalue problem, $\hat{H}v = \varepsilon\hat{Q}v$ [1], where $\hat{H}$ and $\hat{Q}$ are the Hamiltonian and overlap matrices.

We solve the generalized eigenvalue equation iteratively for each value of angular momentum in the ground state and the resultant eigenvectors are used to construct the ground- and excited-state wavefunctions. The central potential is spherically symmetric in the case of closed-shell systems, whereas for open shells a spherically averaged approximation is used. Convergence is improved by first running the algorithm for the inner orbitals to self-consistency, before successively including the outer ones. Annealing the nuclear charge during iterations also speeds convergence [2].

Figure 1 shows the ground state wavefunctions for neutral Kr (Z=36), calculated using $n = 100$ splines of order $k = 9$ with a box size $R = 40$ a.u. (Note that inner wavefunctions display characteristic additional nodes due to exchange interaction [3].) Table 1 shows the corresponding orbital energies are compared against reference HF data [4] and experiment [5]. Overall, we find that the method shows good numerically accuracy in addition to fast convergence.

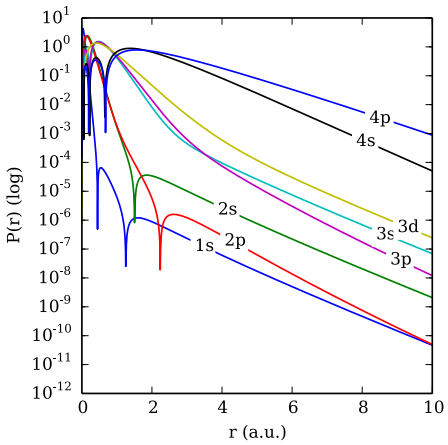

Fig. 1: Ground state wavefunctions for Kr demonstrating additional nodes in inner shells due to exchange interaction.

The B-spline basis provides a particularly efficient representation for many-body theory calculations of atomic processes, e.g., positron annihilation in atoms [6], where it yields a compact and effectively complete set of positron and electron basis states covering both bound states and the positive-energy continuum. Our intention is to extend the calculations of the ground- and excited-state wavefunctions to the relativistic (Dirac-Fock) case, before using them in diagrammatic many-body theory calculations of positron interactions with heavy atoms Xe, Hg, Rn etc.

Table 1: Ground-state energies (in a.u.) for neutral Kr against reference Hartree-Fock and experimental values.

nl	Present	Ref. [4]	Rel. Err.	Abs. Err.	Expt. [2]	Rel. Err.
E_{tot}	−2752.054 982 444	−2752.054 977 350	1.85×10^{-9}	5.09×10^{-6}		
1s	−520.165 468 002	−520.165 468 000	3.73×10^{-12}	1.94×10^{-9}	−526.507 585	0.012
2s	−69.903 082 341	−69.903 082 000	4.88×10^{-9}	3.41×10^{-7}	−70.668 953	0.011
2p	−63.009 785 490	−63.009 785 000	7.78×10^{-9}	4.90×10^{-7}	−62.152 297	0.014
3s	−10.849 466 647	−10.849 466 000	5.96×10^{-8}	6.47×10^{-7}	−10.767 552	0.008
3p	−8.331 501 615	−8.331 501 000	7.38×10^{-8}	6.15×10^{-7}	−7.954 391	0.045
3d	−3.825 234 561	−3.825 234 000	1.47×10^{-7}	5.61×10^{-7}	−3.463 624	0.095
4s	−1.152 935 491	−1.152 935 000	4.26×10^{-7}	4.91×10^{-7}	−1.010 974	0.123
4p	−0.524 187 023	−0.524 187 000	4.39×10^{-8}	2.30×10^{-8}	−0.514 476	0.019

References

[1] C. Froese Fischer, Comp. Phys. Comm. **182**, 1315 (2011).
[2] M. Ya. Amusia and L. V. Chernysheva, *Computation of Atomic Processes* (IoP Publishing, Bristol, 1997).
[3] M. G. Kozlov and V. V. Flambaum, Phys. Rev. A **87**, 042511 (2013).
[4] S. L. Saito, At. Data Nucl. Data Tables **6**, 836 (2009).
[5] A. A. Radtsig and B. M. Smirnov, *Parameters of Atoms and Atomic Ions: Handbook* (Energoatomizdat, Moscow, 1986).
[6] D. G. Green, J. A. Ludlow, and G. F. Gribakin, Phys. Rev. A **90**, 032712 (2014).

*Corresponding author: dwaide01@qub.ac.uk

To the list of contents

Radiative Lifetimes of HeLi$^+$($b^3\Sigma^+$)

Martina Zámečníková[*1], **P. Soldán**[†1]
1. Charles University, Faculty of Mathematics and Physics, Department of Chemical Physics and Optics, Ke Karlovu 3, CZ-12116 Prague 2, Czech Republic

Helium-lithium molecular ion HeLi$^+$ is believed to exist in the early Universe [1]. Its electronically excited states take part in various processes, for example, radiative association [2], non-radiative processes [3], and dissociative recombination [4]. It was also shown that the depopulation of the lowest asymptotically degenerate states of HeLi$^+$($1^3\Pi$, $c^3\Sigma^+$) occurs mainly to the energetically lower excited states $b^3\Sigma^+$ and $a^3\Sigma^+$ [5]. The study, however, did not include spontaneous emission, which could change the abundancies of $b^3\Sigma^+$ and $a^3\Sigma^+$ states.

Our most recent study deals with the radiative lifetimes of HeLi$^+$($b^3\Sigma^+$) [6]. The lifetimes have been calculated quantum mechanically within the dipole approximation. The computational procedure for radiative lifetimes has been adopted from [7], [8] and implemented in our in-house programme, and it includes both bound-bound and bound-free processes.

The radiative lifetimes of ro-vibrational initial bound states with the rotational number J_i equal to $J_i = 0, 1, 2$ have been calculated [6]. The total radiative lifetimes τ_{v_i,J_i} of HeLi$^+$($b^3\Sigma^+$) for the rotationless molecular ion ($J_i = 0$) are shown in Table 1 for several ro-vibrational states. The corresponding energy of the initial ro-vibrational states E_{v_i,J_i}, radiative widths Γ_{v_i,J_i} and their bound-bound $\Gamma^{\mathrm{BB}}_{v_i,i}$ and bound-free $\Gamma^{\mathrm{BF}}_{v_i,J_i}$ contributions are given in Table 1 as well.

The shortest living ro-vibrational state of all the computed states is the lowest one with $v_i = 0, J_i = 0$; its lifetime is 1.30×10^{-6} s.

Table 1: Total radiative lifetimes of several ro-vibrational states with $J_i = 0$ of HeLi$^+$($b^3\Sigma^+$) are shown in seconds. The radiative widths $\Gamma_{v_i,0}$, $\Gamma^{\mathrm{BB}}_{v_i,0}$ and $\Gamma^{\mathrm{BF}}_{v_i,0}$ are in a.u. The energies of the initial ro-vibrational bound states $E_{v_i,0}$ are given in cm^{-1}. The results are in the form $x(-y) = x \times 10^{-y}$.

v_i	$E_{v_i,0}$	$\Gamma^{\mathrm{BB}}_{v_i,0}$	$\Gamma^{\mathrm{BF}}_{v_i,0}$	$\Gamma_{v_i,0}$	$\tau_{v_i,0}$
0	-829.6309	1.86(-11)	2.90(-20)	1.86(-11)	1.30(-6)
1	-746.7588	1.80(-11)	1.80(-18)	1.80(-11)	1.34(-6)
2	-668.5136	1.73(-11)	2.11(-17)	1.73(-11)	1.40(-6)
3	-595.0019	1.65(-11)	1.27(-16)	1.65(-11)	1.46(-6)
4	-526.3181	1.57(-11)	1.64(-15)	1.57(-11)	1.54(-6)
14	-102.1505	5.00(-12)	5.99(-13)	5.60(-12)	4.32(-6)
16	-65.64634	3.63(-12)	4.42(-13)	4.07(-12)	5.94(-6)
27	-1.047121	1.66(-13)	1.97(-14)	1.86(-13)	1.30(-4)
28	-0.509753	9.70(-14)	1.15(-14)	1.08(-13)	2.23(-4)
29	-0.211758	5.02(-14)	5.94(-15)	5.61(-14)	4.31(-4)
30	-0.068538	2.16(-14)	2.55(-15)	2.41(-14)	1.00(-3)
31	-0.014103	6.61(-15)	7.82(-16)	7.39(-15)	3.27(-3)
32	-0.000959	8.97(-16)	1.06(-16)	1.00(-15)	2.41(-2)

References

[1] A. Dalgarno, Journal of Physics: Conference Series **4**, 10 (2005).
[2] L. Augustovičová, M. Zámečníková, W. P. Kraemer, and P. Soldán, Chemical Physics **462**, 65 (2015).
[3] A. K. Belyaev, D. S. Rodionov, L. Augustovičová, P. Soldán, and W. P. Kraemer, Monthly Notices of Royal Astronomical Society **449**, 3323 (2015).
[4] R. Čurík, and F. A. Gianturco Physical Review A **87**, 012705 (2013).
[5] M. Zámečníková, W. P. Kraemer, and P. Soldán, Journal of Quantitative Spectroscopy & Radiative Transfer **191**, 88 (2017).
[6] M. Zámečníková, and P. Soldán, in preparation.
[7] M. I. Chibisov, F. B. Yousif, P. J. T. van der Donk, and J. B. A. Mitchell, Physical Review A **54**, 4997 (1996).
[8] S. Kotochigova, and E. Tiesinga, Journal of Chemical Physics **123**, 174304 (2005).

[*]Corresponding author: martina.zamecnikova@mff.cuni.cz
[†]Corresponding author: pavel.soldan@mff.cuni.cz

To the list of contents

Spectroscopy of ultracold dipolar $^6Li^{40}K$ molecules

Sambit B. Pal[1], Mark Lam[1], Anbang Yang[1], Andrew Laugharn[1], and Kai Dieckmann*[1,2]

1. Centre for Quantum Technologies (CQT), 3 Science Drive 2, 117543 Singapore
2. Department of Physics, National University of Singapore, 2 Science Drive 3, 117542 Singapore

With the creation of dipolar molecules in their ro-vibrational ground state in several expariments, a long-standing scientific goal has been achieved [1-6]. At high phase-space density, such molecules are promising tools for the quantum simulation of a large class of many-body effects and for quantum bit manipulation based on the dipole-dipole interaction. Ultracold heteronuclear dimers of $^6Li^{40}K$ in their deeply-bound ro-vibronic states possess a large electric-dipole moment of 3.6 debye, which makes them a suitable candidate for exhibiting strong effects of the long-range and anisotropic nature of the dipole-dipole interaction. Starting from a sympathetically-cooled, quantum-degenerate mixture of ^6Li and ^{40}K, we create weakly-bound $^6Li^{40}K$ molecules via a magnetic-Feshbach association at 215.6 G. High-resolution laser spectroscopy of the electronically-excited $(1)^1\Sigma$ and $(2)^1\Pi$ potentials of $^6Li^{40}K$ Feshbach-molecules is performed to identify intermediate vibrational states suitable for coherent Raman transfer to the electronic ground state. On the basis of the asymptotic bound state model [7] we discuss the possibility how to address a sole singlet state of the excited state manifold for purpose of efficient transfer. Subsequently, Autler-Townes spectroscopy is performed to investigate the deeply-bound ro-vibrational levels of the electronic ground state of $^6Li^{40}K$ molecules. Here, we present an overview results of the single and two-photon molecular spectroscopy.

References

[1] K. - K. Ni., *et al.*, Science, **322**, 231 (2008).
[2] M. Debatin, doctoral thesis (2013). T. Takakoshi, et al. Phys. Rev. Lett, **113**, 205301 (2014).
[3] Peter K. Molony, *et al.*, Phys. Rev. Lett., **113**, 255301 (2014).
[4] J. W. Park, S. Will, M. W. Zwierlein, Phys. Rev. Lett., **114**, 205302, (2015).
[5] J. W. Park, S. Will, M. W. Zwierlein, New Journ. Phys., **17**, 075016, (2015).
[6] M.Y. Guo, *et al.*, Phys. Rev. Lett., **116**, 205303 (2016).
[7] T. G. Tiecke, *et al.*, Phys. Rev. A, **82**, 042712 (2010).

*Corresponding author: phydk@nus.edu.sg

To the list of contents

Stability of a frequency-comb-based transfer-lock using a passive Fabry-Perot resonator

Sambit B. Pal[1], **Mark Lam**[1], **and Kai Dieckmann**[*1,2]

1. Centre for Quantum Technologies (CQT), 3 Science Drive 2, 117543 Singapore
2. Department of Physics, National University of Singapore, 2 Science Drive 3, 117542 Singapore

We demonstrate a transfer-lock laser frequency stabilization [1] that utilizes a frequency comb (FC) and a radio frequency counter referenced to a GPS frequency standard to compensate for the frequency drifts of two lasers, which are locked to a single passive FabryPerot resonator (FPR). The method requires only one optical phase lock with the FC and allows transfer locking of lasers at wavelengths beyond the usable range of the FC. To attain a large frequency tuning range for the lasers, we implement optical serrodyning. We further demonstrate an effcient scheme to suppress residual amplitude modulation, thereby improving the stability of the Pound-Drever-Hall lock used in this case. The absolute frequency stability was found to be better than 2×10^{-13} on timescales up to 300 s. Hence, together with the frequency stability on short timescales provided by the FPR, this scheme facilitates coherent Raman spectroscopy as needed for an example for the production of ultracold dipolar heteronuclear molecules.

References

[1] S. B. Pal, M. M. Lam, and K. Dieckmann, Optics Letters, **41**, 23, 5527-5530 (2016).

*Corresponding author: phydk@nus.edu.sg

To the list of contents

Experimental characterisation of the double minimum $3^1\Sigma_u^+$ state in Rb_2 up to the dissociation limit

W. Jastrzebski[*1], **P. Kowalczyk**[†2], **J. Szczepkowski**[1]

1. Institute of Physics, Polish Academy of Sciences, Al.Lotników 32/46, 02-668 Warszawa, Poland

2. Institute of Experimental Physics, Faculty of Physics, University of Warsaw, ul. Pasteura 5, 02-093 Warszawa, Poland

Spectacular progress in experiments on ultracold diatomic alkali metal molecules has brought about particular interest of the cold physics community in molecular states with broad potential wells, such as double minimum and 'shelf' states. Such states can be effectively excited to the highest bound levels close to the dissociation limit in photoassociation or magnetoassociation processes. They can be also conveniently used as the intermediate states for resonantly enhanced multiphoton ionization of cold molecules. Finally, as they simultasneously display high probability of transitions to low levels in the ground electronic state, they may enable transfer of cold molecules to the absolute rovibrational ground state. It should be also noted that states with broad potential wells are well suited for investigation of wave packet dynamics, because their closely spaced vibrational levels allow for creation of packets with long spreading times.

In this contribution we present an experimental study of the $3^1\Sigma_u^+$ state of rubidium dimer, characterised by a potential curve with two minima, resulting from avoided crossing with the higher lying $4^1\Sigma_u^+$ state [1]. The state is observed through the $3^1\Sigma_u^+ \leftarrow X^1\Sigma_g^+$ transition recorded under rotational resolution using the highly sensitive V-type optical-optical double resonance polarisation labelling spectroscopy technique [1]. Rb_2 molecules (natural isotopic composition) are produced in a linear heat pipe oven in a presence of a few Torr of helium buffer gas. The apparatus provided us with rotationally resolved molecular spectra with both resolution and accuracy of about 0.05 cm^{-1}. In the investigated spectral range of 21700 - 23900 cm^{-1} we identify more than 2000 molecular lines, the frequencies of which are converterd to energies of the upper state levels using the precisely known ground state level energies [2]. The highest observed rovibrational level, ($v = 136$, $J = 86$) is located ca. 2.5 cm^{-1} below the atomic asymptote. The data are used to construct the potential energy curve of the $(3)^1\Sigma_u^+$ state with the pointwise Inverted Perturbation Approach (IPA) method [3]. The resulting potential (Fig. 1) reproduces the observed energy levels with a standard deviation of 0.07 cm^{-1} and is isotopically consistent with regard to the $^{85}Rb_2$ and $^{85}Rb^{87}Rb$ molecules.

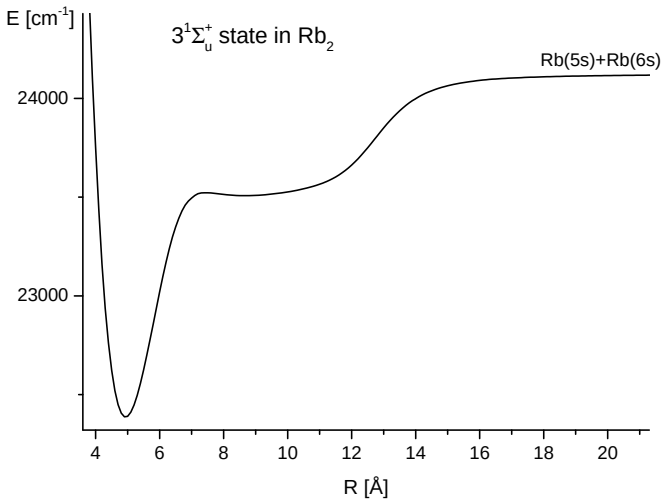

Fig. 1: The experimentally derived potential energy curve of the $3^1\Sigma_u^+$ state in Rb_2. The outer turning point for the highest observed level is $R_{out} \approx 20.1$ Å.

References

[1] W. Jastrzebski, J. Szczepkowski, P. Kowalczyk, A. R. Allouche, P. Crozet, and A. J. Ross, J. Chem. Phys. **143**, 044308 (2015).
[2] J. Y. Seto, R. J. Le Roy, J. Vergès, and C. Amiot, J. Chem. Phys. **113**, 3067 (2000).
[3] A. Pashov, W. Jastrzebski, and P. Kowalczyk, Comp. Phys. Commun. **128**, 622 (2000).

[*]Corresponding author: jastr@ifpan.edu.pl
[†]Corresponding author: Pawel.Kowalczyk@fuw.edu.pl

To the list of contents

X-Ray Spectroscopy of the KLL-Dielectronic Recombination Transitions with a Heidelberg Compact EBIT

P. Micke[*1,2], **S. Bernitt**[1,3], **S. Kühn** [1], **A. Surzhykov**[2], **T. Leopold**[2], **S. A. King**[2], **T. Pfeifer**[1], **P. O. Schmidt**[2,4], **J. R. Crespo López-Urrutia**[1]

1. Max-Planck-Institut für Kernphysik, Saupfercheckweg 1, 69115 Heidelberg, Germany
2. Physikalisch-Technische Bundesanstalt, Bundesallee 100, 38116 Braunschweig, Germany
3. Institut für Optik und Quantenelektronik, Friedrich-Schiller-Universität Jena, 07737 Jena, Germany
4. Institut für Quantenoptik, Leibniz Universität Hannover, Welfengarten 1, 30167 Hannover, Germany

Highly charged ions (HCIs) are of great spectroscopic interest as they are predominant in the visible universe. However their production in the laboratory is demanding. Electron beam ion traps (EBITs) are devices dedicated for that purpose. An electron beam is focused by a strong and inhomogeneous magnetic field in order to ionize neutral atoms and breed high charge states efficiently. After production, HCIs are radially confined by the negative space charge of the electron beam and axially by the electrostatic potential of the trap electrodes. Interaction of the keV electron beam with the trapped ion cloud results in the emission of X-ray radiation.

To ease experimental access to HCIs with the largest possible solid angle for the observation of the ions, we have developed a novel set of high performance room-temperature, compact EBITs [1]. The electron beam has a tunable energy from < 0.1 keV up to 8 keV and a current of up to 80 mA. The beam is compressed by a 0.86 T magnetic field at the trap center. The geometry offers an outstanding large angle of view of 58° along 16 mm for each of four slits through the trap electrode. One of the EBITs, the PTB-EBIT which will later be operated at the Physikalisch-Technische Bundesanstalt, features a retractable in-vacuum germanium X-ray detector. The Ge crystal can be operated at a very close distance of only a few centimeters from the ion cloud.

We are currently carrying out accurate X-ray measurements covering KLL dielectronic resonances. In this resonant process, a keV electron of the beam is captured in the L shell while the released energy is used to excite a second bound electron from the K to the L shell. The excited state decays by emitting K_α radiation. The resonances appear at different electron beam energies for different charge states. The goal of this work is to precisely determine the relative peak positions and to compare them with theoretical calculations in order to benchmark atomic structure calculations and make comparisons of the relative resonance strengths.

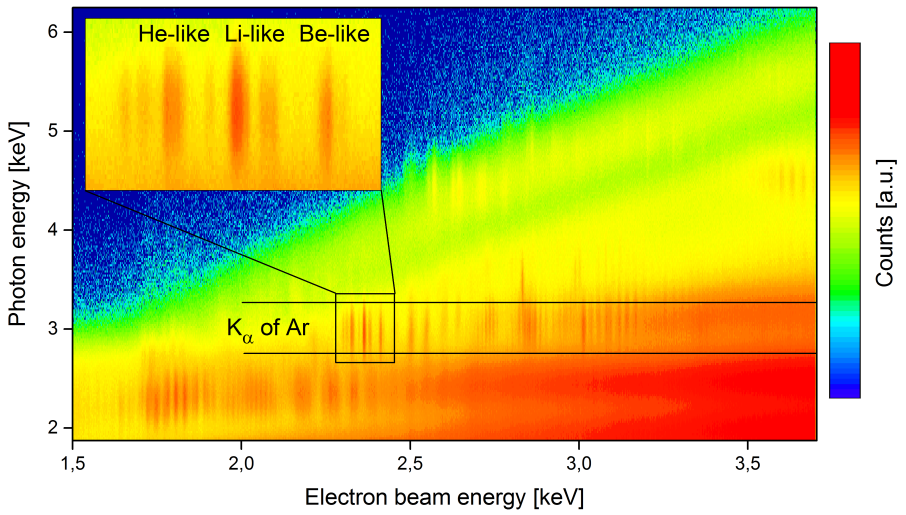

Fig. 1: X-ray spectra of highly charged Argon. The electron beam energy was tuned from 1.5 keV to 3.7 keV. The inset shows the KLL dielectronic recombination, revealing He-like, Li-like, and Be-like Argon. Resonances of Ba and W from the thermionic cathode are also visible.

References

[1] P. Micke *et al.*, in preparation.

*Corresponding author: peter.micke@quantummetrology.de

To the list of contents

Single photon transient hot electron ionization of C_{60}

K. Hansen[*] [1] **V. Zhaunerchyk**[2]

1. Tianjin International Center of Nanoparticles and Nanosystems, Tianjin University, 92 Weijin Road, Nankai district, Tianjin 300072, P.R.China

2. Department of Physics, University of Gothenburg, Sweden

One photon molecular ionization is conventionally understood as emission of an electron in state-to-state processes, involving only a few, well defined electronic states. Multiphoton ionization, on the other hand, may proceed via several different mechanisms, such as above threshold ionization, field ionization and thermionic emission. In addition, electrons can be emitted in a quasi-thermal process where the electronic degrees of freedom act as a thermal subsystem which is heated by e.g. laser pulses while the vibrational motion remains cold for a good fraction of a picosecond [1].

This mechanism has been shown to be responsible for the ionization of a number of large polycyclic aromatic hydrocarbons exposed to light with photon energy far below the ionization energy [2]. The ionization requires a laser pulse of duration on the order of the electron-vibration coupling time or shorter, to avoid the premature dissipation of excitation energy into the vibrational motion.

We have recently shown that C_{60} also ionizes with this mechanism after absorption of a *single* photon [3]. The measurements were performed at the ELETTRA Synchrotron Light Source in Trieste (Italy) with photons of energies between 13.5 and 60 eV. The primary experimental evidence is a persistent and strong component of low kinetic energy electrons in the photoelectron spectra. The electron momenta are spherically distributed with no remaining sign of the light polarization and can be described with a Boltzmann factor with a temperature of 1-2 eV, or $1\text{-}2\cdot10^4$ K[4]. Additionally, the threshold and channel (viz. single and double C_2 loss from C_{60}^+) for subsequent fragmentation of the produced cation agrees quantitatively with the previously measured thermal behavior. The presence of this type of ionization for photon energies above 30 eV which reach beyond the valence band requires that the photon creates a particle-hole state with at least two particles and two holes.

References

[1] E .E.B. Campbell, K. Hansen, K. Hoffmann, G. Korn, M. Tchaplyguine, M. Wittmann, I.V. Hertel, *From Above Threshold Ionization to Statistical Electron Emission: The Laser Pulse Duration Dependence of C_{60} Photoelectron Spectra* Phys. Rev. Lett. **8**4 2128 (2000).

[2] M . Kjellberg, A.V. Bulgakov, M. Goto, O. Johansson, and K. Hansen, *Femtosecond electron spectroscopy of coronene, benzo[GHI]perylene and anthracene* J. Chem. Phys. **1**33 074308 (2010).

[3] K lavs Hansen, Robert Richter, Michael Alagia, Stefano Stranges, Luca Schio, Peter Salén, Vasyl Yatsyna, Raimund Feifel, and Vitali Zhaunerchyk, *Single Photon Thermal Ionisation of C_{60}* Phys. Rev. Lett. **1**18 103001 (2017)

[4] K . Hansen, to be published

[*]Corresponding author: klavshansen@tju.edu.cn

To the list of contents

EUV/SXR spectroscopy of Ge Laser-Produced Plasma

O. Maguire[*1], **D. Kos**[1], **E. Sokell**[1]
1. Atomic, Molecular and Plasma (Spec) group, School of Physics, University College Dublin, Belfield Dublin 4 Ireland

Laser-Produced Plasmas (LPP) may be used to form EUV/SXR light sources with a high conversion efficiency. The wavelength of the source for EUV lithography was chosen to be 13.5 nm due to the availability of MoSi multilayer mirrors. MoSi multilayer mirrors have a high reflectivity of 72% at $13.5 \pm 2\%$ nm into the bandwidth of the mirrors [1]. Tin LPPs can be used as light sources for EUV lithography because of their high conversion efficiency experimentally $\approx 6\%$ [2] and steady state models showing a possible conversion efficiency of $\approx 9\%$ [3]. $4p^6 4d^n - 4p^5 4d^{n+1}$, $4d^n - 4d^{n-1}5p$ and $4d^n - 4d^{n-1}4f$ transitions of Sn VII - Sn XIV each form an Unresolved Transition Array (UTA). These UTAs all combine at 13.5 nm [4]. LPPs of Ge emit in this spectral region and could be used as an EUV/SXR light source [5].

In this work the Hartree-Fock with Configuration-Interaction (HFCI) code of Cowan [6] was used to identify previously unreported open 3d transitions of Ge VII - Ge X, and previously identified transitions of Ge VI and Ge VII [7]. The spectra were recorded on an EUV Jenoptik spectrometer with a spectral range of 9.7 to 18 nm. The spectrometer has been wavelength and intensity calibrated at BESSY II. The spectra of Ge plasmas were created with 2 different lasers. A Q-switched Nd:YAG laser with a pulse energy of 978 ± 6 mJ in 5.4 ± 0.3 ns, focused using a 13 cm uncoated BK7 plano-convex lens and a TEA CO_2 laser, with a plasma shutter [8] to remove the 2 μs N_2 tail, leaving a 50 mJ in 50 ns laser pulse, focused using a 5 cm ZnSe lens. The spectrometer was at 45^o to the incident laser beam focused normal to a planar target. The experimental rms error on the calibration using known lines of oxygen is ± 0.0042 nm. The table below details some of the identified lines within the spectral region. Line identification of Ge VII - Ge X $3p^6 3d^n - 3p^5 3d^{n+1}$, $3d^n - 3d^{n-1}4p$, $3d^n - 3d^{n-1}4f$ of an optically thin Ge plasma will be presented. A comparison between the optically thick Nd:YAG and optically thin CO_2 laser-produced plasmas will be given.

Table 0: Some previously identified and unidentified GeVI, GeVII and GeVIII lines.

Experiment	Cowan	Sugar[7]	Transition
12.1436	12.1508	12.8309	Ge VI $3p^6 3d^9(^2D_{3/2}) - 3p^5 3d^{10}(^2P_{1/2})$
12.8426	12.8374	12.2638	Ge VI $3p^6 3d^9(^2D_{5/2}) - 3p^5 3d^{10}(^2P_{3/2})$
14.0359	14.0405	14.0015	Ge VI $3d^9(^2D_{5/2}) - 3d^8 4f^1(^2D_{5/2})$
14.1373	14.1253	14.0914	Ge VI $3d^9(^2D_{3/2}) - 3d^8 4f^1(^2D_{3/2})$
14.1967	14.1946	14.0465	Ge VI $3d^9(^2D_{5/2}) - 3d^8 4f^1(^2F_{7/2})(^3P)$
14.3156	14.3163	14.1561	Ge VI $3d^9(^2D_{5/2}) - 3d^8 4f^1(^2F_{7/2})(^1D)$
17.1393	17.1464	17.1380	Ge VII $3d^8(^1G_{8/2}) - 3d^7 4p^1(^1F_{6/2})(^2D)$
16.6463	16.6383	16.6609	Ge VII $3d^8(^3P_{4/2}) - 3d^7 4p^1(^3D_{6/2})(^2D)$
17.2220	17.1981	17.2096	Ge VII $3d^8(^3P_{4/2}) - 3d^7 4p^1(^3P_{4/2})(^2D)$
12.4790	12.4849		Ge VII $3d^8(^3P_{4/2}) - 3d^7 4f^1(^3P_{4/2})(^4F)$
11.4689	11.4872		Ge VII $3d^8(^3F_{8/2}) - 3d^7 4f^1(^3D_{6/2})(^2H)$

References

[1] C. Wagner and N. Harned, Nature Photonics 4, 24 - 26 (2010) .
[2] A. Cummings, G. O'Sullivan, P. Dunne, E. Sokell, N. Murphy and J. White, Journal of Physics D: Applied Physics **38**, 604–616 (2005).
[3] M. M. Basko, Physics of Plasmas **23**, 083114 (2016).
[4] P. Hayden, A. Cummings, N. Murphy, G. O'Sullivan, P. Sheridan, J. White, and P. Dunne, Journal of Physics D: Applied Physics **99**, 093302 (2006).
[5] B. Li, H. Hara, Y. Suzuki, G. Arai, T. Higashiguchi, H. Ohashi, W. Jiang, T. Makimura, H. A. Sakaue, C. Suzuki, D. Kato, I. Murakami, P. Dunne, E. Long, P. Sheridan, X. Chen, and G. O'Sullivan, Journal of Applied Physics **118**, 073302 (2015)
[6] R. D. Cowan, The Theory of Atomic Structure and Spectra, University of California Press, Berkeley, (1981).
[7] J. Sugar and A. Musgrave, Journal of Physical and Chemical Reference Data **22**, 1213 (1993)
[8] N. Hurst, and S. S. Harilal, Review of Scientific Instruments **80**, 035101 (2009)

*Corresponding author: oisin.maguire@ucdconnect.ie

To the list of contents

Intra-cavity high-order harmonic generation for XUV spectroscopy of highly charged ions

Janko Nauta[*1], **Andrii Borodin**[1], **Julian Stark**[1], **Peter Micke**[1,2], **Lisa Schmöger**[1,2], **Maria Schwarz**[1,2], **José R. Crespo López-Urrutia**[1], **Thomas Pfeifer**[1]

1. Max-Planck-Institut für Kernphysik, Saupfercheckweg 1, 69117 Heidelberg, Germany
2. Physikalisch-Technische Bundesanstalt, Bundesallee 100, 38116 Braunschweig, Germany

Highly charged ions (HCI) with just a few tightly bound electrons offer many advantages over neutral and singly charged atomic systems for probing fundamental physics. They have been recently proposed as future frequency standards [1-4]. Their low polarizability decreases the sensitivity to external perturbations such as black body radiation and laser-induced shifts, which opens possibilities for reaching relative accuracies in the range of 10^{-19} [4]. Furthermore, specific HCI are extremely sensitive to possible variation of the fine-structure constant α [5].

In order to exploit these advantages of HCI, one needs to determine their transition energies with ultra-high accuracy. Recent progress at the MPIK has enabled the transfer of HCI from an electron beam ion trap (EBIT), where MK temperatures prevail, into a cryogenic linear Paul trap, where they are sympathetically cooled down to the mK regime with Be^+ ions [6]. This paves the way for the first high resolution laser spectroscopy of HCI.

Since the electronic transitions in HCI are shifted to higher photon energies in comparison to neutral atoms, this new project aims at performing spectroscopy in the extreme ultraviolet (XUV) region. To this end, we are developing an XUV light source, using high-order harmonic generation to coherently transfer all modes of an infrared frequency comb towards the XUV [7]. The resulting XUV comb will enable us to perform spectroscopy on HCI at unprecedented accuracies.

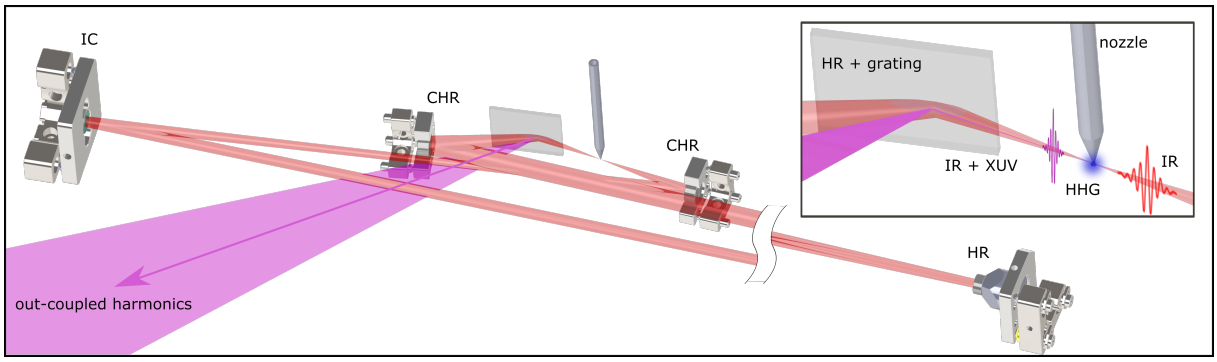

Fig. 1: Overview of the femtosecond enhancement cavity. Infrared (IR) pulses are coupled in through the in-coupling mirror (IC) and circulate in the cavity composed of four other high-reflective (HR) mirrors. In one of this mirrors, a shallow grating structure is etched. The inset shows high-order harmonic generation (HHG) inside the tight focus of the cavity, created by the two curved mirrors in the middle (CHR). The high-order harmonics (labeled XUV) propagate collinearly with the IR beam, and are coupled out of the cavity using the minus-first order diffraction of the grating.

For reaching the laser-intensity required for HHG ($\sim 10^{13}$ W/cm^2) we use an enhancement cavity (shown in Figure 1) to amplify the femtosecond pulses of a stabilized frequency comb with a repetition rate of 100 MHz. The cavity is designed to have a very tight focus ($w_0 \approx 15\ \mu$m) and resides in an ultra-high vacuum chamber. At the focus, a target gas is introduced and an XUV spectrum is generated, containing a copy of the IR frequency comb at odd multiples of the original frequency. We use a shallow, 2000 lines/mm diffraction grating to separate the XUV light from the IR light circulating in the cavity [8]. The different harmonic orders are spatially separated and only the wavelength of interest will be guided to the cold and trapped HCI, of which finally absolute transition energies can be determined.

References

[1] M. S. Safronova, V. A. Dzuba, V. V. Flambaum, U. I. Safronova, S. G. Porsev, and M. G.Kozlov, Phys. Rev. Lett. **113**, 030801 (2014).
[2] V. A. Dzuba, V. V. Flambaum, and Hidetoshi Katori Phys. Rev. A **91**, 022119 (2015).
[3] M. S. Safronova, V. A. Dzuba, V. V. Flambaum, U. I. Safronova, S. G. Porsev, and M. G. Kozlov, Phys. Rev. A **90**, 042513 (2014).
[4] A. Derevianko, V. A. Dzuba, and V. V. Flambaum, Phys. Rev. Lett. **109**, 180801 (2012).
[5] J. C. Berengut, V. A. Dzuba, V. V. Flambaum, and A. Ong, Phys. Rev. Lett. **109**, 070802 (2012).
[6] L. Schmöger, O. O. Versolato, M. Schwarz, M. Kohnen, A. Windberger, B. Piest, S. Feuchtenbeiner, J. Pedregosa-Gutierrez, T. Leopold, P. Micke, A. K. Hansen, T. M. Baumann, M. Drewsen, J. Ullrich, P. O. Schmidt, and J. R. Crespo López-Urrutia, Science **347**, 6227 (2015).
[7] C. Benko, T. K. Allison, A. Cingöz, L. Hua, F. Labaye, D. C. Yost, and J. Ye, Extreme ultraviolet radiation with coherence time greater than 1 s, Nat. Photon. **8**, 530 (2014).
[8] D. C. Yost, T. R. Schibli, and J. Ye, Efficient output coupling of intracavity high-harmonic generation, Opt. Lett. **33**, 1099-1101 (2008).

*Corresponding author: nauta@mpi-hd.mpg.de

To the list of contents

Ultracold Lithium for Sympathetic Cooling of Dipolar Molecules

S. Wright*, **Thomas Wall, Michael Tarbutt**
Blackett Laboratory, Imperial College, London, SW7 2BZ, UK

The ability to produce large ensembles ($N \sim 10^6$) of ultracold dipolar molecules would be beneficial to many precision measurement experiments, and presents exciting opportunities for quantum simulation and cold chemistry. A number of molecule traps suitable for cold molecules have been realized, most recently magneto-optical trapping of the monofluoride radicals SrF [1] and CaF [2].

A viable option for further cooling of molecules is sympathetic cooling with an ultracold atomic gas. We present progress towards using an ultracold Lithium gas as a refrigerant for cold molecules in a microwave trap. Currently we have samples of ^{7}Li at 50 μK and intend to use these to characterise our microwave trap.

References

[1] J. F. Barry, D. J. McCarron, E. B. Norrgard, M. H. Steinecker, and D. DeMille. Magneto-optical trapping of a diatomic molecule. Nature, 512(7514):286–289, Aug 2014.
[2] S. Truppe, H. J. Williams, M. Hambach, L. Caldwell, N. J. Fitch, E. A. Hinds, B. E. Sauer, M. R. Tarbutt, Molecules cooled below the Doppler limit, arXiv:1703.00580 [physics.atom-ph].

*Corresponding author: s.wright15@imperial.ac.uk

To the list of contents

Rydberg spectroscopy of ytterbium

H. Lehec[*1], **A. Zuliani**[1], **W. Maineult**[1], **E. Luc-Koenig**[1],**P. Pillet**[1], **P. Cheinet**[1]
1. Laboratoire Aimé Cotton, Bat. 505 Campus d'Orsay,
91405 Orsay, France

Rydberg atoms offers an ideal platform for the study of strongly interacting systems. However, usual techniques for imaging or trapping atoms are unavailable in alkali Rydberg atoms. The aim of this experiment is to optically manipulate atoms in Rydberg states using a divalent atom: ytterbium.

We present our results[1] of laser and microwave spectroscopy of highly excited Rydberg levels of Ytterbium. We have improved the precision over previous absolute measurements[2] by two or more orders of magnitude, now reaching around 10 MHz, which opens new perspectives on two-electron atoms. Our analysis based on Multichannel Quantum Defect Theory (MQDT) demonstrates, as shown in figure 1 for the $^1S_0$ series, a good understanding of the interactions between the two electrons in such levels. In particular, we need for the first time to include in the theory a channel with no bound state to account accurately for the level perturbations.

Once excited to the Rydberg state, the atom has still a valence electron to optically manipulate its external degrees of freedom. In this purpose, we have recently performed ionic core spectroscopy, these results will also be presented.

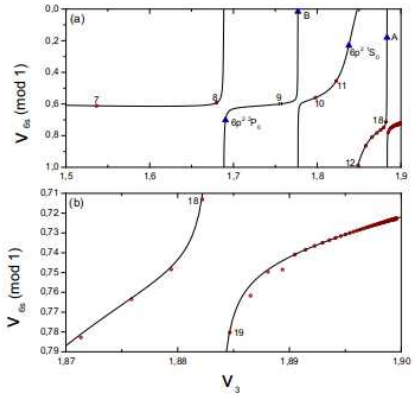

Fig. 1: Result of the MQDT analysis for the $^1S_0$ Rydberg serie presented in a Lu-Fano plot. (a) combines previous data for low levels up to n=22 and our measurements from n=23 to n=80 of the 6sns $^1S_0$ levels. (b) shows a zoom on levels from n=15 to n=80 allowing to observe the precision improvement.

References

[1] H. Lehec et al., in preparation for PRA
[2] Aymar et al., J. Phys. B. **13**, 1089 (1980).

*Corresponding author: henri.lehec@u-psud.fr

To the list of contents

Inverse crossover resonances applied to ^{171}Yb laser cooling

J. J. McFerran[*1], **L.A. Salter**[1] **Emeric de Clercq**[†2]
1. School of Physics, University of Western Australia, 6009, Crawley, Australia
2. LNE-SYRTE, Observatoire de Paris, PSL Research University, CNRS, Sorbonne Universités, UPMC Univ. Paris VI, 61 avenue de l'Observatoire, 75014 Paris, France

Explorations in degenerate Fermi gases [1–3], quantum many body simulations with lattices [4–6], and atomic clocks [7–9] each make use of neutral ytterbium. A common approach to producing atomic cloud temperatures at a few tens of micro-Kelvin is to employ two stages of laser cooling with 399 nm and 556 nm light, where the latter exploits the $(6s^2)\ ^1S_0 - (6s6p)\ ^3P_1$ inter-combination line ($\Gamma/2\pi$= 184 kHz and corresponding Doppler cooling limit of 4.4 μK). To generate frequency-stable 556 nm light, stabilization by locking to a high-Q optical cavity is often employed is [10, 11]. Rather than take this approach, and despite the low scattering rate associated with the intercombination line, we employ sub-Doppler spectroscopy upon a thermal Yb beam that leads to a Zeeman slower and magneto-optical trap. In doing so, we have identified an inverted Lamb dip with the $^1S_{0F=1/2} - {}^3P_{1F'=3/2}$ and $^1S_{0F=1/2} - {}^3P_{1F'=1/2}$ hyperfine transitions in ^{171}Yb. The enhancement in fluorescence is found to be due to an inverted crossover resonance (ICR), where the principal lines involved in the crossover are symmetrically separated Zeeman transitions. We use a four-level rate equation model to help validate the nature of the resonance [12]. In the case of $F' = 3/2$ (upper state) the ICR can be used to frequency stabilize laser light for cooling of ^{171}Yb. While that of the $F' = 1/2$ ICR acts as a rather robust frequency reference with an overall fractional frequency uncertainty in the low 10^{-11} range.

An example of the ICR is shown in Fig. 1(a) for the $F' = 1/2$ hyperfine line, a bias B-field of 0.10 mT and first harmonic detection. The amplitude of the FM was 0.4 MHz and the intensity 53 I_{sat}. The discriminator provides a narrow-line feature for laser frequency stabilization. Fig. 1(b) shows that changing the instability of the laser frequency does not influence the temperature of a cloud of ^{171}Yb atoms in at dual-wavelength magneto-optical trap (over the range tested). Cycle-to-cycle temperature fluctuations exhibit a standard deviation of $\sim 2\mu$K.

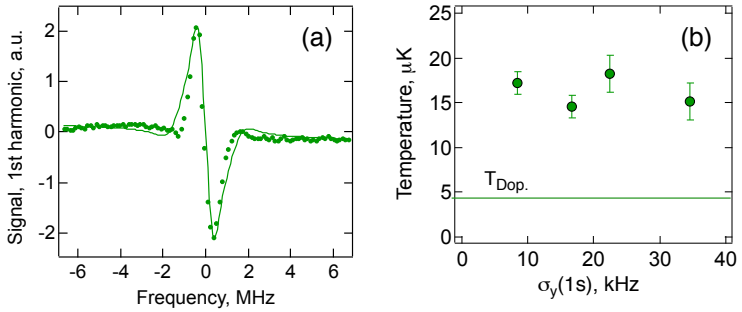

Fig. 1: (a) The ICR resonance for the $^1S_0 - {}^3P_1(F' = 1/2)$ line with first harmonic signal detection. Overlaid is a curve generated with a four-level rate equation model based on the experimental parameters. (b) ^{171}Yb cloud temperature for a range of frequency instabilities (at $\tau = 1$ s).

Similar inverted crossover resonances are expected to occur whenever the atom has a nuclear spin of 1/2 and the transition has a sufficiently narrow natural linewidth; other examples include the intercombination lines in ^{199}Hg ($\Gamma/2\pi$=1.3 MHz), ^{111}Cd and ^{113}Cd ($\Gamma/2\pi$=65 kHz). In the case of ^{173}Yb where $I = 5/2$ we see that the ICR is extremely weak.

References

[1] Hansen, A. *et al. Phys. Rev. A* **84**, 011606 (2011).
[2] Fukuhara, T., Takasu, Y., Kumakura, M. & Takahashi, Y. *Phys. Rev. Lett.* **98**, 030401 (2007).
[3] Dorscher, S. *et al. Rev. Sci. Instrum.* **84**, 043109 (2013).
[4] Scazza, F. *et al. Nature Physics* **10**, 779–784 (2014).
[5] Schreiber, M. *et al. Science* **349**, 842–845 (2015).
[6] Yamamoto, R., Kobayashi, J., Kuno, T., Kato, K. & Takahashi, Y. *New Journal of Physics* **18**, 023016 (2016).
[7] Schioppo, M. *et al. Nature Photonics* **11**, 48–52 (2017).
[8] Takamoto, M. *et al.* their applications. *Comptes Rendus Physique* **16**, 489 (2015).
[9] Nemitz, N. *et al. Nat. Photon.* **10**, 258–261 (2016).
[10] Kuwamoto, T., Honda, K., Takahashi, Y. & Yabuzaki, T. *Phys. Rev. A* **60**, 745 (1999).
[11] Maruyama, R. *et al. Phys. Rev. A* **68**, 011403 (2003).
[12] Salter, L. A., de Clercq, E. & McFerran, J. J. *arXiv* 1611.03249v3

[*]Corresponding author: john.mcferran@uwa.edu.au
[†]Corresponding author: emeric.declercq@obspm.fr

To the list of contents

Laser- induced fluorescence and optogalvanic spectroscopy used to find Lande g_J factors of La I.

Ł. M. Sobolewski[1,2*], **Laurentius Windholz**[2], **Jerzy Kwela**[†1]

1. Institute of Experimental Physics, Faculty of Mathematics, Physics and Informatics, University of Gdańsk, 80-308, Poland

2. Institute of Experimental Physics, Graz University of Technology, Petersgasse 16, A-8010 Graz, Austria

Landé- g_J factors of 61 energy levels of La I, found from investigations of 66 spectral lines in the wavelength range 562.959÷609.537 nm, were determined.

As a source of free La atoms a hollow cathode lamp with argon as a buffer gas was used. In order to investigate the Zeeman effect, we placed a strong permanent magnet inside a container with liquid nitrogen, which was used for cooling the hollow cathode lamp. In that way we obtained a field of about 800 G in the observation region. The cooling helps to maintain the stability of the discharge and also reduces the Doppler width of the spectral lines (down to some hundreds of MHz). The Zeeman effect studies were performed for two states of linear polarization of the exciting laser light (produced by a half- wave plate and a Glan prism polarizer).

For the observation of the Zeeman hf structure we used the optogalvanic spectroscopy and the LIF technique. Setups for both these measuring techniques were described in our papers [1, 2]. As an example the figure below presents the spectra of the 595.275 nm line (π and σ patterns).

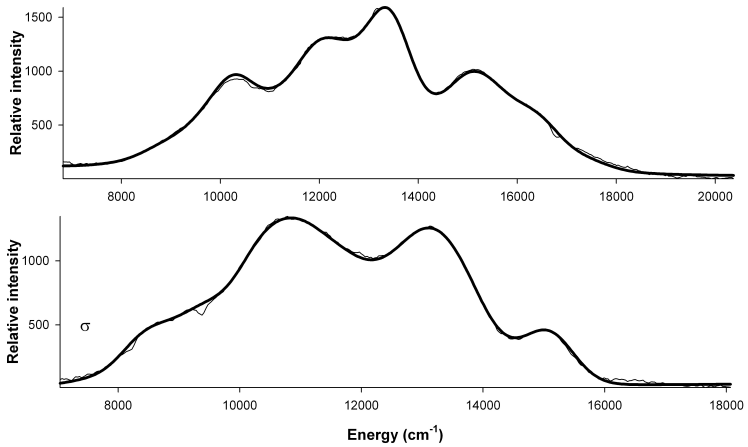

Fig. 1: Experimental and simulated Zeeman structures of 595.275 nm line (π and σ patterns).

Our experiments proved that optogalvanic spectroscopy and LIF method can be successfully used for measurements of Lande g_J- factors. An advantage of optogalvanic spectroscopy is the ability to observe the Zeeman effect of very weak atomic lines unobservable by other spectroscopic methods. However, in the case of close lying neighbouring lines the optogalvanic spectrum contains overlapping structures what can create problems in the analysis. The LIF technique is free from this problem, but can be used only for relatively strong lines.

Ł. S. would like to thank University of Gdańsk for support by BMNiD grant - 2017.

References

[1] Ł. M. Sobolewski, L. Windholz, J. Kwela, "Zeeman effect of weak La I lines investigated by the use of optogalvanic spectroscopy", J. Quant. Spect. Rad. Transfer 189 221 - 227 (2017).

[2] Ł. M. Sobolewski, L. Windholz and J. Kwela, "Laser Induced Fluorescence spectroscopy used for the investigation of Landé g_J factors of praseodymium energy levels", J. Quant. Spect. Rad. Transfer 194 24-30 (2017).

*Corresponding author: lukasz.sobolewski@ug.edu.pl

†Corresponding author: fizjk@ug.edu.pl

To the list of contents

Lifetimes and Transition Probabilities for High-Lying Levels in Astrophysically Interesting Atoms Using Multi-Photon Excitation

L. Engström*[1], H. Lundberg[1], H. Nilsson[2], H. Hartman[2,3]

1. Department of Physics, Lund University, Box 118, 221 00 Lund, Sweden
2. Lund Observatory, Lund University, Box 43, 22100 Lund, Sweden
3. Applied Mathematics and Material Science, Malmö University, 20506 Malmö, Sweden

In spectroscopy of stellar atmospheres the atomic transitions most often appear as absorption lines. To use these lines for quantitative analysis of the population distribution and abundance determinations, reliable transition probabilities or f-values must be available. A standard technique for this purpose is to combine measurements of the lifetime of the upper level with experimentally determined branching fractions from an intensity calibrated source. Since experimental studies are naturally limited in the number of levels that can be investigated, it is very fruitful to use the experimental data to benchmark detailed and comprehensive theoretical calculations.

We will discuss the recent progress at the Lund Laser Centre, aiming to extend previous studies to more highly excited levels and also to levels with the same parity as the ground configurations. The lifetime measurements are performed using the Time-Resolved Laser-Induced Fluorescence (TR-LIF) technique, and the key element to reach the new levels is by either two-photon excitation (from a single laser) or by two step excitations (from two different lasers). Most of these experimental studies are combined with theoretical investigations by P. Palmeri and P. Quinet from the theory group at the Université de Mons in Belgium.

Recent results using two-photon excitations in Cr II, Fe II, Ti II, Co II, Ni II and Y II can be found in [1-6]. A current project is Sc II, where the experimental lifetime measurements are complemented by measured branching fractions, from a Hollow Cathode using a Fourier Transform spectrometer, to obtain absolute transitions probabilities. [7]

References

[1] L. Engström *et al.* Astron. Astrophys. (2014) doi:10.1051/0004-6361/201424762
[2] H. Hartman *et al.* Astron. Astrophys. (2015) doi: 10.1051/0004-6361/201525738
[3] H. Lundberg *et al.* MNRAS (2016). doi:10.1093/mnras/stw922
[4] H. Hartman *et al.* Astron. Astrophys. (2015) doi: 10.1051/0004-6361/201629615
[5] P. Quinet *et al.* MNRAS (2016). doi:10.1093/mnras/stw1900
[6] P. Palmeri *et al.* Submitted to MNRAS 2017
[7] A. Pehlivan, To be submitted 2017

*Corresponding author: lars.engstrom@fysik.lth.se

To the list of contents

Probing variations of the fundamental constants with Cs clock referenced acetylene lines

Florin Lucian Constantin[*1]
1. Laboratoire PhLAM, CNRS UMR 8523, 59655 Villeneuve d'Ascq, France

Possible time- or potential gravitational-dependences of the fundamental constants allowed in theories beyond the Standard Model [1], can be detected by precision measurements. The molecular spectra are principally sensitive to the proton-to-electron mass ratio. The measurement of the frequency of a molecular clock against the frequency of an atomic clock provided an efficient strategy to address the question of the stability of the fundamental constants. Previous approaches were based, for example, on ammonia inversion transitions detected in a fountain [2], on rovibrational transitions of trapped molecular hydrogen ions [3] or of diatomic molecules in optical traps [4] and on a two-photon rovibrational transition in a molecular beam [5] that constrained the variation of m_e/m_p at 5.6×10^{-14} yr^{-1}. This contribution proposes to exploit frequency splittings between near-resonant rovibrational transitions of acetylene with enhanced sensitivity to a variation of m_e/m_p [6].

The experimental setups developed in many laboratories (see for example [7]) are based on an extended cavity laser diode with external electro-optic modulation that is locked with the Pound-Drever-Hall method to a Fabry-Perot cavity filled with acetylene. The metrological performances are a short term (<1 s) laser linewidth of ~ 50 kHz, a fractional stability of $\sim 10^{-12}$ at 1 s and a reproducibility of ~ 1 kHz on a day-to-day timescale. Acetylene transitions have been measured with an accuracy of ~ 1 kHz using frequency comb techniques. The proposed approach is to count the optical beat at a microwave frequency X between two similar systems locked to adjacent acetylene lines against the Cs clock frequency f_{Cs}. The Cs clock frequency depends as $f_{Cs} \sim g_{Cs}a^{2.83}m_e/m_p$, where a is the fine structure constant and g_{Cs} is the Cs g-factor. Small linear time variations of the fundamental constants lead to a small linear time variation of the frequency ratio X/f_{Cs}. The contribution of the fractional time variation of m_e/m_p to the temporal drift of X/f_{Cs} can be discriminated by the sensitivity coefficient $d(lnX)/d(ln(m_e/m_p))$.

The rovibrational energy levels of $^{12}C_2H_2$ are modelised with a Hamiltonian [8] that accounts for rotation, centrifugal distortion, vibration, anharmonicity and different rovibrational interactions. The sensitivities to a variation of m_e/m_p of the rovibrational transitions of the $\nu_1+\nu_3$, respectively the $\nu_1+\nu_2+\nu_4+\nu_5$ band are calculated (Fig. 1 a). Near resonant transitions arise from the cancellation of the rotational intervals with frequency shifts associated to the isotopic effect, the origins of the vibrational bands, the anharmonicity or the rovibrational interactions. The frequency splittings between near resonant transitions have sensitivity coefficients up to the $\pm10^3$ level (Fig. 1 b). The systematic frequency shifts of the frequency splittings may be smaller than those of one transition. The systematic effects are conservatively estimated at 96 Hz for actual experimental setups and may constrain a measurement of the fractional variation of m_e/m_p at the 10^{-10} level.

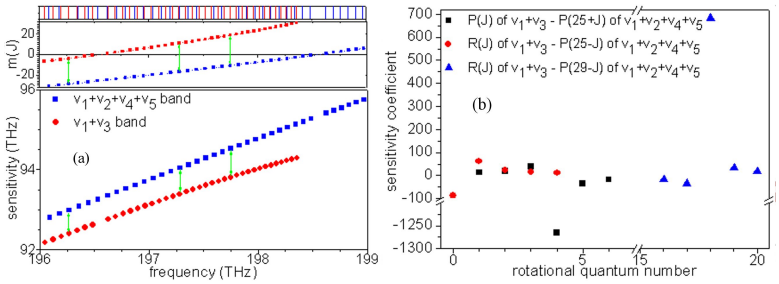

Fig. 1: a. Dependence of the sensitivity of the $\nu_1+\nu_3$ and the $\nu_1+\nu_2+\nu_4+\nu_5$ band transitions of $^{12}C_2H_2$ on the calculated rovibrational frequency and Fortrat diagram. b. Dependence of the sensitivity coefficient for selected pairs of near resonant transitions on the rotational quantum number of the $\nu_1+\nu_3$ band transition.

References

[1] for a review, see for example : J. -P. Uzan, Rev. Mod. Phys. **75**, 403 (2003).
[2] H. L. Bethlem *et al.*, Eur. Phys. J. Special Topics **163**, 55 (2008).
[3] S. Schiller and V. Korobov, Phys. Rev. A **71**, 032505 (2005).
[4] M. Kajita, Phys. Rev. A **84**, 022507 (2011).
[5] A. Shelkovnikov *et al.*, Phys. Rev. Lett. **100**, 150801 (2008).
[6] F. L. Constantin, Vibrational Spectroscopy **85**, 228 (2016).
[7] C. S. Edwards *et al.*, J. Mol. Spectrosc. **234**, 143 (2005).
[8] K. A. Keppler *et al.*, J. Mol. Spectrosc. **175**, 411 (1996).

*Corresponding author: FL.Constantin@univ-lille1.fr

To the list of contents

Multifrequency generation with an ac-biased photomixer

Florin Lucian Constantin[*1]
1. Laboratoire PhLAM, CNRS UMR 8523, 59655 Villeneuve d'Ascq, France

The generation of phase-coherent optical frequency combs with mode-locked lasers allowed many advances in the fields of frequency metrology, precision measurements and sensing. THz frequency combs were generated with the THz-TDS technique [1] and mode-locked THz quantum cascade lasers [2]. This contribution reports a different approach based on electrical modulation. Early approaches on THz-wave modulation exploited external devices [3]. The optoelectronic frequency down-conversion (photomixing) with two lasers and a dc-biased low-temperature-grown (LTG) GaAs photoconductive antenna (photomixer) allowed broadband generation of THz-waves [4]. Optical modulation of a photomixing signal was demonstrated by transferring high-speed modulation from two telecom lasers to the THz domain [5]. The coupling of an alternative voltage on a LTG-GaAs photomixer is exploited here for the modulation of a photomixing signal.

A photoconductive model based on one-dimensional carrier drift is presented. The carrier velocities [6] and the carrier lifetimes [7] depend nonlinearly on the electric field in LTG-GaAs. They have time dependences oscillating at harmonics of the modulation frequency upon application of an alternative electric field on the photomixer. The current density has spectral components at the sum and the difference between the frequency of the optical beat and a harmonic of the modulation frequency. Their phases and amplitudes are numerically calculated from an expansion in power series of the amplitude of the alternative electric field. The signal in the microwave regime at zero dc-bias field with radiofrequency modulation has spectral components with stable phases and supralinear dependence of the amplitudes in function of the alternative electric field (Fig. 1.a).

The experimental setup, described in [8] (Fig. 1.b), is based on two extended cavity laser diodes at 820 nm and a LTG-GaAs interdigitated photomixer with a self-complementary log-spiral antenna. The device is addressed with a 50-ohm semirigid microwave line through a bias-T with a dc-voltage applied through a choke and a capacitively coupled low-frequency ac-voltage. The photomixing signal in the microwave regime is recorded with a spectrum analyser. Multifrequency generation in the microwave regime is demonstrated by electrical modulation of a photomixing signal (Fig. 1.c), with qualitative agreement between the model and the experimental results.

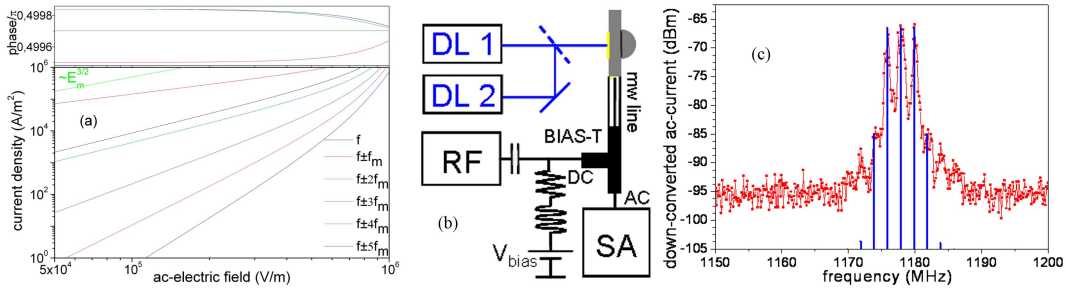

Fig. 1: a.Alternative electric field dependences of the amplitudes and the phases of selected spectral components of the current density. LTG-GaAs electrical conduction parameters from [6,7], photoconductive width 2×10^{-6}m, depth 2×10^{-6}m, area 12×10^{-12}m^2. Optical beat at $f=1$ GHz, modulation frequency $f_m=1$ MHz, laser power 2×10 mW. Dependence on the electric field as $E_m{}^{3/2}$ plotted as the green line b. Experimental setup. DL diode lasers, RF synthesizer, SA spectrum analyzer. c. Modulation of a photomixing signal. Optical beat at 1178 MHz, modulation frequency 2 MHz, optical power 2×20 mW. RBW 300 kHz, sweep time 4 ms. Spectral components are calculated for a set of experimental parameters and plotted with bars.

References

[1] C. A. Schmuttenmaer, Chem. Rev. **104**, 1759 (2004).
[2] S. Barbieri *et al.*, Nat. Photonics **5**, 306 (2011); J. R. Freeman *et al.*, Appl. Phys. Lett. **101**, 181115 (2012).
[3] M. Rahm, J. -S. Li and W. J. Padilla, J. Infrared Milli Terahz Waves **34**, 1 (2013).
[4] E. R. Brown *et al.*, Appl. Phys. Lett. **62**, 1206 (1993).
[5] M. Martin *et al.*, Appl. Phys. Lett. **93**, 131112 (2008).
[6] J. P Ibbetson and U. K. Mishra, Appl. Phys. Lett. **68**, 3781 (1996).
[7] N. Zamdmer *et al.*, Appl. Phys. Lett. **75**, 2313 (1999).
[8] F. L. Constantin, in *Proceedings of SPIE Vol. 9894, Nonlinear Optics and its Applications IV*, edited by B. J. Eggleton, N. G. R. Broderick, A. L. Gaeta (SPIE, Bellingham, 2016).

*Corresponding author: FL.Constantin@univ-lille1.fr

To the list of contents

Long term comparison between Raman atom interferometry based gravimeter and FG5 absolute gravimeter

LingXiao Zhu[1], Anthony Rodgers[1], Victoria Smith[2], Graham Appleby[2], Yu-Hung Lien*[1], Michael Holynski†[1], Kai Bongs[1]

1. Quantum Technology Hub for Sensors and Metrology and School of Physics and Astronomy, University of Birmingham, Edgbaston, Birmingham, West Midlands, United Kingdoms

2. NERC Space Geodesy Facility, Herstmonceux Castle, East Sussex, United Kingdoms

The Raman atom interferometry (RAI) based gravity sensors are becoming more popular and attracting the attentions for diverse field applications. Consequently we are developing a high precision RAI gravimeter as a transportable reference platform in UK quantum technology hub. The gravimeter is based on a ^{87}Rb atomic fountain cooled to a few μk via the moving molasses technique and employing the Raman pulses as atom optical components. The practical interrogation time is 120 ms limited by seismic noise and the theoretical sensitivity is estimated to be around 200 ng$/\sqrt{\text{Hz}}$ based on the current experimental parameters. In order to evaluate the potential systematic biases, we are planning to move the apparatus to the UK space geodesy facility later this year. We will proceeds a three months comparison between our transportable gravimeter and a cluster of de facto FG5 absolute gravimeters possessed by the facility. Some preliminary results would be presented in the conference.

The figure 1 shows the interferometric signals acquired with different interrogation times. Currently the S/N is largely limited by the seismic noise of local lab environment and expects to be improved by moving to the more quiet environment, e.g. the space geodesy facility.

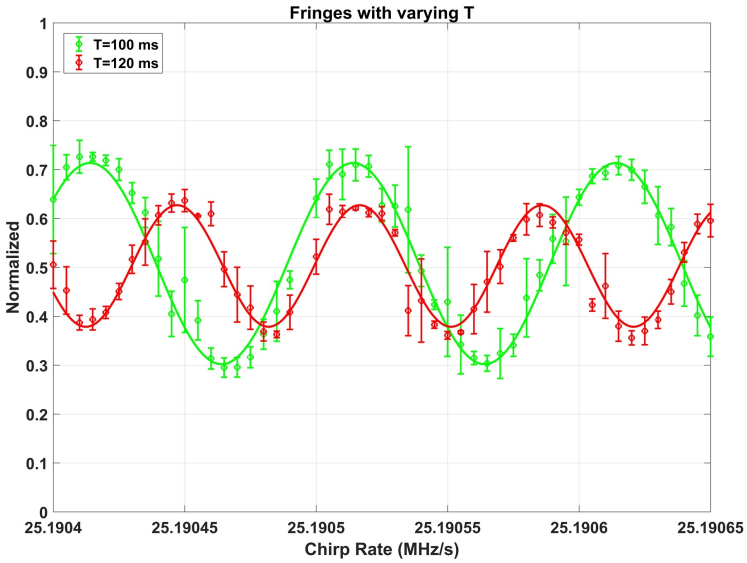

Fig. 1: The interferometric fringes are acquired by scanning the Raman frequency chirp rate with the interrogation time 100 and 120 ms.

*Corresponding author: y.lien@bham.ac.uk

†Corresponding author: m.holynski@bham.ac.uk

To the list of contents

Ultrafast diffraction with cold electrons from laser-cooled atoms

A. J. McCulloch[*1], **R. W. Speirs**[1] **D. Murphy**[1] **D. J. Thompson**[1] **J. Torrance**[1] **B. M. Sparkes**[1] **R. E. Scholten**[1]

1. School of Physics, The University of Melbourne
Parkville, Victoria, Australia

The CAEIS cold-atom electron/ion source, based on photoionisation of laser-cooled atoms, has achieved competitive nanoscale ion imaging [1] and offers unique properties for future application to ultrafast electron diffractive imaging [2,3]. Electron bunches produced by these sources have intrinsically high transverse coherence due to the very low source temperature, enabling single-shot high resolution diffraction [4]. Achieving practical imaging will require application of a diverse range of atomic physics. For example, optical excitation and ionisation allow generation of ultrafast bunches, but the bunch duration can vary by up to six orders of magnitude for relatively small changes in laser wavelength that enhance or inhibit specific photoexcitation pathways and below-threshold tunneling. Using streak methods, we have explored those pathways and demonstrated bunch durations of tens of picoseconds [5]. We have also explored two avenues for increasing brightness: using stimulated Raman adiabatic passage (STIRAP) [6] and selective field ionisation [7]. We are now developing a CAEIS with simultaneous extraction of both electrons and ions to enable correlated electron-ion imaging, and production of heralded single ions using Rydberg blockade in the photoexcitation and ionisation volume.

References

[1] J.J. McClelland *et al.*, Appl. Phys. Rev. **3**, 011302 (2016).
[2] M.W. van Mourik *et al.*, Struct. Dynam. **1**, 034302 (2016).
[3] A.J. McCulloch, B.M. Sparkes, R.E. Scholten, J. Phys. B **49**, 164004 (2016).
[4] R.W. Speirs *et al.*, J. Phys. B **48**, 214002 (2015).
[5] R.W. Speirs *et al.*, Phys. Rev. A, in press.
[6] B.M. Sparkes *et al.*, Phys. Rev. A **94**, 023404 (2016).
[7] A.J. McCulloch *et al.*, unpublished.

*Corresponding author: mccaj@unimelb.edu.au

To the list of contents

Towards an optical thermometer based on molecular spectroscopy to implement the new kelvin

E. Moufarej[*1,2], **O. Kozlova**[3], **B. Darquie**[1,2], **S. K. Tokunaga**[1,2], **S. Briaudeau**[3], **C. Daussy**[1,2]
1. Université Paris 13, Sorbonne Paris Cité, Laboratoire de Physique des Lasers
F-93430 Villetaneuse, France
2. CNRS, UMR 7538, LPL, F-93430 Villetaneuse, France
3. Laboratoire Commun de Métrologie LNE-CNAM
F-93210, La Plaine Saint-Denis, France

In 2018, the international System of Units (SI), including the kelvin, will be redefined by the International Comity of Weight and Measurements. This reform aims at relating each unit to a fundamental constant instead of relating them to materiel objects. Thereby, the temperature unit will be related to a fixed value of the Boltzmann constant k_B (instead of being related to the triple point of water). For the implementation of the new kelvin, several different primary thermometry methods are currently being developed (acoustic gas thermometry, Johnson noise thermometry, Doppler-broadening thermometry(DBT), etc...).

We proposed and previously used the spectroscopic method, based on the measurement of the Doppler broadening, on ammonia ro-vibrational transitions at the triple point of water for the determination of the Boltzmann constant [1][2]. Once the value of k_B will be fixed in the new SI, the DBT will be used as a primary spectroscopic method for thermodynamic temperature measurements.

In the frame of the Joint Research Project INK-2 of the European Metrology Programme for Innovation and Research, we will develop, test and optimize DBT in the temperature range 300 - 430 K, in order to demonstrate its potential and to study its limitations beyond the temperatuer of triple point of water. The measurement is based on precise spectroscopy of an ammonia ro-vibrational transition in the mid-infrared range ($\sim$10 μm). We present our on-going work towards this objective. The existing set-up (used for the k_B determination) is currently being upgraded. The spectroscopic cell is be placed in a variable thermostat, the temperature stability and gradient is currently being characterized. The influence of the line-mixing will be investigated theoretically and experimentally.

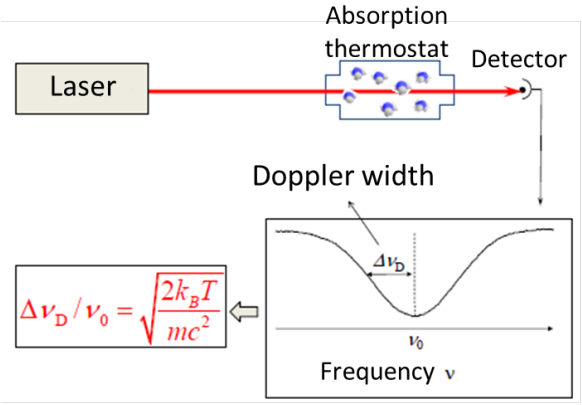

Fig. 1: Experimental Setup.

References

[1] C. Daussy *et. al.*, Physical Review Letters,**98**, Issue 25, 250801 (2007)
[2] S. Mejri *et. al.*, **52**, S314-S323, (arXiv:1506.01828) (2015)

*Corresponding author: elias.moufarej@univ-paris13.fr

To the list of contents

Coherent and efficient microwave-to-optical conversion via six-wave mixing in Rydberg atoms

Thibault Vogt[*1,2], **J. Han**[1], **C. Gross**[1], **D. Jaksch**[3], **M. Kiffner**[1,3], **W. Li**[1,4]

,

1. Centre for Quantum Technologies, National University of Singapore, 3 Science Drive 2, Singapore 117543
2. MajuLab, CNRS-UNS-NUS-NTU International Joint Research Unit UMI 3654, Singapore 117543
3. Clarendon Laboratory, University of Oxford, Parks Road, Oxford OX1 3PU, United Kingdom
4. Department of Physics, National University of Singapore, 117542, Singapore

Demonstrating efficient interconversion of millimetre waves and optical fields for future quantum technologies remains a challenge. Here we realize a coherent, broadband, microwave-to-optical converter and achieve an efficiency of more than 1% in conversion of a field of 84 GHz frequency into a field of 384 THz frequency. Our approach is based on frequency mixing in a cloud of Rubidium atoms, where the microwave fields are coupled to atomic transitions between Rydberg energy levels [1]. The strong coupling between the microwave field and these transitions allows for free-space conversion, in contrast to other physical systems already demonstrated. Electromagnetically induced transparency is used in our scheme in order to maximize the non-linearity responsible for the process, and opens the prospect for reaching much higher efficiencies. Eventually, if this technique were successful in reaching near-unity conversion efficiency, the large number of available transitions in the microwave and THz range would be very beneficial for applications.

In this presentation, I will describe the experimental setup that was used to obtain our results. I will also discuss the strategies for improving this efficiency and the efforts currently deployed towards this goal.

References

[1] J. Han, T. Vogt, Ch. Gross, D. Jaksch, M. Kiffner, and W. Li, arXiv:1701.07969.

*Corresponding author: cqtttv@nus.edu.sg

To the list of contents

Probing superfluidity in a quasi two-dimensional Bose gas through its local dynamics

C. De Rossi[1], R. Dubessy*[1], K. Merloti[1], M. de Goër de Herve[1], T. Badr[1], A. Perrin[1], L. Longchambon[1] and H. Perrin[1]

1. Laboratoire de physique des lasers, CNRS - Université Paris 13 UMR 7538
99 av. Jean-Baptiste Clément, 93430 Villetaneuse, France

We report direct evidence of superfluidity in a quasi two-dimensional Bose gas by observing its dynamical response to a collective excitation, the scissors mode[1]. The collective behaviour of the atomic cloud is identified by applying principal component analysis to a series of in-situ absorption pictures[2]. Relying on a novel local average analysis, we are able to probe inhomogeneous clouds and reveal their local dynamics[3]. We identify in this way the superfluid and thermal phases inside the gas and locate the boundary at which the Berezinskii–Kosterlitz–Thouless crossover occurs. This new analysis also allows to evidence the coupling of the two fluids which induces at finite temperatures damping rates larger than the usual Landau damping.

Our measurement scheme relying on the weak global excitation of a gas close to equilibrium probed locally is symmetric to the measurement of the critical velocity in an inhomogeneous quasi-2D Bose gas[4], where the effect of a strong local perturbation is probed through a global observable, the total heat deposited over the whole cloud.

References

[1] D. Guéry-Odelin and D. Stringari, Phys. Lett. **83**, 4452 (1999).
[2] R. Dubessy, C. De Rossi, T. Badr, L. Longchambon and H. Perrin, New J. Phys. **16**, 122001 (2014).
[3] C. De Rossi, R. Dubessy, K. Merloti, M. de Goër de Herve, T. Badr, A. Perrin, L. Longchambon, and H. Perrin, New J. Phys. **18**, 062001 (2016).
[4] R. Desbuquois, L. Chomaz, T. Yefsah, J. Léonard, J. Beugnon, C. Weitenberg and J. Dalibard, Nat. Phys. **8**, 645 (2012).

*Corresponding author: romain.dubessy@univ-paris13.fr

To the list of contents

Quantum chaos in ultracold collisions between Yb($^1S_0$) and Yb($^3P_2$)

Dermot G. Green[*1,2], **Christophe L. Vaillant**[1,3], **Matthew D. Frye**[1], **Masato Morita**[1], **Jeremy M. Hutson**[†1]

1. Joint Quantum Centre (JQC) Durham-Newcastle, Department of Chemistry, Durham University, South Road, Durham DH1 3LE, United Kingdom

2. School of Mathematics and Physics, Queen's University Belfast, University Road, Belfast BT7 1NN, United Kingdom

3. Department of Chemistry, University of Cambridge, Lensfield Road, Cambridge CB2 1EW, UK

Signatures of quantum chaos have recently been observed in ultracold collisions of the complex atoms Er and Dy in magnetic fields [1-3]. Such chaos may have very important consequences for ultracold physics: it is likely to make it impossible to assign quantum numbers to resonances and near-threshold states, and may make it difficult or impossible to determine interaction potentials by fitting to observed resonances. In addition, it may cause long-lived 2-body collisions that result in fast 3-body loss [4]. It is thus important to understand the nature of chaos in ultracold collisions, and determine when and why it occurs.

We calculate and analyse Feshbach resonance spectra for ultracold Yb($^1S_0$) + Yb($^3P_2$) collisions as a function of an interatomic potential scaling factor λ and external magnetic field [5]. We find clear signatures of chaos in this system which become stronger with increasing magnetic field, reaching a level that is similar to that observed experimentally in Er and Dy (see Fig. 1). In addition, we show that the resonances in magnetic field in the experimentally accessible range 400 to 2000 G are chaotically distributed, with strong level repulsion that is characteristic of quantum chaos [5].

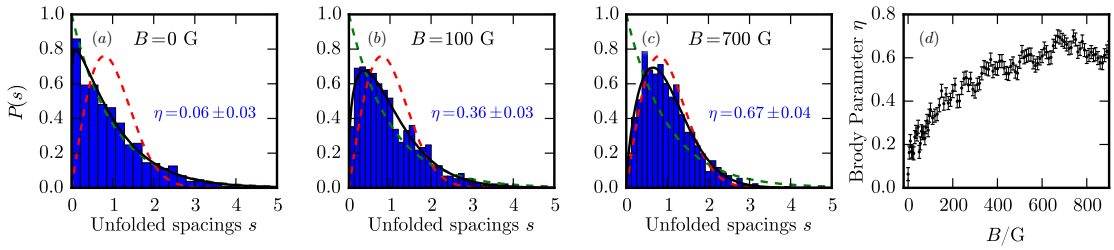

Fig. 1: Statistical analysis of Feshbach resonance positions in ultracold Yb($^1S_0$) + Yb($^3P_2$) collisions with respect to potential scaling factor λ. (a), (b) and (c) show the nearest-neighbour distributions $P(s)$, which is the probability density of two neighbouring levels having the spacing s (on a dimensionless scale in which the levels have unit number density). The nearest-neighbour spacing distribution of a randomly distributed set of levels is of Poisson type, while that of a chaotically distributed set is of Wigner-Dyson type. The Wigner-Dyson distribution exhibits strong level repulsion, i.e., vanishingly small probabilities of finding levels that coincide. The Brody distribution interpolates between Poisson and Wigner-Dyson ones, via a single parameter that takes values between zero (Poisson) and unity (Wigner-Dyson). Coupled-channel results (blue histograms); fitted Brody distributions (black lines, with the corresponding Brody parameters stated); Poisson and Wigner-Dyson distributions (green and red dashed lines, respectively). (d) shows the calculated Brody parameter as a function of magnetic field. Figure adapted from that appearing in [5].

We have shown strong signatures of chaos in a remarkably simple system, which has strong anisotropy but only 3 electronic curves correlating with the $^3P_2$ threshold. This is very many fewer electronic states than Er+Er and Dy+Dy. The results demonstrate that a complex electronic structure is not a prerequisite for chaos in ultracold collisions. This also suggests that chaos is likely to be widespread in ultracold collisions, which will have important consequences for the study and understanding of ultracold species.

References

[1] A. Frisch *et al.*, *Quantum chaos in ultracold collisions of gas-phase erbium atoms*, Nature London **507**, 475 (2014).
[2] T. Maier *et al.*, *Emergence of Chaotic Scattering in Ultracold Er and Dy*, Phys. Rev. X **5**, 041029 (2015).
[3] T. Maier *et al.*, *Broad universal Feshbach resonances in the chaotic spectrum of dysprosium atoms*, Phys. Rev. A **92**, 060702 (2015).
[4] M. Mayle, B. P. Ruzic, and J. L. Bohn, *Statistical aspects of ultracold resonant scattering*, Phys. Rev. A **85**, 062712 (2012).
[5] D. G. Green, C. J. Vaillant, M. D. Frye, M. Morita and J. M. Hutson, *Quantum chaos in ultracold collisions between Yb($^1S_0$) and Yb($^3P_2$)*, Phys. Rev. A. **93**, 022703 (2016).

[*]Corresponding author: d.green@qub.ac.uk
[†]Corresponding author: j.m.hutson@durham.ac.uk

To the list of contents

Avoided crossings in near-threshold bound states of space-fixed dipoles.

John D. Reddel[1], **Matthew D. Frye**[*1], **Jeremy M. Hutson**[†1]
1. Joint Quantum Centre (JQC) Durham-Newcastle, Department of Chemistry, Durham University, South Road, Durham DH1 3LE, United Kingdom

The Bohn-Cavagnero-Ticknor (BCT) model [1] is a useful simple model of dipole-dipole scattering. Here we investigate near-threshold bound states of this model.

The BCT model is based on the approximation that the orientations of both dipoles are fixed in space and parallel to each other. This approximation may be appropriate when a dipole is polarised by an external field and the interaction potential is smaller compared to the energy which is polarising the dipole [1]. Therefore, this model is expected to be useful for describing low-energy scattering and near-threshold bound states.

We have implemented the BCT model in the computer program BOUND [2], and used it to calculate bound states using parameters which correspond to the dipoles of different physical systems, such as the weak magnetic dipoles of Dy+Dy and the much stronger dipoles induced by an electric field in KCs+KCs. In the latter system, it is possible to vary the effective dipole by varying the polarising electric field, which provides an experimental mechanism for controlling the parameters of the model.

We investigate how the levels shift as we vary the parameters of the model, and we observe numerous avoided crossings of a variety of strengths. In particular, we find states which approach threshold slowly as a function of the effective dipole strength, which are crossed by numerous steeper states in a way which is similar to features observed experimentally in near-threshold bound states of Dy+Dy [3].

References

[1] J. L. Bohn, M. Cavagnero, and C. Ticknor, *Quasi-universal dipolar scattering in cold and ultracold gases*, New J. Phys. **11**, 055039 (2009).

[2] J. M. Hutson, BOUND computer code

[3] T. Maier *et al.*, *Broad universal Feshbach resonances in the chaotic spectrum of dysprosium atoms*, Phys. Rev. A **92**, 060702 (2015).

[*]Corresponding author: matthew.frye@durham.ac.uk
[†]Corresponding author: j.m.hutson@durham.ac.uk

To the list of contents

Imprinting Knotted Optical Vortices onto Atomic Bose–Einstein Condensates

S. A. Gardiner[*1], **I. G. Hughes**[†1], **F. Maucher**[‡1]
1. Joint Quantum Centre (JQC) Durham–Newcastle, Department of Physics, Durham University
South Road, Durham DH1 3LE, UK

Recently there has been a growing interest in the dynamics of knotted vortex lines in BECs, without necessarily considering concrete experimental means to excite such matter waves in a controlled fashion.We have studied the theoretical creation of knotted ultracold matter waves in Bose-Einstein condensates via coherent two-photon Raman transitions with a Λ level configuration, and their subsequent dynamics [1]. We have done this by taking advantage of the possibility to create knotted light fields (in the paraxial limit) through astute superpositions of Laguerre–Gauss modes [2],[3], and by numerical modelling three-dimensional Gross–Pitaevskii equation. The Raman transition allows an indirect transfer of atoms from the internal state $|a\rangle$ to the target state $|b\rangle$ via an excited state $|e\rangle$, that would be otherwise dipole-forbidden, as shown in Fig. 1(a). This setup enables us to imprint three-dimensional knotted vortex lines embedded in the probe field to the density in the target state. With this work we believe we have presented a setup with physically realistic parameters to create such knotted vortex lines in ultracold matter waves, although the subsequent dynamics can quickly become quite involved.

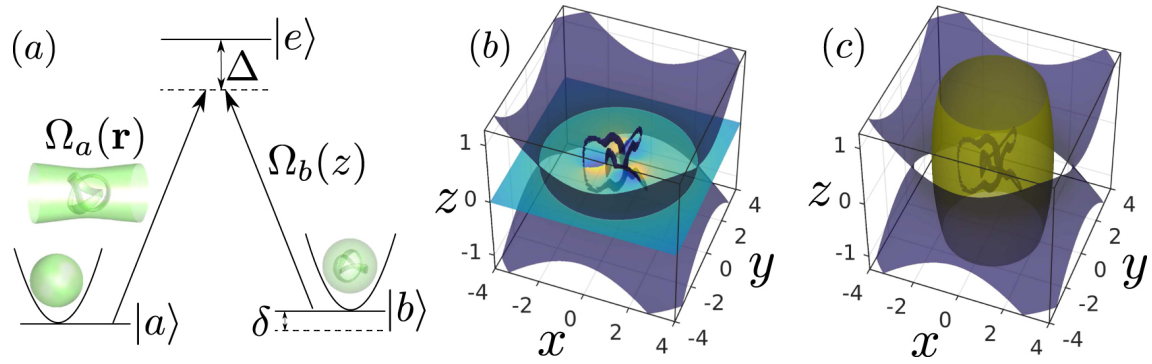

Fig. 1: (a) Schematic sketch of a Raman-type transition with Λ-configuration. The state $|a\rangle$ is off-resonantly coupled to state $|b\rangle$ with two-photon detuning δ. The knotted light field $\mathscr{E}$ associated with $\Omega_a(\mathbf{r})$ off-resonantly couples state $|a\rangle$ to $|e\rangle$ with detuning Δ. The final state $|b\rangle$ then reflects the involved structure of the light field $\mathscr{E}$ associated with $\Omega_a(\mathbf{r})$. (b) depicts an isosurface of the intensity (purple) of the light-field $\mathscr{E}$ at a low isointensity value and a slice showing the phase in the (x,y)-plane. In addition to the vortex lines in the centre of the beam, the usual diffraction cones become visible. (c) Illustration of the situation at $t = 0$, when the light field is imprinted, before any subsequent dynamics in the atomic Bose–Einstein condensate take place. The isodensity of the cigar-shaped wave function ψ_a (yellow) is subject to the knotted light field (purple) from Fig. (b).

References

[1] F. Maucher, S. A. Gardiner, and I. G. Hughes, New J. Phys. **18**, 063016 (2016)
[2] M. R. Dennis, R. P. King, B. Jack, K. O'Holleran, and M. J. Padgett, Nat. Phys. **6**, 118 (2010)
[3] M. R. Dennis, J. B. Götte, R. P. King, M. A. Morgan, and M. A. Alonso, Opt. Lett. **36**, 4452 (2011)

[*]Corresponding author: s.a.gardiner@durham.ac.uk
[†]Corresponding author: i.g.hughes@durham.ac.uk
[‡]Corresponding author: fabian.maucher@durham.ac.uk

To the list of contents

Strong Coupling of a Cold Potassium Gas and a Ring Cavity

R. Culver[1], **A. Lampis**[1], **B. Megyeri**[1], **G. Harvie**[1], **Jon Goldwin**[*1]
1. School of Physics & Astronomy, University of Birmingham,
Edgbaston, Birmingham B15 2TT, UK

Collective strong light-matter coupling was induced between a cold potassium gas and a high-finesse ring cavity. Potassium-39 atoms were pre-cooled in a two-dimensional magneto-optical trap, and continuously transferred to a three-dimensional trap intersecting the cavity mode. Cavity transmission spectra revealed the normal mode splitting characteristic of strong coupling. By varying the bare cavity resonance frequency, the avoided crossing of the normal modes was observed (see Fig. 1). This was used as a benchmark to characterise the strength of the atom-light coupling.

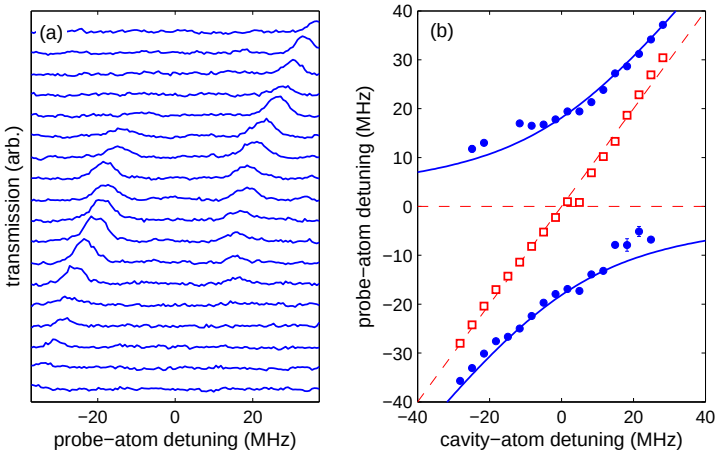

Fig. 1: Normal mode spectroscopy of a coupled atom-cavity system [1].

I will describe recent progress on the experiment and our plans for the near future. Sub-Doppler cooling has reduced the temperature by an order of magnitude. Currently we are working to extend the coherence time, now limited by stray magnetic fields, to enable studies of electromagnetically induced transparency (EIT). This follows our previous work in a heated vapour cell, where steep dispersion led to group indices approaching 10^4 [2]. Combining EIT with the ring cavity experiment will set the stage for more general control of gain and dispersion in the strongly coupled system. Fundamental studies and applications in sensing and metrology will be described.

References

[1] R. Culver et al., New J. Phys. **18**, 113043 (2016).
[2] A. Lampis et al., Opt. Express **24**, 015494 (2016).

[*]Corresponding author: j.m.goldwin@bham.ac.uk

To the list of contents

Spin-orbit coupled interferometry with ring–trapped Bose–Einstein condensates.

J. L. Helm[*1,2], **T. P. Billam** [3], **A. Rakonjac** [2], **S. L. Cornish** [2], **S. A. Gardiner**[2]

1. Dodd-Walls Centre for Photonic and Quantum Technologies, Department of Physics, University of Otago, Dunedin 9016, New Zealand
2. Joint Quantum Center (JQC) Durham-Newcastle, Department of Physics, Durham University, Durham DH1 3LE, United Kingdom
3. Joint Quantum Center (JQC) Durham-Newcastle, Department of Mathematics and Statistics, Newcastle University, Newcastle University, Newcastle upon Tyne, NE1 7RU, United Kingdom

We propose a method of atom-interferometry using a spinor Bose–Einstein (BEC) and the well-established experimental technique of time-varying magnetic fields as a coherent beam-splitter. Our protocol creates long-lived superpositional counterflow states, which are of fundamental interest and can be made sensitive to both the Sagnac effect and magnetic fields on the sub micro-Gauss scale. We split a ring-trapped condensate, initially in the $m_f = 0$ hyperfine sub-level, into superpositions of both internal spin state and condensate superflow [1], which are spin-orbit coupled. After interrogation a relative phase accumulation can be inferred from a population transfer to the $m_f = \pm 1$ states [2]. We present numerical and analytical treatments of our system [3].

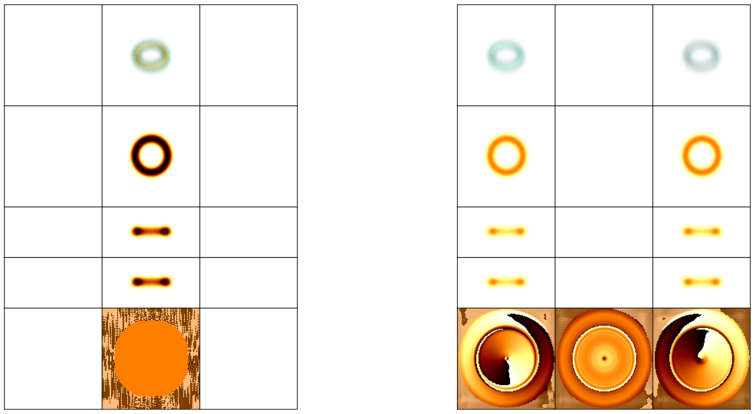

Fig. 1: Numerically generated density vapour, column densities (top, front and side views), and phase plot for (left panel) initial condition and (right panel) counterflow state. Note the opposite phase windings in the $m_f = \pm 1$ components (depicted in the left and right columns of each panel respectively).

References

[1] T. Isoshima, M. Nakahara, T. Ohmi, and K. Machida, Phys. Rev. A **61**, 063610 (2000).
[2] P. L. Halkyard, M. P. A. Jones, and S. A. Gardiner, Phys. Rev. A **81**, 061602 (2010).
[3] J. L. Helm, T. P. Billam, A. Rakonjac, S. L. Cornish, S. A. Gardiner, arXiv:1701.02154.

*Corresponding author: john.helm@otago.ac.nz

To the list of contents

KCs: refinement of interaction potential and prediction of Feshbach resonances

C. Ruth Le Sueur*, **Jeremy M. Hutson**†
Joint Quantum Centre (JQC) Durham–Newcastle, Department of Chemistry, Durham University
South Road, Durham DH1 3LE, UK

Feshbach resonances have recently been observed in an ultracold ^{39}K-^{133}Cs mixture[1]. In that work we used the positions of these resonances to refine the triplet interaction potential [2], [3] and thus to make improved predictions of the positions and widths of all the Feshbach resonances (between 0 and 1000 G) that are due to s-wave or d-wave states crossing the lowest asymptotic threshold, as well as a map of the bound states just under that threshold, for all three isotopic combinations. The new triplet potential gives a triplet scattering length for ^{40}K^{133}Cs that is not as close to the singlet scattering length, producing significantly broader resonances. This improves the prospects of using the resonances to produce fermionic ^{40}KCs molecules, and also makes them more suitable for precise tuning of the interactions in a K-Cs Fermi-Bose mixture.

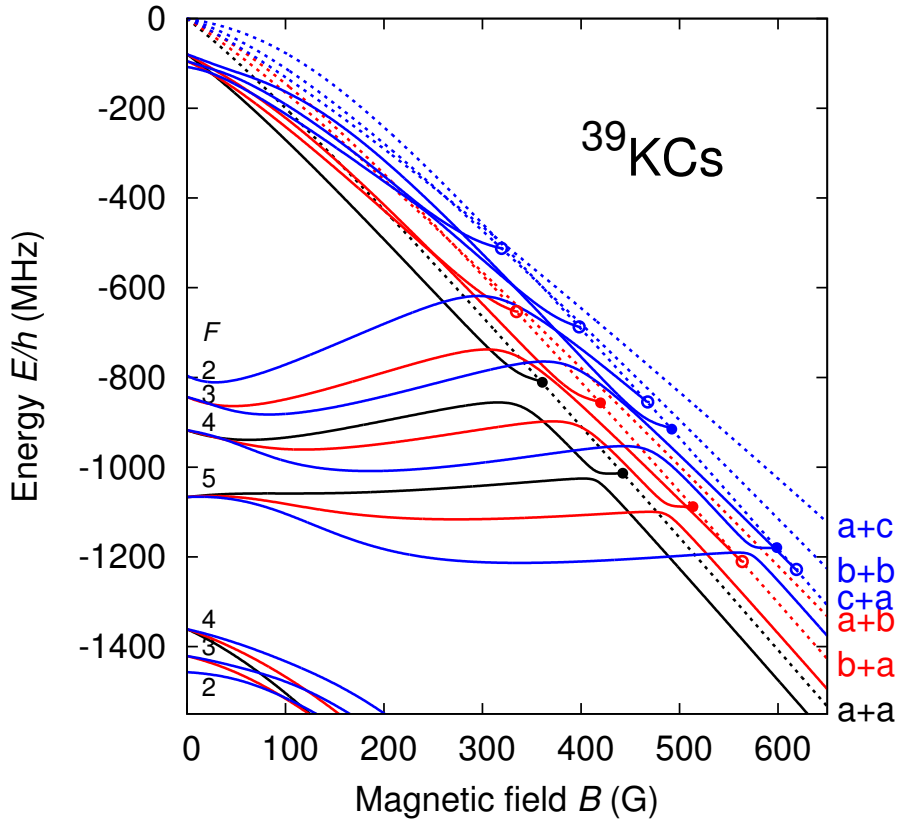

Fig. 1: Bound states of ^{39}KCs with $M_F = 2$ (blue), 3 (red) and 4 (black), together with the corresponding thresholds, calculated using our refined potential [1]. The threshold crossings that produce observed crossings are shown with filled circles and those so far unobserved with open circles.

References

[1] M. Gröbner, P. Weinmann, E. Kirilov, H.-C. Nägerl, P. S. Julienne, C. R. Le Sueur and J. M. Hutson, arXiv preprint **arXiv:1612.07196** 2016
[2] R. Ferber, O. Nikolayeva, M. Tamanis, H. Knöckel, and E. Tiemann, Phys. Rev. A **88**, 012516 (2013)
[3] H. J. Patel, C. L. Blackley, S. L. Cornish, and J. M. Hutson, Phys. Rev. A **90**, 032716 (2014)

*Corresponding author: c.r.lesueur@dur.ac.uk
†Corresponding author: j.m.hutson@dur.ac.uk

To the list of contents

BOUND: a program for bound states of atomic and molecular pairs

C. Ruth Le Sueur*, **Jeremy M. Hutson**†
Joint Quantum Centre (JQC) Durham–Newcastle, Department of Chemistry, Durham University
South Road, Durham DH1 3LE, UK

BOUND is a program for locating bound states of a pair of weakly interacting atomic or molecular partners, in external fields if desired. It can be used for many different interacting partners, including pairs of alkali-metal atoms in magnetic and radiofrequency fields. Such calculations are of great importance in understanding Feshbach resonances and in designing experiments for magnetoassociation to form ultracold molecules. Such molecules can then be transferred to the absolute ground state by using STIRAP [1], [2], [3] at which point they are available for further use as a collection of particles with long-range and tunable interactions.

BOUND uses the method of coupled channels, which handles the interatomic distance coordinate by direct numerical integration and all the other coordinates using a basis set. The Schrödinger equation is recast in terms of the log-derivative matrix, which allow stable propagation even in the presence of deeply closed channels.

Here we present the capabilities of BOUND (and the partner program FIELD) to find and characterise high-lying bound states in the ^{87}RbCs system. This system is particularly challenging because it has a molecular state lying about 0.11 MHz beneath the lowest hyperfine threshold (1 part in 10^9 of the well depth), with multiple avoided crossings with other states (see figure 1). Mapping these states as a function of magnetic field and energy is a task that BOUND performs well.

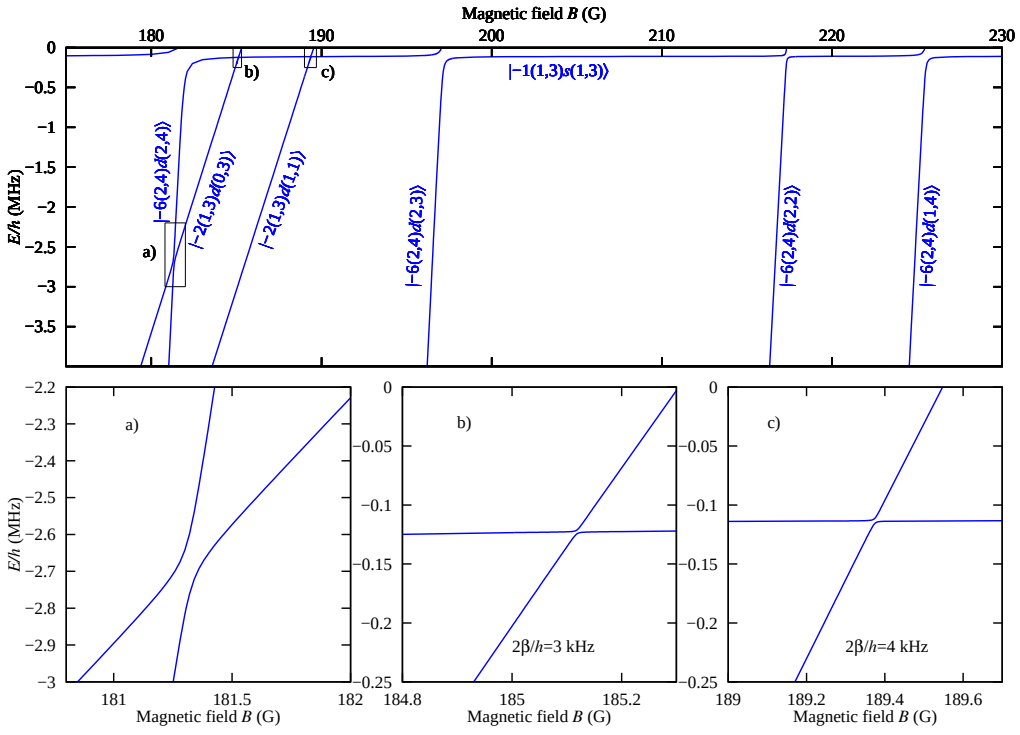

Fig. 1: Weakly bound states of ^{87}RbCs shown relative to dissociation limit Rb$|1,1\rangle$+Cs$|3,3\rangle$ at the given magnetic field value B. Panels a), b) and c) show close-ups of the areas boxed and labelled in the top panel.

References

[1] K.-K. Ni, S. Ospelkaus, M. H. G. de Miranda, A. Pe'er, B. Neyenhuis, J. J. Zirbel, S. Kotochigova, P. S. Julienne, D. S. Jin and J. Ye, Science **322**, 231 (2008).
[2] T. Takekoshi, L. Reichsöllner, A. Schindewolf, J. M. Hutson, C. R. Le Sueur, O. Dulieu, F. Ferlaino, R. Grimm and H.-C. Nägerl, Phys. Rev. lett. **113**, 205301 (2014).
[3] P. K. Molony, P. D. Gregory, Z. Ji, B. Lu, M. P. Köppinger, C. R. Le Sueur, C. L. Blackley, J. M. Hutson and S. L. Cornish, Phys. Rev. Lett., **113**, 255301 (2014)

*Corresponding author: c.r.lesueur@dur.ac.uk
†Corresponding author: j.m.hutson@dur.ac.uk

To the list of contents

Theoretical Study on the Stability of a Vortex Ring in an Axisymmetrically and Harmonically Trapped Dipolar Condensate

I-Kang Liu (Gary)[*1] **and Shih-Chuan Gou**[†1]
1. Department of Physics and Graduate Institute of Photonics, National Changhua University of Education, Changhua 50058, Taiwan

We theoretically study the stability of a vortex ring in an axisymmetrically and harmonically trapped dipolar condensate. Specifically, we focus on the case in which the dipoles are all aligned along the axial direction. Assuming a condensate of large size, we approach the problem by taking into account the velocity formula derived from the time-dependent Gross-Pitaevskii equation by the method of matched asymptotic expansion in the Thomas-Fermi limit for the filament model of a circular vortex ring subject to bending-wave instability [1]. The stable region (the shaded area in Fig. 1), where the vortex ring is robust against the linear instability of bending waves, is determined for wide ranges of scaled dipole strength and aspect ratio of the trapping potential. To visualize the locomotion and probe more into the dynamical aspect of the vortex ring traversing in a realistic dipolar BEC, we numerically solve the time-dependent Gross-Pitaevskii equation related to the recently demonstrated dysprosium BEC [2]. Furthermore, the quantum fluctuation in such dipolar BECs, which originates from the Lee-Huang-Yang effect [3], can act to influence the stability of the vortex ring, and we also address this issue in this presentation.

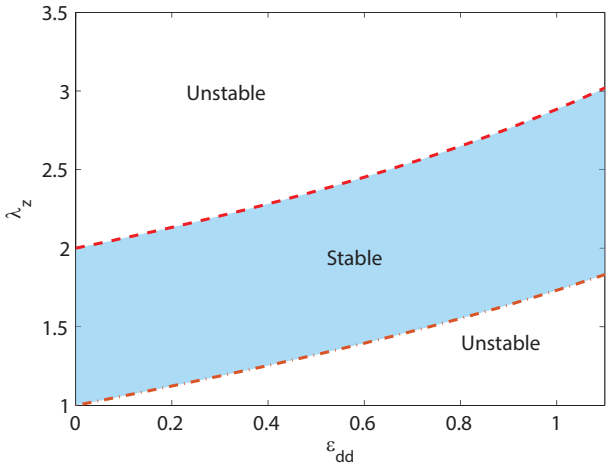

Fig. 1: The stability of a vortex ring in an axisymmetrically and harmonically trapped dipolar condensate in the Thomas-Fermi approximation as a function of ε_{dd}, the scaled dipole strength, and $\lambda_z = \omega_z/\omega_\perp$, the aspect ratio of the harmonic trap. The shaded area indicates the stable region of a circular vortex ring.

References

[1] T.-L. Horng, S.-C. Gou and T.-C. Lin, Phys. Rev. A **74**, 041603 (2006).
[2] H. Kadau, M. Schmitt, m. Wenzel, C. Wink, T. Maier, I. Ferrier-Barbut and T. Pfau, Nature **500**, 194-197 (2015).
[3] F. Wächtler and L. Santos, Phys. Rev. A **93**, 061603 (2016), and H. Saito, J. Phys. Sco. Jpn. **85**, 053001 (2016).

[*]Corresponding author: ikliu@cc.ncue.edu.tw
[†]Corresponding author: scgou@cc.ncue.edu.tw

To the list of contents

Control of quantum dynamics on an atom chip

Cosimo Lovecchio[*1], **H.-V. Do**[1], **F. S. Cataliotti** [1,2]
1. LENS and Dipartimento di Fisica ed Astronomia, Università di Firenze, Via Nello Carrara 1, 50019 Sesto Fiorentino, Italy
2. Istituto Nazionale di Ottica INO-CNR, Largo Enrico Fermi 3, 50125 Firenze, Italy

We produce a Bose-Einstein condensate of ^{87}Rb with an Atom-Chip. The Atom-Chip is also equipped with RF sources for coherent transfer of atoms between internal states in order to realize an atom interferometer [1]. We demonstrate a novel scheme for the tomographic reconstruction of atomic states that combines the inherent stability of the atom chip setup with the flexibility of optimization schemes [2]. This scheme allowed confirming of the superb control on parameters allowed by the experimental set-up and put it to use on improved control algorithms to realise arbitrary superposition states [3]. In the same set-up we can further control the available Hilbert space for quantum evolution exploiting Quantum Zeno dynamics [4]. This can be used to create two separate subspaces in the hyperfine ground states of ^{87}Rb. We choose the 4 logical input state of a 2 q-bit gate among the two subspaces. With D-CRAB optimization [5] we design a control RF pulse to perform a phase gate. Since in the same system we can make use of Raman and microwave transitions between the different hyperfine manifolds in order to perfom single q-bit operations, our use of QZD allows the demonstration of a complete set of logical gates within a single rubidium atom.

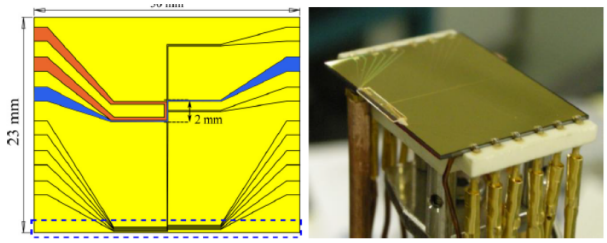

Fig. 1: The atom chip on which condensation and manipulations are performed.

Finally we show a possible route for controlling the coupling to an environment by experimentally demonstrating the stochastic Quantum Zeno effect; i.e. we prove an ergodicity relation between the survival probabilities of different stochastic series that respectively correspond to time and ensemble averages [6]. These experiments prove that Atom Chips can be ideal tools for the control of quantum dynamics opening a new way to realizing novel quantum logical gates.

References

[1] J. Petrovic, *et al.*, New J. Phys. **15** (4), 043002 (2013)
[2] C. Lovecchio, *et al.*, New J. Phys. **17**, 093024, (2015)
[3] C. Lovecchio, *et al.*, Phys. Rev. A **93**, 010304(R) (2016)
[4] F. Schaefer, *et al.*, Nature Communications **5**:3194 (2014)
[5] N . Rach *et al.*, Phys. Rev. A **92**, 062343 (2015)
[6] S. Gherardini, *et al.*, Quantum Sci. Technol. **2**, 015007 (2017)

*Corresponding author: lovecchio@lens.unifi.it

To the list of contents

Probing correlations of cold-atom systems using multiple atomic impurities

M. Streif[1,2], **A. Buchleitner**[2], **D. Jaksch**[1,3], **J. Mur-Petit**[*1]
1. Clarendon Laboratory, University of Oxford, Parks Road, Oxford OX1 3PU, United Kingdom
2. Physikalisches Institut, Albert-Ludwigs-Universität Freiburg, Hermann-Herder-Straße 3, 79104 Freiburg, Germany
3. Centre for Quantum Technologies, National University of Singapore, 3 Science Drive 2, 117543 Singapore

Experimental advances in the control and measurement of quantum systems are driving the development of quantum technologies across multiple experimental platforms, from trapped ions and cold atoms, to superconducting circuits and nanomechanical setups [1]. Among the most promising practical applications of these devices lies quantum-enhanced sensing, where individual or quantum-correlated particles are used to accurately measure observables, from magnetic fields to gravity. Extending this paradigm, recent work has highlighted the potential of single quantum systems to probe strongly-correlated quantum systems [2]. Yet it is clear that in general a single qubit probe cannot suffice to exhaustively characterise a complex quantum system, since the probe's diagnostic horizon will generally be limited to a finite subset of the system's Hilbert space.

In a first step to address this issue, we have considered probing a quantum with two impurity atoms separated a distance Δc. We have found [3] that nonlocal density-density correlations of the gas,

$$g^{(2)}(\Delta c) = \frac{\langle \rho(0)\rho(\Delta c)\rangle - \langle \rho(0)\rangle\langle \rho(\Delta c)\rangle}{\langle \rho(0)\rangle^2},$$

where $\rho(x)$ is the density of the system at position x, can be measured in a nondestructive way by monitoring the evolution of the two-probe reduced density matrix after a change of the probe-system interaction strength. Our findings, illustrated in Fig. 1, are supported with analytic and numerical calculations for the Bose-Hubbard model, from the weakly to the strongly interacting regimes, under conditions of temperature, density, and impurity-gas interactions relevant to ongoing experiments in two-species cold-atom systems [4]-[5].

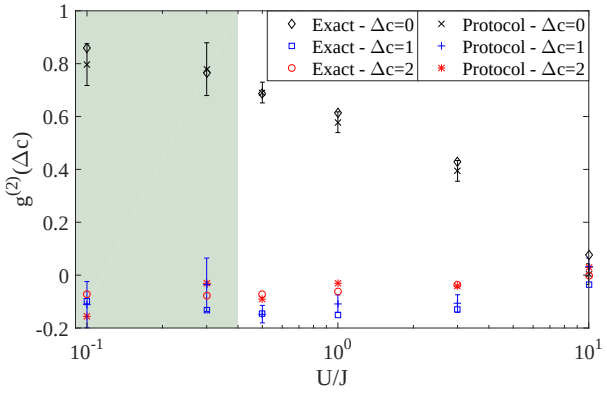

Fig. 1: Two-point density-density correlation function $g^{(2)}(\Delta c)$ of the one-dimensional Bose-Hubbard model for separation $\Delta c = 0, 1, 2$ (in units of the lattice constant) and different values of U/J, where U and J are the on-site interaction energy and the hopping energy, respectively, of the Bose-Hubbard Hamiltonian. Empty symbols stand for the theoretical predictions based on Bogoliubov theory for $U/J \leq 0.4$ with a thermal state with inverse temperature $\beta = 1000/J$ (shaded region), and on tensor network theory (TNT) calculations for $U/J > 0.4$. Symbols $\times, +, *$ show the results of our measurement protocol, with the associated error bars for $N_{\text{exp}} = 10^4$ simulated measurements. For clarity, we do not include error bars for the $\Delta c = 2$ calculations; they are similar to those for $\Delta c = 1$. Reproduced from Ref. [3].

References

[1] G. Kurizki *et al.*, PNAS **110**, 3866 (2014); K. Bongs *et al.*, Proc. SPIE 9900, Quantum Optics 990009 (2016), doi:10.1117/12.2232143.
[2] See, *e.g.*, D. Hangleiter *et al.*, Phys. Rev. A **91**, 013611 (2015); T. H. Johnson *et al.*, Phys. Rev. A **93**, 053619 (2016); F. Cosco *et al.*, arXiv:1511.00833v2 (2016).
[3] M. Streif, A. Buchleitner, D. Jaksch, and J. Mur-Petit, Phys. Rev. A **94**, 053634 (2016).
[4] S. Ospelkaus *et al.*, Phys. Rev. Lett. **96**, 180403 (2006); S. Palzer *et al.*, Phys. Rev. Lett. **103**, 150601 (2009); N. Spethmann *et al.*, Phys. Rev. Lett. **109**, 235301 (2012); J. Catani *et al.*, Phys. Rev. A **85**, 023623 (2012); T. Fukuhara *et al.*, Nature Phys. **9**, 235 (2013); R. Scelle *et al.*, Phys. Rev. Lett. **111**, 070401 (2013); M. Hohmann *et al.*, Phys. Rev. A **93**, 043607 (2016).
[5] E. Bentine, T. L. Harte, K. Luksch, A. J. Barker, J. Mur-Petit, B. Yuen, and C. J. Foot, J. Phys. B **50**, 094002 (2017).

[*]Corresponding author: jordi.murpetit@physics.ox.ac.uk

To the list of contents

Phase Profiles of Atomic Bose-Einstein Condensate Mixtures

K. L. Lee[1], I.-K. Liu[1], N. Jorgensen[2], L. Wacker[2], M. G. Skou[2], K. T. Skalmstang[2], J. J. Arlt[2] and Nick Proukakis*[1]

1. Joint Quantum Centre (JQC) Durham–Newcastle, School of Mathematics and Statistics, Newcastle University Newcastle upon Tyne NE1 7RU, UK

2. Institut for Fysik og Astronomi, Aarhus Universitet, Ny Munkegade 120, 8000 Aarhus C, Denmark

We characterize the phase profiles of interacting atomic Bose-Einstein condensates, presenting the precise conditions for phase mixing or separation. Considering equilibrium patterns, we demonstrate a new criterion for the in-situ spatial distributions, which offers a significant improvement over the homogeneous condition typically used to analyse experiments; using a state-of-the-art finite temperature kinetic model, recently extended by us to two-component condensates [1]-[2], we establish the measurement of collective modes as a unique tool probing the mixture (im)miscibility [3]. Investigating images after time-of-fight expansion, in a scheme which also accounts for the thermal mean field, we show through a detailed theoretical-experimental comparison [4] that immiscibility can actually emerge in expanded images of two initially spatially-separated condensates (see figure), as a result of the effective mean-field potentials during expansion. We also briefly comment on the coupled condensate thermalization dynamics [5] and the extent to which the coupled condensate formation dynamics can affect the observed quasi-equilibrated profiles through the spontaneous emergence of composite structures during the phase transition crossing [6].

We acknowledge financial support from the EPSRC and discussions with Tom Billam, Simon Cornish, Simon Gardiner, Shih-Chuan Gou and Nick Parker.

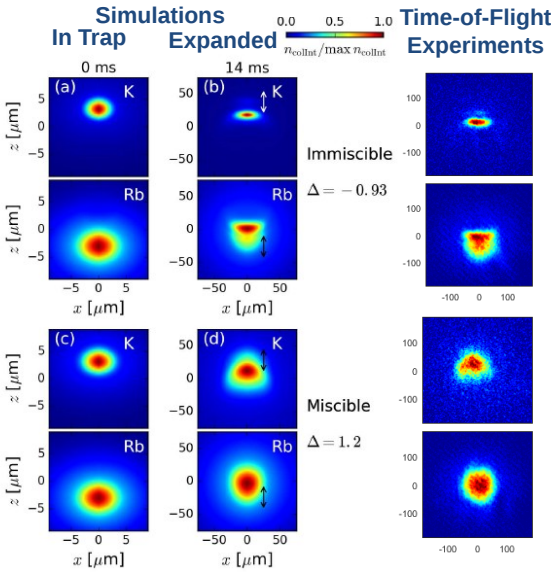

Fig. 1: Comparison of simulated *in situ* and *expanded* coupled condensate profiles (left two columns), and corresponding experimentally-measured ones (right column) for a harmonically-confined ^{87}Rb-^{39}K mixture, with a large *in situ* phase separation. These images show clearly that the observation of characteristic structures after time-of-flight imaging does not necessarily reflect the *in situ* physics.

References

[1] M. J. Edmonds, K.-L. Lee, N. P. Proukakis, Phys. Rev. A **91**, 011602(R) (2015).
[2] M. J. Edmonds, K.-L. Lee, N. P. Proukakis, Phys. Rev. A **92**, 063607 (2015).
[3] K.-L. Lee, N. B. Jorgensen, I.-K. Liu, L. Wackers, J. J. Arlt, N. P. Proukakis, Phys. Rev. A **94**, 013602 (2016).
[4] K.-L. Lee, N. Jørgensen, L. Wacker, M. G. Skou, K. T. Skalmstang, J. J. Arlt, N. P. Proukakis, in preparation.
[5] K.-L. Lee, N. P. Proukakis, J. Phys. B **49**, 214003 (2016).
[6] I.-K. Liu, R. W. Pattinson, T. P. Billam, S. A. Gardiner, S. L. Cornish, T.-M. Huang, W.-W. Lin, S.-C. Gou, N. G. Parker, N. P. Proukakis, Phys. Rev. A **93**. 023628 (2016).

*Corresponding author: nikolaos.proukakis@ncl.ac.uk

To the list of contents

Decay of Josephson Superflow via Vortex-Ring Emission

K. Xhani[1], K. L. Lee[1], L. Galantucci[1], C. F. Barenghi[1], A. Trombettoni[2], G. Valtolina[3], F. Scazza[3], A. Amico[3], C. Fort[3], M. Zaccanti[3], A. Burchianti[3], G. Roati[3], and Nick Proukakis[*1]

1. Joint Quantum Centre (JQC) Durham–Newcastle, School of Mathematics and Statistics, Newcastle University Newcastle upon Tyne NE1 7RU, UK

2. CNR-IOM and SISSA, Italy

3. INO-CNR and LENS, Italy

Josephson oscillations in fermionic superfluids across the BEC-BCS crossover [1] have been recently experimentally observed to decay through the emission of vortical excitations at the barrier connecting the two parts of the superfluid in a double-well trap. By performing full 3D numerical simulations in the molecular BEC regime at both zero and finite temperatures, we explicitly demonstrate the generated structures to be excited vortex rings, and study their propagation, dynamical instability and subsequent decay (see figure below) [2], shedding more light into this nonlinear process, the role of interactions of vortex rings with other rings and background sound, and the effect of gradually removing the barrier (experimental step undertaken before time-of-flight imaging). By self-consistently coupling the Gross-Pitaevskii equation to a quantum Boltzmann equation ("ZNG" model) [3] we also discuss the role of finite temperature in damping both Josephson oscillations and macroscopic quantum self-trapping.

We acknowledge financial support from the EPSRC.

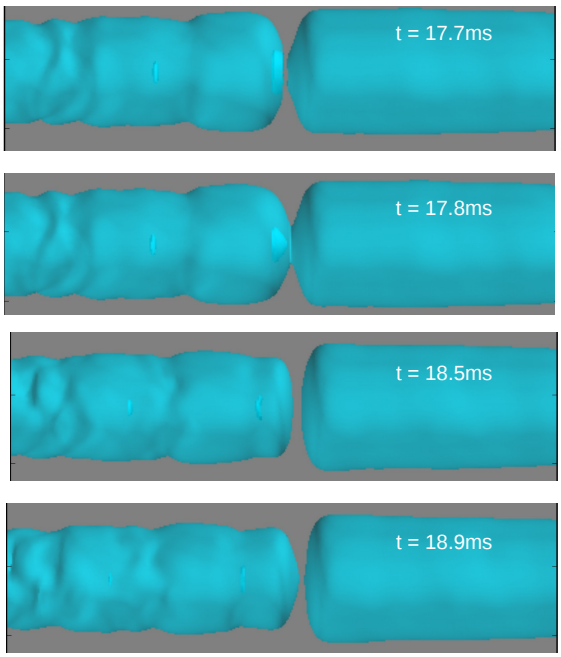

Fig. 1: Snapshots of the evolving condensate density, clearly highlighting the creation of a vortex ring in, and subsequent emergence from, the barrier region, and subsequent decay, in the presence ofan underlying Josephson current.

References

[1] Valtolina et al., Science **350**, 15050 (2015).
[2] Xhani et al., in preparation
[3] K.-L. Lee, N. P. Proukakis, J. Phys. B **49**, 214003 (2016).

*Corresponding author: nikolaos.proukakis@ncl.ac.uk

To the list of contents

Manipulating cold atoms with low frequency electromagnetic radiation.

G. A. Sinuco-Leon[*1], **B. M. Garraway** [1]
1. Department of Physics and Astronomy, University of Sussex, Brighton, BN1 9QH, UK

Low frequency electromagnetic radiation constitutes a superb tool for coherent control of the internal state of a wide variety of quantum systems (e.g. NV centres, superconducting circuits and trapped atoms and ions). It is usual to describe the dynamics of such systems neglecting their multilevel nature via perturbative expansions and applying the rotating wave approximation (RWA). However, modern experimental implementations let us explore the regime of strong matter-radiation coupling where all relevant energy scales can be of the same order of magnitude, which renders inaccurate the standard simplifications. In this work, we present a study of the dynamics of a multilevel quantum system coupled to strong fields in the context of ultracold alkali atoms under the influence of multiple radio-frequency and microwave electromagnetic fields.

We describe the atomic dynamics corresponding to typical atom-chip configuration and highlight the range of relevant energy scales achievable with state-of-the-art technology. We discuss novel effects associated with non-equal energy spacing between internal states (corresponding to non-linear Zeeman shifts) and its utility to reduce the sensitivity of atomic clock transitions via RF and MW dressing [1], and to implement addressed manipulation of atomic qubits trapped in a lattice [2]. Following this, we consider qubits encoded by atomic RF dressed states and evaluate beyond RWA effects on its transition frequency and coupling to microwave radiation. The relevance of this work for applications in atomic interferometry [3] and quantum information processing are demonstrated with concrete examples.

References

[1] G. A. Sinuco-Leon and B.M. Garraway, NJP **14**, 123008 (2012). G.A. Kazakov and T. Schumm, PRA **91**, 023404 (2015). L. Sarkany, et al., PRA **90**, 053416 (2014)
[2] G. A. Sinuco-Leon and B.M. Garraway, NJP **17**, 053037 (2015). G. A. Sinuco-Leon and B.M. Garraway, NJP **18** 035009 (2016).
[3] G.A. Sinuco-Leon, et al., Nat. Comm. **5**, 5289 (2014).

[*]Corresponding author: g.sinuco@sussex.ac.uk

To the list of contents

Observation of attractive and repulsive polarons in a Bose-Einstein condensate

N. B. Jørgensen[1], L. Wacker[1], K. T. Skalmstang*[1], M. M. Parish[2], J. Levinsen[2], R. S. Christensen[1], G. M. Bruun[1], J. J. Arlt[1]

1. Institut for Fysik og Astronomi, Aarhus Universitet 8000 Aarhus C, Denmark
2. School of Physics & Astronomy, Monash Unversity, Victoria 3800, Australia

The problem of an impurity particle moving through a bosonic medium plays a fundamental role in physics, ranging from organic electronics to the Standard Model. However, despite intense theoretical investigation, the canonical scenario of a mobile impurity immersed in a Bose-Einstein condensate (BEC) has not yet been realized. Here, we use radio frequency spectroscopy of ultracold bosonic ^{39}K atoms to experimentally demonstrate the existence of a well-defined quasiparticle state of an impurity interacting with a BEC [1]. We measure the energy of the impurity both for attractive and repulsive interactions, and find excellent agreement with theories that incorporate three-body correlations. The spectral response consists of a well-defined quasiparticle peak at weak coupling, while for increasing interaction strength, the spectrum is strongly broadened and becomes dominated by the many-body continuum of excited states. Crucially, no significant effects of three-body decay are observed. Our results open up exciting prospects for studying mobile impurities in a bosonic environment and strongly interacting Bose systems in general.

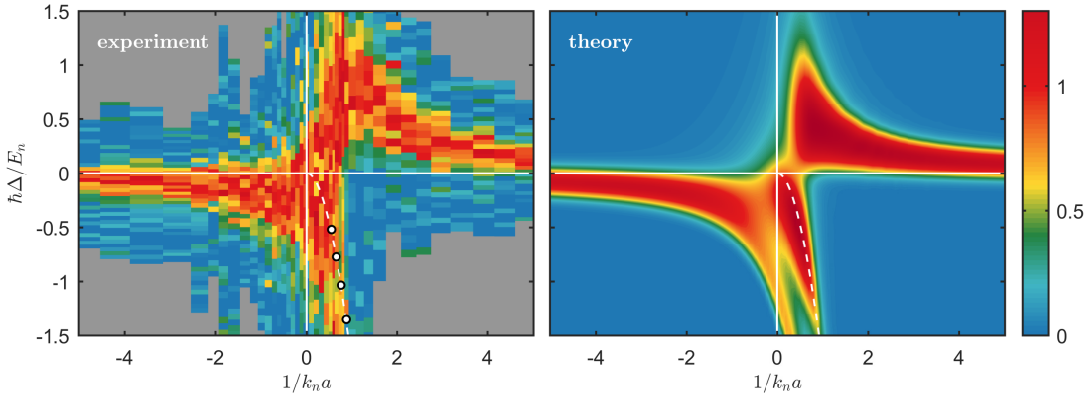

Fig. 1: The spectral response of an impurity in a BEC as a function of detuning Δ and interaction strength $1/k_n a$. Both experiment and theory show a clear shift in in spectral weight due to the interaction between the impurity and the BEC

References

[1] N. B. Jørgensen *et al.*, in *Phys. Rev. Lett.* ***117***, 055302 (2016).

*Corresponding author: kt.skalmstang+au@gmail.com

To the list of contents

Spatially distributed multipartite entanglement and Einstein-Podolsky-Rosen steering of atomic clouds

Philipp Kunkel[*1], **Maximilian Prüfer** [1], **Daniel Linnemann** [1], **Anika Frölian** [1], **Helmut Strobel**[†1], **Thomas Gasenzer** [1], **Martin Gärttner** [1], **and Markus K. Oberthaler** [1]

1. Kirchhoff-Institut für Physik, Universität Heidelberg, Im Neuenheimer Feld 227, 69120 Heidelberg, Germany

A key resource for distributed quantum-enhanced protocols is entangled states between spatially separated modes. Here, we use spin mixing in a tightly confined Bose-Einstein condensate of ^{87}Rb to generate a squeezed vacuum state in a single spatial mode. We show experimentally that the corresponding local entanglement can be spatially distributed by self-similar expansion of the atomic cloud in a waveguide potential. Spatially resolved spin read-out is used to reveal Einstein-Podolsky-Rosen (EPR) steering between distinct parts of the expanded cloud. Building on the ability to partition the system arbitrarily, we also show threeway steering. To quantify the connection between the strength of EPR steering and genuine multipartite entanglement we construct a witness, which testifies up to genuine five-partite entanglement.

[*]Corresponding author: steering@matterwave.de
[†]Corresponding author: helmut.strobel@kip.uni-heidelberg.de

To the list of contents

Non-adiabatic quantum phase transition in a trapped spinor condensate

Tomasz Świsłocki[*1], **E. Witkowska**[2], **M. Matuszewski**[2]
1. Faculty of Applied Informatics and Mathematics, Warsaw University of Life Sciences, ul. Nowoursynowska 159, 02-786 Warsaw, Poland
2. Institute of Physics, PAS, Aleja Lotnikow 32/46, 02-668 Warsaw, Poland

We study the effect of an external harmonic trapping potential on an outcome of the non-adiabatic quantum phase transition from an antiferromagnetic to a phase-separated state in a spin-1 atomic condensate. Previously, we demonstrated that the dynamics of an untrapped system exhibits double universality with two different scaling laws appearing due to conservation of magnetization [1]. We show that in the presence of a trap double universality persists. However, the corresponding scaling exponents are strongly modified by transfer of local magnetization across the system. The values of these exponents cannot be explained by the effect of causality alone, as in the spinless case. We derive the appropriate scaling laws based on a slow diffusive-drift relaxation process in the local density approximation [2].

References

[1] Tomasz Świsłocki, Emilia Witkowska, Jacek Dziarmaga, and Michał Matuszewski, Phys. Rev. Lett. **110**, 045303 (2013).
[2] Tomasz Świsłocki, Emilia Witkowska, and Michał Matuszewski, Phys. Rev. A **94**, 043635 (2016).

*Corresponding author: tomasz_swislocki@sggw.pl

To the list of contents

Synthetic clock transitions and Rashba spin-orbit coupling

Dimitris Trypogeorgos[*1], **Ana Valdés-Curiel**[1], **Nathan Lundblad**[2], **I. B. Spielman**[1]
1. Joint Quantum Institute, University of Maryland and National Institute of Standards and Technology, College Park, Maryland, 20742, USA
2. Department of Physics and Astronomy, Bates College, Lewiston, Maine 04240, USA

Decoherence of a quantum system due to uncontrolled environmental fluctuations presents a fundamental obstacle in quantum science. 'Clock' transitions that are insensitive to low frequency fluctuations are used to extend the coherence time, however these may not always exist in a particular system. Here, we use dynamical decoupling in a spin-1 Bose-Einstein condensate to create a trio of 'dynamical' clock transitions, with only quadratic sensitivity to magnetic field fluctuations, as with the naturally occurring clock transitions present near zero magnetic field. Using a concatenated scheme, we also suppress the sensitivity to fluctuations in our control fields. The new field insensitive states represent an ideal starting place for a new generation of experiments with artificial gauge fields and spinor Bose-Einstein condensates.

The loss of coherence due to uncontrolled coupling to fluctuations of the surrounding environment, is the limiting performance factor for quantum technologies. In select cases, 'clock' transitions exist that are first order insensitive to the dominant noise sources, however, in most cases, such transitions are absent. This limitation can be lifted using dynamical decoupling protocols, in which the system is continuously driven by an external field, resulting in a dynamically protected 'dressed' system. A number of dynamical decoupling methods, pulsed or continuous, have been shown to isolate a quantum system from the low frequency noise of its immediate environment. Continuous dynamical decoupling (CDD) relies on the application of time-periodic, continuous control fields, rather than a series of quantum-logic pulses. To date, CDD has been used to produce protected two level systems in nitrogen-vacancy center experiments, NMR, and trapped ions. We implemented CDD in an atomic Bose-Einstein condensate (BEC) producing a protected *three* level system, suitable for quantum simulation experiments. Moreover, the energy differences of the dressed eigenstates are proportional to the amplitude of the dressing field, and hence tunable, and the quantization axis can be arbitrarily rotated so that two separate quantum systems can be strongly coupled.

These techniques adds no heating or loss mechanisms, yet within the protected subspace retains the full complement of cold-atom coherent control tools such as optical lattices and Raman laser coupling, and permit new first order transitions that are absent in the unprotected subspace [2]. For example, a fully connected geometry is required for engineering exotic topological states such as topological insulators, the spin-Hall effect, and two-dimensional Rashba spin-orbit coupling in ultracold atomic systems [3].

References

[1] D. Trypogeorgos, A. Valdés-Curiel, N. Lundblad, I. B. Spielman, unpublished.
[2] D. L. Campbell and I. B. Spielman, New Journal of Physics, 18, 033035, 2016.
[3] Gediminas Juzeliūnas, Julius Ruseckas, and Jean Dalibard, Phys. Rev. A 81, 053403, 2010.

To the list of contents

Spatial entanglement patterns and Einstein-Podolsky-Rosen steering in a Bose-Einstein condensate

T. Zibold[*1], **M. Fadel** [1], **B. Décamps** [1], **P. Treutlein**[1]
1. Department of Physics, University of Basel, Klingelbergstrasse 82, 4056 Basel, Switzerland

We investigate the spatial entanglement in a spin squeezed Bose-Einstein condensate of rubidium atoms. We experimentally prepare two-component Bose-Einstein condensates of several hundreds of atoms on an atom-chip [1]. Using state-selective potentials to tune the collisional interactions we prepare spin squeezed atomic states through one axis twisting [2]. By letting the atomic cloud expand and using high resolution absorption imaging we are able to access the spatial spin distribution of the many-body state. The observed spin correlations between different regions go beyond classical correlations and reveal spatial non-separability. Furthermore they allow for Einstein-Podolsky-Rosen (EPR) steering of a sub-region of the atomic spin. By inferring measurement outcomes of non-commuting observables in one region based on measurements in a separate region we are able to seemingly beat the Heisenberg uncertainty relation, realizing the EPR paradox with an atomic system [3]. Our findings of spatial entanglement in ultracold atomic clouds pave the way for future quantum enhanced measurements of spatially varying observables such as electromagnetic fields.

References

[1] P. Böhi, et al., Nature Physics **5**, 592 (2009)
[2] M. F. Riedel, et al., Nature **464**, 1170 (2010)
[3] M. D. Reid, et al., Rev. Mod. Phys. **81**, 1727 (2009)

*Corresponding author: tilman.zibold@unibas.ch

To the list of contents

Study of ICD time evolution with THz – field - driven XUV streak camera

F. Karimi[1,2] **M.Pfau**[1,2] **M. Ranke**[1,2] **S. Walther**[1,2] **A. Dimitriou**[*1,2], **U.Frühling**[†1,2]
1. Center for Ultrafast Imaging, Luruper Chaussee 149, 22761 Hamburg, Germany
2. Institut für Experimentalphysik, Universität Hamburg, Luruper Chaussee 149, 22761 Hamburg, Germany

Interatomic Coulombic Decay (ICD), a non-local auto-ionization process, is an efficient decay channel used by atoms in loosely bound van der Waals rare gas molecules and clusters [1]. The aim of this study is the investigation of the ICD lifetime in Ne-Kr dimers formed in a co-expansion of a NeKr gas mixture under high pressure through an aperture in vacuum with the use of THz-streaking [2], [3].

In order to ionize an inner valence electron of Ne and therefore initiate the ICD process we generate few fs Ultrashort XUV pulses with High Harmonic Generation (HHG). The relaxation energy of Ne is transferred to the neighbouring Kr atom in form of a virtual photon. The whole process leaves two ionized atoms in a dimer which consequently undergoes a coulomb explosion.

The continuum electron wave packet will be probed with an intense THz field, which is superimposed with the XUV pulses, and is created by optical rectification of NIR laser pulses on a $LiNbO_3$ nonlinear crystal. Efficient velocity matching of NIR and THz pulses is achieved by tilting the pulse front with the use of a diffraction grating [4]. The temporal profile of this wave carries the desired temporal information about the underlying dynamics. Our group has pioneered in adapting the THz- field streaking technique [5].

Within this project we have already built an experimental chamber to efficiently create van-der-Waals clusters. Our set up also consists of an already operational XUV monochromator designed and constructed by our group in order to choose the desired harmonic [6]. The whole set up is close to become fully operational for streaking measurements and the most recent developments as well as the experimental set up and the techniques used for this study will be presented in the conference.

References

[1] L.S. Cederbaum *et al.*, Phys. Rev. Lett. **79**, 4778 (1997).
[2] U. Frühling *et al.*, Nat. Phot. **3**, 523 (2009).
[3] B. Schütte *et al.*, Opt. Expr. **19**, 18833 (2011).
[4] J. Hebling *et al.*, Opt. Expr. **10**, 1161 (2002).
[5] U. Frühling Jour. Phys. B **44**, 243001 (2011).
[6] F. Frassetto *et al.*, Opt. Expr. **19**, 19169 (2011).

[*]Corresponding author: anastasios.dimitriou@cfel.de
[†]Corresponding author: ulrike.fruehling@desy.de

To the list of contents

4d - 4f Photoabsorption in Laser-Produced Thulium Plasmas

R. Stefanuik[1,3] **E. Sokell**[1], **E. Long**[1], **P. Hayden**[2], **P. Dunne**[*1]
1. UCD School of Physics, University College Dublin
Belfield, Dublin 4, Ireland
2. School of Physical Sciences, Dublin City University,
Dublin 9, Ireland.
3. Department of Physics and Astronomy, Uppsala University,
751 05 Uppsala, Sweden

The dual laser plasma (DLP) technique [1] exploits the continuum emission from a laser produced plasma, formed on a high-Z solid target to probe the ions present in a second plasma, formed on a target of the material of interest. By varying the time delay between the formation of the plasma containing the ions to be observed and the creation of the continuum, it is possible to probe successively lower stages of ionisation. Typically the absorbing plasma is formed as a column in which the plasma electron temperature is below 5 eV and the time delays between plasmas range from 25 ns to 1000 ns. The continuum is generated on a tungsten, samarium or hafnium target, where individual line emission is not observed [2]. This is due to emission by extremely high numbers of weak lines which is submerged in plasma continuum and bremsstrahlung radiation.

In this work, spectra revealing photoabsorption due to Tm, Tm^{+} and Tm^{2+} ions have been observed in the spectral region between 6 and 8 nm where 4d to 4f photoabsorption is the dominant process. These ions are of particular interest as they have $4d^{10}4f^{13}6s^{n}$ ground states where $n = 2$, 1 and 0 in the case of Tm, Tm^{+} and Tm^{2+}, respectively. Thus in each ion the 4d – 4f transitions are of the form $4d^{10}4f^{13}$ - $4d^{9}4f^{14}$ with the 6s electrons effectively playing a spectator role where present. Only photoabsorption from the lower $^{2}F_{7/2}$ term in neutral thulium has been observed prior to this work[3] by Radtke, using a furnace as the source of thulium vapour and synchrotron radiation as the probe.

Large resonances, peaking in the region around 7.1 nm are present at delays ranging from 25 to 1000 ns, reflecting the similar photoabsorption processes that occur through each of the first three ion stages. For each ion stage the absorption profile can be explained in terms of two spin-orbit components, fitted to combined Fano profiles. Analysis was aided by the use of a Hartree Fock with configuration interaction atomic structure code [4].

References

[1] J. T. Costello *et al.* Physica Scripta **T34**, 77 (1991).
[2] G. O'Sullivan *et al.*, Opt. Eng. **33(12)**, 3993 (1994).
[3] E.R. Radtke, J. Phys. B: At. Mol. Phys. **12**, L71 (1979).
[4] R. D. Cowan, in *The Theory of Atomic Structure and Spectra*, Berkeley, CA, (University of California Press, 1981).

*Corresponding author: padraig.dunne@ucd.ie

To the list of contents

Photo-ionization in Presence of Circularly Polarized Fundamental and Odd Order Harmonic Fields.

I.A.Ivanov[*1,3], **Chang Hee Nam**[1,2], **Kyung Taec Kim**[†1,2]
1. Center for Relativistic Laser Science, Institute for Basic Science, 123 Cheomdangwagiro, Buk-gu, Gwangju, 61005, Korea
2. Department of Physics and Photon Science, GIST, Gwangju 61005, Republic of Korea
3. Research School of Physics and Engineering, The Australian National University, Canberra ACT 0200, Australia

Strong field ionization process driven by a circularly polarized laser pulse and its second harmonic received recently considerable attention in the literature [1-3]. A natural generalization of this setup would be a field configuration consisting of the circularly polarized fundamental field and its higher harmonics.

We present a study of the photo-electron spectra for the ionization process driven by counter- and co-rotating circularly polarized fundamental and odd order harmonic fields. General features of the photo-electron spectrum for the field configurations we consider can be inferred from the simple SFA picture of ionization, in which ionization occurs at the times t_m of the peak field strength of the pulse, with the final electron velocity given by the value of the vector potential at this moment of time. One can easily see that for the flat pulse envelope and the counter-rotating geometry, the total electric field of the pulse has $q+1$ peak values of equal magnitude per each optical cycle of the fundamental field at times $t_m = \dfrac{mT}{q+1}$ $(m = 0,\ldots,q)$ (here T is an optical cycle), with vector potential components:

$$A_x(t) = -\frac{E_1}{\omega\sqrt{2}}\left(1-\frac{C}{q}\right)\sin\omega t_m \ , A_y(t) = \frac{E_1}{\omega\sqrt{2}}\left(1-\frac{C}{q}\right)\cos\omega t_m \ . \tag{1}$$

Here $C = \dfrac{E_q}{E_1} = 0.1$, E_1 and E_q are, respectively, the field strengths of the fundamental and harmonic fields. According to this simple picture, for the counter-rotating geometry the photo-electron spectra should form a regular structure with $q+1$ lobes in the polarization plane of the pulse. For the case of the co-rotating circularly polarized fundamental field and its q-th harmonic the photo-electron spectra should exhibit a structure with $q-1$ lobes in the polarization plane of the pulse.

A TDSE calculation, organized along the lines we described in [4], confirms this picture as spectra shown in Fig.1. demonstrate.

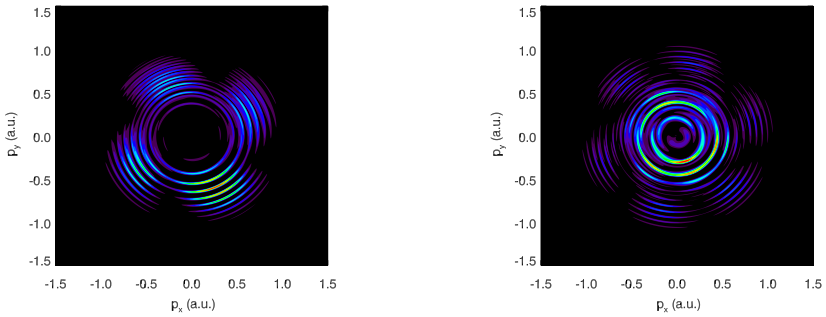

Fig. 1: Ionization probability distribution in the polarization plane for the counter-rotating fundamental and third harmonic (left panel), and fundamental and fifth harmonic (right panel) fields. Pulse parameters: intensity and frequency of the fundamental field are $I = 10^{14}$ W/cm^2, $\omega = 0.057$ a.u. (wavelength of 790 nm). Intensities of the third and fifth harmonics were 10^{12} W/cm^2.

Main difference with the SFA predictions is presence of the low energy structures (LES). Of all the field configurations we considered, LES were present only for the case of ionization driven by the counter-rotating fundamental field and its fifth harmonic. We tried to elucidate this phenomenon, and found that Rydberg states populated by a combined absorption of the photons from the fundamental and harmonic fields are responsible for its origin.

References

[1] C. A. Mancuso *et al.*, Phys. Rev. A **91**, 031402(R) (2015).
[2] J. L. Chaloupka and D. D. Hickstein, Phys. Rev. Lett. **116**, 143005 (2016).
[3] M. Richter, M. Kunitski, M. Schöffler, T. Jahnke, L. P. H. Schmidt, and R. Dörner, Phys. Rev. A **94**, 033416 (2016).
[4] I. A. Ivanov, Phys. Rev. A **90**, 013418 (2014).

[*]Corresponding author: Igor.Ivanov@anu.edu.au
[†]Corresponding author: kyungtaec@gist.ac.kr

To the list of contents

Fano-CI method for decay widths of metastable excited states of atomic and molecular systems

Přemysl Kolorenč[*1]
1. Charles University, Faculty of Mathematics and Physics, Institute of Theoretical Physics, V Holešovičkách 2, 180 00 Prague, Czech Republic

Electron correlation is an essential driver of a variety of relaxation processes in metastable excited atomic and molecular systems. These are phenomena which often lead to autoionization involving two-electron transitions, such as Auger effect or inter-atomic Coulombic decay (ICD). Recently, even higher-order multi-electron decay processes has come into focus since their significance increases in multiply excited systems produced, e.g., after irradiation by high-intensity free electron lasers [1]. Among fundamental characteristics of a metastable state belongs decay width, directly related to its lifetime. Wide range of computational approaches can be chosen to determine this quantity. Number of studies employ the golden rule formula for transition probabilities combined with various many electron wave function models, usually specifically tailored to the particular problem. Alternatively, decay widths can be computed using complex absorbing potential (CAP) in combination with various tools of excited-state quantum chemistry, such as configuration interaction (CI), algebraic diagrammatic construction (ADC) or equation-of-motion coupled-cluster methods.

The CAP-based methods represent possibly the most generic approach to study lifetimes of autoionizing states and, furthermore, can build on the highly developed foundations of computational quantum chemistry if standard square-integrable ($\mathscr{L}^2$) basis sets are used. Major disadvantage of the method is that only the total decay widths can be determined, partial widths for individual channels are not accessible. Also, the approach is rather demanding with respect to the quality of the basis set necessary for reliable representation of the CAP since it has to be localized in a region sufficiently distant from the system.

Another class of $\mathscr{L}^2$ methods is based on the Fano theory of resonances, again in combination with CI or ADC expansions for the description of the many-electron wave functions. These methods were established as very accurate and possibly the most efficient tools for computation of intra- and inter-atomic decay widths and have been utilized in several important studies of ICD [3]. Fano-ADC was applied successfully also to study collective decay processes involving more than two electrons [4] or to large molecules with hundreds of decay channels [5]. In contrast to CAP, this class of methods can be used to calculate also the partial decay widths, even though the use of square integrable still prohibit rigorous definition of the decay channels and the partial widths are therefore only approximate. Furthermore, since only the coupling matrix elements between the discretized continuum and a compact discrete state wave functions are needed, less diffuse basis sets are usually sufficient to obtain converged results.

At the heart of the Fano theory is separation of the Hilbert space into background continuum subspace $\mathscr{P}$ and complementary subspace $\mathscr{Q}$ containing the discrete states representing the resonances. Since the natural distinction between the continuum and $\mathscr{L}^2$ wave functions associated with the discrete states is lost when standard Gaussian or other $\mathscr{L}^2$ one-particle basis set is employed, other criteria for the separation have to be devised. Recently, universal procedure for the classification of individual many-electron configurations appearing in the CI or ADC expansions has been developed [6]. However, it is restricted to configurations characterized by only a single electron occupying virtual orbital and cannot be used, in the case of ADC for ionized systems, beyond the second-order. The task becomes significantly more complicated when configurations with two or more electrons in virtual orbitals are involved. Such configurations are found in higher-order ADC or CI expansions or already in the second-order ADC scheme for polarization propagator needed to study decay of excited states of electronically neutral systems. Therefore, universal Fano-ADC method for the latter is missing.

We will present generic Fano-CI method for electronically neutral systems in which the projectors on the $\mathscr{P}$ and $\mathscr{Q}$ subspaces are constructed using separate CI calculation for singly-ionized decay channels. Unfortunately, such a straightforward approach cannot be applied to the more accurate ADC schemes. However, the method can be utilized in the future for testing different classification procedures generalizing the approach of Ref. [6].

The work was funded by the Czech Science Foundation under the project GAČR 17-10866S.

References

[1] P. Kolorenč *et al.*, J. Phys. B **49**, 082001 (2016).
[2] T. Takanashi *et al.* , *Phys. Rev. Lett.* **118**, 033202 (2017).
[3] N. Sisourat *et al.* , *Nat. Phys.* **6**, 508 (2010); K. Gokhberg *et al.*, *Nature* **505** 664 (2014).
[4] R. Feifel *et al.* , *Phys. Rev. Lett.* **116**, 073001 (2016).
[5] A. Sanchez-Gonzales *et al.* , J. Phys. B **48**, 234004 (2015).
[6] P. Kolorenč and N. Sisourat, *J. Chem. Phys.* **143**, 224310 (2015).

*Corresponding author: kolorenc@gmail.com

To the list of contents

The ALPHA Experiment: Laser and Microwave Spectroscopy of Antihydrogen Atoms

Daniel Maxwell[*1], **the ALPHA Collaboration**
1. Swansea University, Singleton Park, Swansea, Wales, SA2 8PP, UK

In 2016, the ALPHA collaboration at CERN observed the first optical transition in antihydrogen atoms [1]. Along with microwave transitions observed in 2012 [2], these measurements constitute milestone steps towards direct spectroscopic comparisons between hydrogen and antihydrogen as a test of CPT (charge-parity-time) symmetry [3]. The immediate goal of the ALPHA experiment is to improve the precision of these spectroscopic measurements, with the ultimate aim of matching the levels of precision that have been achieved with hydrogen, where the absolute frequency of the 1S-2S transition has been measured to 4 parts in 10^{15} [4].

We will present the experimental apparatus and techniques that have made spectroscopy of antihydrogen possible. At the heart of the 1S-2S spectroscopic measurement is the optical enhancement cavity, inside the cryogenic atom trap. New techniques in antihydrogen trapping developed in 2016 mean that we can now trap and perform spectroscopy on ten's of antihydrogen atoms simultaneously, compared to the 1-2 atoms previously demonstrated [5].

We will also present developments towards increasing the antihydrogen trapping rate. The current trapping rate of antihydrogen will eventually put restrictions on the precision that future experiments are likely to achieve. The positron temperature is thought to play a vital role in both the rate of antihydrogen formation, and on the trapping rate of antihydrogen [6],[7]. Currently, positron temperatures reach around 50 K. By lowering the positron temperature, significantly more antihydrogen atoms should be trapped. We propose to sympathetically cool the positrons using laser-cooled beryllium ions, $^{9}Be^{+}$, a technique that has previously been demonstrated [8]. Simulations in ALPHA have shown that the temperature of the positrons could potentially be reduced to less than 5K if cooling is maintained during antihydrogen formation [9]. We have recently demonstrated a Beryllium ion source suitable for operation under significant constraints imposed by the ALPHA apparatus, which is being installed before the 2017 antiproton run.

References

[1] ALPHA Collaboration, Nature **541**, 506-510 (2017).
[2] ALPHA Collaboration, Nature **483**, 439-443 (2012).
[3] T. Hansch *et al*., Hyperfine interact. **76**, 47-57 (1993).
[4] A. Matveev *et al*., Phys. Rev. Lett. **110**, 230801 (2013).
[5] ALPHA Collaboration, Nature **529**, 373-376 (2016).
[6] G. Gabrielse *et al*., Phys. Lett. A **129**, 38 (1988).
[7] ATHENA Collaboration, Phys. Lett. B **583**, 59 (2004).
[8] B. M. Jelenkovic *et al*., Phys. Rev. A **67**, 063406 (2003).
[9] N. Madsen *et al*., New J. Phys **16**, 063046 (2014).

*Corresponding author: daniel.thomas.maxwell@cern.ch

To the list of contents

Configuration Interaction Effects in Unresolved np^6nd^{N+1} - np^5nd^{N+2}+$np^6nd^Nnf^1$ Transition Arrays; Contrasting Behaviour for n = 4 and n = 5

Luning Liu[*1,2], **Deirdre Kilbane**[2], **Padraig Dunne**[2], **John Sheil**[2], **Xinbing Wang**[1] **and Gerry O'Sullivan**[†2]

1. Wuhan National Laboratory for Optoelectronics, Huazhong University of Science and Technology, Wuhan 430074, China

2. School of Physics, University College Dublin, Belfield, Dublin 4, Ireland

The extreme ultraviolet (EUV) and soft x-ray (SXR) spectra of medium and high Z-ions are known to be dominated by emission from unresolved transition arrays (UTAs), the most intense of which originate from $\Delta n = 0$, $4p^64d^{N+1} - 4p^54d^{N+2} + 4p^64d^N4f^1$ transitions [1]. Indeed, their intensity is such, that sources based on such emission are being developed for applications ranging from lithography to microscopy [2, 3]. Configuration interaction (CI) effects can greatly influence the spectral profile and intensities of these UTAs [4 - 6]. Changing the principle quantum number n, from 4 to 5, changes the origin of the UTA from $\Delta n = 0$, $4p^64d^{N+1} - 4p^54d^{N+2} + 4p^64d^N4f^1$ to $\Delta n = 0$, $5p^65d^{N+1} - 5p^55d^{N+2} + 5p^65d^N5f^1$ transitions. This causes unexpected and significant changes in the impact of configuration interaction from that observed in the heavily studied $n = 4 - n = 4$ arrays. In this study, the properties of $n = 5 - n = 5$ arrays have been investigated theoretically in ions of elements from Z = 79 (Au) to Lr (Z = 103) with the aid of Hartree-Fock with configuration interaction (HFCI) calculations and compared with their $n = 4 - n = 4$ counterparts. At the beginning of the sequence, 5f wavefunction contraction effects are clearly evident. In addition to predicting the wavelengths and spectral details of the anticipated features, the calculations show that the effects of configuration interaction are quite different for the two different families of $\Delta n = 0$ transitions, a conclusion which is reinforced by comparison with experimental results.

References

[1] H. Ohashi, T. Higashiguchi, Y. Suzuki, G. Arai, Y. Otani, T. Yatagai, B. Li, P. Dunne, G. O'Sullivan, W. Jiang, A. Endo, H. A. Sakaue, D. Kato, I. Murakami, N. Tamura, S. Sudo, F. Koike, and C. Suzuki *Appl. Phys. Lett.* **104**, 234107 (2014)

[2] G. O'Sullivan, B. Li, R. D'Arcy, P. Dunne, P. Hayden, D. Kilbane, T. McCormack, H. Ohashi, F. O'Reilly, P. Sheridan, E. Sokell, C. Suzuki and T. Higashiguchi *J. Phys. B: At. Mol. Opt. Phys.* **48**, 144025 (2015)

[3] T. Higashiguchi, T. Otsuka, N. Yugami, W. Jiang, A. Endo, B. Li, P. Dunne, and G. O'Sullivan *Appl. Phys. Lett.* **100**, 014103 (2012)

[4] P. Mandelbaum, M. Finkenthal, J. L. Schwob, and M. Klapisch *Phys. Rev. A* **35**, 5051 (1987)

[5] J. Bauche, C. Bauche-Arnoult, M. Klapisch, P. Mandelbaum and J. L. Schwob *J. Phys. B: At. Mol. Opt. Phys.* **20**, 1443 (1987)

[6] S. Kucas, R. Karazija, V. Jonauskas, and A. Momkauskaite *J. Phys. B: At. Mol. Opt. Phys.* **42**, 205001 (2009)

[*]Corresponding author: luningliu@outlook.com

[†]Corresponding author: gerry.osullivan@ucd.ie

To the list of contents

Variation of the fine-structure constant and the electron-proton mass ratio in simple ions

Natalia S. Oreshkina[*1], **Stefano M. Cavaletto**[1], **Niklas Michel**[1], **Christoph H. Keitel**[1], **Zoltán Harman**[1]
1. Max-Planck-Institut für Kernphysik, Saupfercheckweg 1, 69117 Heidelberg, Germany

Numerous few-electron atomic systems are considered, which can be effectively used for observing a potential variation of the fine-structure constant α and the electron-proton mass ratio m_e/m_p. We examine magnetic dipole transitions between hyperfine-structure components in heavy highly charged H-like and Li-like ions with observably high sensitivity to a variation of α and m_e/m_p. The experimental spectra of the proposed systems consist of only one, strong line, which simplifies significantly the data analysis and shortens the necessary measurement time. Furthermore, we propose systems for an experimental observation of the variation of quark masses and discuss the expected level of accuracy in assessing limitations on the variation of the quark masses. Finally, we establish which constraints on the variation of the fundamental constants could be provided by measurements with a hyperfine-structure highly-charged-ion clock and some reference clock, showing that the improvement of the current limitations can be reached even for a conservative scenario.

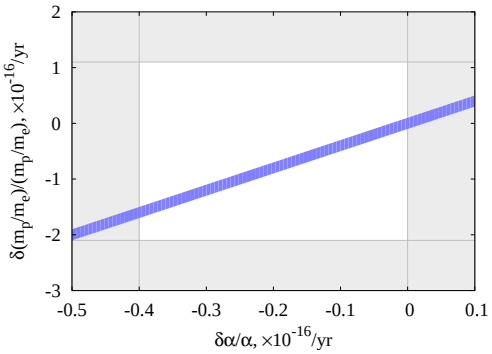

Fig. 1: The current limits for the variation of the fine-structure constant $\frac{\delta\alpha}{\alpha} = -2.0(2.0)\times 10^{-17}/\text{yr}$ and electron-proton mass ratio $\frac{\delta(m_e/m_p)}{m_e/m_p} = 0.5(1.6)\times 10^{-16}/\text{yr}$ together with the new limitations based on the comparison of HFS clocks with insensitive atomic clocks on the level of $10^{-17}/\text{yr}$.

References

[1] N. S. Oreshkina, S. M. Cavaletto, N. Michel, C. H. Keitel, and Z. Harman, arXiv: 1703.09943 (2017).

*Corresponding author: oresh@mpi-hd.mpg.de

To the list of contents

High-density effects on the atomic structure and inner-shell transitions of astrophysical interest in oxygen ions

J. Deprince[1], P. Palmeri[1], P. Quinet[1,2], S. Fritzsche[3,4], M.A. Bautista[5], C. Mendoza[5], T.R. Kallman[6] and J. Garcia[7]

[1] Physique Atomique et Astrophysique, Université de Mons, B-7000 Mons, Belgium
[2] IPNAS, Université de Liège, B-4000 Liège, Belgium
[3] Helmholtz Institut Jena, 07743 Jena, Germany
[4] Theoretisch Physikalisches Institut, Friedrich Schiller Universität Jena, 07743 Jena, Germany
[5] Department of Physics, Western Michigan University, Kalamazoo, MI 49008, USA
[6] NASA Goddard Space Flight Center, Code 662, Greenbelt, MD, USA
[7] Department of Astronomy, California Institute of Technology, Pasadena, CA 91125, USA

X-ray emission lines from accreting black holes, most notably K-lines, have observed widths and shifts which imply an origin very close to the compact object [1]. The intensity of these lines can provide insight into the effects of special and general relativity in the emitting region as well as insight into some properties of the compact object itself. According to the magnetohydrodynamic simulations of accreting black holes (M = 10 $M_{\rm Sun}$, accretion rate = 0.1) due to Schnittman *et al*. [2], the plasma conditions in such an environment should be characterized by an electronic temperature, $T_{\rm e}$, ranging from 10^5 to 10^7 K and an electronic density, $n_{\rm e}$, ranging from 10^{18} to 10^{21} cm^{-3}. This may affect the atomic structure and processes corresponding to the ionic species present in the plasma.

In order to estimate the influence of plasma environment on the atomic parameters in oxygen ions, a time averaged Debye-Hückel potential for both the electron-nucleus and electron-electron interactions has been considered within the framework of two independent atomic structure computational approaches, namely the purely relativistic multiconfiguration Dirac-Fock (MCDF) method [3,4] and the Breit-Pauli relativistic approximation, as implemented in the AUTOSTRUCTURE code [5,6]. In the present work, new sets of results related to the plasma environment effects on ionization potentials, K-thresholds, K-line transition energies and radiative emission rates in all oxygen ions, from O I to O VII, are reported.

[1] C.S. Reynolds and M.A. Nowak, Phys. Rep. 377, 389, 2003.
[2] J.D. Schnittman, J.H. Krolik and S.C. Noble, Astrophys. J. 769, 156, 2013.
[3] F.A. Parpia, C. Froese Fischer and I.P. Grant, Comput. Phys. Commun. 94, 249, 1996.
[4] S. Fritzsche, Comput. Phys. Commun. 183, 1525, 2012.
[5] N.R. Badnell, J. Phys. B : At. Mol. Opt. Phys. 30, 1, 1997.
[6] N.R. Badnell, Comput. Phys. Commun. **182**, 1528, 2011.

To the list of contents

Theoretical insight into the atomic structure of neutral astatine, the rarest element on Earth

P. Quinet[1,2] and G. Sicorello[1]

[1] Physique Atomique et Astrophysique, Université de Mons, B-7000 Mons, Belgium
[2] IPNAS, Université de Liège, B-4000 Liège, Belgium

In view of the high radioactivity of all its isotopes, astatine (Z = 85) is the rarest naturally occurring element on the Earth's crust with an estimated total abundance of less than one gram at any given time [1]. Because of its extreme rarity, the chemical and physical properties of astatine are almost totally unknown. Many of these have only been estimated based on its position in the periodic table, making of At the heaviest of halogens, i.e. the group of elements including fluorine, chlorine, bromine and iodine. As regards its electronic structure, the ground state of the astatine atom is $6p^5\ ^2P_{3/2}$ while the lowest excited configurations are of the type $6p^4nl$ (with nl = 7s, 7p, 6d, 5f, ...). Nevertheless, only two excited levels ($6p^47s\ ^4P_{3/2,5/2}$) were clearly classified until now [2], although some additional tentative identifications of higher-lying states were suggested from recent laser spectroscopy experiments using the resonance ionization laser ion source (RILIS) of the ISOLDE radioactive beam facility at CERN [3] or using the Isotope Separator and Accelerator (ISAC) facility at TRIUMF [4]. As support to further experimental investigations of astatine, it is however useful to know the atomic structure of this element in the most complete possible way.

In the present work, different physical models based on the pseudo-relativistic Hartree-Fock method including intravalence, core-valence and core-core electron correlation [5-7] have been used for modeling the atomic structure and for computing radiative parameters in neutral astatine. These calculations allowed us to provide for the first time a reliable spectroscopic designation to some energy levels experimentally observed [3,4] but not clearly classified in the $6p^5$, $6p^47s$, $6p^47p$, $6p^49p$ and $6p^410p$ configurations. Moreover, a semi-empirical approach based on the quantum defect formula has also been used for predicting level energies along the $6p^4np$ and $6p^4nd$ (n = 8 – 50) Rydberg series. This new theoretical investigation is expected to provide a useful support to future laser-spectroscopy experiments at ISOLDE and to check other theoretical methods that will be used to model the atomic structure and radiative processes in At I.

[1] A.F. Holleman and E. Wiberg E., *Inorganic Chemistry*, Academic Press, 2001.
[2] R. McLaughlin, J. Opt. Soc. Am. 54, 965-967, 1964.
[3] S. Rothe, A.N. Andreyev, S. Antalic et al., Nature Commun. 4, 1835-1840, 2014
[4] S. Raeder, J. Lassen, H. Heggen and A. Teigelhöfer, Hyperfine Interact. 227, 77-83, 2014
[5] R.D. Cowan, *The Theory of Atomic Structure and Spectra*, University of California Press, Berkeley, 1981
[6] P. Quinet, P. Palmeri, E. Biémont, M.M. McCurdy, G. Rieger, E.H. Pinnington, M.E. Wickliffe and J.E. Lawler, Mon. Not. R. Astron. Soc. 307, 934-940, 1999.
[7] P. Quinet, P. Palmeri, E. Biémont, Z.S. Li, Z.G. Zhang and S. Svanberg, J. Alloys Comp. 344, 255-259, 2002.

To the list of contents

High-precision relativistic calculations of isotope shifts in neutral antimony

S. Gamrath[1], P. Palmeri[1], P. Quinet[1,2], S. Bouazza[3] and M.R. Godefroid[4]

[1] Physique Atomique et Astrophysique, Université de Mons, B-7000 Mons, Belgium
[2] IPNAS, Université de Liège, B-4000 Liège, Belgium
[3] LISM, E.A. 4695 Université de Reims-Champagne-Ardenne, F-51687 Reims Cedex 2, France
[4] Chimie Quantique et Photophysique, Université Libre de Bruxelles, B-1050 Brussels, Belgium

The spectroscopic measurements of isotope shifts (IS) for any element are carried out to test the atomic structures, to deduce the changes in the nuclear mean-square charge radius and to give information on electron behaviour inside the nucleus. Antimony (Sb, Z= 51), has only two stable isotopes, ^{121}Sb and ^{123}Sb, with natural abundances of 57.21% and 42.79%, respectively. It also has 36 known radioactive isotopes with mass numbers A ranging from 103 to 140 and with corresponding half-lives spanning from 93 ms (^{139}Sb) to 2.7586 years (^{125}Sb) [1]. By constrast, the mean nuclear charge radius, $\langle r^2 \rangle^{1/2}$, is only known for the two stable isotopes, i.e. 4.6802 ± 0.0026 fm for ^{121}Sb and 4.6879 ± 0.0025 fm for ^{123}Sb [2]. To our knowledge, there are only two measurements of IS published in the literature and they concern exclusively the stable isotopes [3,4].

In the present study we have used a very extensive electron-correlation model based on the fully-relativistic multiconfiguration Dirac–Hartree–Fock (MCDHF) method [5] to calculate the IS electronic parameters, K_{RNMS}, K_{RSMS} and F, for 49 fine-structure levels belonging to the configurations $5s^25p^3$, $5s^25p^26s$, $5s^25p^26p$ and $5s^25p^27p$ in Sb I. These parameters can be used to determine IS of the transitions involving these levels for any pair of Sb isotopes along with their different *NMS* (Normal Mass Shift), *SMS* (Specific Mass Shift) and *FS* (Field Shift) contributions and to deduce the corresponding changes in mean-square nuclear charge radius. Our ab initio calculations agree very well with the recent measurements of Sobolewski *et al* [4] and also show the importance of the relativistic effects on the different IS contributions confirming the breakdown of the scaling law for the *NMS* [6,7].

[1] Table of Nuclides, Nuclear Data Center at KAERI (Korea Atomic Energy Research Institute)[http://http://atom.kaeri.re.kr/nuchart/ (last accessed February 17, 2017)]
[2] I. Angeli, K.P. Marinova, At. Data Nucl. Data Tables 99, 69, 2013
[3] B. Buchholz, H.D. Kronfeldt, G. Müller, M. Voss, R. Winkler, Z. Physik A 288, 247, 1978
[4] L.M. Sobolewski, S. Bouazza , L. Windholz, J. Kwela, J. Opt. Soc. Am. B 33, 1921, 2016
[5] P. Jönsson, G. Gaigalas, J. Bieron, C. Froese Fischer, I.P. Grant, Comput. Phys. Comm. 184, 2197, 2013
[6] J.G. Li, C. Nazé, M.R. Godefroid, G. Gaigalas, P. Jönsson, Eur. Phys. J. D 66, 290, 2012
[7] P. Palmeri, P. Quinet , S. Bouazza, J.Q.S.R.T. 185, 70, 2016

To the list of contents

Electron-impact-induced long-chain modified arylpiperazine molecule fragmentation

L. G. Romanova[1], V. S. Vukstich[1], A. V. Snegursky*[1], A. V. Papp[1], T. A. Snegurskaya[2]
1. Institute of Electron Physics, Ukrainian National Academy of Sciences, 21 Universitetska street, 88017 Uzhgorod, Ukraine
2. Uzhgorod National University, 3 Narodna square, 88000 Uzhgorod, Ukraine

An electron-molecule interaction is a fundamental and very important process involved in various fields, e.g. in radiation biology. In this area, low-energy electrons represent the most predominant species formed during a very short time after the deposition of high-energy ionizing quanta into a biological medium. The study of sustainability of a potent ligand of $5-HT_{1A}$ and $5-HT_{2A}$ receptors [1] is an important step to understand the degradation way of such molecules as a biosystem sub-units under the low-energy electron impact. In our investigation, we studied interactions of low-energy electrons with a highly privileged $5-HT_{1A}$ receptor pharmacophore-o-methoxyphenylpiperazine 4,5- connected with four methylene group alkyl chain to amino acids (named by authors as PZ-68 [1]) in order to probe the intrinsic properties of the molecule and trace its change(s) under the electron impact. We have measured the mass-spectra of the PZ-68 (m/z=470 a.m.u.) molecule at the electron ionizing energies of 70, 20 and 18 eV (the mass spectrum at 18 eV and the structure of PZ-68 are presented in Fig. 1). The crossed-beam method with the mass separation of the collision products by means of a magnetic mass-spectrometer was applied. The experimental technique used in this work was described in detail in [2]. All the mass-spectra measured are characterized by a lack of selectivity and the absence of a peak corresponding to the parent molecular ion. This testifies to the parent molecule instability at ionization. The lack of the distinct fragmentation channels is due to the 8 heteroatoms located along the skeleton chain. The most specific direction of fragmentation of the molecule is the 'β-break', i.e. the homolitic splitting of the $C-C$ or $C-H$ bond being β-located with respect to a heteroatom. Besides the 'β-break', a considerable role is also played by the α-bond dissociation (with respect to the charge 'localization' site), in particular, at the chain branching sites. In the higher-mass region (i.e. at $m/z > 300$ a.m.u.), no high-intensity and average-intensity peaks are observed. This indicates, probably, the instability of not only the primary molecular ion, but of the large positively charged molecular fragments as well.

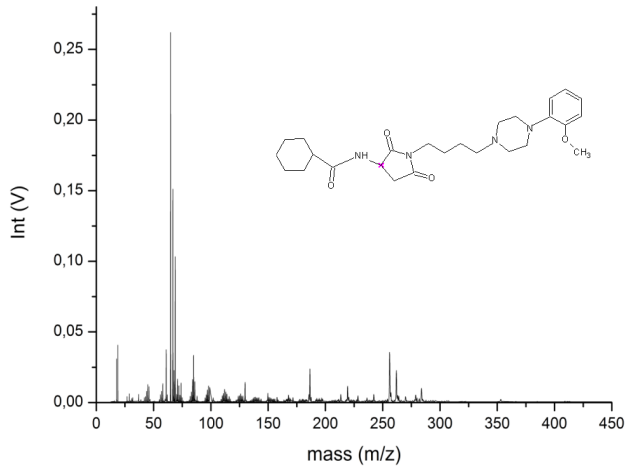

Fig. 1: PZ-68 molecule structure and mass-spectrum measured at the 18 eV electron energy.

References

[1] P. Zajdel, et al., *Bioorganic and Medicinal Chemistry Lett.* 16, 3406 (2006).
[2] V.S. Vukstich, A.I. Imre, A.V. Snegursky, *Tech. Phys. Lett.* 15, 1071 (2009).

*Corresponding author: snegursky.alex@gmail.com

To the list of contents

Structure and relative stabilities of chlorobenzene dications and trications produced by electron, proton and photon impact

Wania Wolff[1], Benedikt Rudek[2], Woon Yong Baek[2], Felipe Fantuzzi[3], Marco A. C. Nascimento[3]

1. Instituto de Física, Universidade Federal do Rio de Janeiro, Rio de Janeiro, RJ 21941-972, Brazil

2. Physikalisch-Technische Bundesanstalt, Bundesallee 100, 38116 Braunschweig, Germany

3. *Departamento de Físico-Química, Universidade Federal do Rio de Janeiro, Rio de Janeiro, RJ 21941-909, Brazil*

Monochlorobenzene (C_6H_5Cl) is proposed as a prototypical molecule for studying substituent effects on the benzene ring, demonstrating the advantages of combining theoretical and experimental techniques to probe the molecular structure and dynamic. A literature survey has shown limited insights on monosubstituted benzene derivatives, especially on the formation of multiply-charged parent ions [1]. This report presents the structure and relative stabilities of chlorobenzene dications and trications generated by the multiple ionization of C_6H_5Cl induced by electron, proton and photon impact. The most stable structure and low-lying isomers of multiply-charged parent ions are analysed by Density Functional Theory calculations [2], which revealed unusual carbon-chlorine bonding patterns. The results indicate that the great majority of the most stable ions is composed of a terminal C=Cl double bond in a formyl-like CHCl moiety (**1**$^{2+}$ and **2**$^{3+}$, Fig. 1a). An unprecedented nitrile-like C≡Cl triple bond (**3**$^{2+}$ and **4**$^{3+}$, Fig. 1b) is also found among the most stable isomers of C_6H_5Cl dication and trication. Experimentally, direct evidence of the formation of stable doubly- and triply-charged molecular parent ions is observed by time-of-flight mass spectroscopy. Mass spectra and ion yields give the measure of the dications and trications formation and their stability against dissociation is analysed through the ratios of dications and trications to the molecular ion (Fig. 1c). Both aspects were investigated using keV energetic photons around the chlorine K-edge, electrons with energies from the double ionization threshold [3] to 2000 eV and low-energy protons in the 50-155 keV range. From the chemist's point of view, the authors hope that the results presented herein will encourage experimentalists to synthesize novel chlorine-containing species with unusual bonding pattern. Similarly, from the physicist's point of view it is expected that these results will enable investigation into the competition between direct double ionization and auger emission channels in the formation of stable multiply-charged parent ions.

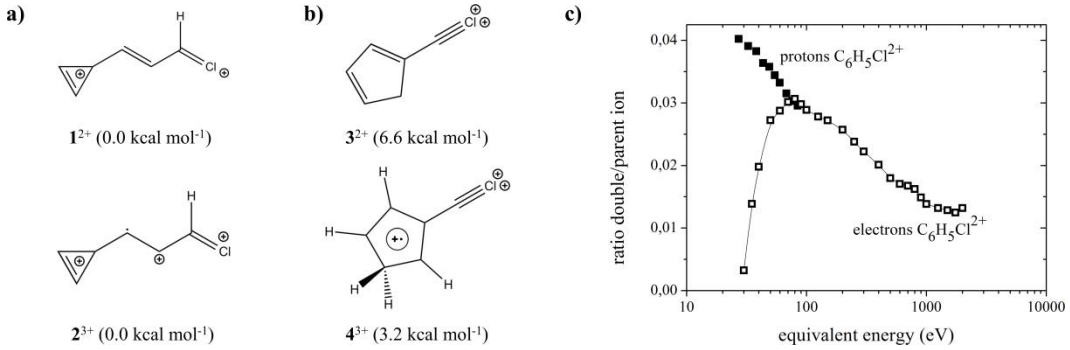

Fig. 1 a) Lewis structures of the most stable C_6H_5Cl dication and trication species at the PBE0/cc-pVTZ(-f) level of calculation. b) Lewis structures of species containing a nitrile-like C≡Cl^{2+} moiety. c) Ratio of doubly-charged to neutral parent molecular ion. Closed square: proton impact; open square: electron impact as function of (equivalent) electron energy.

References

[1] S. Singh, R. Naghma, J. Kaur, and B. Antony, Calculation of total and ionization cross sections for electron scattering by primary benzene compounds, *J. Chem. Phys*. **145**, 034309 (2016).

[2] T. Monfredini, F. Fantuzzi, M.A.C. Nascimento, W. Wolff, H. M. Boechat-Roberty, Single and double photoionization and photodissociation of toluene by soft X-rays in a circumstellar environment, *Astrophys. J.* **821**, 4 (2016).

[3] F. M. Harris, P. J. Jackson and J. A. Rontree, Experimental Investigations of Double Ionization to Ground and Electronically Excited States of Chlorobenzene, 1,2-, 1,3- and 1,4-Dichlorobenzene, 1,2,3-, 1,2,4 and 1,3,5-Trichlrobenzene, 1,2,3,4- and 1,2,4,5-Tetrachlrobenzene and Pentachlorobenzene Dications, *Org. Mass Spectrom.* **27** 261 (1992).

To the list of contents

Ionization and fragmentation of building blocks of the DNA by electron, proton and nitrogen-ion impact

Benedikt Rudek[*1], **Wania Wolff**[†2]
1. Department for Ionizing Radiation (6.53), Physikalisch-Technische Bundesanstalt
Bundesallee 100, 38116 Braunschweig, Germany
2. Instituto de Fisica, Universidade Federal do Rio de Janeiro
Av. Athos da Silveira Ramos 149, Rio de Janeiro 21941-901, Brazil

DNA damage is considered to be the molecular origin of tumour creation and radiation-induced DNA damage to be the basis for radiation cancer therapy. The ionization of molecular DNA building blocks by photons, ions or most often by secondary electrons is the first step of direct DNA damage. The negatively charged molecule may then rearrange its geometry or dissociated into fragments, with both processes possibly leading to DNA strand breaks. The ionization cross section has been shown to be up to 20% higher for actual building blocks compared to water which is commonly used in dosimetry and Monte Carlo track structure codes [1]. We thus have previously investigated several interaction cross sections for tetrahydrofuran (THF) and pyrimidine, that are chemical analogues to the sugar and base of the DNA, respectively. In particular, we reported ionization cross sections of THF [2][3] and relative fragmentation cross sections of THF, pyrimidine and trimethylphosphate [4] irradiated with protons of energies from 75 kev or 300 keV, respectively, up to several MeV.

In the present work, we extend our fragmentation measurements with heavy charged particles to proton energies down to 20 keV to fully cover the Bragg peak region and singly-charged nitrogen ions with energies from 30 keV to 155 keV. For comparison, fragmentation have also been measured for electron impact with energies ranging from 10 eV to 2000 eV. The data has been corrected for mass-dependent detection efficiency and normalized on to absolute scale. We present absolute partial dissociation cross sections (PDCS) and fragmentation matrices to propose the underlying dissociation channels and ionized molecular orbitals as previously reported for a smaller parameter set [5]. The relative fragmentation cross sections of THF depicted in Fig. 1 show a weak dependence on the projectile velocity. For pyrimidine, however, we observed steadily stronger fragmentation for lower velocities. Below an electron impact velocity of 2.3 v_{Bohr} (70 eV electron energy), the fragment yield decreases and the parent ion dominates as the appearance energies of the fragments lie between 10 eV and 20 eV.

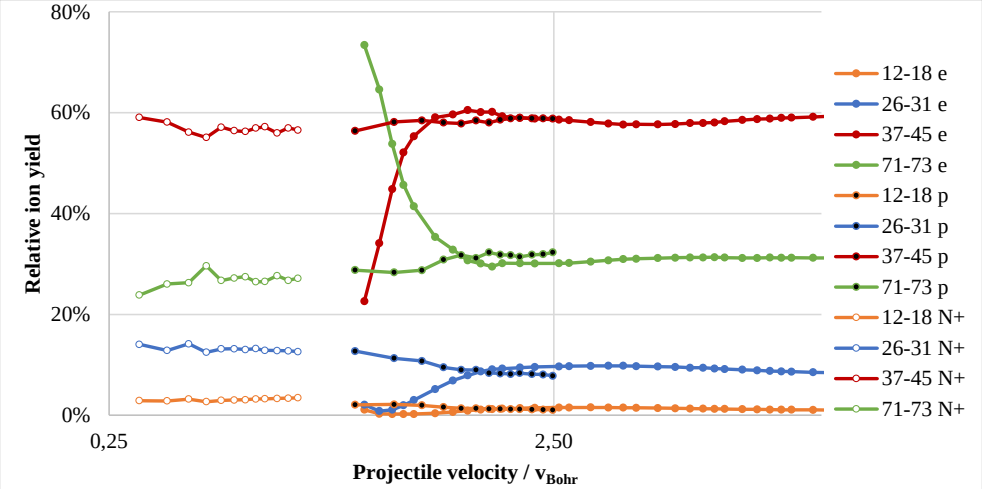

Fig. 1: Relative fragmentation cross sections for THF (C4H8O) for nitrogen-ion, proton and electron impact. The four lines group fragments of a fixed number of oxygen and carbon atoms and varying number of hydrogen atoms, namely the parent ion C4HnO (mass 71-73 amu), and the fragment ions C_2H_nO/C_3H_n (37-45 amu), C_1H_nO/C_2H_n (26-31 amu), and H_nO/CH_n (12-18 amu).

References

[1] M. Bug, Ph.D. Thesis, Wollongong University, 2014.
[2] M. Wang, B. Rudek, D. Bennett, P. de Vera, M. Bug, T. Buhr, W. Y. Baek, G. Hilgers, and H. Rabus, Phys. Rev. A **93**, 52711 (2016)
[3] B. Rudek, D. Bennett, M. Bug, M. Wang, W. Y. Baek, T.Buhr, G. Hilgers, C. Champion, and H. Rabus, J. Chem. Phys. **145**, 104301 (2016)
[4] B. Rudek, A. Arndt, D. Bennett, M. Wang, and H. Rabus, Eur. Phys. J. D **69**, 237 (2015)
[5] W. Wolff, H. Luna, L. Sigaud, A. C. Tavares and E. C. Montenegro, J. Chem. Phys. **140**, 52711 (2014)

[*]Corresponding author: benedikt.rudek@ptb.de
[†]Corresponding author: wania@if.ufrj.br

To the list of contents

Ion Desorption from Nitrile-bearing Astrophysical Ice Analogues Studied by Electron and Heavy Ion Bombardment

F. de A. Ribeiro[*1,2], **G. C. Almeida**[4], **W. Wolff**[†3], **E. F. da Silveira**[4], **H. M. Boechat-Roberty**[5] **and M. L. Rocco**[2]

1. Federal Institute of Rio de Janeiro
R. Sen. Furtado, 121 - Maracanã, Rio de Janeiro - RJ, 20270-021, Brazil
2. Institute of Chemistry, Federal University of Rio de Janeiro
Av. Athos da Silveira Ramos , 149 – Centro de Tecnologia, Bloco A, Cidade Universitária, Rio de Janeiro - RJ, 21941-909, Brazil
3. Institute of Physics, Federal University of Rio de Janeiro
Av. Athos da Silveira Ramos , 149 – Centro de Tecnologia, Bloco A, Cidade Universitária, Rio de Janeiro - RJ, 21941-909, Brazil
4. Physics Departament, Pontifical Catholic University of Rio de Janeiro
Rua Marques de São Vicente, 225 - Gávea, Rio de Janeiro - RJ, 22453-900, Brazil
5. Valongo Observatory, Federal University of Rio de Janeiro
Ladeira Pedro Antônio, 43 - Centro, Rio de Janeiro - RJ, 20080-090, Brazil

Nitriles (molecules bearing the CN functional group) represent a quite abundant class of molecules in the gas-phase of a variety of astrophysical environments. The organic nitriles acetonitrile (CH_3CN), propionitrile (C_2H_5CN), acrylonitrile (C_2H_3CN) and isobutyronitrile ($i-C_3H_7CN$) have been detected towards star-forming regions in the interstellar medium (ISM), and some of them are also present in Solar System bodies, like the Titan's atmosphere and cometary coma. Despite their relevance, little is known about their formation and processing under astrophysical conditions. In the ISM, these molecules are expected to condense onto the ice mantles of cold dust grains, which are constantly bombarded by cosmic rays. At the Solar System, nitriles may be incorporated in the ice matrix of cold objects, like comets and on Titan's organic haze particles, being exposed to the solar wind and to energetic charged particles trapped in planetary magnetospheres. The incidence of high-energy radiation onto icy surfaces triggers a radiation induced surface chemistry, which constitutes an important route for leading new neutral or ionized molecular species back to the gas phase in interstellar/circumstellar and planetary environments, enhancing the molecular complexity. In this work, we have studied the ion desorption of cations from pure CH_3CN, C_2H_5CN, C_2H_3CN and $i-C_3H_7CN$ ices due to the impact of electrons and energetic heavy ions from the 252Cf fission, simulating the incidence of cosmic rays and/or solar wind particles onto icy surfaces. The desorbed cations from each sample were identified by time-of-flight mass spectrometry (TOF-MS), by means of the Electron Stimulated Ion Desorption (ESID) and Plasma Desorption Mass Spectrometry (PDMS) techniques. Several ionic species were identified, indicating strong fragmentation on surface. Proton-transfer processes are suggested to play an important role in ion desorption, as evidenced by the abundant desorbed protonated parent molecules CH_3CNH^+, $C_2H_5CNH^+$, $C_2H_3CNH^+$ and $i-C_3H_7CNH^+$ and ion clusters such as $(CH_3CN)_2H^+$, $(C_2H_5CN)_2H^+$, $(C_2H_3CN)_2H^+$ and $(i-C_3H_7CN)_2H^+$. The energy dependence on the positive ion desorption yield indicates that ion desorption is initiated by Coulomb explosion following Auger electronic decay [1]. Ion desorption induced by electrons or heavy ions onto nitrile-bearing ices is suggested to constitute an important non-thermal route by which new neutral or ionized molecular species may be delivered to the gas-phase, contributing to the production of more complex molecules. The derived desorption yields per projectile impact may contribute to chemical evolution models in different cold astrophysical objects, especially where the abundance of nitriles is expected to be high.

References

[1] F. de A. Ribeiro, G. C. Almeida, Y. Garcia-Basabe, W. Wolff, H. M. Boechat-Roberty and M. L. M. Rocco, Phys. Chem. Chem. Phys. **17**, 27473-27480 (2015).

[*]Corresponding author: fabio.ribeiro@ifrj.edu.br
[†]Corresponding author: wania@if.ufrj.br

To the list of contents

Population Transfer in five level atoms

E. Gazazyan[*1]
1. Institute for Physical Research, Ashtarak-2, 0203, NAS of Republic of Armenia

Effective population transfer in multilevel atomic system to the target state still remains one of main problem in atomic physics, specially for Rydberg state excitation. In addition to well-known method STIRAP [1] there are other possibilities. In [2, 3], an alternative method of transferring the populations based on the intuitive sequence of pulses has been experimentally demonstrated, in which the pump pulse is switched before the Stokes pulse. In contrast to the STIRAP method, in which the transfer of populations is carried out through a dark state, in an intuitive sequence of laser pulses the transfer of populations is done through the bight state. Such transfer of atomic populations has been named by the authors of [2] as the b-STIRAP. The possibility of such a transfer on a single atom has been predicted and theoretically analyzed in [4], and in the medium in [5] in details. In a multi-level system, the possibility of an effective transfer of populations with the use of the STIRAP chain has also been considered in [1]. In [6], the alternative schemes of population transfer in the five-level systems have been proposed and their advantages in comparison with the STIRAP chain have been analyzed. Here we consider another method of population transfer in the five-level atomic M-type system. The interaction Hamiltonian for this system is given by

$$H = \Omega_p^{(1)} e^{i\Delta_p^{(1)} t} \sigma_{21} + \Omega_s^{(1)} e^{i\Delta_s^{(1)} t} \sigma_{32} + \Omega_p^{(2)} e^{i\Delta_p(2)t} \sigma_{43} + \Omega_s^{(2)} e^{i\Delta_s^{(2)} t} \sigma_{54} + h.c. \tag{1}$$

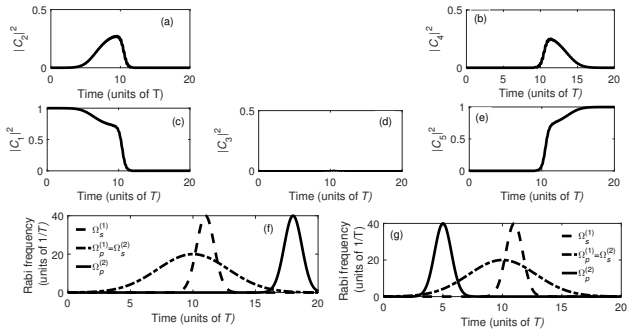

Fig. 1: Total transfer of populations from state $|1\rangle$ to $|5\rangle$

The full transfer of a populations is demonstrated in Fig.1, when the region of overlapping of two of the three pulses is not vanishing, independently of the sequence of switching of internal adjacent transitions and the time delay between these pulses. The possibility of transfer in a large region of two-photon detunings is demonstrated, as well as the partial transfer of populations depending on the two-photon detuning at its values $\delta_2 T > 20$.

This work was supported by the SCS MES of Armenia (15T-1C066 theme) and IRMAS project.

References

[1] Vitanov, N.V., Fleischhauer, M., Shore, B.W., and Bergmann, K., Advan. Atom., Mol., Opt. Physics,**46**, 55. (2001)
[2] Klein, J., Beil, F., and Halfmann, T, Phys. Rev. A, **78**, 033416, (2008)
[3] Klein, J., Beil, F., and Halfmann, T, Phys. Rev. Lett, **99**, 113003, (2007)
[4] Rangelov, A., Vitanov, N., Yatsenko, L.P., Shore, B.W., Halfman, T., and Bergmann, K., Phys. Rev. A, **72**, p. 053403 (2005)
[5] Grigoryan, G.G., Nikoghosyan, G., Halfmann, T., Pashayan-Leroy, Y.T., Leroy, C., and Guerin, S., Phys. Rev. A, **80**, 033402 (2009)
[6] Grigoryan, G., Gazazyan, E., Chaltykyan, V., and Tikhova, O, Laser Physics, **24**, 035301 (2014)

*Corresponding author: emilgazazyan@gmail.com

To the list of contents

g factor of lithium-like ions: higher-order interelectronic-interaction effects

D. A. Glazov* [1,2], **A. V. Volotka** [1,3] **V. M. Shabaev** [1] **I. I. Tupitsyn** [1,4] **G. Plunien** [5]

1. Department of Physics, St. Petersburg State University
Oulianovskaya 1, Petrodvorets, 198504 St. Petersburg, Russia
2. State Scientific Centre "Institute for Theoretical and Experimental Physics" of National Research Centre "Kurchatov Institute"
B. Cheremushkinskaya st. 25, 117218 Moscow, Russia
3. Helmholtz-Institut Jena, Fröbelstieg 3, D-07743 Jena, Germany
4. Center for Advanced Studies, Peter the Great St. Petersburg Polytechnic University
Polytekhnicheskaja 29, 195251 St. Petersburg, Russia
5. Institut für Theoretische Physik, Technische Universität Dresden
Mommsenstraße 13, D-01062 Dresden, Germany

Recent investigations of the g factor of highly charged ions have lead to the most precise up-to-date determination of the electron mass [1]. They have also provided the stringent tests of the various bound-state QED effects in the presence of magnetic field [2,3], including the relativistic nuclear recoil effect [4]. Moreover, it was proposed to determine the fine structure constant from the g factors of light [5] and heavy [6] few-electron ions. Apart from the corresponding high-precision measurements, these proposals demand significant improvement of the theoretical accuracy. Presently, for low- and medium-Z lithiumlike ions it is limited by the interelectronic-interaction effects. In this work, we improve the accuracy of this contribution by calculating the third- and higher-order terms in $1/Z$ in the Breit approximation within the recently developed perturbative approach. It is based on the recursive formulation of the perturbation theory and provides an efficient access to the higher-order contributions. The interelectronic-interaction contributions of the first and second orders are evaluated within the bound-state QED. Application of this method to the binding energies of lithiumlike and boronlike systems has been presented in our recent papers [7,8].

References

[1] S. Sturm *et al.*, Nature **506** 467 (2014).
[2] A. Wagner *et al.*, Phys. Rev. Lett. **110**, 033003 (2013).
[3] A. V. Volotka *et al.*, Phys. Rev. Lett. **112**, 253004 (2014).
[4] F. Köhler *et al.*, Nature Communications **7**, 10246 (2016).
[5] V. A. Yerokhin *et al.*, Phys. Rev. Lett. **116**, 100801 (2016).
[6] V. M. Shabaev *et al.*, Phys. Rev. Lett. **96**, 253002 (2006).
[7] D. A. Glazov *et al.*, Nucl. Instr. Meth. Phys. Res. B, in press, DOI:10.1016/j.nimb.2017.04.089.
[8] A. V. Malyshev *et al.*, Nucl. Instr. Meth. Phys. Res. B, in press.

*Corresponding author: d.glazov@spbu.ru

To the list of contents

Cross-relaxation Studies with Optically Detected Magnetic Resonances in Nitrogen – Vacancy Centres in Diamond in External Magnetic field

Marcis Auzinsh[*1], **Andris Berzins**[1], **Laima Busaite**[1], **Ruvins Ferbers**[1], **Forian Gahbauer**[1], **Reinis Lazda**[1]
1. Laser Centre, University of Latvia, 19 Raina boulevard, Riga, LV-1586, Latvia

Electron as well as nuclear magnetic resonance methods are very powerful tool to characterise the electron and nuclear structure of different materials. Recently it was demonstrated that the nitrogen - vacancy (NV) centres in diamond crystals can be used as a very efficient probe to examine internal structure and point defects of diamond crystals [1] [2]. Authors of those papers demonstrated all-optical approach employing the measurements of the dependance of the quantum relaxation time T_1 of electron spins in the ground state of NV centres on the magnetic field strength, to study the electron spin structure and nuclear spin structure in the point defect formed by the substitutional nitrogen ^{14}N in a diamond crystal.

Recent developments in the magnetic field sensing with negatively charged nitrogen-vacancy centers in a diamond employ magnetic-field dependent features in the photoluminescence. These features can be studied in presence of the microwave radiation or this radiation can be eliminated [3]. Some of these features are directly related to the cross-ralaxation processes in the diamond crystals.

In present study we demonstrate the possibility to study the internal electronic and nuclear structure of diamond crystals by means of optically detected magnetic resonance methods (ODMR).

We examine the contrast and line-width dependance of the optically detected magnetic resonance signals on the magnetic field strength in two different regions of the magnetic field. One region is around 512 G strong magnetic field. Another region is around 600 G strong magnetic field. In both regions in detected ODMR signals we observe several cross relaxation transitions. These transitions occur when the energy splitting between NV centre ground state electron spin component magnetic sublevels $m_S = 0$ and $m_S = -1$ coincide with some of the energy splitting intervals in such point defects in diamond crystal as subsitutional nitrogen ^{14}N or carbon ^{13}C.

For the magnetic field strength around 512 G we study ODMR signals in two frequency regions. One region is around 1440 MHz when the microwave radiation causes transitions between hyperfine components of the NV centre ground state electron spin magnetic sublevels $m_S = 0$ and $m_S = -1$. These sublevels are directly involved in the cross-relaxation processes with the substitutional nitrogen ^{14}N [2].

We compare these signals with signals obtained in the frequency range of 4320 MHz. In this region microwave radiation excites transitions between the hyperfine components of the NV centre ground state electron spin magnetic sublevels $m_S = 0$ and $m_S = +1$. For these transitions one of the magnetic sublevels of electron spin ($m_S = +1$) is not directly involved in the cross relaxation process with the substitutional nitrogen.

We compare the measured signals with the model simulations based on the hyperfine structure hamiltonian analysis both for the substitutional nitrogen as well as for the NV centres.

All the studies are supported by the model of NV centre interaction with light in the presence of the magnetic field and microwave radiation, based on our previous experience of similar studies in atomic systems [4].

References

[1] James D.A. Wood et. al Phys. Rev. B 94, 155402, (2016).
[2] L.T. Hall et. al Nature Communications, (5 January 2016).
[3] Huijie Zheng et. al arXiv:1701.06838v1, 24 Jan 2017; Proc. of SPIE Vol. 10119 (2017).
[4] M. Auzinsh, D. Budker, S. Rochester, Optically Polarised Atoms, Oxford University Press, (2014).

*Corresponding author: Marcis.Auzins@lu.lv

To the list of contents

Optically Detected Magnetic Resonance Studies of Level Anticrossing in Nitrogen – Vacancy Centres in Diamond Crystals

Marcis Auzinsh[*1], **Andris Berzins**[1], **Laima Busaite**[1], **Ruvins Ferbers**[1], **Forian Gahbauer**[1], **Reinis Lazda**[1]
1. Laser Centre, University of Latvia, 19 Raina boulevard, Riga, LV-1586, Latvia

Recent developments in the magnetic field sensing with negatively charged nitrogen-vacancy (NV) centers in diamond employ magnetic-field dependent features in the photoluminescence. These features can be studied in presence of the microwave radiation or this radiation can be eliminated [1].

One set of the resonant features in the photoluminescence dependance on the magnetic field strength in the absence of microwave radiation in the NV centres appear at the magnetic field strength around 1024 G. At this field NV centre electron spin $S = 1$ magnetic sublevels with quantum numbers $m_S = 0$ and $m_S = -1$ undergo level crossing.

If studied in detail, due to hyperfine interaction of NV centre electron spin angular momentum states with the nitrogen ^{14}N nuclear spin $I = 1$ states, each electron spin component is split into three hyperfine components. When external magnetic field is applied, some of these hyperfine state components are mixed together by the field and as a result several of these hyperfine components in the magnetic field have real crossing, but several undergo anticrossings. Besides in the vicinity of the magnetic field of 1024 G the wave functions of these states are strongly mixed, that leads to a substantial alternation of magnetic dipole transition probabilities between these hyperfine levels in the microwave field.

In the present study we examine the NV centre hyperfine level anticrossing in the vicinity of the magnetic field of 1024 G experimentally and compare measured resonance signals with numerical calculations based on the hyperfine structure hamiltonian analysis.

For experimental studies we employ optically detected magnetic resonance signal measurements in two different microwave frequency ranges. When the microwave field frequency is in the range of $5.7 - 5.9$ GHz and the magnetic field is scanned around 1024 G, we study microwave radiation caused resonant depolarisation of the NV centres in the ground state due to transitions between mixed hyperfine levels in the vicinity of anti-crossing point and a distant spin state magnetic sublevel $m_S = +1$ hyperfine components.

Dependence of the contrast of optically detected magnetic resonances and width of these resonances on the strength of the magnetic field is measured. Measured signals are compared with a numerical model that accounts for the hyperfine interaction of NV electronic angular momentum with the nitrogen nuclear spin and magnetic field.

The influence of the cross relaxation between hyperfine components of the the NV centres and a nuclear spin components of substitutional nitrogen ^{14}N, which is a point defect in a diamond crystal but is not a part of the NV centre, were examined in the optically detected magnetic resonance spectrum in the vicinity of 1024 G magnetic field.

If the microwave field frequency is much lower, below 100 MHz, but strength of the external magnetic field still is around 1024 G, we measure the NV centre angular momentum resonant depolarisation by the microwave radiation causing transitions between hyperfine magnetic sub-levels in the vicinity of the anti-crossing point. Again, the width and contrast of these signals as they depend on the external magnetic field, are examined. The experimental results are compared with the numerical model.

References

[1] Huijie Zheng et. al arXiv:1701.06838v1, 24 Jan 2017; Proc. of SPIE Vol. 10119 (2017).

*Corresponding author: Marcis.Auzins@lu.lv

To the list of contents

Shell Model Calculation of The Atomic Scattering Factor in Electric Field

S Y Yousif Al-Mulla*
University of Borås/College of Engineering/ S-50190 Borås/ Sweden
EGAS 49th Conference of the European Group of Atomic Systems/ Durham University/ Durham / UK / July 17-21, 2017

The study of the effectiveness of the shell model calculations in specifying charge deformation of atoms and ions are presented. This has been done by comparing quantum mechanical calculations of perturbed X-ray scattering form factor of an atom/ion in an electric field with shell model predictions. In computing the shell scattering factors it is assumed that only the outermost ns and np wave functions contribute [1 - 4]. The results are shown in Fig.1 for Ar and K^+, and the correspondence between the two models is remarkable. There is a good agreement between the two models for Neon-like atoms/ions; Argon-like atoms/ions and Krypton-like atoms/ions.

The X-ray atomic scattering factor for an unperturbed atom with N electron is given by:

$$f_0 = \sum_{j=1}^{N} \psi_0^* \exp(i\chi S \cdot r_j)\psi_0 d\tau = \sum_{j=1}^{N} \psi_0^* \exp(iKr_j \cos\theta_j)\psi_0 d\tau$$

In the presence of an electric field F, the wave function is perturbed,

$$f = f_0 + if_1F + O(F^2) \text{ where } if_1F = 2F\sum_{j=1}^{N}\int \psi_0^* \exp(iKS\cdot r_j)\psi_1 d\tau$$

We use the Kirkwood - Pople-Schofield approach for the wave function

$$\psi = \psi_0\left[1+\sum_j u(r_j)\right] \text{ where } u(r) = F(\mu r + \nu r^2 + \eta r^3) \text{ and the } f_1 \text{ is given by}$$
$$if_1F = 2F\sum_i\sum_j \psi_0^* \exp(iKS\cdot r_j)(\mu r_i + \nu r_i^2 + \eta r_i^3)\cos\theta_i \psi_0 d\tau$$

The optimal values of μ, ν and η are determined variationally and calculated from various moments of the unperturbed charge distribution using a single Slater determinant.

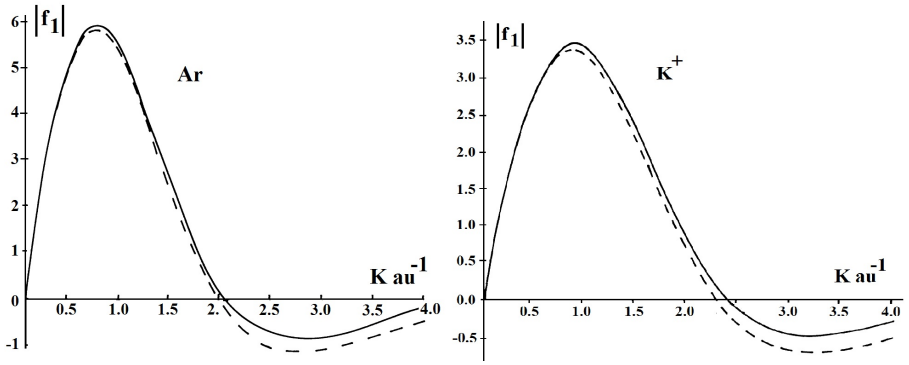

Fig. 1: Comparison of the magnitude of the modified X-ray scattering factor per unit applied field with scattering vector K (au^{-1}) for the shell model calculation - - - - - and the quantum mechanical model ——— for Ar and K^+

References

[1] JAD. Matthew and S.Y. Yousif, , Acta Crys. **A 40**, 716 (1984).
[2] JAD. Matthew and S.Y. Yousif , Molec. Phys. **51**, 175 (1984).
[3] S.Y. Yousif Al-Mulla, Physica Scripta **61**, 417 (2000).
[4] S.Y. Yousif Al-Mulla, EGAS 46th (2014)

*samir.al-mulla@hb.se

To the list of contents

STIRAP-like quantum search

Nicholas Chancellor[*1], **Viv Kendon**[†1]
1. Department of Physics, Durham University
South Road, Durham DH1 3LE, UK

The STImulated Raman Adiabatic Passage (STIRAP) protocol is a workhorse of atomic and molecular physics [1][2][3]. This protocol allows efficient transfer between long lived 'initial' and 'target' state via a highly excited short lived intermediate state. This is achieved by first driving a transition between the target and intermediate state and then adiabatically turning this driving off, while simultaneously turning up driving between the initial and intermediate state. This is effectively a traditional adiabatic protocol, but run in reverse so that the first excited state of the three state system is occupied rather than the ground state. Since this energy eigenstate has a node on the intermediate state, decay is strongly suppressed.

We find that for the unstructured search problem, where one state is 'marked' by having a lower energy than all of the others, properly constructed STIRAP inspired protocols can achieve the same quantum speedup as traditional adiabatic protocols. The quickest any classical protocol can solve this problem scales as the number of states N, while the best quantum protocols [4], which we show include our STIRAP inspired protocol, take a time proportional to $\sqrt{N}$. Moreover, we find that the picture of how such protocols work is exactly analogous to how STIRAP works, the system is initialized in an excited state and a protocol is run backward though an avoided level crossing. Up until our work, the only two protocols based on continuously evolving systems which have been shown to be able to obtain this speedup are traditionally formulated adiabatic protocols which keep the system in its ground state by the adiabatic theorem of quantum mechanics and continuous time quantum walks which are based on evolution with a fixed Hamiltonian. Our work adds a third protocol to this list. Fig. 1 depicts the results of these three strategies for a time dependent 'hypercube' search Hamiltonian with $N = 2^n$ states, $H(\frac{t}{T}) = -A(\frac{t}{T})\sum_{i=1}^{n}\sigma_i^x - B(\frac{t}{T})\,|m\rangle\langle m|$, where the starting state is taken to be a uniform positive superposition of all states.

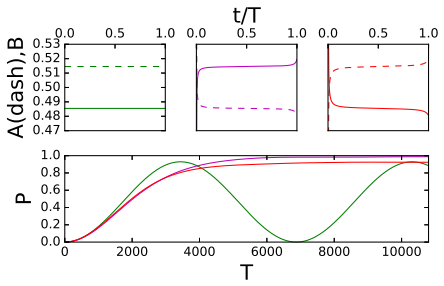

Fig. 1: Example of the three protocols for a $N = 2^{20} \approx 10^6$ state system. A is the strength of the 'search' Hamiltonian which hops between states and B is the strength of the 'marked' state Hamiltonian which gives a single state lower energy. A quantum walk is depicted in green, traditionally formulated adiabatic protocol in magenta, and STIRAP inspired protocol in red. The time dependence of the Hamiltonians is depicted on the top row, and the success probability P versus total runtime T is depicted on the bottom figure.

This project relates to other work we have done which demonstrates that there is actually a continuum of protocols which exist between the two extremes of adiabatic protocols and STIRAP inspired reverse adiabatic protocols and includes continuous time quantum walks as an intermediate point. I explain how this interpolation is analogous to the timing of a laser pulse sequence in an atomic physics setting, where the pulse order and duration determines the character of the protocol as ground state adiabatic, quantum walk like (Rabi flopping), or a STIRAP like excited state adiabatic protocol.

References

[1] U. Gaubatz, P. Rudecki, S. Schiemann, and K. Bergmann, "Population transfer between molecular vibrational levels by stimulated Raman scattering with partially overlapping laser fields. A new concept and experimental results," J. Chem. Phys. 92, 5363. (1990).
[2] P. Marte, P. Zoller, and J. L. Hall "Coherent atomic mirrors and beam splitters by adiabatic passage in multilevel systems" Phys. Rev. A 44, R4118(R) (1991).
[3] Nikolay V. Vitanov, Andon A. Rangelov, Bruce W. Shore, and Klaas Bergmann "Stimulated Raman adiabatic passage in physics, chemistry, and beyond" Rev. Mod. Phys. 89, 015006 (2017).
[4] Charles H. Bennett, Ethan Bernstein, Gilles Brassard, and Umesh Vazirani, "Strengths and weaknesses of quantum computing," SIAM J. Comput. 26, 151–152 (1997).

[*]Corresponding author: nicholas.chancellor@durham.ac.uk
[†]Corresponding author: viv.kendon@durham.ac.uk

To the list of contents

Adiabatic passage of Förster resonances for two-qubit gates and generation of Bell states of Rb and Cs atoms

I. I. Beterov[*1,2,3] , **G. N. Hamzina**[1,3], **M. Saffman**[4] , **D. B. Tretyakov**[1,2], **V. M. Entin**[1,2], **E. A. Yakshina**[1,2], **S. Bergamini**[5], **E. A. Kuznetsova**[6,1], **I. I. Ryabtsev**[1,2]

1. Rzhanov Institute of Semiconductor Physics SB RAS, 630090, Novosibirsk, Russia
2. Novosibirsk State University, 630090, Novosibirsk, Russia
3. Novosibirsk State Technical University, 630073, Novosibirsk, Russia
4. University of Wisconsin-Madison, Madison, Wisconsin, 53706, USA
5. The Open University, Walton Hall, MK7 6AA, Milton Keynes, UK
6. Institute of Applied Physics RAS, 603950, Nizhny Novgorod, Russia

Generation of entangled two-qubit states is required for building a universal quantum computer. High-fidelity Bell states are of great interest in modern quantum physics. Entanglement of ultracold neutral atoms in two spatially separated optical dipole traps is promising for implementation of quantum computing and quantum simulation and for investigation of Bell states of material objects. We propose to entangle two atoms via long-range Rydberg-Rydberg interaction. However, high-fidelity two-qubit gates with Rydberg atoms have not been demonstrated yet [1]. Alternatively to previous approaches, based on Rydberg blockade, we consider Stark-tuned Förster resonances. The external electric field adjusts the Rydberg energy levels in such a way that the Rydberg state $|r\rangle$ is located midway between two other Rydberg states of the opposite parity $|r'\rangle$ and $|r''\rangle$. Rydberg-Rydberg interaction leads to coherent exchange of the population of the collective two-atom states $|rr\rangle \leftrightarrow |r'r''\rangle$ [2]. In general, the fidelity of this method is sensitive to fluctuations of the interatomic distance which lead to fluctuations of the interaction energy. To reduce this effect, we propose to use double adiabatic passage across the Stark tuned Förster resonance, which results in the deterministic phase shift of the two-atom state [3].

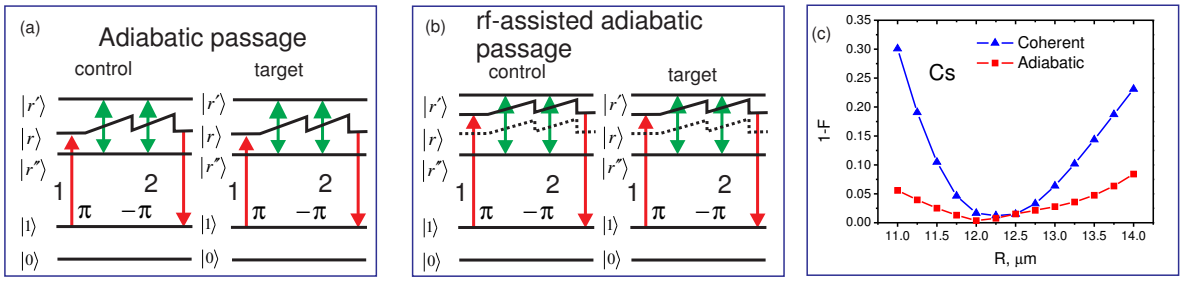

Fig. 1: (a) Scheme of CZ gate using adiabatic passage of Stark tuned Förster resonance; (b) Scheme of CZ gate using adiabatic passage of Stark-tuned radiofrequency-assisted Förster resonance; (c) The calculated dependence of the infidelity of Bell states on interatomic distance for Cs atoms.

Scheme of two-qubit CZ gate is shown in Fig. 1(a). Two trapped atoms are excited into Rydberg states $|r\rangle$. The Förster resonance is passed two times in the time-dependent electric field. After the end of the adiabatic passage the system returns to the initial two-atom state $|rr\rangle$ with a π phase shift. However, implementation of this scheme requires well isolated Förster resonances for Rydberg states, which have substantially long lifetimes. Such resonances are difficult to find. More flexibility can be achieved if radiofrequency (rf)-assisted Förster resonances are used [4]. They are observed for Floquet sidebands which are induced by external rf electric field. Scheme of CZ gate based on double adiabatic passage of rf-assisted Förster resonances is shown in Fig. 1(b).

We have calculated the dependence of the infidelity of the Bell states for Rb and Cs atoms on the interatomic distance [see Fig. 1(c) for Cs]. We compare the fidelity of the Bell states, generated using rf-assisted Förster resonance $|80P, 80P\rangle \rightarrow |80S, 81S\rangle$ via double adiabatic passage or via single Rabi oscillation between collective two-atom states. The reduced sensitivity of the fidelity on the interatomic distance, when adiabatic passage is used, confirms that the proposed method has advantages for generation of high-fidelity Bell states of ultracold atoms.

This work was supported by the RFBR Grants No. 16-02-00383 and 17-02-00987, the Russian Science Foundation Grant No. 16-12-00028, and the Novosibirsk State University.

References

[1] K. M. Maller, M. T. Lichtman, T. Xia, Y. Sun, M. J. Piotrowicz, A. W. Carr *et al.*, Phys. Rev. A 92, 022336 (2015).
[2] S. Ravets, H. Labuhn, D. Barredo, L. Beguin, T. Lahaye, and A. Browaeys, Nat. Phys. 10, 914 (2014).
[3] I. I. Beterov, M. Saffman, E. A. Yakshina, D. B. Tretyakov, V. M. Entin, S. Bergamini, E. A. Kuznetsova, and I. I. Ryabtsev, Phys. Rev. A 94, 062307 (2016).
[4] E. A. Yakshina, D. B. Tretyakov, I. I. Beterov, V. M. Entin, C. Andreeva, A. Cinins, A. Markovski, Z. Iftikhar, A. Ekers, and I. I. Ryabtsev, Phys. Rev. A 94, 043417 (2016).

*Corresponding author: beterov@isp.nsc.ru

To the list of contents

Response of Electron Crystal to External Excitation. Modeling

V. Syvokon[*1], **Iryna Sharapova**[†1]
1. B.Verkin Institute for Low Temperature Physics and Engineering of the National Academy of Sciences of Ukraine
47 Prospekt Nauky, 61103 Kharkiv, Ukraine

The Wigner crystal at the liquid helium surface is a spatially ordered state of a two-dimensional system of classical particles with the Coulomb interaction.

When the crystal is exposed to an external electric field directed along the surface of the liquid (guiding field), the layer conductivity varies nonmonotonically with the increasing field.

It is found [1] that the conductivity of a Wigner crystal changes drastically as the holding potential decreases. The sharp changes in the conductivity may be accounted for by the disturbance of the crystalline order when the holding field decreases and a solid disordered phase is formed. "Evaporation" of the electrons onto the higher-lying surface levels was assumed as a possible mechanism in [2].

In this paper, we carry out some additional experimental studies of the conductivity of electron crystals as the holding potential is reduced and, based on model calculations, we propose another possible explanation for the observed conductivity behavior.

The above analysis confirms that the change in the impedance of the test cell when the holding potential is reduced is not a consequence of changes in the resistance of the layer, as assumed previously [1], so there is no justification for assuming that any kind of structural transitions take place in the electron crystal. The observed behavior arises from features of capacitive measurements of the transport characteristics of two-dimensional electron systems. These features are related to the finite size of the measured sample and the nonzero dimensions of the excitation electrode, which lead to a distinctive distribution of the excitation field in the cell. In some cases, the combined current in the cell, which is detected by an external receiver electrode, can be extremely sensitive to small variations in the experimental parameters.

References

[1] K. A. Nasyedkin, V. E. Syvokon, A. S. Neoneta, Pisma v ZhETF Lett. **91**, 652 (2010).
[2] V. V. Slavin, A. A. Krivchikov, Fiz. Nizk. Temp. **38**, 1390 (2012).

[*]Corresponding author: sivokon@ilt.kharkov.ua
[†]Corresponding author: sharapova@ilt.kharkov.ua

To the list of contents

Theoretical study of Rydberg–EIT in thermal Rb atoms

Arturs Cinins[*1], **T. Kirova**[1], **M. Auzinsh**[2], **Y. H. Chen**[3], **Ite. A. Yu**[3]

1. *Institute of atomic physics and spectroscopy, University of Latvia, Skunu street 4, Riga, LV1586, Latvia*
2. *Faculty of physics and mathematics, University of Latvia, Zellu street 23, Riga, LV1002, Latvia*
3. *Department of Physics and Frontier Research Center on Fundamental and Applied Sciences of Matters, National Tsing Hua University, Hsinchu 30013, Taiwan*

A key signature of electromagnetically induced transparency (EIT) is a sharp dip in absorption profile of an atomic transition. Combination of the high signal contrast of EIT spectra and large polarizability of highly excited atomic Rydberg states have enabled development of many novel techniques, including weak electromagnetic field measurements [1] and Rydberg–Rydberg interaction probing [2].

A recent experimental study of Rydberg EIT in room temperature rubidium vapor [3] has shown that normalized EIT peak height is initially enhanced with increasing probe laser intensity, reaches maximum and falls if the probe intensity is further increased. Improvement of normalized EIT peak height by 2–4 times compared to the weak probe field scenario is possible by optimal choice of probe laser intensity. At the expense of slight power broadening of the EIT peak, increased probe laser intensity boosts measurement signal to noise ratio. Moreover, experimental data demonstrate remarkable stability of the optimal probe laser intensity with respect to other experimental parameters - intensity of control laser radiation, laser polarizations and the selected Rydberg state. The observed behavior renders thermal Rydberg EIT a good candidate for laser frequency locking in Rydberg–relevant research. In contrast, in cold atoms increased probe intensity generally leads to worse EIT parameters [4]. The present research aims to develop a theoretical model for room temperature Rydberg EIT and to provide physical interpretation for the experimental observations reported in [3].

The observed EIT peak height enhancement is partially reproduced in a simple three level model system (Fig. 1), where Doppler effect is accounted for via an additional decoherence rate. However, the simple model fails to fully account for all the features of experimental data. In addition to the Doppler effect–induced decoherence, transit relaxation [5] takes place due to thermal motion of atoms. The transit relaxation counteracts optical pumping, and, for tightly focused EIT laser beams, it can lead to complete vanishing of the optical pumping. Furthermore, Doppler broadening of the D_2 line in ^{87}Rb at room temperature is comparable with hyperfine splitting of the $5P_{3/2}$ fine structure level, and additional excitation pathways to the selected Rydberg state must also be accounted for. To properly describe EIT in thermal atomic systems, we have developed an elaborate model accounting for Zeeman structure of multiple hyperfine energy levels involved in each step of laser excitation. Numerical simulations suggest that transit relaxation–induced redistribution of ground state populations results in additional enhancement of normalized EIT peak height.

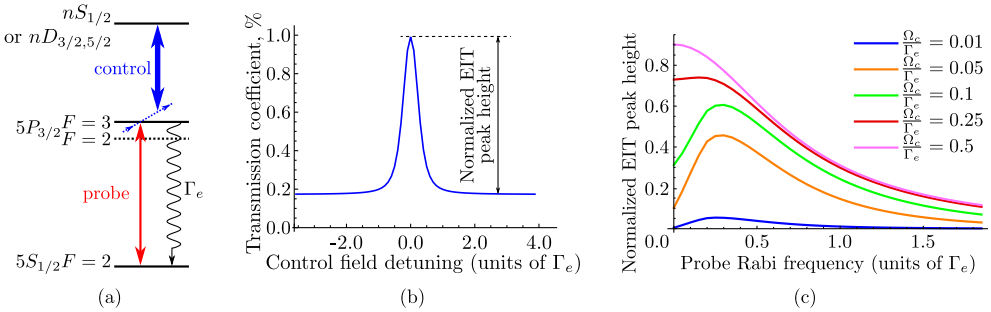

Fig. 1: (a) Three–level model system. Frequency of the strong control field is swept across transition resonance between $5P_{3/2}F=3$ level and the selected long–lived Rydberg state. Frequency of the probe field is fixed to transition resonance between ground level $5S_{1/2}F=2$ and $5P_{3/2}F=3$. Nearby $5P_{3/2}F=2$ level is ignored in the simple model. (b) EIT is observed as a narrow peak(s) in light transmission coefficient of the medium. (c) Enhancement of normalized EIT peak height with increasing probe laser Rabi frequency (simulation results). The maximum position is almost stationary for a wide range of control field Rabi frequencies.

References

[1] R.P. Abel, C. Carr, U. Krohn, C.S. Adams, Phys. Rev. A **84**, 023408 (2011)
[2] K.J. Weatherill, J.D. Pritchard, R.P. Abel, M.G. Bason, A.K. Mohapatra, C.S. Adams, J. Phys. B: At. Mol. Opt. Phys. **41**, 201002 (2008)
[3] B.H. Wu, Y.W. Chuang, Y.H. Chen, J.C. Yu, M.S. Chang, I.A. Yu, arXiv:1704.03139, unpublished.
[4] S. Wielandy, A.L. Gaeta, Phys. Rev. A **58**, 2500 (1998)
[5] M. Bruvelis, J. Ulmanis, N.N. Bezuglov, K. Miculis, C. Andreeva, B. Mahrov, D. Tretyakov, A. Ekers Phys. Rev. A **86**, 012501(2012)

*Corresponding author: arturs.cinins@lu.lv

To the list of contents

Analytical evaluation of non-adiabaticity and efficiency of STIRAP using the saddle-point method

Arturs Cinins[*1], **M. Bruvelis**[2], **D. K. Efimov**[3], **K. Miculis**[1], **N. N. Bezuglov**[4], **A. Ekers**[5]

1. Institute of Atomic Physics and Spectroscopy, University of Latvia, Riga, LV-1586, Latvia
2. Laser Centre, University of Latvia, Riga, LV-1002, Latvia
3. Instytut Fizyki im. Mariana Smoluchowskiego, Uniwersytet Jagielloski, Krakw, 30-348, Poland
4. Faculty of Physics, St. Petersburg State University, St. Petersburg, 198904, Russia
5. Computer, Electrical and Mathematical Sciences and Engineering Division, King Abdullah University of Science and Technology, Thuwal, 23955-6900, Saudi Arabia

Stimulated Rapid Adiabatic Passage (STIRAP) has become an important tool in a variety of applications beyond gas phase atomic and molecular physics physics [1]. In its simplest original configuration, STIRAP is used to transfer population from an initial stable state Ψ_1 to a final stable or quasi-stable (e.g., Rydberg) state Ψ_3 in a three-state system with states arranged in a Λ- or a ladder-type scheme, whereby the intermediate state Ψ_2 acts as a "spectator" that is not populated during the transfer process. The highest transfer efficiency is achieved using pulsed laser fields in a counterintuitive sequence, whereby the laser field coupling of states Ψ_2 and Ψ_3 precedes the field coupling of Ψ_1 and Ψ_2. There is a certain overlap between both laser pulses, and the timing is chosen such that adiabaticity is maintained throughout the population transfer process [2].

There are only two models of STIRAP with ideal ramp pulse shapes that allow for exact analytical description of the population transfer dynamics [3]. In all other cases, including Gaussian laser pulses, the adiabaticity criterion is found either by qualitative estimates or by numerical calculations [4]. Analytically, the effect of non-adiabaticity on the STIRAP efficiency is usually assessed using the Dykhne-Davis-Pechukas (DDP) method [5] – a generalization of the Landau-Zener model [6] that is strictly valid only for two-level systems. However, this method fails in finding the pre-exponential multipliers in quasi-classical asymptotes in the case of typical three-level STIRAP schemes. The optimized version of STIRAP described in [7] requires very accurate estimates of those multipliers in order to predict the fidelity and robustness of the STIRAP process against the variations of intensities and laser field detunings.

In this presentation, we explore the approach described in [8] for integral representation of matrix elements describing mixing between the adiabatic states. We choose a new basis of bright and dark states to determine the accuracy range of the Sun-Metcalf approximation [8] for the case of exponential ramp pulses that can be treated analytically [3]. We then employ the saddle-point method [9] to obtain an asymptotic analytical result, with correct pre-exponential multipliers, for the efficiency of STIRAP upon coupling by two Gaussian laser pulses that are assumed to be of equal durations and intensities. This analysis reveals occurrence of saddle points that the DDP method fails to identify; those saddle points lead to the well-known oscillations of STIRAP efficiency [3]. The optimum STIRAP efficiency is achieved when the ratio between the FWHM durations Δ_τ of both Gaussian laser pulses and the delay time τ between them satisfy the condition $(\tau/\Delta_\tau)^2 = 1/(4\ln 2)$. The obtained analytical results are validated by comparing them with exactly solvable reference models for somewhat modified ramp pulses [3] and with the results of numerical calculations for the case of Gaussian laser pulses.

References

[1] N. V. Vitanov, A. A. Rangelov, B. W. Shore, and K. Bergmann, Rev. Mod. Phys. **89**, 015006 (2017).
[2] K. Bergmann, H. Theuer, and B. W. Shore, Rev. Mod. Phys. **70**, 1003 (1998).
[3] T. A. Laine and S. Stenholm, Phys. Rev. A **53**. 2501 (1996).
[4] B. Shore, *Manipulating Quantum Structures Using Laser Pulses* (Cambridge University Press, 2011.
[5] J. P. Davis and P. Pechukas, The Journal of Chemical Physics **64**, 3129 (1976).
[6] L. Landau and E. Lifshitz, *Quantum Mechanics: Non-Relativistic Theory, Course of Theoretical Physics,v.3* (Elsevier Science, 1981).
[7] G. Vasilev, A. Kuhn, and N. Vitanov, Physical Review A **80**, 013417 (2009).
[8] JY. Sun and H. Metcalf, Phys. Rev. A **90**, 033408 (2014).
[9] A. Erdlyi, *Asymptotic Expansions*, Dover Books on Mathematics (Dover Publications, 1956).

*Corresponding author: arturs.cinins@lu.lv

To the list of contents

Toward optical detection of zero- and ultra-low field nuclear magnetic resonance

S. Pustelny[*1], **and P. Put**[1]
1. Institute of Physics, Jagiellonian University, Łojasiewicza 11, 30-348 Kraków, Poland

For several decades, nuclear magnetic resonance (NMR) conducted in ultra-low or truly-zero magnetic fields was considered as an exotic incarnation of NMR. While problems with magnetic-field strength vs magnetic-field homogeneity, magnetic artefacts, necessity of cryogenic cooling of superconducting magnets, etc. are important challenges for NMR, the improvement of signal-to-noise ratio and hence increase of spatio-temporal resolution of the technique has been a main drive for development and application of yet stronger magnetic fields.

The need for operation at strong magnetic fields stems from two particular origins. The first is pumping. As most of currently explored NMR applications uses thermal polarization of samples, the stronger field implies larger polarization of the samples and hence larger NMR signals. Simultaneously, the strong field is also implied by a traditionally used inductive detection scheme applied for observation of NMR signals; stronger magnetic fields correspond to the faster spin precession and hence faster magnetic-flux changes. Thereby, stronger fields improve sensitivity of NMR signal detection. Some of novel techniques of polarization improvement (hyperpolarization) do not require strong magnetic field at the polarization level. This either excludes of at least alleviates necessity of implementation of the strong magnetic field for spin polarization. Moreover, replacement of the pickup coil with a nonconventional detection scheme, being more sensitive at slowly-varying magnetic fields (low Larmor frequency) will address the challenge at the probing stage. These two fact, in conjunction with analysis of J spectra, enables one to detect strong NMR signals even without any magnetic field and triggered changes in reception of zero- and ultra-low-field (ZULF) NMR [1].

We are presenting our activities on development of a magnetometric scheme, enabling detection of NMR signals at ZULFs. The scheme is based on application of optical magnetometry [2], i.e., the technique, in which detection of magnetic field is performed based on monitoring properties of light traversing media subject to the external magnetic field. As the field may be induced by spin-polarized NMR samples, the technique enable detection of NMR signals. The detection of NMR signals is envisioned at the field between truly zero (spectroscopy) up to 100 μT (imaging). A particular example of application of the magnetometer in detection of magnetization of spin-exchange polarized xenon [3] will be given. The measurement will demonstrate the potential of ZULF NMR for spectroscopy and imaging.

References

[1] J. W. Blanchard and D. Budker, EMagRes **5**, 1395 (2016).
[2] W. Chalupczak, R. M. Godun, S. Pustelny, and W. Gawlik, Appl. Phys. Lett. **10**, 242401 (2012).
[3] http://chaos.if.uj.edu.pl/∼ksenon/

*Corresponding author: pustelny@uj.edu.pl

To the list of contents